UNIVERSITY OF SOUTHAMPTON

Driving an Ecosystem Simulation Model with Spatial Estimates of LAI

Toby E. Wicks

A thesis submitted for the degree of Doctor of Philosophy

Department of Geography
Faculty of Science

March 2000

UNIVERSITY OF SOUTHAMPTON

ABSTRACT

FACULTY OF SCIENCE
GEOGRAPHY

Doctor of Philosophy

DRIVING AN ECOSYSTEM SIMULATION MODEL WITH REMOTELY SENSED DATA

by Toby E. Wicks

To estimate the net primary production (NPP) hence, carbon sequestration, for large areas of terrain, an ecosystem simulation model (ESM) can be driven using biophysical data in a spatially-extensive format. Such information is needed to implement the United Nations' Framework Convention on Climate Change (Kyoto Protocol) as it will reduce uncertainty in national and global carbon budgets for terrestrial ecosystems.

Ground and remotely sensed data were collected between 1994 and 1998 as part of the BOReal Ecosystem-Atmosphere Study (BOREAS) and Boreal Ecosystem Research and Monitoring Sites (BERMS) initiatives in northern Canada. A pilot investigation 'optimised' the FOREST-BGC (Bio-Geochemical Cycling) ESM to obtain accurate estimates of NPP for a number of BOREAS sites and ascertained model sensitivity to input variables. Subsequently, FOREST-BGC was 'automated' using remotely sensed estimates of leaf area index (LAI) from the Landsat Thematic Mapper (TM) sensor, in order to produce a 20 km^2 map of NPP. The pilot study emphasised the need for accurate spatial estimates of LAI. Consequently, three refinements were investigated with the aim of maximising the accuracy with which remotely sensed data could be used to estimate boreal forest LAI:

First, the joint issues of scale and the choice of an *optimum* sampling unit for forested landscapes were investigated through the development of a new technique for the partitioning of remotely sensed images into relatively homogeneous 'areal sampling units' (ASU). More representative estimates of LAI were attained as the ASU captured spatial variation of the landscape, removing high spatial frequency features (some associated with noise in the data). Further increases in accuracy were attained by excluding edge pixels from the ASUs.

Second, three alternative methods for producing spatially-extensive estimates of LAI were explored: Aspatial regression, cokriging and conditional simulation. Although theory suggested cokriging may produce the most accurate spatial estimates, aspatial regression was adopted because the estimation of spatial covariance was not robust in this case.

Third, the potential of using data acquired by the Advanced Very High Resolution Radiometer (AVHRR) satellite sensor was assessed by investigating the relationship between LAI and several spectral vegetation indices. The value of remotely sensed radiation reflected at middle infrared (MIR) wavelengths (3.0-5.0 μm) was demonstrated as the VI3 vegetation index (incorporating reflected MIR) was related more strongly to LAI than the more widely used normalised difference vegetation index.

The final phase of this research explored the impact of future climates on the carbon budget of the boreal forest. FOREST-BGC was run with climate change predictions (derived from three different CO_2 emission scenarios) together with spatial estimates of LAI (from both Landsat TM and AVHRR) that were a result of the preceding research chapters. Results suggested that boreal forests continued to provide a substantial 'brake' on the rate of increase in atmospheric CO_2, provided anthropogenic emissions of CO_2 were reduced dramatically to within the imposed limits of the Kyoto Protocol. However, if emissions followed the unmitigated (i.e., 'business as usual') scenario, carbon sequestration of the boreal forests increased to a maximum by 2050 but thereafter collapsed, resulting in a disappearance of the carbon sink by approximately 2080. There is still a considerable amount of work to be done in order to estimate accurately future carbon sequestration of the boreal forest. However, it was concluded that driving FOREST-BGC with accurate spatial estimates of LAI derived from remotely sensed data is a powerful tool with which to gain a quantitative understanding of current and future biogeochemical cycling through the boreal forest ecosystem.

Declaration

I declare that the work within this thesis is my own, unless otherwise stated. It has not been submitted for any other degree. This work was done wholly whilst registered as a postgraduate at the Universities of Southampton and Toronto.

Toby Wicks
8 March 2000

'If the Lord Almighty had consulted me
before embarking on the Creation,
I would have recommended something simpler'.

Alfonso X of Castile, 'The Learned',
1221–1284.

Acknowledgements

Over the past three years I am so fortunate to have 'interacted' with a great number of people to whom I am indebted. I hope that this page expresses, in some small way, my gratitude.

First, my supervisor, Prof. Paul Curran, an inspiration in all aspects of research, whose energy and infectious enthusiasm were a pleasure to witness.

Next, I wish to acknowledge those people who have facilitated this research. Dr. Geoff Smith (NERC ITE, Monks Wood), Dr. Terry Dawson (ECU, University of Oxford) and Dr. Paul Aplin (University of Nottingham) were particularly encouraging as well as Dr. Doreen Boyd, Dr. Neil Lucas (Kingston University), Dr. Jennifer Dungan (Johnson Controls, NASA Ames) and Dr. David Viner (Climate Research Unit, University of East Anglia). Thanks also to the staff of the Department of Geography (University of Southampton), especially, Dr. Peter Atkinson, Dr. Duncan Baldwin, Dr. Jim Milne, Prof. Nigel Arnell, Dr. Ted Milton and the staff of the Cartographic Unit. The environmental research community generated by the BOReal Ecosystem Atmosphere study (BOREAS) (of which Prof. Paul Curran was a PI) and in particular, Dr. Steven Plummer (NERC ITE, Monks Wood), Val Ungless (NPA) and Beth Nelson (BORIS) for facilitating my access to the data. In addition, Prof. Steve Running and Dr. Peter Thornton (University of Montana) for providing the FOREST-BGC ecosystem simulation model. The climate scenario data used within this thesis were supplied by the Climate Impacts LINK project on behalf of the Hadley Centre and UK Meteorological Office.

Whilst in Canada, Dr. Richard Fournier (Natural Resources Canada), Prof. Ferko Csillag (Department of Geography, University of Toronto), Dr. Ian Campbell (Northern Forest Centre, Edmonton), Dr. Alan Barr (AES, Saskatoon) and Paula Pacholek (BERMS, Waskesiu) made my time so enjoyable.

The research was supported financially by the Natural Environment Research Council (studentship GT4/96/273/EO). RSS travel bursaries enabled me to present at international conferences: Courchevel (April, 1997) and Tromso (June, 1998) and an EU 'special grant' funded my attendance at a two week 'Remote Sensing Risks' residential course at the International Space University (Strasbourg).

On a more personal level, all my fellow postgraduates and sub-wardens at Southampton and Toronto, especially: Andy, Anjana, Chris, Graeme, Jamie, John, Mark, Pamela, Philip, Robin, Rose, Sally, Süha, Tatiana and Will. In particular, Pete Langdon, Paul Aplin and Rich Waller deserve special praise. Apologies to the long-term sufferers of the EO lab., Research Computing and especially my office who were witness to my frequent over excitement!

Kate deserves a mention for her distracting influence and for attempting to calm my hyper-activity! Finally, thanks to my 'support team' in Bristol for their continued interest and encouragement.

Contents

List of Figures

List of Tables

List of Plates

Abbreviations and acronyms found within this thesis:

AATSR	Advanced Along-Track Scanning Radiometer
AES	Atmosphere Environment Service
AFM	Airborne Flux and Meteorology
AMS	Automatic Mesonet Station
APAR	Absorbed photosynthetically active radiation
ASCII	American Standard Code for Information Interchange
ASU	Areal sampling unit
ATM	Airborne Thematic Mapper
ATSR	Along-Track Scanning Radiometer
AUX	Auxiliary site
AVHRR	Advanced Very High Resolution Radiometer
AVIRIS	Airborne/Visible Infrared Imaging Spectrometer
BATS	Biosphere-Atmosphere Transfer Scheme
BERMS	Boreal Ecosystem Research and Monitoring Sites
BFTCS	Boreal Forest Transect Case Study
BGC	Biogeochemical Cycling
BOREAS	BOReal Ecosystem-Atmosphere Study
BORIS	BOREAS Information System
BRDF	Bi-directional reflectance distribution function
BTDF	Bi-directional transmittance distribution function
CASI	Compact Airborne Spectrographic Imager
CC	Cubic convolution
CCRS	Canadian Centre for Remote Sensing
CD-ROM	Compact Disk - Read Only Memory
CEV	Carbon evaluation site
CO_2	Carbon dioxide
CUE	Carbon use efficiency
DAAC	Distributed Active Archive Centre
dbh	Diameter at breast height
DEM	Digital elevation model
DETR	Department of the Environment, Transport and the Regions
DN	Digital number
EFEDA	European Field Experiment in a Desertification threatened Area
EO	Earth observation
EOS	Earth Observing System
ERS	European Remote Sensing Satellite
ESA	European Space Agency
ESM	Ecosystem simulation model
ETM+	Enhanced Thematic Mapper-Plus
FFC	Focussed field campaign
FOREST-BGC	Forest Biogeochemical Cycling
FPAR	Fraction of PAR absorbed by the vegetation canopy
GAC	Global Area Coverage
GAIM	Global Analysis Integration and Modelling
GCM	Global climate model
GEOCOMP	Geocoding and Compositing System
GICS	Geocoded Image Correction System

GIS	Geographical Information System
GPP	Gross primary production
GPS	Global Positioning System
GTOS	Global Terrestrial Observing System
GVI	Global Vegetation Index
GWR	Geographically weighted regression
HAPEX	Hydrological Atmospheric Pilot Experiment
HRPT	High resolution picture transmission
HRV	High Resolution Visible sensor
HYD	Hydrology
IFC	Intensive field campaign
IFOV	Instantaneous field-of-view
IGBP	International Geosphere-Biosphere Programme
IGIS	Integrated Geographical Information System
IPCC	Intergovernmental Panel on Climate Change
ITRDB	International Tree-Ring Data Bank
LAC	Local Area Coverage
LAI	Leaf area index
LGSOWG	Landsat Ground Stataion Operations Working Group
LNC	Leaf nitrogen concentration
LSP	Land Surface Process
LUT	Look-up table
MAUP	Modifiable Areal Unit Problem
MERIS	Medium Resolution Imaging Spectrometer
MIR	Middle infrared
MODIS	Moderate Resolution Imaging Spectrometer
MSE	Mean square error
MSS	Multispectral Scanner
MTPE	Mission to Planet Earth
NAD	North American Datum
NASA	National Aeronautics and Space Administration
NDVI	Normalised difference vegetation index
NEE	Net ecosystem exchange
NEP	Net ecosystem production
NERC	Natural Environment Research Council
NIR	Near infrared
NN	Nearest neighbour
NOAA	National Oceanic and Atmosperic Administration
NPP	Net primary production
NPP_A	Aboveground net primary production
NSA	Northern Study Area
NSERC	Natural Science and Engineering Research Council
OA	Old aspen
OBS	Old black spruce
OJP	Old jack pine
OTTER	Oregon Transect Research Project
PAL	Pathfinder AVHRR Land data
PANP	Prince Albert National Park

Chapter 1

Introduction

This research investigated the value of driving a forest ecosystem simulation model (ESM) with remotely sensed data. This chapter explains the rationale behind the research, states the specific objectives and concludes with a description of the thesis structure.

1.1 Rationale

Among the most important research initiatives of the new millennium is the study of global environmental change. One key issue within this initiative is the relationship between biogeochemical cycles and the Earth's climate. In particular, it is evident that there is a 'discernible human influence on global climate' and of primary concern is the magnitude and rate of increase in the concentration of atmospheric carbon dioxide (CO_2) (O'Riordan 2000, p.172). A key to understanding the causes of this increase in atmospheric CO_2 is to further the knowledge of interactions operating in the global carbon cycle and to quantify its budget (Sedjo 1993). Indeed, in 1997, the United Nations Framework Convention on Climate Change (UNFCCC) agreed upon the 'Kyoto Protocol', recognising the need to preserve and increase the amount of carbon in the terrestrial biosphere (Grubb *et al.* 1999), most of which is stored in forests and soil (Dawson and Wicks 1998) in order to provide a substantial reduction in the rate of increase of atmospheric CO_2 (DETR 1999).

Although considerable research has been undertaken to determine the rôle of the terrestrial biosphere on the global carbon cycle, exact relationships are still a matter of great debate (Tans *et al.* 1990; Grainger 1993; Dixon *et al.* 1994; Houghton *et al.* 2000), primarily because of the complex interaction of natural and anthropogenic factors (Solomon *et al.* 1993). To date, tropical terrestrial ecosystems have received most attention, where extensive deforestation and burning have altered atmospheric chemistry and land surface climatology (Houghton *et al.* 2000). Boreal forests, however, have an equally important rôle in the global carbon budget, especially over long time periods (White *et al.* 1999; Chen *et al.* 1999).

Consequently, there is a need to gain a quantitative understanding of biogeochemical cycling through the boreal forest ecosystem. Net primary production (NPP) is one of the most important fluxes characterising the performance of an ecosystem. It is the difference between the total carbon uptake (sequestration) from the atmosphere through photosynthesis and carbon loss due to respiration by living plants. Direct measurements of NPP can be made but only for small portions of space and time. Current techniques are, therefore, unsuitable for deriving NPP estimates over large areas. Computer simulation models of ecosystem behaviour, however, are a valuable experimental alternative for investigating responses and feedbacks of processes controlling NPP (such as photosynthesis, respiration and transpiration) operating over a range of spatial and temporal scales.

Indeed, forest ecosystem simulation models have the potential to increase our understanding of the dynamic behaviour of forest processes and how they react to natural and anthropogenic pressures (Lucas and Curran 1999). Landsberg *et al.* (1991) identified three reasons for developing such models:

1. essential as a framework for any research into the functioning of forest ecosystems (e.g., Running *et al.* 1999);
2. useful management tool (e.g., Franklin *et al.* 1997a) and
3. can be used in a prognostic capacity to analyse the effects of future climate on forest ecosystems (e.g., Nilson *et al.* 1999; Siddiqui *et al.* 1999).

Hence, over the past ten to fifteen years a number of models, designed to estimate forest productivity on the basis of physiological processes, have been developed. Whilst these models may vary in their conceptual approach and scale of operation, all are simplifications (Stoddart 1986) *aspatial* (Curran 1994a) and 'data hungry' (Coops 1999, p. 1149). The latter two characteristics have made it extremely difficult to 'scale-up' data or processes in order to understand the functioning of forest ecosystems, in particular, their interaction with hydrospheric and atmospheric processes (Hobbs and Mooney 1990; van Gardingen *et al.* 1997).

Indeed, as "the most pressing ecological questions being asked today address ecosystem processes at regional to global scales" (Curran and Foody 1994, p.2), a number of scale-independent deterministic models were developed that require spatial estimates of key driving variables (Lucas *et al.* 2000). However, it is often technically and financially impossible to acquire the necessary input data with the precision required by an ESM over large areas (van Rompaey *et al.* 1999). Hence to date, the majority of such models have 'only been used as research tools' (Coops 1999, p. 1149), although their ultimate aim was to provide prognostic capabilities (Hibbard and Sahagian 1997).

Therefore, to estimate accurately carbon fluxes at regional scales, such scale-independent, process-based models require accurate spatial estimates of biophysical variables (e.g., leaf area index (LAI)) as inputs. Traditionally, estimates of LAI have been acquired *in-situ* using extremely labour-intensive sampling techniques (e.g., Franklin *et al.* 1997a; Wülder *et al.* 1998a; Gower *et al.* 1999). However, it is now acknowledged widely that remotely sensed observations provide the only practical and accurate means of estimating the variables needed to drive such models at regional to global scales (Aber *et al.* 1993; Lucas and Curran 1999).

To evaluate variation in ecological processes over large areas, enhanced coupling between remote sensing technology and ecosystem theory must occur as reasonable predictions require accurate representation of biosphere-atmosphere interaction (Wickland 1991; van Gradingen *et al.* 1997). This was one of the primary motivations behind the BOReal Ecosystem-Atmosphere Study (BOREAS), a comprehensive international ecological investigation focused on increasing understanding of the exchanges between the boreal forest and the lower atmosphere (Sellers *et al.* 1997). A specific objective was to collect the data needed to increase the accuracy of estimates from computer simulation models of the processes controlling these exchanges.

The ultimate aims of developing process-based forest ESMs are to increase (i) the accuracy of estimates and (ii) understanding of biosphere-atmosphere interaction. The research pursued in this thesis was conducted in response to such development, with three specific objectives:

1. to drive a forest ESM with biophysical variable estimates derived from remotely sensed data in order to produce a map of NPP for an initial area of 20 km^2 of boreal forest;
2. to increase the accuracy of spatial LAI estimates over large areas of boreal forest and
3. to investigate the impact of future climate on the carbon budget of the boreal forest.

A realistic aim, for the not too distant future, is the routine production of accurate regional NPP maps on a daily, monthly and/or annual basis (Running *et al.* 1999). Such information is

essential to (i) increase environmental understanding and (ii) enhance environmental management so policy makers can make environmentally-sound decisions on strategies for the sustainable development of natural resources. This thesis presents a series of original techniques that have potential to increase the accuracy of current NPP estimates with fine to moderate spatial resolution (0.03~1 km) for the boreal forest at regional scales (10,000 km^2). Such quantification of the rôle boreal forests within the global carbon cycle (in particular their interaction with anthropogenic atmospheric CO_2 emissions), would enable researchers to better predict how the carbon cycle will be affected by future climate change and *vice versa*.

1.2 Thesis Structure

This thesis has been written in 9 chapters (Figure 1.1). In response to a review of existing theory and empirical evidence (**Chapter 2**), the enormous potential of driving an ESM with biophysical variable estimates derived from remote sensing in order to estimate carbon fluxes over large areas of boreal forest was apparent.

Chapter 3 introduces the study site, data acquisition and fieldwork: The BOREAS Southern Study Area (SSA) in Saskatchewan, Canada was chosen as the primary location for developing and testing the techniques within this thesis because of the ecosystem conditions and availability of the requisite data sets.

Chapter 4 details a pilot study including a sensitivity analysis of FOREST-BGC (-Biogeochemical Cycling), the forest ESM to be used (Running and Coughlan 1988). The model was 'initialised', 'optimised' and 'automated' in order to produce an accurate map of NPP for 20 km^2 of boreal forest. The subsequent three chapters are focussed on increasing the accuracy with which biophysical variables (notably, LAI) can be estimated from remotely sensed data.

Chapter 5 addresses the issues of scale and the choice of an 'optimum' sampling unit for the study of forested landscapes over large areas using remotely sensed data. A new technique was developed to partition remotely sensed images into relatively homogeneous 'areal sampling units' in order to optimise estimates of biophysical variables.

Three alternative methods for producing spatially extensive estimates of LAI are compared in **Chapter 6**. The theory behind each method was discussed before exploring the most appropriate for this investigation.

The potential of using radiation acquired by the National Oceanic and Atmosperic Administration (NOAA) Advanced Very High Resolution Radiometer (AVHRR) satellite sensor to estimate boreal forest LAI is the subject of **Chapter 7**. Particular attention was given to radiation acquired in middle infrared (MIR) wavelengths (3.0–5.0 μm). The relationships between LAI and several spectral vegetation indices were assessed and the strongest relationship used to produce a LAI map.

Given the need to predict and anticipate the effects of global change on the boreal forest and the associated implications for the global carbon cycle, **Chapter 8** investigates the effect of possible future climatic scenarios on the productivity of the boreal forest. The automated FOREST-BGC model was run with climate change predictions as well as input data that were a result of the preceding four chapters of this thesis. Attention was given to whether the boreal forest would remain a terrestrial carbon sink under different scenarios of climate change.

Finally, **Chapter 9** provides a summary of this research and concluding remarks. The contribution and limitations of this research were discussed, together with areas of uncertainty that need to be addressed by future investigations.

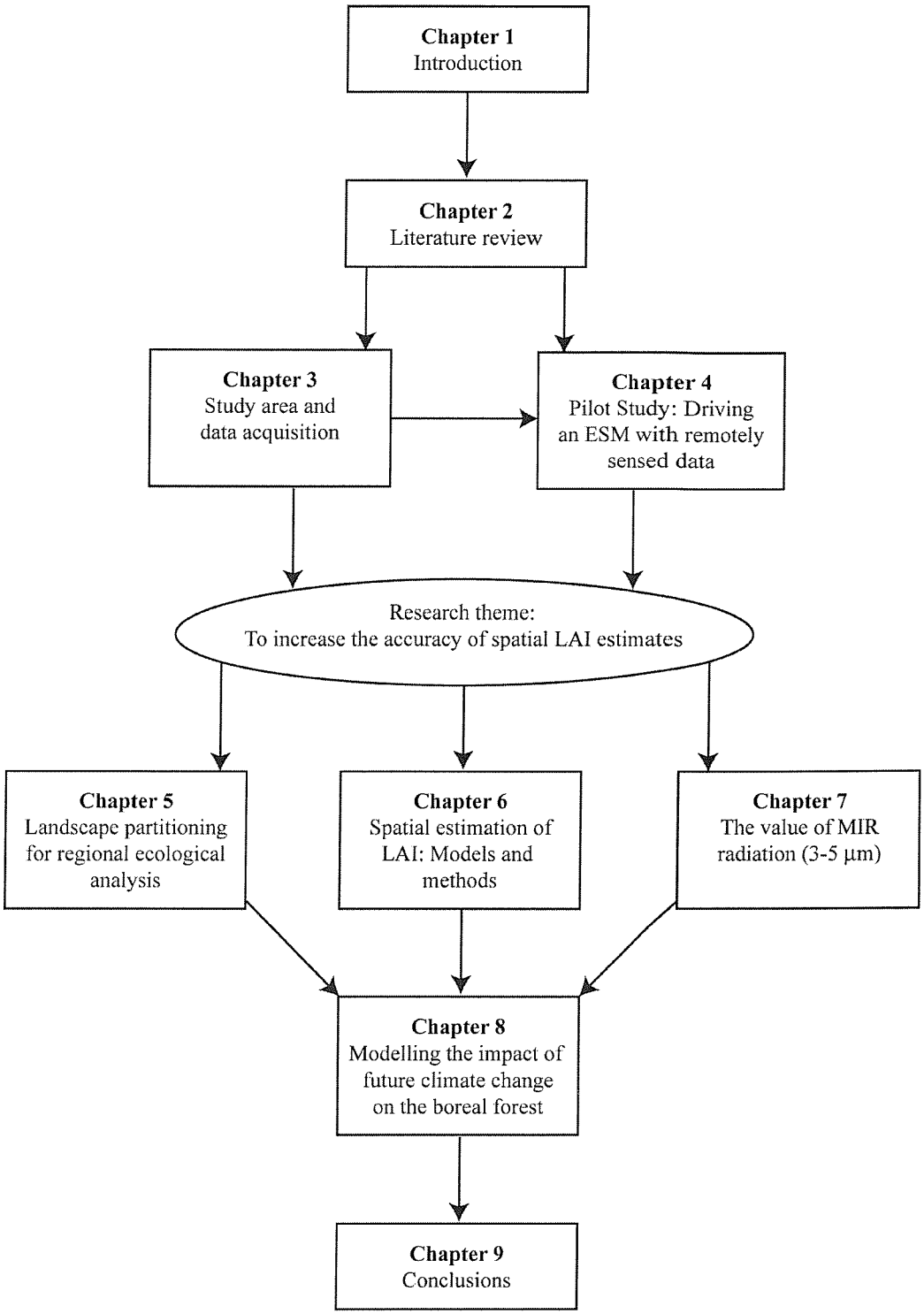

Figure 1.1 Schematic representation of the structure of this thesis.

Chapter 2

Literature Review

This aim of this chapter is to review the literature relevant to driving a forest ESM with remotely sensed data to reduce uncertainties surrounding the rôle of the boreal forest in the global carbon budget. This review concerns six broad topics: (i) the global carbon budget and the rôle of boreal forests; (ii) the need for forest ESMs; (iii) using remote sensing to estimate biophysical properties of forests; (iv) the FOREST-BGC ESM of Running and Coughlan (1988); (v) field experiments and data acquisition (particular attention is given to the BOREAS) and finally, (vi) future directions: The need to develop new methods to increase the accuracy of ESM outputs over large areas.

2.1 The Global Carbon Budget and Boreal Forests

Knowledge concerning the location and movement of carbon within the Earth system is of fundamental importance to the management of the planet. However, considerable uncertainty exists as to the influence of different processes on the global carbon cycle (Sampson *et al.* 1993; Houghton *et al.* 2000). Uncertainty stems from limitations in the understanding of environmental processes and owing to the importance of atmospheric CO_2 as a greenhouse gas, hinders the ability of researchers to predict future global environmental change (Solomon and Leemans 1997; O'Riordan 2000). Consequently, the identification and quantification of all sources and sinks within the global carbon cycle are of critical importance (Sampson *et al.* 1993; Waring and Running 1998; Running *et al.* 1999).

The fundamental difficulty in quantifying all aspects of the global carbon budget arises because of the disparity in size between the predominantly large pools and relatively small fluxes (Fan *et al.* 1998). Indeed, uncertainty surrounding the magnitude of these fluxes, especially the time scales required to affect atmospheric carbon is of greatest concern (Figure 2.1).

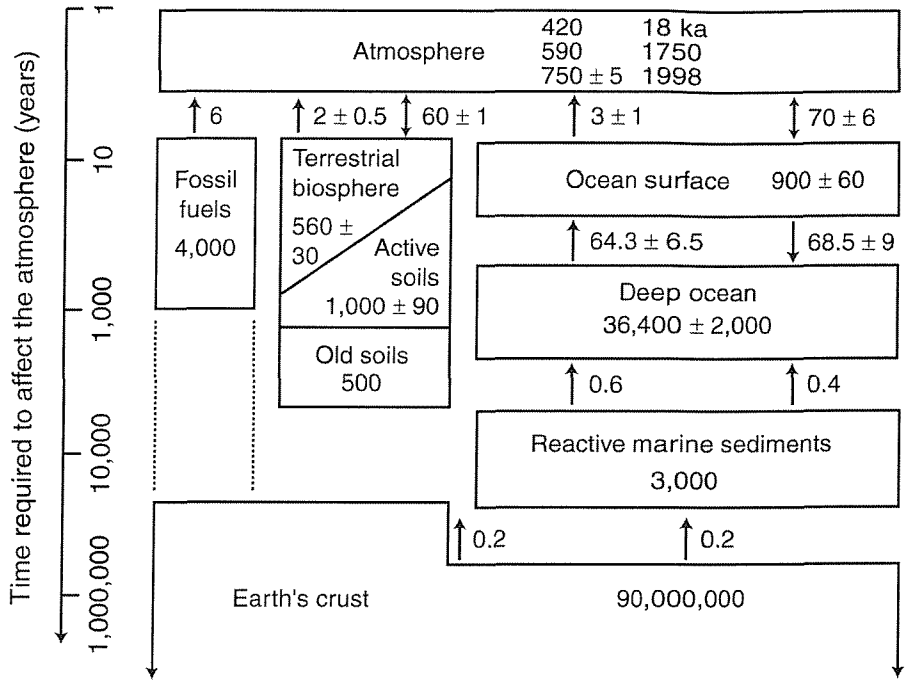

Figure 2.1 Principal pools (Pg) and fluxes (Pg yr^{-1}) in the global carbon cycle. Vertical placements relative to scale on the left show approximate time required for pools and fluxes to affect atmospheric CO_2. Single arrows to and from the atmosphere are approximate estimates of anthropogenic fluxes for 1990. Terrestrial uptake of anthropogenic CO_2 is likely but not illustrated because of considerable uncertainties (Wisniewski and Sampson 1993).

Recent quantification of current carbon pools (e.g., White *et al.* 1999; Houghton *et al.* 2000) continues to be hindered by poor understanding of responses and feedbacks to both natural and anthropogenically-induced fluxes (Turner *et al.* 1997). This has led to uncertainty concerning the *background* natural exchanges of carbon that were assumed by many researchers to be in carbon balance before eighteenth century industrialisation (Wisniewski and Sampson 1993), which conflicts with considerable evidence from Antarctic ice cores (e.g., Smith *et al.* 1993).

Despite this apparent contention, there is reasonable agreement that current atmospheric CO_2 loading is increasing by approximately 3.3 Pg C yr^{-1} (Table 2.1) (Schimel 1995; Trenberth *et al.* 1996). The primary anthropogenically-induced net sources of this carbon are (i) burning of fossil fuels and (ii) deforestation of forest ecosystems, particularly in the low latitudes (Houghton *et al.* 2000). These sources are thought to contribute around 5.5 and 1.6 Pg yr^{-1} to the atmosphere, respectively (Hunt *et al.* 1996).

The opposing and predominantly natural net sinks are known to a lesser extent because they are an order of magnitude less (in size of flux) than the anthropogenic sources (Detwiler and Hall 1988). Uptake of carbon by the deep ocean and sequestration by forests are thought to fix approximately 2.0 and 0.5 Pg C yr^{-1} respectively (Houghton *et al.* 1998; White *et al.* 1999). However, together these two sinks constitute a very inadequate representation of the potential for the terrestrial biosphere to cycle carbon (Sampson *et al.* 1993). Consequently, considerable confusion remains as to the contribution of both natural and anthropogenically-induced terrestrial net sinks to balancing the carbon budget (Houghton *et al.* 2000).

Given the magnitude of the known sources and sinks of carbon and accepting the associated uncertainty, the current rate of atmospheric CO_2 increase is less than half that expected (Tans *et al.* 1990; Sundquist 1993; Houghton *et al.* 1996; Murray *et al.* 1996) (Table 2.1). This discrepancy, termed the 'missing carbon', has been estimated as a sink of approximately 1.3 Pg C yr^{-1}, a figure too large to be considered as the error associated with the other carbon budget terms (Craig and Holmén 1995; Chen *et al.* 1999). Hence, an inadequate understanding of carbon pools and fluxes as well as the effects of rising concentrations of atmospheric CO_2 on natural ecosystems is manifest in the unbalanced global carbon budget.

CO_2 sources		
1	Emissions from fossil fuel combustion and cement production	5.5 ± 0.5
2	Net emissions from changes in tropical land use	1.6 ± 1.0
3	Total anthropogenic emissions (1 + 2)	7.1 ± 1.5
Partitioning amongst pools		
4	Storage in the atmosphere	3.3 ± 0.2
5	Ocean uptake	2.0 ± 0.8
6	Uptake by Northern Hemisphere ecosystems	0.5 ± 0.5
7	Inferred 'missing carbon sink' (4 + 5 + 6 – 3)	1.3 ± 1.5

Table 2.1 Average annual anthropogenic carbon budget for 1980–1989. CO_2 sources, sinks and storage in the atmosphere expressed in Pg C yr^{-1} (Trenberth *et al.* 1996).

The 'search' for this missing carbon was initiated (on its discovery during the late 1980s), with positive attempts to reduce uncertainties associated with the global carbon budget (Bailey 1997). For example, Denning *et al.* (1995) found that the seasonal sequestration of atmospheric CO_2 by photosynthesis and subsequent release by respiration involved fluxes that were stronger than the anthropogenic emission rate by an order of magnitude (Schimel 1994). These fluxes account for the very large seasonal amplitude of the annual cycle of CO_2 concentrations.

Denning *et al.* (1995) concluded that the contribution of seasonal terrestrial biota to the sinks of atmospheric CO_2 in the Northern Hemisphere must be stronger than suggested previously. A decrease in the estimated potential of the oceanic pool to act as a significant sink (Siegenthaler and Sarmiento 1993) left the search for the missing carbon directed firmly towards the terrestrial biosphere (Tans *et al.* 1990; Beerling 1999). Indeed, increased understanding of the fluxes and pools within the terrestrial biosphere is essential if progress is to be made balancing the budget (Boyd *et al.* 1996; Foody *et al.* 1996).

2.1.1 Forest ecosystems

Forest ecosystems cover approximately 4.1 billion ha (31%) of the Earth's land surface and are of major importance in the global carbon cycle as they dominate the cycling of carbon within the terrestrial biosphere (Sedjo 1993; Culotta 1995). As with most of the elements of the global carbon cycle, estimates of carbon fluxes to and from forests vary greatly. However, forests are estimated to account for approximately 90% (70 to 90 Pg) of the annual carbon flux between the atmosphere and terrestrial ecosystems via photosynthesis, respiration, decomposition and land use change (Dixon *et al.* 1994).

Given the possibility for changing carbon fluxes at the global scale, it has become critical to investigate whether forests act as net sources or sinks of carbon under present conditions and assess their development with respect to carbon dynamics in a changing climate (Perruchoud and Fischlin 1995; Chen *et al.* 1999). To date, the effects of climate on terrestrial ecosystems have received most attention in the tropics, where extensive deforestation and burning have altered atmospheric chemistry and land surface climatology (Houghton *et al.* 2000). However, 'a significant portion of the net uptake of CO_2 occurs at mid-latitudes of the Northern Hemisphere' (Tans *et al.* 1990; Ciais *et al.* 1995; Running *et al.* 1999). Therefore, boreal forests have an equally important rôle in the global budgets of atmospheric carbon, especially over long temporal scales, when terrestrial vegetation undergoes significant geographic redistribution in response to climate change (Tans *et al.* 1990; White *et al.* 1999). The following sub-sections introduce the boreal forest biome and detail its susceptibility to change.

2.1.2 An introduction to boreal forests

The boreal forest covers approximately 17% of the world's land surface area in a circumpolar complex of forested and partially forested ecosystems (Larsen 1980). About two thirds lies in Eurasia and one third in North America (Slaughter *et al.* 1995). The boreal forest is, thus, circumpolar in extent, occupying a belt as wide as 1000 km in certain regions (Figure 2.2).

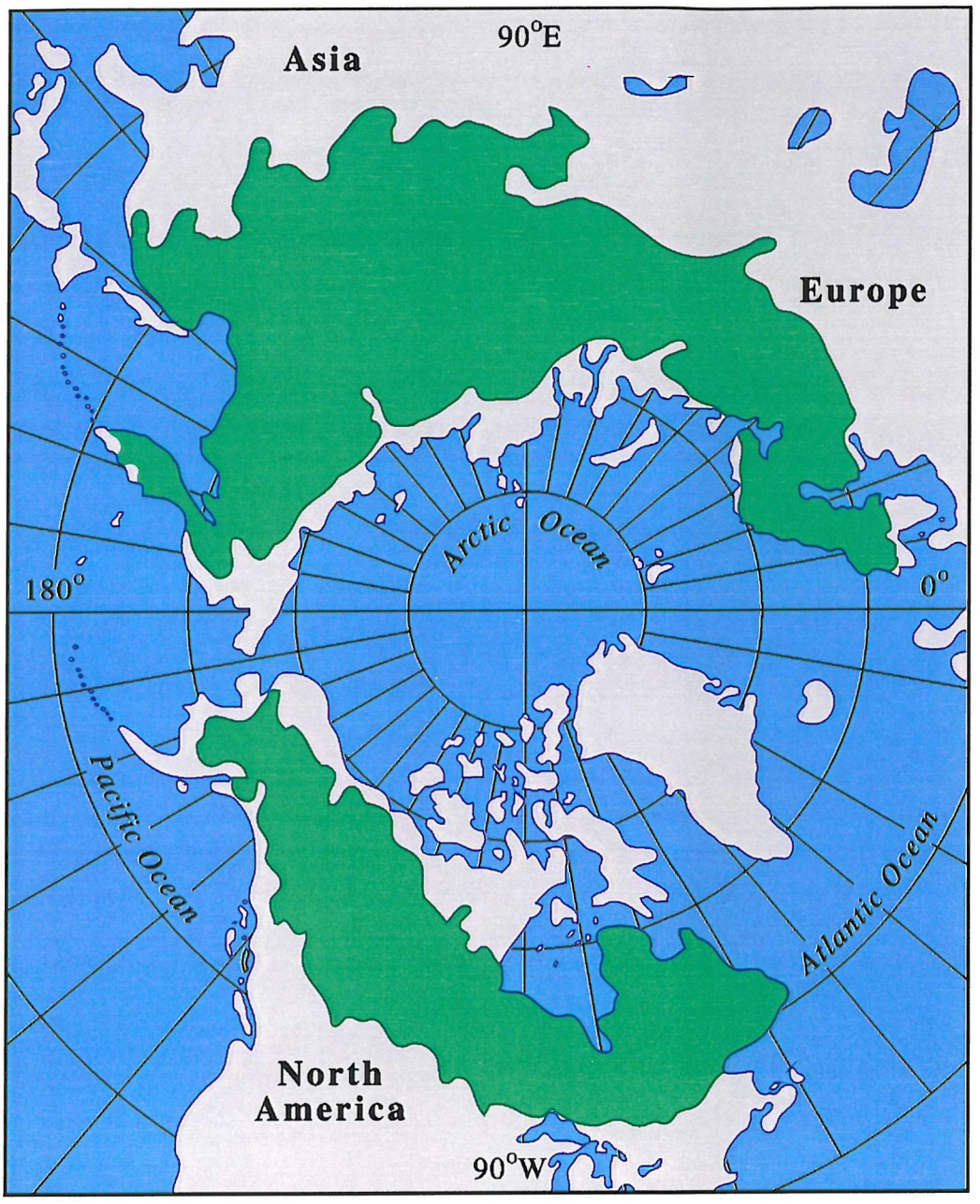

Figure 2.2 The circumpolar extent of the boreal forest. Note that approximately two-thirds lies within Eurasia and that the area in eastern Canada is the furthest south (adapted from Apps *et al.* 1993).

Throughout its range the forest is surprisingly uniform in species composition (Larsen 1980). Conifers include spruce (*Picea* sp.), fir (*Abies* sp.), pine (*Pinus* sp.) and larch (*Larix* sp.); hardwoods typically include aspen or cottonwood (*Populus* sp.), birch (*Betula* sp.), alder (*Alnus* sp.) and willow (*Salix* sp.). Many shrubs of the boreal forest exhibit similar circumpolar commonality at the genus and species level (Bliss and Matveyeva 1992).

2.1.2.1 Species and environment

For a complete understanding of the vegetational composition of the boreal forest it is important to know something of the history of the species. Such knowledge requires an appreciation of the relationship between evolving plants and their environment.

Historical flora composition

Fossil evidence has failed to provide a lucid record of the origins of boreal floras, although it has been inferred that such flora developed throughout the Tertiary period, beginning about 70 million years ago (Price and Apps 1996). Interpretation of this evidence suggested that prevailing conditions favoured development of tropical flora in the southern portions of North America that graded northward into an "Arcto-Tertiary flora" in which deciduous trees and conifers were predominant. With the steadily declining temperatures of the late Tertiary it is probable that the modern species, now characteristic of both the arctic and boreal zones, evolved from species of the northern portions of the hemisphere (Halliwell *et al.* 1995).

Climate

The word *boreal* carries climatic implications since it is derived from a Greek name for the 'Goddess of the North Wind'. The climate of the boreal ecosystem is characterised by strong seasonal variation: with short, moderately warm and moist summers and long, extremely cold and dry winters (Hare and Hay 1971). Appreciable snow cover lasts for more than one-half of the year in most parts of the region (Slaughter *et al.* 1995). The annual temperature range is considerable, especially in the mid-continental areas, where seasonal fluctuations can be as great as 100 °C (Johnson *et al.* 1994)!

Given that the boreal forest extends in a broad band over both North America and Eurasia, climatic conditions vary considerably. Researchers, therefore, tend to study vegetation in terms of its relationship to microclimate, rather than to the macroclimate characteristics of the 'sub-arctic' zone in which it is found (Hall 1995; Price and Apps 1996).

The distribution of boreal flora appears to be primarily in response to climate, with related edaphic factors (environmental characteristics determined by soil characteristics) such as moisture availability, playing a secondary rôle (Larsen 1980). Indeed, the position of the boreal forests' borders are approximately coincident with a number of variables that have been employed to delineate climate, for example, temperature, average pressure and maximum frontal activity (Oliver and Larson 1996). There are also a number of climate-related soil and geomorphological characteristics, notably podzolisation and permafrost, which concur with circumpolar distributions of boreal vegetation (Tedrow 1977; Larsen 1980; Hall 1995).

Ecologically, the most striking characteristic of the northern forest border is its abrupt nature, particularly in view of the virtually continuous and dominant *Picea* cover for hundreds of miles south. Aerial observations support Tyrrell's notes of 1894, in which he states, "within a few miles the forest disappears, or becomes confined to the ravines" (Tyrrell 1897, p.169). Climatic effects alone may be sufficient to accomplish this remarkable transformation, however, energy transfer relationships may also have a significant contribution. As such, the considerable biophysical effects of boreal forests on climate show that climate and vegetation exist in a dynamic equilibrium in which climate affects and is affected by the distribution of vegetation.

Radiation and temperature

Radiation is the primary factor establishing temperature and moisture regimes, therefore, is of fundamental significance for the climatology of vegetational communities. For Canada, total incoming solar radiation per annum increases by 22%, on average, with progression south through the boreal forest (Bonan *et al.* 1995). Zonal divisions of vegetation appear to correlate closely with such patterns in radiation. Hence, the most important aspects of solar radiation in the boreal region are related to latitude. For a significant part of the year the radiation balance is negative and for the remainder, relatively low, compared with that for temperate or tropical zones (Canadian Forest Service 1999).

By masking the high albedo of snow and through the partitioning of net radiation into sensible and latent heat, boreal forests have a significant impact upon the seasonal and annual climatology of much of the Northern Hemisphere (Smith *et al.* 1993). The low albedo of dense forest permits more rapid warming in spring, hence a longer above freezing season than in the tundra (on average by 50 days), hence vegetation type can have an influence on climate (Bonan *et al.* 1995).

Precipitation

Around 50% of the annual precipitation of the boreal region falls between June and August (Larsen 1980). Rainfall is derived largely from summer convective activity, hence highly variable in time and space. Periods of high rainfall are usually the result of invasion of the interior by moist air originating from the lower latitudes of the North Pacific. The region is relatively dry, with precipitation ranging from 400 to 450 mm yr^{-1}, approximately one-third of which falls as snow (Houghton *et al.* 1996).

Permafrost

Much of the boreal forest in Eurasia, Alaska and Northwest Canada is underlain by sporadic permafrost (material which is perennially frozen). The proportion of the landscape underlain increases with latitude, increasing northern exposure and greater soil moisture (Brown and Péwé 1973; Slaughter *et al.* 1995).

Permafrost exerts a profound influence upon vegetation by impeding the uptake of water and nutrients by the roots, which in relation to the boreal forest is often linked to the restriction of northward expansion. Obviously, parallels can be drawn with incident radiation patterns.

Species distribution

There are fundamental biochemical and physiological connections between climatic regimes and the distinctive geographical ranges of many boreal plant species. However, the nature of these connections will remain obscure until the physiology of temperature and moisture relationships as well as growth induced environmentally and reproductive hormonal responses are better understood (Larsen 1980).

Minor variations in topography and vegetational community composition and structure can be correlated with variations in climatic variables. Temperature is the single most important factor limiting the growth and development of vegetation in boreal regions and four temperature-dependent physiological processes (i.e., translocation, water absorption, photosynthesis and respiration), are most important in this relationship. It is ultimately gene structure that establishes the tolerance limits of a plant species and it seems likely that distribution in northern regions is not simply a response to frost but is conditioned by many specific temperature-dependant requirements. Billings and Mooney's (1968) work illustrated the complexity of such physiological responses of the boreal forest to environmental changes.

2.1.3 Sensitivity of the boreal forest to change

Boreal ecosystems are subject to change from a variety of agents and processes. Wildfire is the primary driving successional force and has remained so despite fire suppression activities and extensive harvesting (Burke *et al.* 1997). Depending on the severity of fire and adjacent seed sources, the landscape is eventually re-vegetated in a successional cycle. Insects and disease also cause extensive damage (Oliver and Larson 1996). Indeed, the forest mosaic has been 'designed' by the stresses of long, snowy winters, a short growing season and repeated naturally occurring forest fires. The boreal forests are adapted to these stresses and can be expected to recover (Hall 1995).

The majority of simulation studies carried out to assess climatic impact of increasing CO_2 indicate that the greatest warming will occur at higher latitudes (45-65 °N) (IPCC 1996; Sellers *et al.* 1997), with the most marked effects within continental interiors (Mitchell 1983; Hasenauer *et al.* 1999). For this reason, there is a general consensus that climate change will have greater impact on boreal forests than on tropical and perhaps temperate forests. However, large uncertainty exists in the ability of researchers to project future forest distribution, composition and productivity under transient or non-transient global climate change scenarios (Dixon and Wisniewski 1995; Houghton *et al.* 1998; White *et al.* 1999).

Pastor and Post (1988) investigated the possible responses of north-eastern North American forests to a warmer and generally drier climate by driving a linked forest productivity / soil process model with climate model predictions corresponding to a doubling of atmospheric CO_2. They found that responses were strongly dependent on climate induced changes in water and nitrogen availability; increased productivity was observed where soil water was not limiting and nitrogen availability had been enhanced. Hence, there was positive feedback between carbon and nitrogen cycles that was bounded by negative constraints of soil moisture availability and temperature.

Indeed, forest responses to climate change may be as sensitive to the indirect effects of climate and vegetation on soil properties as they are to the direct effects of temperature on tree growth (Salisbury and Ross 1992). Therefore, the heterogeneity of the landscape (e.g., the distribution of soil types), becomes an important factor determining forest response.

2.1.3.1 Biophysical feedbacks on the physical climate system

Changes in the ecological functioning of the biome could ensue following changes in the physical climate system. Albedo, surface roughness, and the biophysical control of evapotranspiration are the most likely surface biophysical characteristics to experience alterations, with the implication of further feedback effects on the near-surface climatology. Such notions have contributed to the launch of a series of broad scale experiments that attempt to examine the net ecosystem exchange of CO_2 between the atmosphere and portions of the terrestrial biosphere. The BOREAS, a collaborative experiment co-ordinated primarily by the National Aeronautics and Space Administration's (NASA) Biospheric Research Division, is an example of such an experiment (§2.5).

The hypothetical equilibrium of global warming driven by higher atmospheric concentrations of greenhouse gases leading to increased terrestrial carbon storage, initiating negative feedback between the global vegetation / soil system and atmospheric CO_2 concentration was disputed by Smith and Shugart (1993). They realised changes in vegetation and soil type that result in a net release of CO_2 to the atmosphere could be more rapid than changes that result in a net increase in terrestrial carbon storage under non-transient climate change. For example, most vegetation transitions would involve a considerable taxonomic shift. "Vegetation and soil changes could prove to be a significant source of CO_2 in the first 50 to 100 years following a climate warming, thereby increasing atmospheric CO_2 concentration by up to a third of the present level" (Smith and Shugart 1993, p.523). However, Bonan *et al.* (1995) support the original mode of thinking, their equilibrium analysis suggests that transient global warming is likely to lead to increased carbon storage (Prentice and Fung 1990).

2.1.3.2 Estimation of future trends in carbon dynamics

Several critical processes can be identified which are likely to modify the current distribution of above and below-ground forest carbon pools. The direct effects of CO_2 on plants (e.g., CO_2 fertilisation) and the response of plants to changing climate patterns are likely to be the most significant.

Direct effects of CO_2

Experimental studies to determine the effects of enhanced atmospheric concentration of CO_2 on productivity have been *en vogue* since the mid-1980s. Initial results suggested CO_2 had the short-term effect of increasing both rates of photosynthesis and water-use efficiency at the level of the individual plant (Mooney *et al.* 1991; Bazzaz *et al.* 1996). Smith *et al.* (1993) hypothesised if this short-term individual-level 'fertilisation' effect (CO_2 substitutes for the

enzyme rubisco, speeding up photosynthesis) extrapolated to patterns of ecosystem NPP, it would represent a large potential for increased terrestrial carbon storage. However, the majority of initial studies concentrated on seedlings and results demonstrated the importance of long-term experiments allowing plants to 'acclimatise' for several growing seasons (Murray *et al.* 1996). Indeed, recent studies have shown that with prolonged exposure some species acclimatise to the higher CO_2 concentrations, with photosynthetic rates returning to values corresponding to those observed prior to treatment (Luxmoore *et al.* 1993). Lee and Jarvis (1995) also emphasised the importance of the degree of maturity of plant tissue in response to elevated CO_2. The extrapolation of the observations on juvenile trees or seedlings to mature trees poses problems, particularly as the longest periods of CO_2 exposure that have been published to date range from 3 to 4 years (Ceulemans and Mousseau 1994).

Data for stand and ecosystem-level response to elevated CO_2 suggested an interaction with other limiting factors. Idso and Idso (1994) found their data, gathered as a review of the past ten years' experiments, showed relative growth enhancing effects of atmospheric CO_2 enrichment to be greatest when resource limitations (e.g., nitrogen availability) and environmental stresses were most severe. Following this argument, the response of the entire biosphere to increased CO_2 may be substantial if plant growth response is greater than it would have been under optimum conditions. Most researchers, however, err on the side of caution, (e.g., Luxmoore *et al.* 1993; Jarvis 1994), suggesting "elevated CO_2 may not necessarily enhance productivity" (Murray *et al.* 1996, p.401).

Climate change

The accuracy of greenhouse gas emission estimates and of climate change predictions are still met with scepticism (Apps and Price 1996; Pate-Cornell 1996; Hulme *et al.* 1999), largely due to a degree of ignorance about feedback processes in assessments of such global change. Despite such uncertainty, the scientific community acknowledges that rising atmospheric concentrations of CO_2 and other greenhouse gases over the next century have the potential to influence global climate patterns, hence carbon storage within forests (Dixon and Wisniewski 1995; Grace and Rayment 2000).

Luxmoore *et al.* (1993) suggested that climate warming and the accompanying increase in mean soil temperature could have a greater effect than CO_2 enrichment on terrestrial sources and sinks of carbon. Soil respiration and nitrogen mineralisation were shown to increase with soil temperature. If plant growth increased with increased nitrogen availability and more carbon was fixed in growth than was released by soil respiration, negative feedback on climate would

occur. Conversely, if warming were to result in a net efflux of CO_2 from forests positive feedback would ensue.

Solomon *et al.* (1993) suggested the processes which respond to rapid climate change are associated predominantly with carbon release to the atmosphere: forest die-back, incomplete tree life cycles, soil carbon oxidation and climate-mediated increases in potential agricultural areas. Smith and Shugart (1993) were also of this opinion. Their findings implied such vegetation and soil changes could prove to be a significant source of CO_2 in the first 50 to 100 years following climatic warming, increasing atmospheric concentrations of the gas by up to a third of the present level.

The degree to which results would differ under a transient scenario (i.e., short duration) would depend on the rate of climate change relative to the rates of transfer associated with the vegetation and soil processes. Vloedbeld and Leemans' (1993) results indicated that as vegetation shifts due to climate change and increased water use efficiency, CO_2 fertilisation decreases net carbon emissions, whilst changed decomposition rates increase CO_2 emissions to the atmosphere considerably. This emphasised the importance of considering a combination of different processes quantitatively. Pastor and Post (1988) illustrated the sensitivity of forests to the indirect effects of climate (e.g., increased productivity where soil water was not limiting and nitrogen availability was enhanced). Hence, the heterogeneity of the landscape becomes an important factor for determining forest responses to climate change.

Watson *et al.* (1996) considered the most likely changes induced by climate change would be in terms of distribution and composition of global vegetation. In particular, they emphasised northern tree-lines were likely to advance slowly into regions occupied currently by tundra and that as the NPP of forests is not limited by water availability it is likely to increase in response to warming. Such speculation is inevitable until mature tree physiological responses to CO_2 enrichment and the effects of temperature on terrestrial sources and sinks of carbon can be determined.

Indeed, given the dynamic and interactive properties of this system, *in situ* classic experimentation (i.e. modifying just one variable at a time, (Rastetter 1996)) is inappropriate / unfeasible. However, computer simulation models of ecosystem behaviour are a valuable experimental alternative for investigating responses and feedbacks of processes operating at a range of spatial and temporal scales. The following section describes the need for ecosystem simulation modelling of forests.

2.2 Forest Ecosystem Simulation Modelling: The Need for Models

> '*Measurements alone are nothing more than data: Models convert these data into scientific understanding*' (Goel and Norman 1992, p.163).

Models may be used to better understand and explain why we observe what we observe, for example, 'instrumentally' as tools for estimation, prediction or synthesis (Curran 1987). In particular, ESMs, including soil-vegetation-atmosphere transfer (SVAT) models, allow investigation of responses and feedbacks of processes operating at a range of spatial and temporal scales, with the ultimate objectives of increasing (i) the accuracy of estimates and (ii) understanding of biosphere-atmosphere interaction (§5.1.2).

Estimates of gross carbon budgets for vegetation (the output of many ESMs) are extremely difficult to construct as field measurements of photosynthesis and foliage respiration are not obtained easily because of the difficulties controlling the environmental conditions in field allometry (Dawson and Wicks 1998). Even when direct measurements of carbon fluxes can be made they usually represent small samples in space and time (e.g., Running *et al.* 1999). Therefore, reliable models are needed to interpolate and extrapolate flux measurements spatially and temporally. Furthermore, the development of such models is needed to improve the simulation of ecosystem dynamics in the spatial domain and provide the means to describe and monitor the state of the biosphere.

2.2.1 Modelling approaches

Process-based models simplify the mechanisms underlying the responses to change (or stimuli) to investigate a system. For example, the objective of forest ESMs is to simulate the growth of forest stands in terms of the underlying physiological processes that determine growth (Waring and Running 1998). Hence, forest growth may be described in terms of radiation interception, climate, photosynthesis and carbon allocation, rather than empirical relations developed from statistical analysis of measurements made on individual trees. Process-based ESMs are much more flexible than empirical equations, particularly when investigating the consequences of change. However, they are not without problems, the most significant of which is that they often require many state and rate variables (that are often difficult to obtain) in order to characterise a system adequately (van Rompaey *et al.* 1999).

Indeed, when devising process-based models researchers have to resist the 'fatal attractions' of (i) over-simplification, which may ignore crucial processes or (ii) over-sophistication, resulting in cumbersome, expensive and data dependent models (Schellnhuber 1999).

The pioneer NPP model, MIAMI (Lieth 1975) used empirical regression to relate annual NPP to annual average temperature and precipitation (without accounting for radiation). However, because of its simplicity and empirical basis, this model is still used as a baseline for the evaluation and development of more sophisticated mechanistic models (Hibbard and Sahagian 1997). Over the past 15 years, a number of models have been developed to estimate forest productivity on the basis of physiological processes. As a consequence, in 1995 the International Geosphere-Biosphere Programme (IGBP) established the Global Analysis, Interpretation and Modelling (GAIM) Task Force (http://gaim.unh.edu) to compare and assess a range of existing ESMs in order to clarify the rôle of terrestrial systems on the carbon cycle (Sahagian 1997).

Figure 2.3 displays just a few of these models, illustrating the diverse array of system complexities and time scales they encompass. Researchers make decisions concerning the level of model complexity for every investigation independently, choosing the least complex model that provides the required precision. For example, the Moderate Resolution Imaging Spectroradiometer (MODIS) sensor's NPP estimate is represented by ε, a model of minimum process complexity. MODIS is the key instrument aboard the Terra satellite (http://modarch.gsfc.nasa.gov/MODIS/) (§2.3). However, models of higher 'process detail' are required to assess the accuracy and interpret the ε models but cannot be run globally because of a lack of data and computing limitations (Running *et al.* 1999).

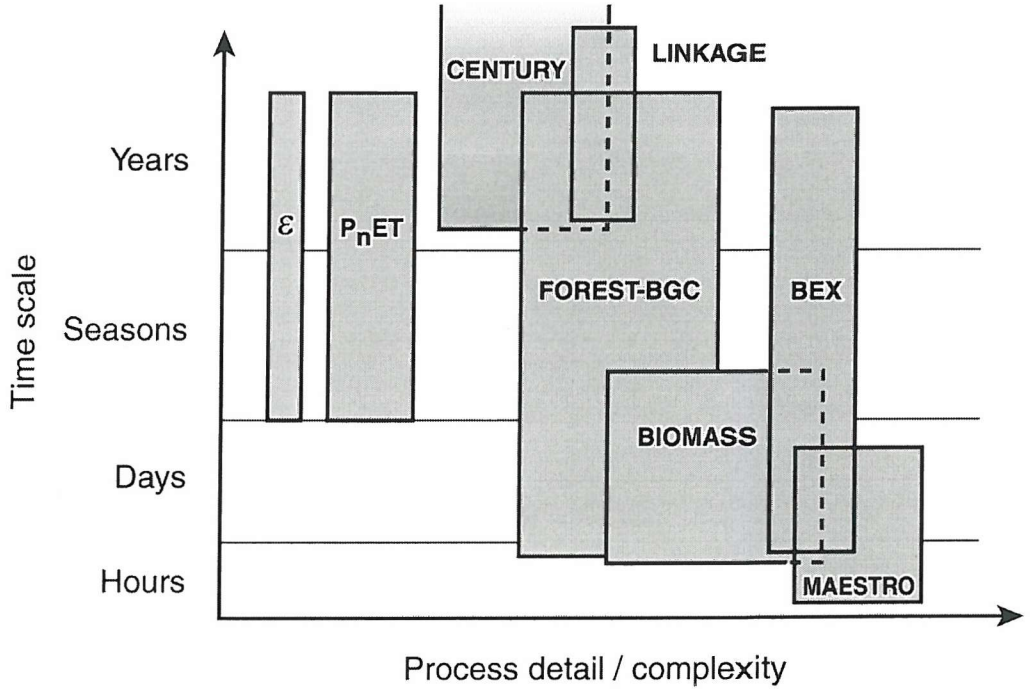

Figure 2.3 A diagrammatic evaluation of the varying time scales and mechanistic complexity inherent in various current SVAT models (adapted from Landsberg and Gower 1997).

Whilst models may vary in their conceptual approach (e.g., use scale-dependent processes, empirical relationships or are entirely process-based) and scale of operation, all are simplified versions of reality (Stoddart 1986) and are typically *aspatial* (Running and Hunt 1993; Curran 1994a). The aspatial nature, combined with data dependency, made it extremely difficult to 'scale up' data or processes in order to understand the functioning of forest ecosystems, in particular, their interaction with hydrospheric and atmospheric processes (Hobbs and Mooney 1990; van Gardingen *et al.* 1997; Lucas *et al.* 2000). This led to the development of a number of scale-independent deterministic models that require spatial estimates of key driving variables (Curran 1994a).

However, using *in situ* sampling techniques in order to provide the necessary model driving variables over large areas, would be impractical logistically. At these spatial scales, it is necessary to develop explicit linkages between the ecosystem processes and the structure of the landscape in space and time (Wessman 1994). Therefore, a number of researchers proposed that variables estimated from remotely sensed data may be used to drive ESMs. Hence extrapolating aspatial models to regional and global scales by means of spatially referenced remotely sensed data (Burke *et al.* 1990; Aber *et al.* 1993; Curran 1994a).

2.2.2 Driving ESMs with variables estimated from remotely sensed data

> "*Driving ecosystem simulation models with remotely sensed data is an intellectually challenging task which has the potential to be the most rewarding use of such data in terms of our understanding of the Earth's land surface*" (Briggs 1991, p. 3).

ESMs that are capable of exploiting the spatial, temporal and spectral capabilities of remotely sensed data to provide driving variables for implementation over a range of spatial scales were classified into two broad groups by Bonnan (1995):

1. Models designed by and for the ecological community. These may be further sub-divided into two groups according to the temporal scale on which they operate:
   - Short term (seasonal to annual) ESMs provide estimates of gas exchange processes (e.g., photosynthesis, respiration and evapotranspiration), allocation, decomposition and soil processes (e.g., mineralisation) all of which cannot be measured directly with optical sensors (Roughgarden *et al.* 1991).
   - Long term (100 to 1,000 years) gap models of forest dynamics predict responses to environmental change in both biogeochemical processes and individual species distribution and dominance patterns.

2. Land Surface Process (LSP) models, designed by atmospheric science researchers, which model biophysics at short time scales over large areas.

Table 2.2 lists a few models, prominent in the literature, that have the capability of being driven with variables estimated from remotely sensed data, according to Bonnan's (1995) classification. Despite the potential for coupling these synergistic technologies, there are relatively few examples where remotely sensed data have been used with models to simulate ecological processes at a range of spatial and temporal scales (Lucas and Curran 1999). Indeed, to date, most of these models have only been used as research tools (Coops 1999), although their ultimate aim was to provide prognostic capabilities (Hibbard and Sahagian 1997).

It is now acknowledged widely that remotely sensed data provide the only accurate means of estimating the variables needed to drive such models at regional to global scales (Aber *et al.* 1992; Lucas and Curran 1999). In particular, Wessman *et al.* (1990) suggested variables that quantify the light interception properties (that scale from leaf to globe), have the greatest potential for ecosystem model inputs.

Joint development of ecosystem models and remote sensing should, therefore, enhance the capabilities of estimating productivity over large areas (Schimel *et al.* 1990). Wessman *et al.* (1990) concluded that sophisticated ecosystem models driven by remote observation would permit monitoring of ecosystem dynamics at local to global scales. Therefore, to evaluate changes in ecological processes accurately at the required spatial and temporal scales, remote sensing technology and ecosystem theory must be considered jointly.

Most recently an array of national and international programmes have inaugurated regular, global satellite observations, critical field measurements of carbon (and water) fluxes and global model development for the purpose of beginning to monitor the biosphere (Running *et al.* 1999) (http://www-eosdis.ornl.gov/eos_land_val/valid.html) (§2.3).

Classification	Model name	Remotely sensed inputs	Model outputs	Key references
Ecosystem models				
Short term	Labile Carbon Model	APAR, LAI and meteorological observations	Simulates labile carbon dynamics, stem growth and root respiration (for Florida slash pine)	Cropper and Gholz 1991
	Modular Global Change Modelling System	Land-use data and biomass production	Calculates regional response of forest ecosystems to climate change	Aber *et al.* 1993
	FOREST-BGC	LAI and meteorological observations	Estimates transpiration, respiration, photosynthesis, canopy interception, carbon allocation and litterfall	Running and Coughlan 1988; Running and Gower 1991
	Physiological Principles Predicting Growth using Satellite data (3-PGS)	Meteorological data and APAR	Calculates regional response of forest ecosystems to climate change	Coops 1999
Long term	HYBRID	LAI and meteorological observations	Predicts response to environmental change in biogeochemical processes, individual species distribution and dominance patterns	Friend *et al.* 1997
	TREE-BGC	APAR and tree height	Allocates stand estimates of photosynthesis to individual trees	Korol *et al.* 1995
Atmospheric models				
	Simple Biosphere (SiB) Model	LAI, canopy reflectance and canopy surface roughness	Evaluates terrestrial vegetation effects on global climate	Sellers 1987; Sellers *et al.* 1996a
	Biosphere-Atmosphere Transfer Scheme (BATS)	LAI, canopy albedo, soil albedo and vegetation classification	Evaluates terrestrial vegetation effects on global climate	Dickenson 1984; Wilson *et al.* 1987; Chase *et al.* 1996

LAI is leaf area index and APAR is absorbed photosynthetically active radiation

Table 2.2 Models that may be driven by inputs derived from remotely sensed data.

2.3 The Remote Sensing of Forests

The science of remote sensing consists of the interpretation of measurements of electromagnetic energy reflected from or emitted by a target from a vantage-point that is distant from the target (Rencz 1999). *Earth Observation* by remote sensing (EO) is the interpretation and understanding of such measurements from the Earth's surface or atmosphere (Mather 1999). Hence within Geography (and other physical sciences), remote sensing may be used as a tool for the location, classification and estimation of features on the Earth's surface or within the atmosphere (Curran 1987; Mather 1999).

Several works have stressed the enormous potential of remote sensing for studying vegetation structural characteristics and functioning processes (e.g., Peterson *et al.* 1987; Gholz *et al.* 1996). This section outlines briefly applications of remote sensing within forestry, before detailing how and why remotely sensed data can "enhance the pursuit and application of knowledge" (Curran 1987, p. 1255), with particular reference to estimating the biophysical variables needed to drive ESMs (§2.2.2).

> *"We have three principal means: Observation of nature, reflection and experiment. Observation gathers the facts, reflection combines them and experiment verifies the result of the combination. It is essential that the observations of nature are assiduous, that reflection is profound and that experimentation is exact. Rarely does one see these abilities in combination. And so, creative geniuses are not common!"*
>
> Denis Diderot (1713-1784)
> Pensées sur l'Interpretation de la Nature, 1753, XV

The rôle of remote sensing in the study of forests became established over many years through the use of aerial photo-interpretation for vegetation inventory (e.g., Murtha 1977, 1983; Edwards and Lowell 1996). More recent techniques, developed for remotely sensing forests, can be applied over a range of spatial scales (Foody and Curran 1994a; Stein *et al.* 1999; Barrett and Curtis 1999). Laboratory spectrometers mounted on ground platforms provide data for the analysis of forest attributes at scales of leaf to tree (e.g., Milton 1980), whilst sensors mounted on airborne and space-borne platforms provide a synoptic view at regional scales.

Ecological and remote sensing priorities are converging as both research communities respond to the challenge of understanding global change. Remote sensing techniques have matured as data gathering capabilities have increased exponentially (Rencz 1999). Interests in applications have shifted to the examination of important natural ecosystems, pattern and process at regional scales (Wickland 1991; Running *et al.* 1999).

Two of the most exciting prospects for global monitoring in the future are the NASA's Mission To Planet Earth (MTPE) and the associated Terra (formerly EOS AM-1) satellite (http://terra.nasa.gov) (Senftle 1997) and the European Space Agency's (ESA) Envisat Mission (http://envisat.estec.esa.nl/). Terra was launched successfully on 18th December 1999, carrying (amongst many other sensors) the Moderate Resolution Imaging Spectroradiometer (MODIS) (Gershon and Miller 1993) (which completed its first "data dump" on 1st February 2000) (http://modarch.gsfc.nasa.gov/MODIS/). Whilst, it is anticipated June 2001 will see the launch of Envisat-1, an advanced polar-orbiting EO satellite carrying amongst others the Medium Resolution Imaging Spectrometer (MERIS) providing measurements of the atmosphere, ocean, land, and ice over a five year period (http://envisat.estec.esa.nl/instruments/MERIS/). Such research projects will play a vital rôle in ensuring the place of remote sensing in the scientific community well into the twenty first century.

2.3.1 Remote sensing: Basic principles

Reflectance from the Earth's surface (ρ), ignoring polarisation effects, may be expressed as a function of five variables: the illumination geometry of the irradiation; the viewing geometry of the reflected radiation; the wavelength of the reflected radiation; the time of the observation and the geographical location of the target (Verstrate and Pinty 1992):

$$\rho = f(\theta_i, \phi_i; \theta_r, \phi_r; \lambda; t; x) \tag{2.1}$$

Where, θ_i and ϕ_i are the zenith and azimuth angles of the irradiation (illumination geometry), θ_r and ϕ_r are the zenith and azimuth angles of the reflected radiation (viewing geometry), λ is the wavelength of the reflected radiation, t is the time of observation and x is the spatial location of the target. By examining these variables as a means of describing the remotely sensed signal from vegetation, the following brief sub-sections provide useful background as to how remotely sensed data may be used to estimate biophysical variables.

2.3.1.1 Illumination and viewing geometry (θ_i, ϕ_i; θ_r, ϕ_r)

The illumination azimuth (ϕ_i) and view azimuth (ϕ_r) angles are defined in relation to a particular reference direction. In comparison, illumination zenith (θ_i) and view zenith (θ_r) angles are referenced with respect to a plane normal to the target surface. The phase angle (θ_L) is the complete angle between the illumination zenith and view zenith angles. The principal plane is defined as the azimuth direction containing the source, sensor and target ($\phi = 0^o$ and 180^o) (in Figure 2.4).

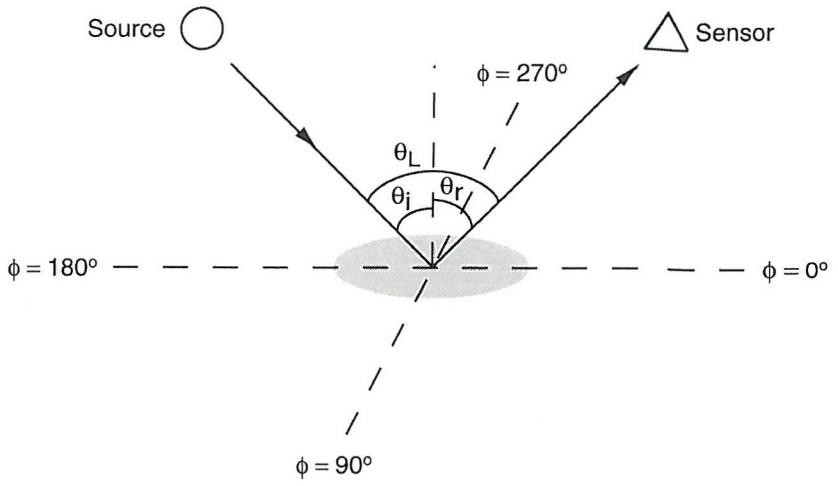

Figure 2.4 The main geometric terms in a remote sensing system (adapted from Cutler 1998).

Incoming solar flux

This can be divided into the direct flux and the diffuse flux, which has been scattered in the downward direction by atmospheric aerosols, hence dependent upon atmospheric conditions. The direction of the direct flux is characterised by the solar zenith angle (θ_s) and the azimuth angle (ϕ_s) whereas the diffuse flux is characterised by its angular distribution.

2.3.1.2 Wavelength (λ)

The most common systems used in the remote sensing of forests operate in one or several of the visible (0.4–0.7 μm), near infrared (NIR) (0.7–1.4 μm) and middle infrared (MIR) (3.0– 5.0 μm) portions of the electromagnetic spectrum. Each range of wavelength has its own strengths in terms of the information it can contribute (Table 2.3). Consequently, systems have been developed that are optimised for and operate within particular spectral ranges (Figure 2.5). Hoffer (1978) gave an excellent review and discussion of the spectral reflectance characteristics of vegetation, soils, water, snow and clouds.

Spectral region	Wavelength (μm)	Primary uses
Visible	0.4–0.7	soil and vegetation differentiation, chlorophyll absorption.
Near infrared	0.7–1.4	biomass surveys, water body delineation, vegetation moisture measurement, snow / cloud differentiation.
Middle infrared	3.0–5.0	vegetation moisture measurement, hydro-thermal mapping.

Table 2.3 The primary uses of the spectral regions of the electromagnetic spectrum (from Lillesand and Kiefer 1999).

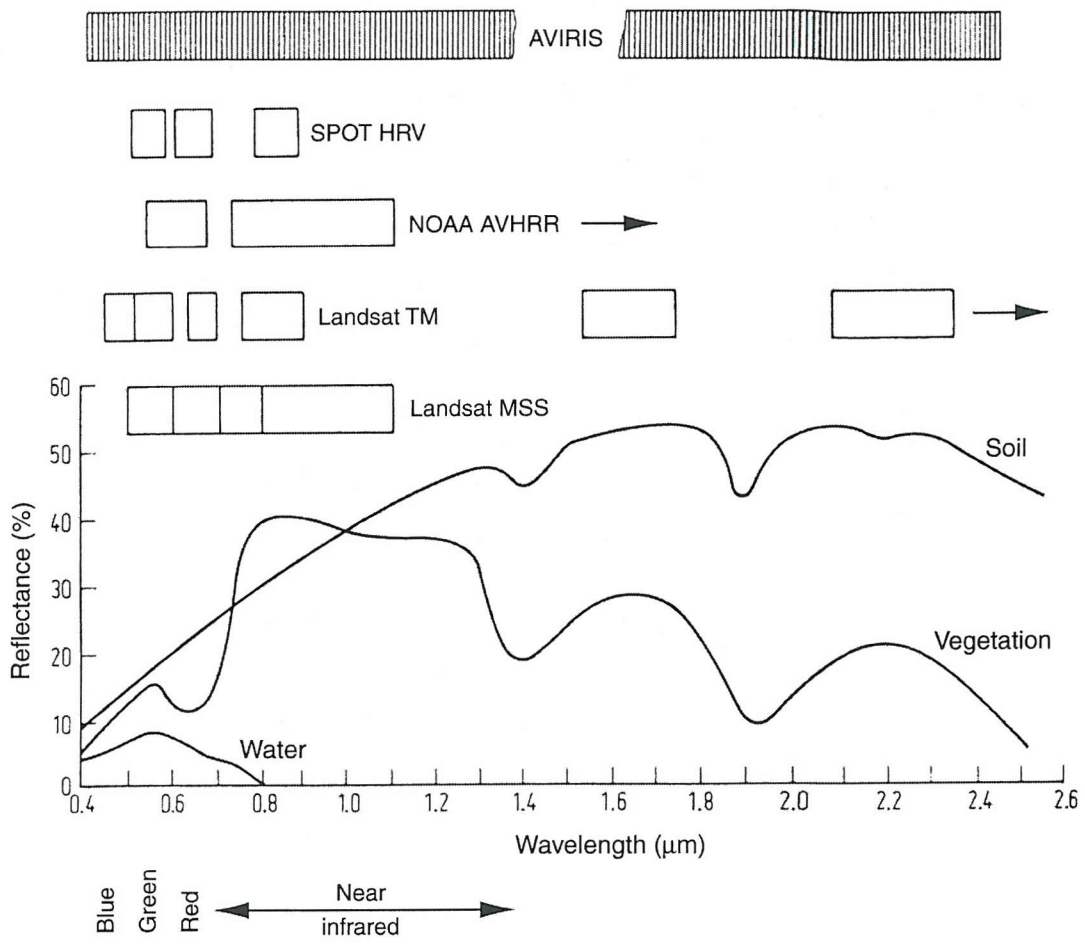

Figure 2.5 Spectral reflectance characteristics of common Earth surface materials in the visible and near-infrared wavelengths. The positions of spectral bands for a few common remote sensing instruments are indicated (adapted from Richards, 1993).

Horler and Ahern (1986) identified that the shortwave infrared (SWIR) spectral region, (represented by TM bands 5 and 7) was particularly sensitive to forest vegetation density. In particular, shadowing and leaf moisture content were identified as having the greatest influence on the spectral reflectance of forests in this region. In part, this prompted the Canadian Centre for Remote Sensing (CCRS) to recommend that users adopt the 'forestry composite' (TM 453 = RGB) for cover-type discrimination.

The use of middle infrared radiation

The potential of using remotely sensed data acquired in MIR wavelengths in particular, (sensitive to canopy water content, surface temperature and canopy structure and roughness) for the estimation of biophysical variables, has yet to be fully realised (Boyd *et al.* 2000).

The level of understanding and documentation regarding the processes operating within the MIR region is small relative to that of the visible and NIR regions (Cracknell 1997; Boyd and

Curran 1998). There are several reasons for this lack of attention. First, the MIR region is hybrid, being sensitive to a combination of both reflected and emitted radiances (Agbu 1993). Second, the longer wavelengths of the MIR are lower in energy than those of the visible and NIR, therefore, are harder to sense remotely and have a lower signal-to-noise-ratio (SNR) (Curran 1985; Landgrebe and Malaret 1986; Smith and Curran 1999). Nonetheless, current literature suggests that MIR radiation may be a useful data source for estimating vegetation biophysical properties (e.g., Boyd *et al.* 1996; Boyd *et al.* 1999). Hence, there is the possibility that MIR radiation data offers the potential for increasing the accuracy with which biophysical variables may be estimated prior to their inclusion within an ecosystem simulation model.

2.3.1.3 Temporal and spatial resolution (t, x)

Temporal and spatial effects influence any remote sensing operation. Temporal effects are any factors that change the spectral characteristics of a feature over time. For example, the spectral characteristics of many species of vegetation are in a dynamic state of change throughout a growing season (Curran *et al.* 1992; Chen 1996a). These changes may influence when remotely sensed data are acquired for a particular application. Indeed, temporal data may be the key to gleaning information sought in an analysis, a most obvious example being change detection (e.g., Brown *et al.* 2000).

Places that are near to each other are more alike than those that are further apart and the degree of dissimilarity depends on both the environment and the nature of our observations (Curran and Atkinson 1998). Therefore questions such as 'what size of sample may be deemed representative?' and 'what size of support should be used?' are also fundamental.

Such issues of temporal effects and spatial variability of natural landscapes must be addressed when undertaking any form of remote sensing analysis.

Some thoughts on spatial resolution

> '*Surprisingly, Earth scientists have as yet largely failed to provide comprehensive quantitative data in a form which is comparable with deriving objective estimates of resolution requirements*' (Townshend 1981, p. 50).

Spatial variability of remotely sensed imagery refers to the size and nature of and relationships between pixels. The most significant spatial element of remotely sensed imagery is the pixel size, which is related closely, although not synonymously, with the more general term of spatial resolution. In fact, no single quantitative definition of spatial resolution exists (Aplin 1999), although in general terms, spatial resolution refers to the spatial detail of remotely sensed imagery. Finer spatial resolution imagery provides increased spatial detail, enabling the

delineation of smaller features than coarser spatial resolution imagery. Sensors now exist with many different spatial resolutions, from over one kilometre (NOAA AVHRR) to 0.8 m panchromatic (Ikonos-2) with finer in prospect (Aplin *et al.* 1999).

Strahler *et al.* (1986) introduced the concept of the L- and H- models of spatial resolution, discussed further by Jupp *et al.* (1988; 1989). In the L- resolution case, Earth surface spatial variability is at a higher frequency than image sampling so features of interest that are smaller than the spatial resolution of the imagery cannot be resolved spatially. Consequently, the 'mixed pixel problem' is manifest when pixels comprise a variety of land cover types (Foody 1997; Petrou and Foschi 1999). In the H- resolution case, spatial variability is at a lower frequency than image sampling so features can be resolved.

Since fine spatial resolution imagery tends to provide more spatial detail and proportionally fewer mixed pixels, than coarser spatial resolution imagery, it would seem beneficial to use the former where possible. However, this is not always the case. For example, where the feature of interest is a forest stand but the spatial resolution of the imagery is sufficiently fine to distinguish between individual trees and patches of grass separating tress, certain pixels may be misidentified (Townshend and Justice 1988). As such, when considering spatial resolution, features on the Earth's surface, as identified by imagery with a specific spatial resolution are generally scale-dependent (Henderson-Sellers *et al.* 1985; Foody and Curran 1994a).

Hence, the unstated implication of traditional classifications (e.g., of land cover type), is that land cover occupies multiples of rectangular spatial units, and that such small areas are homogeneous up to the coarsest pixel. However, characteristics of the natural landscape do not necessarily assume such elemental spatial occupation of the finest pixel. Indeed, the pixel is merely imposed as a division of the space, which is imaged and is unlikely to match the contents of that space (Fisher 1997).

The productive synergy between geostatistics (a set of statistical techniques) and remote sensing resulted in a series of papers in the late 1980s (see Curran and Atkinson 1998 for a review) that discussed images in terms of the spatial autocorrelation between pixels. For example, homogenous areas were seen as having high spatial autocorrelation (neighbouring pixels were similar) such that coarse spatial resolution would be appropriate (Curran and Atkinson 1999). This conclusion was formalised by Woodcock and Strahler (1987) who showed how between-pixel variance varied according to the spatial variability of the scene and the spatial resolution of the sensor and Curran (1988) who used geostatistics to provide a methodological link between pixel size requirements for different land covers. The basis for

this link was a plot of variability against ground distance, otherwise known as the variogram (Atkinson 1993).

As such, the application of geostatistics in remote sensing, particularly research that focuses on (i) the 'support' for measured reflectance (e.g., Woodcock and Strahler 1987; Atkinson and Curran 1995; Curran and Atkinson 1999) and (ii) the extraction of sub-pixel information, offer potential solutions to the 'mixed pixel problem', however, "this research is in its infancy" (Fisher 1997, p. 684).

2.3.2 Estimating biophysical properties of vegetation using remote sensing

The ability to estimate any biophysical property using remotely sensed data requires, at the first instance, the biophysical property to affect the radiance reflected and/or emitted from the target and a relationship derived. Second, the spectral (§2.3.1.2), spatial, temporal (§2.3.1.3) and radiometric resolutions (§2.3.1.1) of the remotely sensed data influence the ability to extract meaningful information about the biophysical property in question. Generally there are two classes of biophysical properties of vegetation that can be remotely sensed (Jensen 1983):

1. Direct relations, e.g., vegetation chlorophyll content (Tucker 1977a), vegetation biomass (Curran 1980), vegetation moisture content (Tucker and Garrett 1977) and vegetation temperature (Price 1983).
2. Indirect relations (i.e., by analysing more than one variable that is estimated directly), e.g., by modelling the vegetation absorption characteristics and moisture content, vegetation stress may be detected (Jackson *et al.* 1983).

Understanding the nature of the relationships between biophysical properties of vegetation and remotely sensed data continues to be an area of much research (e.g., Boyd *et al.* 2000). One approach to achieving this has been to simulate canopy radiative transfer processes through modelling techniques (North 1996). Such models (e.g., Li and Strahler 1986; Sellers *et al.* 1992) provide valuable insights into the fundamental factors driving the relationships between remotely sensed data and vegetation biophysical properties (Chen and Cihlar 1996). However, the use of these models with remotely sensed data are not yet fully operational (Privette *et al.* 1996; Dawson *et al.* 2000) Factors such as the heterogeneity of vegetation canopies, dynamic characteristics of canopy optical properties and external effects such as atmospheric path radiance and absorption have hindered the development of such models (Boyd 1996). Alternatively, empirical techniques, whereby remotely sensed data and various derivatives (e.g., vegetation indices) are related to known vegetation biophysical properties. The following sections of this chapter provide a broad overview of such empirical research in relation to the estimation of boreal forest biophysical properties.

2.3.2.1 Boreal forest LAI

Of the many types of biophysical property that influence the radiation from a forest canopy, LAI is perhaps the most important (Danson 1995a) as it is a primary determinant of the productive capacity of forests (Gholz *et al.* 1996; Nemani *et al.* 1993a). LAI is defined as the one-sided leaf area per unit ground surface area (Chen 1996a) (§3.2.1.1). It is an important variable in modelling estimates of photosynthetic and evapotranspiration rates so accurate estimation by remote sensing would enable calculation of such processes over large areas at relevant time intervals (Spanner *et al.* 1990; Running and Coughlan 1988; Running 1984) (§2.3).

Initially LAI estimation was based on inversion of the Beer-Lambert Law (Marshall and Waring 1986; Lang 1987) as the proportion of light transmitted through a canopy to the proportion of direct solar beam that has been passed only through the gaps in the canopy can be related to LAI (Pierce and Running 1988; Curran 1991; Sellers *et al.* 1992; Nel and Wessman 1995; Gower *et al.* 1999).

Subsequent investigations suggested that a relationship exists between the LAI of forest canopies and remotely sensed data acquired in visible and NIR wavelengths, particularly when combined in vegetation indices (Spanner *et al.* 1984; Running *et al.* 1986). Increases in LAI result in more absorption by visible radiation due to increases in pigmentation (e.g., chlorophyll content) in the leaves and more reflectance in NIR radiation due to increases in internal leaf scattering (Curran 1985). Further studies re-enforced these relationships (e.g., Peterson *et al.* 1987; Gong *et al.* 1995; Myneni *et al.* 1997) and recognised that research focussing on forests with (i) open stands with different understorey conditions; (ii) a mixed canopy of conifer and broadleaf trees; (iii) very uneven structural properties and (iv) stands across a variety of successional stages, would be necessary to refine relationships (North 1996; Boyd 1996).

More recent research (e.g., Running *et al.* 1999; Gower *et al.* 1999) discussed a number of other variables that influence the relationship between remotely-sensed visible and NIR radiation and LAI of a forest canopy. These include external variables such as the atmosphere and the geometrical arrangement of Sun and sensor in relation to the forest target (Ranson *et al.* 1986; Guyot *et al.* 1989) and internal variables such as canopy geometry and terrain characteristics (Walsh 1987). Canopy closure also has an effect, since this determines the amount of spatially variable understorey vegetation and soil background exposed to the sensor (Spanner *et al.* 1990; Nemani *et al.* 1993a; Goward *et al.* 1994). Phenology also needs consideration as the LAI of many canopies varies seasonally (Badhwar *et al.* 1986; Curran *et*

al. 1992). The exact influence of these variables and ways of overcoming (or utilising) their effects continues to be a topic of investigation (e.g., Chen *et al.* 1999; Gower *et al.* 1999).

Following investigation of current forest ESMs (§2.2) and the ability to estimate LAI spatially from remotely sensed data (§2.3), the natural progression would be to drive an ESM that incorporates spatial estimates of LAI. The following sections describe the FOREST-BGC model, developed by Running and Coughlan (1988), a process-based ESM designed specifically to calculate the cycling of carbon, water and nitrogen through forest ecosystems.

2.4 FOREST-BGC: Model Logic and Development

FOREST-BGC uses LAI as the principal independent driving variable to calculate canopy interception, transpiration, respiration, photosynthesis, carbon allocation and litterfall (Running and Coughlan 1988).

The model requires the input of 41 '*parameters*' or state variables (prefix B) to define the initial conditions and 20 driving variables (prefix X) (§4.3.1, Table 4.2) (Running and Gower 1991). These include daily input data of standard meteorological conditions combined with key site and vegetation variables (e.g., soil water capacity, LAI and leaf nitrogen concentration (LNC)). The model uses default values derived and tested in other applications for all critical variables if no data exist (Running 1994). Canopy interception and evaporation, transpiration, soil outflow of water; photosynthesis, growth and maintenance respiration, allocation (above and below-ground), litterfall and decomposition of carbon; and deposition, uptake, litterfall and mineralisation of nitrogen are the model outputs, all of which cannot be observed directly with remote sensors (Roughgarden *et al.* 1991). FOREST-BGC has a split time resolution, to facilitate the modelling of processes at time scales optimum for the process dynamics (Running and Coughlan 1988): with hydrologic, photosynthetic and maintenance respiration processes computed daily and the remaining carbon and all nitrogen processes computed annually (Figure 2.6).

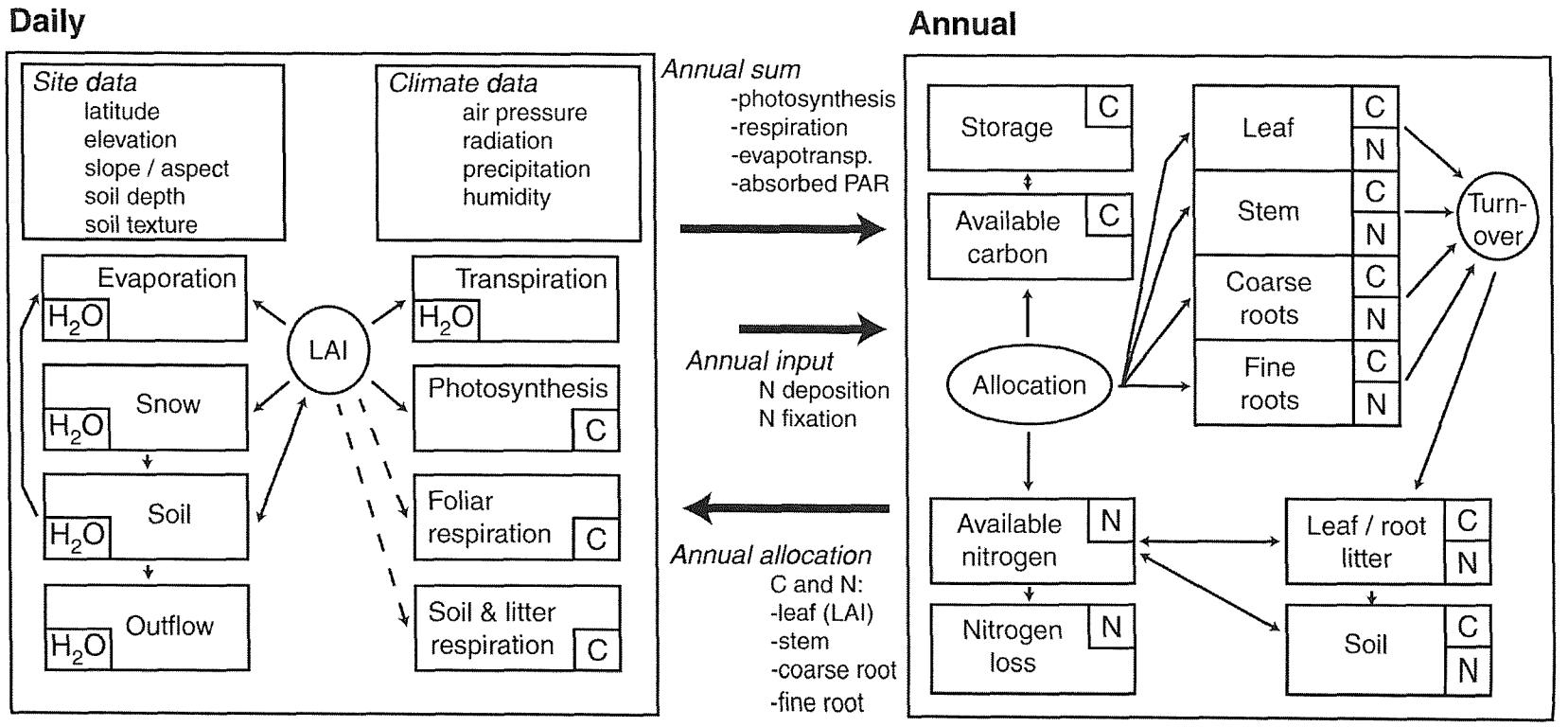

Figure 2.6 A system diagram of FOREST-BGC (adapted from Running and Coughlan 1988; Running and Gower 1991).

The model has been used for a variety of different applications, however, whilst these studies have all found FOREST-BGC simulations capable of estimating field measurements of small forest stands, accuracy assessment at regional scales is essential. Indeed, many ecosystem process models have been built from and used to simulate the dynamics of a study plot, often 10m x 10m or smaller. However, FOREST-BGC is different in that a conscious compromise between mechanistic detail and simplifying generality, by for example, including minimal species-specific data, was adopted to allow implementation for regional scale research. A common thread evident through the development of the model was that 'scaling decisions were a continuous, progressive optimisation' as each new version of the model answered a specific question (Nemani *et al.* 1992, p.298). To ensure successful future global scale extrapolation the new generation of models must interface with remote sensing drivers (Running *et al.* 1999). FOREST-BGC emphasises LAI as the principal, independent structural attribute to quantify the forest structure important for energy and mass exchanges: A key simplification for regional scale applications. The aim is to derive as much of the ecosystem structure as possible from LAI, in order to allow the use of remote sensing for regional extrapolation. This logic is very similar to that used by Ryan (1991) to estimate gross carbon budgets for forests. Hydrologic variables are calculated as one-dimensional depths in metres as is common in hydrology (e.g., Schmugge and Jackson 1996). Stand and site conditions are based on 1 ha ground area, with carbon and nitrogen variables in kg ha^{-1}.

Daily sub-model

The daily sub-model calculates a site hydrologic balance and a photosynthesis-respiration balance for each day. Depending on air temperature, daily precipitation is routed to snowpack or soil: a distribution that influences the timing of future hydrologic activity significantly. Canopy interception fraction is subtracted and evaporated as a function of LAI. The remaining water is available for transpiration from the soil compartment. Transpiration is calculated with a Penman-Monteith equation, using vapour pressure deficits and incident radiation as driving variables (Monteith 1965). Should ambient air temperature, a major factor determining the active physiological season, fall below 0 °C canopy conductance is reduced to cuticular levels. Night canopy respiration, calculated from night average air temperature and LAI, is subtracted from daylight photosynthesis to give daily net carbon fixation. Maintenance respiration of the stem and root mass is calculated as a function of compartment size and mean air and soil temperature. Hence, a complex string of equations produces the daily output data. Running and Coughlan (1988) gave a complete description of the daily half of the model. Carbon fixation and respiratory losses are accumulated daily and respiration subtracted from fixation to give a final measure of carbon available for growth, which is forwarded to the annual sub-model.

Annual sub-model

Running and Gower (1991) replaced the 'static' carbon budget of the annual half of the old model with dynamic and interacting carbon and nitrogen budgets. This version of the model begins the 'optimisation' process by calculating the LAI that could be produced if net carbon, water or nitrogen alone were limiting. The transferred available carbon is partitioned annually to the leaf, stem and roots. Temperature independent growth respiration is subtracted as a fixed fraction of the carbon allocated to each compartment, with the inherent assumption that whilst instantaneous growth rate is temperature dependant, the annual "construction costs" of biomass are not (Lucas 1995). Litterfall, implying carbon turnover, is defined by coefficients, whereas decomposition is derived from the annual weight-loss of fresh litter using an equation based on annual evapotranspiration and initial lignin concentration.

2.4.1 Previous use and accuracy assessment of FOREST-BGC

Running and Coughlan (1988) used the model to simulate the annual hydrologic balance and NPP for a hypothetical forest stand in seven contrasting environments across North America for 1984. Hydrological partitioning ranged from 14, 86 and 0% for evaporation, transpiration and outflow, respectively, at Fairbanks, Alaska (annual precipitation of 313 mm) to 10, 27 and 66% in Jacksonville, Florida (annual precipitation of 1244 mm). These balances changed as LAI was increased from 3 to 9 during successive simulations. NPP ranged from 0 t C ha^{-1} $year^{-1}$ at Tuscon, Arizona, to 14.1 t C ha^{-1} $year^{-1}$ at Knoxville, Tennessee, corresponding well with observed values at each site ($r^2 = 0.87$). Running and Coughlan (1988) emphasised the possibility of "parameterising" FOREST-BGC at regional scales in the future with forest LAI estimates derived from satellite sensor imagery.

Running and Nemani (1988) found that FOREST-BGC was sensitive to extreme differences in climate as single-year simulations of NPP were similar to remotely sensed data over a wide range of climates, from Florida to Alaska. Nemani and Running's (1989) study only used the daily sub-model, as their primary interest was in transpiration. They found agreement between measured and simulated seasonal soil moisture extraction values for lodgepole pine (*Pinus contorta*) stands was strong ($r^2 = 0.90$ for un-thinned and $r^2 = 0.93$ for thinned stands). Predicted seasonal trends in water stress, measured as pre-dawn leaf water potentials, were also very accurate. Indeed the model has a decisive advantage over conventional methods of water budget computation as it allows for physiological controls over water loss and better hydrologic partitioning.

With regard to estimating gross carbon budgets, Ryan (1991) compared readily-available data from ecosystem studies together with empirical relationships against estimates from the FOREST-BGC model for young and old stands of lodgepole pine and Pacific silver fir (*Abies amabilis*) chrono-sequences. For the lodgepole pine site, estimated annual carbon flux was 95% of the FOREST-BGC estimate in the young stand and 69% of the FOREST-BGC estimate in the older stand. The low estimate of carbon flux compared with the model estimate, particularly in the older stand, suggests that by using canopy demographics to estimate canopy production and litterfall, true values may be underestimated. It could also be hypothesised that FOREST-BGC overestimates stomatal conductance and photosynthesis for larger mature trees because the model variables were developed initially on 2-8 m tall saplings. For the silver fir stands, FOREST-BGC estimates were roughly equivalent to the estimated total annual carbon flux for both stands (Ryan 1991). Coupling simple estimates of net canopy carbon fixation illustrated the utility of the model as a tool for identifying problem areas in annual carbon budgets. Hunt *et al.* (1991) found FOREST-BGC sensitive to the effects of annual climate variation on annual stem growth. Nemani *et al.* (1993a) reinforced these observations, more specifically concluding that FOREST-BGC could better integrate the effects of climate on stem carbon gain than multiple linear regression models.

Field measurements from the Oregon Transect Research project (OTTER) were used by Running (1994) to assess the accuracy of selected process simulations in FOREST-BGC. Strong correlation between estimates and measured data were found for aboveground net primary production ($r^2 = 0.82$); 100 year stem biomass ($r^2 = 0.79$) and average LNC ($r^2 = 0.88$).

More recently, Lucas *et al.* (1995) reported an investigation to examine whether FOREST-BGC could estimate stem carbon production (SCP) for a forest in mid-Wales. Data acquired using a Compact Airborne Spectrographic Imager (CASI) sensor were used to calculate the point of maximum slope in the vegetation spectra, the red edge position (REP). A strong linear correlation was found between LAI and the REP ($r^2 = 0.88$). Subsequently, REP was used to obtain spatial estimates of LAI (Green *et al.* 1997).

However, it is extremely difficult and costly to obtain rigorous initialisation and complete independent accuracy assessment data for complex ecosystem models. At regional scales there are far fewer field-measurable state variables to choose from because of the increasing tendency to represent physiology in a general way (§2.2.1). Watershed stream runoff and vegetation index dynamics (Nemani *et al.* 1993a) may be the only choices for accuracy assessment at these greater scales. Ecosystem gas exchange processes, relying on expensive, erratic curette measurements, are unsuitable for accuracy assessment. Yoder (1992) attempted

to measure the photosynthetic capacity (A_{max}), a key system flux capacity and was unsuccessful in obtaining dependable data for even just one site. Regional studies should concentrate on critical integrating system variables that can be measured reasonably accurately and repetitively; Running (1994) suggested NPP, LAI and canopy litterfall. Progressive extrapolation of process-based ESMs requires a changing array of model drivers and accuracy assessment procedures. Confidence developed for model logic at one scale is not lost as the model is implemented at a broader scale provided the logic and model structure remains intact and only key variables are defined in a new way.

Although not exhaustive, Tables 2.4 a and b summarise the use of FOREST-BGC reported in the literature. The investigations are listed in chronological order. Species, input data and model outputs are detailed, with particular attention given to accuracy assessment. Two trends in these investigations are of note. First, although the potential to drive FOREST-BGC with variables estimated using remotely sensed data was highlighted by Running and Coughlan (1988), such investigations were not prominent in the literature until the mid 1990s. Second, accuracy assessment of model estimates with independent observed data has only been emphasised comparatively recently (Lucas and Curran 1999; Running *et al.* 1999).

Year	Researchers	Location (Ecosystem/ species)	Driven with remote sensing	Output variables	Accuracy assessment with independent ground data / Conclusions
1988	Running and Coughlan	North America (7 contrasting environments)	x	ET, outflow, NPP	$r^2 = 0.87$ with NPP data.
	Running and Nemani	Jacksonville and Missoula (simulated forest)	x	ET, PSN, NPP	Comparison between 2 sites of contrasting climate, no accuracy assessment.
1989	Nemani and Running	(Lodgepole pine) daily sub-model only	x	ET LWP	$r^2 = 0.90$ and 0.93 for ET (un-thinned and thinned stands respectively).
1991	Running and Gower	Madison and Missoula (simulated forest)	x	SCP, GPP	Comparison between 2 sites of contrasting climate, no accuracy assessment.
	Ryan	(Lodgepole pine, Pacific silver fir)	x	NPP	FOREST-BGC slightly underestimates NPP (for older stands).
	Hunt *et al.*	Montana (Ponderosa pine)	x	SCP	$r^2 = 0.47$ with SCP data ($r^2 = 0.65$ when previous year's simulated de-trended increment was included). FOREST-BGC more sensitive to annual climate variation than multiple linear regression.
	Band *et al.*	Elk Creek, Montana	x	ET, NPP	Introduces RHESSys framework. No accuracy assessment.
	Running and Hunt	(simulated grassland, coniferous forest and deciduous broadleaf forest)	x	NPP	Comparison between vegetation types: no accuracy assessment.
	Korol *et al.*	Kamloops, BC (Douglas fir)	x	SCP	$r^2 = 0.95$ with SCP data for an individual tree ($r^2 = 0.87$ without competition algorithm).

LAI is leaf area index; LWP is leaf water potential; SCP is stem carbon production; NPP is net primary production; GPP is gross primary production; ET is evapotranspiration; PSN is photosynthesis; RHESSys is Regional Hydro-Ecological Simulation System.

Table 2.4 a Summary of the use and accuracy assessment of FOREST-BGC (1988-1991).

Year	Researchers	Location (Ecosystem/ species)	Driven with remote sensing	Output variables	Accuracy assessment with independent ground data / Conclusion
1991 (cont.)	Running and Nemani	Montana and Jacksonville (simulated forest)	x	ET, PSN, NPP	Comparison between 2 sites of contrasting climate, no accuracy assessment.
1994	Running	Oregon Transect Ecological Research (OTTER) (Pacific silver fir, Douglas fir, Sub-alpine fir and Ponderosa pine)	x	NPP, SCP	$r^2 = 0.82$ and 0.79 for NPP and SCP respectively.
1997	Green *et al.*	Tywi forest, central Wales (Sitka spruce)	✔ (AIRSAR)	SCP	$r^2 = 0.11$ for SCP (increased to $r^2 = 0.64$ using LAI, LNC and biomass as inputs).
1998	Cienciala *et al.*	Sweden (Norway spruce)	x	ET, NPP	$r^2 = 0.95$ and 0.66 for ET and NPP respectively.
1999	Hasenauer *et al.*	Australia (Norway spruce)	x	NPP, LOGS	Increase in temperature controlled LOGS by 11 days from 1961 to 1990.
2000	Lucas *et al.*	Llyn Brianne, central Wales (Sitka spruce)	✔ (CASI)	SCP	$r^2 = 0.33$ for SCP (increased to $r^2 = 0.68$ using LAI, LNC and biomass as inputs).

LAI is leaf area index; LNC is leaf nitrogen concentration; SCP is stem carbon production; LOGS is length of growing season; NPP is net primary production; ET is evapotranspiration; PSN is photosynthesis; CASI is Compact Airborne Spectrographic Imager; AIRSAR is Airborne Synthetic Aperture Radar.

Table 2.4 b Summary of the use and accuracy assessment of FOREST-BGC (1991-2000).

2.4.2 The evolution of FOREST-BGC in the scientific user community

Following the dynamic carbon and nitrogen budgets of Running and Gower (1991) there have been several significant developments to the original model, most notably by combining FOREST-BGC with other models of ecosystem processes.

The conceptual model design provides the opportunity to merge it with the detailed representation of biophysics in land surface process models and with the demography of gap models. For example, the formulation of CO_2 exchange in terms of canopy physiology and energy exchange is calculated over short time periods and is, therefore, compatible with the temporal resolution of LSMs (Lucas 1995; Hunt *et al.* 1996).

Nemani *et al.* (1992) combined three simulation models to perform the computation of ecosystem flux rates across the landscape. The resulting Regional Hydroecological Simulation System (RHESSys) includes a complement of digital terrain analytical methods. The simple "bucket-type logic" of FOREST-BGC fails to account for the horizontal distribution of soil water. This was resolved by the incorporation of TOPMODEL (Band *et al.* 1991), which defines lateral flow of soil water explicitly from topography and soil properties. The surface redistribution of soil water, for example by saturated throughflow processes, influences spatial forest ecosystem activity, previously ignored in FOREST-BGC logic. RHESSys was employed by Band *et al.* (1991). Their methodology was based on the interface of geographic information processing and remote sensing, with FOREST-BGC as the non-linear deterministic model to give spatial structure, initialise and execute a simulation of forest evapotranspiration and NPP for watersheds in western Montana. Unfortunately, with the most realistic non-linear process models comes significantly greater difficulty in initialisation. However, Band *et al.* (1991) used the RHESSys methodology successfully on watersheds up to 1600 km^2 in western Montana.

Since process models are inherently complex and non-linear, the way in which continuous geographic information is aggregated has far-reaching effects on model output. Choosing an appropriate scale is difficult as it is dependent upon (i) the processes being modelled, (ii) the inherent variation in the subscale phenomenon, (iii) data availability and (iv) computational limitations. Nemani *et al.* (1993a) used RHESSys to calculate ecosystem flux rates at different spatial scales ranging from a single hillslope to a 100 x 50 km region. They concluded that the effectiveness of regional ecosystem modelling depends on the quality of the models used and the effectiveness of the information processing techniques used to integrate various data sources.

Hence, what was initially designed and operated as a point, or stand-level daily water balance simulation model, run for one year (Band *et al.* 1991), became an integrated carbon, nitrogen and water cycle model with dual time-step resolution run for one hundred years (Running and Hunt, 1991). FOREST-BGC became the platform for exploration of a variety of time and space scales. Wide applications included forest site quality definition (Korol *et al.* 1991), air pollution effects on forests (Kremer 1991) and prediction of effects of doubled atmospheric CO_2 (Running and Nemani 1991). Running and Hunt (1991) comment on the evolution of several new directions under current development as scaling decisions being a continuous progressive optimisation. The translation of FOREST-BGC to BIOME-BGC (Running and Hunt 1991) was to generalise the coniferous forest logic in FOREST-BGC to other biomes and develop a more general ecosystem process framework. Two key principles enforced were that models must interface well with remote sensing drivers and should be controlled strongly by climate, incorporating the notion of globally available data sets. An implicit assumption was that the treatment of a number of key physiological responses (e.g., stomatal control), could be treated generically. In this way, a clear hierarchy of the variables that most influence ecosystem processes could be established.

Bossel (1991) advocated that the next generation of forest models should be based on the merging of tree process models, whose dynamics are determined by the physiological processes at tree-level and gap models, whose dynamics are determined by inter-species competition processes at the forest-gap-level. HYBRID (Friend *et al.* 1993) avoids many of the limitations of both gap and ecosystem process models: The growth equations of gap models are replaced with functionally-realistic equations and processes for carbon fixation and partitioning, resulting in a dynamic model in which competition and physiology play vital rôles. Friend *et al.* (1993) used HYBRID to simulate ecosystem dynamics in a lodgepole pine forest in Missoula, Montana. A sensitivity analysis found that NPP estimates were most sensitive to the ratio of CO_2 partial pressure inside the leaf and the atmosphere, relative humidity, precipitation, air temperature and tree allometry. This model is a general forest ecosystem model that simultaneously treats tree demography, competition, physiology and other physical processes mechanistically. Trade-offs at the stomatal level control both the long and short-term dynamics of HYBRID, resulting in realistic predictions at both scales.

The demographic mechanisms underlying forest dynamics operate on very different spatial and temporal scales that may be difficult to reconcile empirically (Shugart and Urban 1989). Each mechanism and feedback has an intrinsic stochastic (random) element, which may be confounded further by chance environmental fluctuations. Urban *et al.* (1991) emphasised the

common theme in recent applications to generalise the models used, with the goal of discovering and explaining those phenomena common to all forests, rather than focusing on site-specific patterns. Thus the recent trend suggests the seeming paradox of incorporating more detail in biophysics (§2.2.1) and abiotic processes, whilst including fewer case-specific ecological or biological details!

Running (1994) enhanced this trend by describing versions of FOREST-BGC that included a second canopy layer competing for light and soil moisture (e.g., understorey grass) as well as simulation of stand recruitment and mortality, to provide a more realistic, though general, forest stand simulator. This promoted development of slight variants of FOREST-BGC. Korol *et al.* (1995) developed TREE-BGC that used a competition algorithm to allocate stand estimates of photosynthesis to individual trees. TREE-BGC was subsequently modified by Keane *et al.* (1996a) to produce FIRE-BGC in order to evaluate the cumulative effects of various fire regimes (to include prescribed burning and fire exclusion) on forest stands (e.g., Keane *et al.* 1996b). These 'individual-tree' modified versions of FOREST-BGC still require further accuracy assessment and are, therefore, unavailable at present (Running *pers. comm.*; Thornton *pers. comm.*).

2.4.2.1 Computer based support for ecosystem modelling

Most recently, FOREST-BGC has been implemented using the Scientists' Intelligent Graphical Modelling Assistant (SIGMA): A research and development effort within the Computational Sciences Division of the Information Systems Directorate at NASA Ames Research Centre (Keller 1995; Keller and Dungan 1999). SIGMA is an interactive, knowledge-based, visual programming environment that assists researchers in prototyping models (Dungan and Keller 1991; Keller 1995). Artificial intelligence and meta-modelling techniques are employed to automate parts of the scientific software development process. A description of the underlying 'modelling scenario' is incorporated to give insight into the process by which the model was constructed, extending the notion of a scientific model beyond simply a set of equations. FOREST-BGC, originally written in FORTRAN, was considered ideal for developing and testing this graphical software development environment: Keller and Dungan (1999) demonstrated successful implementation of FOREST-BGC through SIGMA (http://www.ic.arc.nasa.gov/ic/projects/sigma/fbgc.html).

2.4.3 Assumptions of FOREST-BGC

Given all models are simplified versions of reality (Stoddart 1986) (§2.2.1), assumptions are integral to their design. The following section lists briefly the most important assumptions of FOREST-BGC:

- There are inherent mismatches in spatial scaling that are a consequence of the ecosystem structure defined by FOREST-BGC (effectively a one-dimensional flux model). The model treats fluxes only in the vertical dimension so that horizontal homogeneity is assumed for any defined area, unless cells are specifically classified across a landscape. As such, the forest canopy is viewed as a homogeneous three-dimensional leaf of depth proportional to the LAI (ignoring all of the complexities).
- Derivation has been from a variety of sources. For example, leaf-level measurements have been scaled-up to whole canopy average responses, whilst soil processes are only inferred from their control of canopy processes and states because only above-ground conditions are amenable to routine accuracy assessment by remote sensing.
- FOREST-BGC is considered a 'detailed physiology process model' (Landsberg and Gower 1997, p.42; Waring and Running 1998) yet, Hinckley and Ceulemans' (1989) hypothesis that increasing hydraulic flow resistances in larger, older trees produces canopy water stress unrelated to climate, is just one example of physiological detail not incorporated into the model.
- Friend *et al.* (1993) highlighted that FOREST-BGC does not grow individual trees so it cannot be used either to predict changes in the distribution of species, or to allow for the different physiological and morphological characteristics of different species. The model's photosynthesis and respiration routines are empirically based and are not constrained in respect to each other. Perhaps most importantly, the model does not allow for an internal variation of LAI through a simulation.
- Finally, new comprehensive, regional ecosystem simulations now take into account lateral routing of soil water based on topographic and soil physical properties (Band *et al.* 1993). However, models such as FOREST-BGC simulate average conditions, particularly when general default values are used for initialisation but can only represent peculiar micro-sites with extensive site-specific data.

Many of these assumptions are essential to avoid a cumbersome, data dependent model, however, the need for site-specific data (for initialisation as well as independent accuracy assessment), is essential for the continual development of FOREST-BGC. The following section outlines the potential of international large area field experiments for providing such data.

2.5 Field Experiments and Data Acquisition

Considerable effort and cost goes into taking the measurements and producing high quality data sets for large area, international field experiments such as the Hydrological Atmospheric Pilot Experiment in the Sahel (HAPEX-Sahel) and the BOREAS (Hall *et al.*, 1993; Prince *et al.* 1994). Often, however, financial support is exhausted before the final stage of combining models and measurements to obtain scientific information (the real pay-off) is realised. Combine this with the time taken to complete many field experiments, the movement of investigators and expertise and the progression / development of the subject, then it is less surprising that the full potential of such data sets has yet to be realised.

The following section describes the scientific background and motivations for the BOREAS, before outlining the experimental design and execution.

2.5.1 The Boreal Ecosystem-Atmosphere Study (BOREAS): An overview

The BOREAS was a comprehensive international investigation focused on increasing understanding of the interactions between the boreal forest biome and the atmosphere, in order to clarify their rôles in global change (Sellers *et al.* 1995a)

2.5.1.1 Scientific background

The interactions between the boreal forest and the atmosphere (Figure 2.7) can be divided into three groups:

1. Sensitivity of the boreal forest biome to changes in the physical climate system;
2. Carbon and biogeochemical cycling and
3. Ecological and biophysical feedbacks to the physical climate system.

These mutually dependent scientific issues provided motivation for the design and execution of the co-operative field investigation, involving land surface climatology, biogeochemistry and terrestrial ecology, with remote sensing playing a vital integrating rôle (BOREAS Science Team 1993).

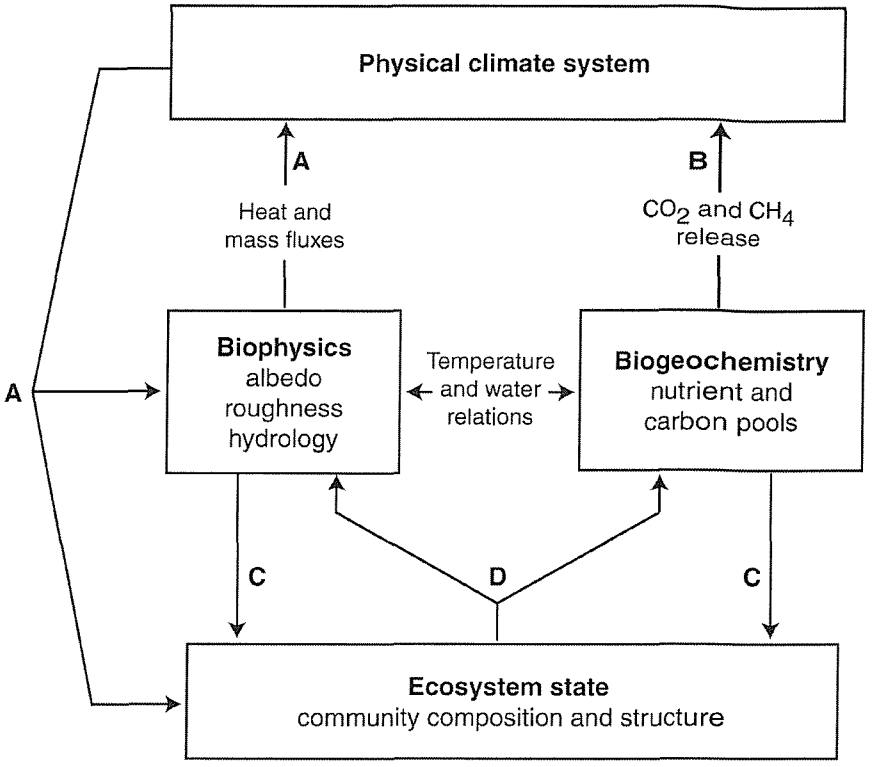

A Influence of changes in the physical climate system on biophysical processes. These may feedback to the atmosphere through changes in energy, heat, water and CO_2 exchange;

B Changes in nutrient cycling rates; release of CO_2 and CH_4 from the soil carbon pool back to the atmosphere;

C Changes in biogeochemical processes and water and nutrient availability influence community composition and structure;

D Change in species composition results in changes in surface biophysical characteristics and biogeochemical rates.

Figure 2.7 Interactions between the boreal forest and the atmosphere with respect to global climate change (adapted from Sellers *et al.* 1997).

2.5.2 Experimental objectives and design

The main objectives of the BOREAS were to collect the data needed to:

1. Increase the accuracy of process-based models that describe the exchanges of radiative energy, sensible heat, water, CO_2 and trace gases between the boreal forest and the lower atmosphere.
2. Develop methods for applying these process-based models over large areas.

These objectives cover a range of spatial scales (local to regional) that had to be reconciled within the experimental design. Therefore, the science team adopted a nested multi-scale measurement strategy to integrate observations and process models over a defined range of spatial scales (§3.1.1, Figure 3.2).

In 1992, 85 science teams were selected from 229 proposals to participate in the BOREAS. Funding of investigators came from a variety of sources, including the NASA, a collaborative special project grant from the Canadian Natural Science and Engineering Research Council (NSERC) as well as the UK's Natural Environment Research Council (NERC).

Six disciplinary 'science groups' were established to aid the organisation of individual projects during the field phases, each with specific objectives (Table 2.5).

Science Group	Acronym	Specific objectives
Airborne fluxes and meteorology	AFM	Study surface-atmosphere interactions.
Tower fluxes	TF	Quantify turbulent energy and mass exchanges.
Terrestrial ecology	TE	Examine biophysical controls on carbon, nutrients, energy and water fluxes and to develop models for scaling-up.
Trace gas biochemistry	TGB	Characterise the flux of trace gases between soil and atmosphere.
Hydrology	HYD	Measure catchment hydrological processes and snow-hydrology components.
Remote sensing science	RSS	Develop links between optical and microwave sensing and boreal zone biophysical variables at scales from single leaf to regional.

Table 2.5 The six science groups of BOREAS.

2.5.3 Experiment execution

A continuous monitoring programme, from 1993 to 1996, incorporated satellite sensor data acquisition, surface meteorological and radiation measurements from ten automatic meteorological stations (AMS) distributed throughout the region (Figure 4.2) and many flux and concentration measurements from several 'flux towers'. However, for most investigations, involving complex equipment and moderate-sized teams, it was not practical or necessary to sustain a continual presence in the field. The bulk of the BOREAS researchers and specialised equipment were, therefore, committed to the field for a series of intensive field campaigns (IFCs) which coincided with the major phenological events (i.e., winter, spring thaw, 'green-up', 'peak greenness' and the beginning of senescence) and augmented the constant monitoring. In addition, focused field campaigns (FFCs) took place in the winter (FFC-W) and thaw (FFC-T) periods to address issues of snow remote sensing and snowmelt processes, respectively (Sellers *et al.* 1995b).

Two intensive study areas allowed the observation of processes associated with the controlling factors of the boreal forests' extent (temperature to the north, moisture to the south) that are most likely to undergo significant change within the biome as a whole (Sellers *et al.* 1995b). Background to the BOREAS study region is given in §3.1.1, whilst §3.2.1 details the collection and distribution of BOREAS data.

2.5.4 BOREAS summary and future directions

Obviously, such an observational period is far too short to measure global change and the associated effects directly but the examination of key processes facilitates the development and accuracy assessment of important process-based models.

The initial focus of the majority of BOREAS researchers has been on accuracy assessment and improvement of local scale energy balance and biophysical process models that operate at relatively short time-scales, amenable to measurement within the three-year BOREAS field programme (e.g., Rayment and Jarvis 1997; Kimball *et al.* 1997; Ryan *et al.* 1997).

The study of ecosystem-level dynamics and land-surface climate interactions at local and regional scales, over longer time periods is the current aim (Sellers *et al.* 1997; Running *et al.* 1999). Whilst application at regional and ultimately global scales is a possibility when combining remote sensing studies with such meso-scale meteorological studies.

To encompass the development of the BOREAS, the initial objectives (§2.5.2) could, therefore, be more simply and comprehensively defined as: The provision of extensive quality data sets that may be used to increase the accuracy of descriptive boreal ecosystem process-based models and develop methods to apply them over large areas using remote sensing and integrative modelling techniques. Ultimately, increasing the accuracy of such models over large areas would enable researchers to better anticipate the effects of global climate change (in particular the effects of altered temperature and precipitation patterns) on the boreal forest.

2.6 Conclusions

The Kyoto Protocol signalled some of the huge socio-economic and political decisions that lie ahead that are heavily reliant on accurate quantitative estimates of future biospheric changes (Grubb *et al.* 1999). Indeed, accurate monitoring of regional scale changes in the terrestrial biosphere is more critical than ever before (Running *et al.* 1999). In particular, there is a need to understand the global carbon cycle.

A comprehensive review of the literature has emphasised the enormous potential that exists for driving FOREST-BGC with accurate spatial estimates of biophysical variables (especially LAI) estimated from remotely sensed data. This powerful combination has been discussed in the context of quantifying the rôle of the boreal forest (which currently sequesters approximately 15% of anthropogenic carbon emissions (DETR 1999)), in the global carbon budget. The remainder of this thesis pursues the challenge of driving FOREST-BGC with accurate spatial data, with the ultimate aim of establishing whether the boreal forests would remain a terrestrial carbon sink under future climates, thus continuing to provide a substantial 'brake' on the rate of increasing atmospheric CO_2.

Chapter 3

Study Area and Data Acquisition

The research issues addressed in this thesis used data from the BOREAS (§2.4) and the Boreal Ecosystem Research and Monitoring Sites (BERMS) research programme. As a prerequisite to the following research chapters (Chapters 4 – 8), a preliminary overview of the study area and ground and remotely sensed data is provided. Accordingly, this chapter is divided into three sections. First, the physical environment of the BOREAS study region (i.e., geographical location, climate, geology, etc.) is described, from which the ground data (§3.2) were collected. The third section outlines the characteristics of the satellite sensors that recorded the remotely sensed data.

3.1 The BOREAS Region

BOREAS was undertaken on the northern and southern edges of the Canadian boreal forest, over a 1000 × 1000 km region, covering most of Saskatchewan and Manitoba. The 'BOREAS Science Steering Committee' conducted the initial study area selection in 1990. The 'BOREAS Science Team' has produced two 'Experiment Plan Documents'. The first, in 1993, detailed the background, objectives and organisation of the study, whilst the later 1996 document, reviewed completed work and gave details of field operations yet to be undertaken. A proportion of the site-specific information contained within this chapter has been compiled using these documents in conjunction with information from hard copy maps and the BOREAS web site (http://boreas.gsfc.nasa.gov/BOREAS/BOREAS_Home.html).

3.1.1 Details of the BOREAS region

The goals of the project (§2.5.2) emphasise the need to study the biome's biophysical, chemical and ecological functioning under different conditions. The governing climatological variables determining these within the biome are:

1. temperature, associated with the length of growing season, radiation budget, etc.,
2. moisture availability, associated with precipitation, snow hydrology and surface hydrological processes (BOREAS Science Team 1993).

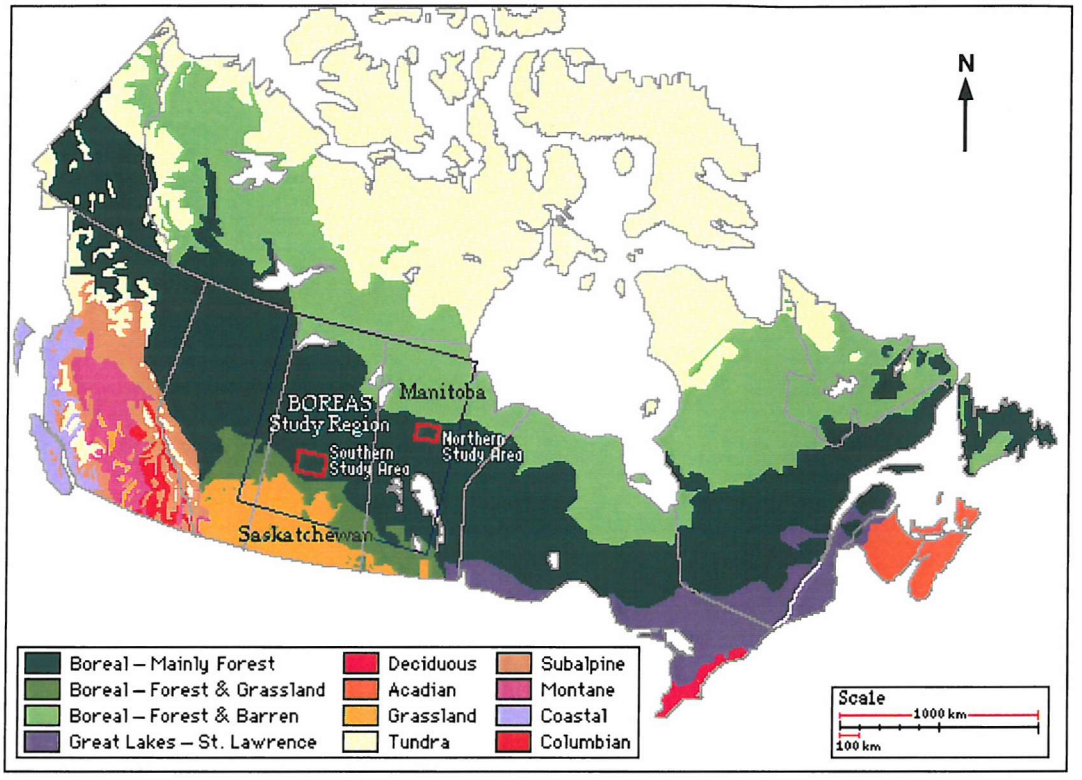

Figure 3.1 Land cover map of Canada showing the location of the BOREAS study areas. (http://boreas.gsfc.nasa.gov/BOREAS/BOREAS_Artwork.html).

Essentially, the northern ecotone (transitional boundary) of the forest is delineated by temperature, whilst the southern boundary is determined by moisture stress and fire frequency in central and western Canada and by ecological competition with temperate deciduous forest to the east of the Great Lakes. Two intensive study areas were desirable as they spanned the environmental gradient and allowed observation of processes associated with the controlling factors (temperature in the north, moisture in the south) most likely to undergo significant change within the biome as a whole (Sellers *et al.* 1995b). Auxiliary sites were chosen to define the variability of surface states and processes and associated remote sensing 'signatures' within and between the Tower Flux Sites (TFS) (BOREAS Science Team 1996).

BOREAS was designed to bridge a wide range of spatial scales because some of the important governing processes can only be studied at fine spatial scales (e.g., the between leaf biochemistry, spectral properties and photosynthesis) but ultimately, the scientific gains must be applied at regional to global scales. Therefore, a nested multi-scale design was developed which permitted knowledge at one scale to be translated and compared to that obtained or inferred at different spatial scales (Figure 3.2).

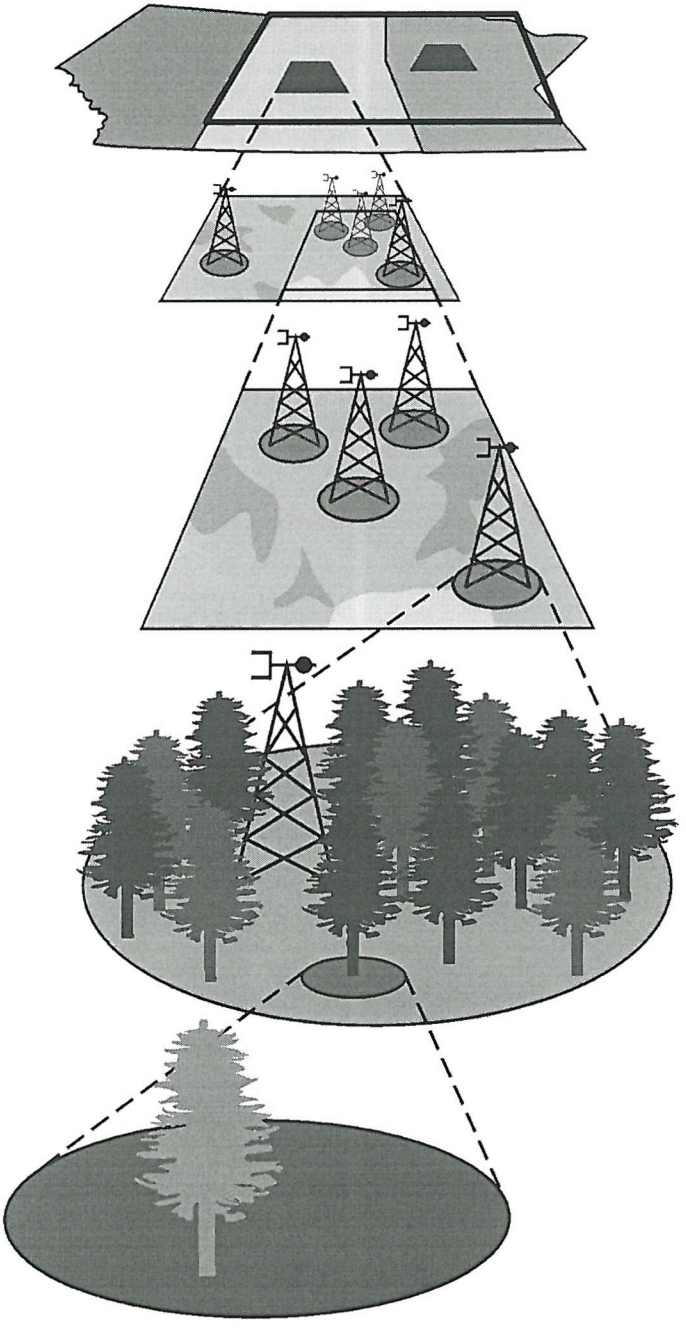

Figure 3.2 The nested multi-scale strategy adopted for the BOREAS (Adapted from Sellers *et al.* 1997).

The scale domains depicted in Figure 3.2 are defined as:

- **Region**: An approximate area of 1000 by 1000 km, covering a large portion of Saskatchewan and Manitoba. The domain of meteorological and satellite sensor data acquisition.
- **Study Areas**: These two areas embedded within the region were the focus of satellite and airborne remote sensing studies, airborne flux measurement and meso-scale modelling. The Southern Study Area (SSA) (11,170 km^2) is located north of Prince Albert, Saskatchewan, and the Northern Study Area (NSA) (8,000 km^2) lies west of Thompson, Manitoba.
- **Transect**: The area connecting and including the NSA and SSA, from Thompson, Manitoba to Prince Albert National Park (PANP), Saskatchewan (approximately 800 km).
- **Modelling Sub-Areas**: The test areas, located within the study areas, for modelling activities and gridded data products. They had the highest priority for airborne remote sensing studies and low-level airborne flux measurements.
- **Tower Flux Sites (TFS)**: Sites located in the centre of 1 square km of relatively homogenous vegetation cover, within the study areas, where flux measurement towers operate. Ten TFS operated during the field campaigns (Plate 3.1).
- **Auxiliary and Process Study Sites**: Approximately 80 auxiliary and process study sites, some located within the TFS, most of the others elsewhere within the study areas, were used for investigator studies or targets for remote sensing investigations. A few were foci for carbon cycle studies, which incorporated measurements of leaf physiology, litterfall and soil CO_2 flux.

Every reasonable effort was made to locate stand types that reflected the objectives of BOREAS (§2.5.2). The criteria for site selection included the following attributes:

- relatively homogeneous tree species;
- relatively even-aged stand: young (or recently disturbed), immature and mature and
- stand size no less than approximately 100 x 100 m.

3.1.2 The BOREAS Southern Study Area (SSA)

The Southern Study Area (SSA) is 130 km by 90 km around Prince Albert, Saskatchewan. The southern boundary is approximately 40 km north of the town of Prince Albert. The SSA topography is gentle, with altitudes between 550 m and 730 m. The western part of SSA is in the Prince Albert National Park (PANP) and the eastern region falls within and around the Narrow Hills Provincial Forest. The Canadian Parks Service manages the PANP land. The two major vegetation zones in the study area are termed mixed wood and aspen grove.

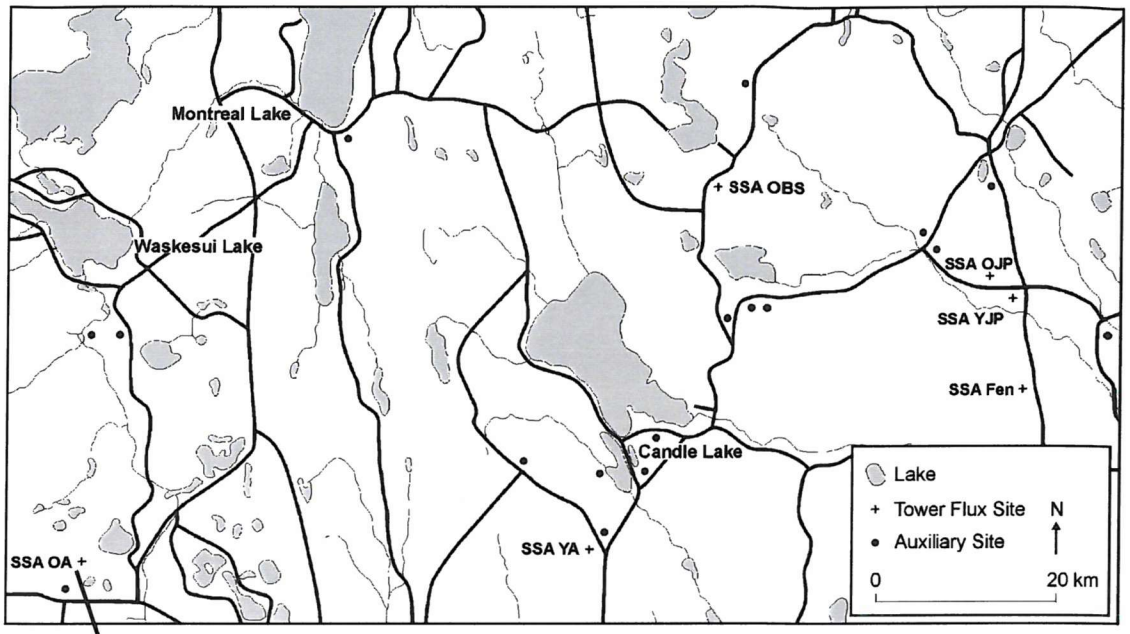

Figure 3.3 The BOREAS SSA.

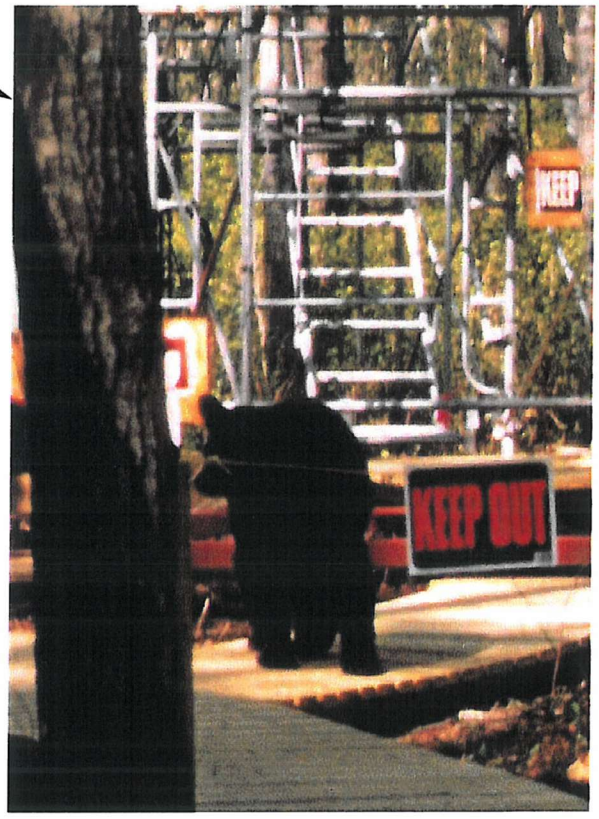

Plate 3.1 My 'fieldwork assistant' at the SSA Old aspen (OA) TFS (September, 1998).

Vegetation

Within the PANP boundary there are large patches of aspen and to a lesser extent jack pine, black spruce and patches of mixed species. Forest cover is often controlled by small changes in relief and soil/soil drainage. Aspen occurs on the uplands, jack pine on minor ridges and black spruce in the lower poorly drained areas. Trees typically range between 50-100 years old and are between 15 and 22 m high, although there are stunted black spruce in bog areas. Local wet patches often result in small (10-30 m diameter) holes in the canopy. To the east of PANP the vegetation is mixed boreal forest. On well drained and or sandy soil the predominant species is jack pine. The poorly drained areas support black spruce. Mixed stands of aspen and white spruce are found on well drained glacial deposits (Halliwell and Apps 1997c).

Fire history

Large fires occurred within the southern half of the PANP during 1940-1950, in the north-east section of the study area during 1977-1978 and west of Montreal Lake in 1989 (Figure 3.3) (Halliwell and Apps 1997b).

Surficial and bedrock geology

The surface deposits are from the Quaternary (Halliwell and Apps 1997c). Pleistocene deposits are of glacial origin, in the form of till, glaciolacustrine and glaciofluvial or outwash materials with thickness from 100-400 m (BOREAS Science Team 1993). Glacial till deposits are shallower in the lowlands and in the depression of Candle Lake. The glacial drift is undifferentiated, mainly grey, calcareous till, containing sand, silt and clay that weathers to an olive or brown colour. Organic deposits date from the Holocene and were deposited after the glacial period.

Directly beneath the surficial deposits are the Lea Park formation, Upper Colorado Group, Ashville Lower Colorado Group and the Swan River Group, all of Cretaceous age. The bedrock topography has a surface that has been glacially eroded indicated by its broad, featureless, gently undulating nature.

Soils and landforms

The soils have developed on thick glacial deposits. The region consists of glacial till and other material of late Wisconsin age, with recent organic deposits (Halliwell and Apps 1997c). The predominant soil orders are brunisolic, gleysolic, chernozemic, luvisolic and organic. The landforms consist of glacial till plains, rolling or hilly moraines, glaciofluvial, glaciolacustrine, fluvial lacustrine, alluvial and aeolian.

Topography

A region of gentle relief with elevations ranging from 400-700 m (Figure 3.4). The Waskesiu and Wapawekka Hills are roughly undulating, often ridged or fluted till plains. The White Gull Creek Plain is rolling outwash plain. Fluvial lacustrine sands, sometimes reworked into sand dunes, are the most common surficial deposits.

Hydrology

Most of the study area belongs to the Saskatchewan River drainage system. Candle Lake is a depression at the headwaters of the Torch River, which drains the surrounding area. Inter-till aquifers, composed of up to 65 m of sand, occur where the sand beds are sufficiently extensive and thick (BOREAS Science Team 1993).

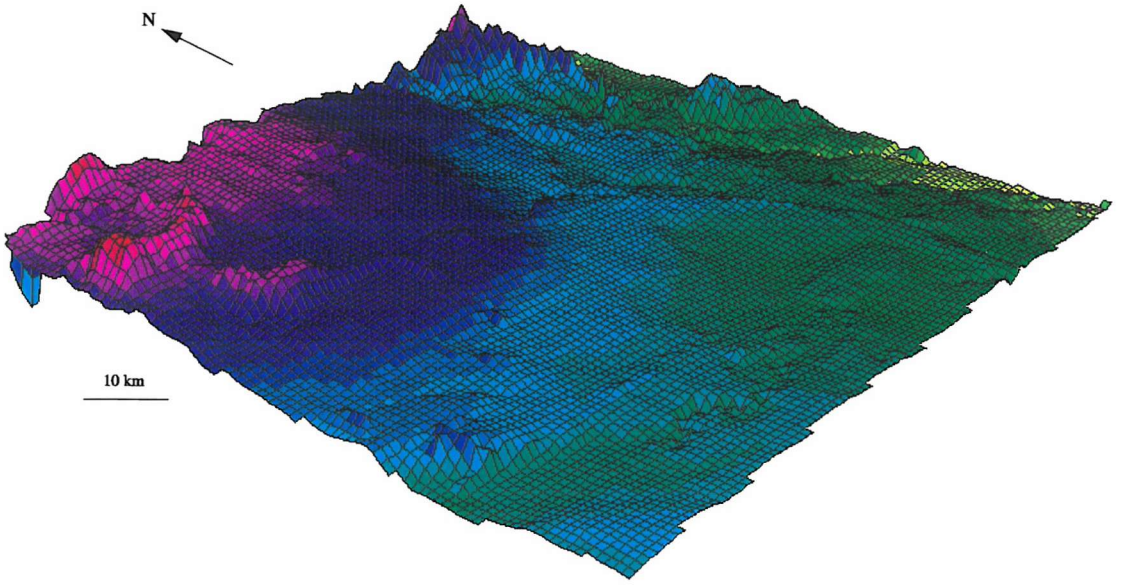

Figure 3.4 Digital elevation model of the BOREAS SSA (vertical exaggeration of 2).

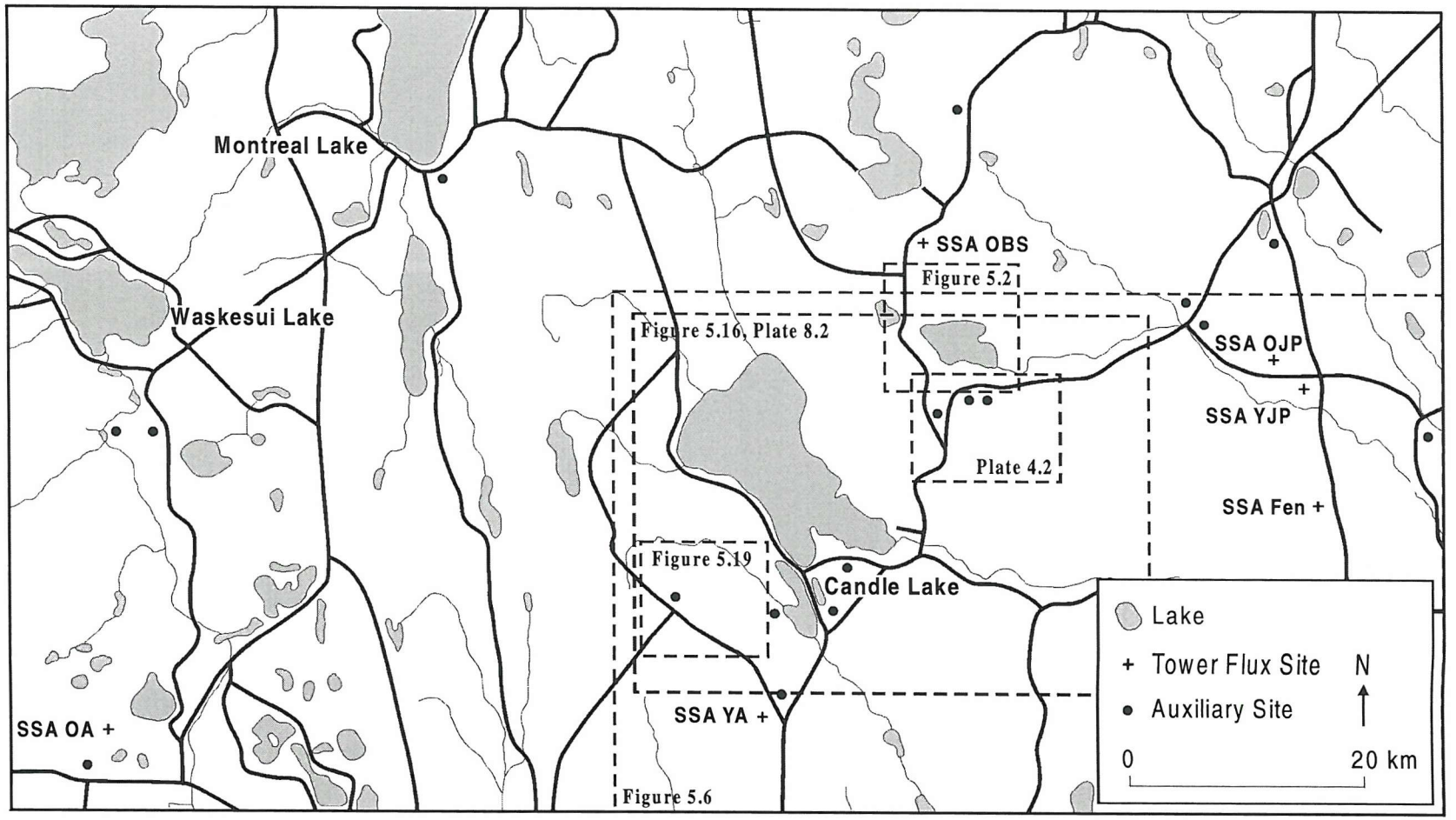

Figure 3.5 The BOREAS SSA. Dashed boxes illustrate the extent of various images (labelled accordingly) throughout the remainder of the thesis.

3.1.3 The BOREAS Northern Study Area (NSA)

The Northern Study Area (NSA) is 100 km × 80 km and located near to Thompson, Manitoba. It is typical of the extreme northern boreal forest, with gentle terrain, containing few lakes and covered primarily with black spruce, scattered birch and some stands of jack pine. Stand ages are variable and are up to 100 years old (Halliwell and Apps 1997a), however, the trees are shorter than in the SSA.

Vegetation

The predominant species is black spruce, which occurs in stands of varying density. It occurs in bogs, drier lichen covered areas and occasional rock outcrops. There are some jack pine stands, mainly to the south of the NSA. The kame deposits have closed to open stands of mainly pure jack pine with other species occurring on patches of clay or beach deposits. Forest stands are generally mature, with some being over 100 years old. Heights vary from stunted black spruce in bog areas to stands of 15m. White birch and trembling aspen are scattered within some of the coniferous stands; pure stands are rare and small. Forest cover is broken by varying density, moisture conditions and especially open treed bogs. Stands and uniform patches are small. No logging or recent burns have occurred in the study area since 1982.

Fire history

Large fires occurred in the eastern section of the study area in 1964, the southern section in 1981 and the western and northern sections in 1989 (BOREAS Science Team 1993)!

Surficial and bedrock geology

Most of the region is composed of clay deposited by glacial Lake Agassiz. In low areas the surficial deposits are mostly varved clays and are thin on the highest areas, or absent. In the low lying areas bogs and fens exist. Permafrost commonly occurs several centimetres below the surface of bogs and to greater depths in clays soils on thickly wooded slopes and ridges. Two major hills composed of sand and gravel (kame deposits) run in the north-south direction with relief up to 60m. The underlying bedrock consists of Pre-Cambrian granite which has been glacially polished (Halliwell and Apps 1997c).

Soils and landforms

Derived predominantly from Glacial Lake Agassiz sediments, the soils consist of clays, organic and some sandy deposits. Depths vary from bare rock outcrops on the top of hills to deep sedimentation basins in the low areas up to 17m in depth (Halliwell and Apps 1997c). The two kame deposits, running approximately north to south, consist of sandy gravel deposits that were reworked by Lake Agassiz wave action and exhibit ancient shorelines along the top of hills. There are occasional outcrops of bedrock. Variations in moisture regime occur due to topographic or soil changes.

The terrain is flat and broadly rolling in low regions and hilly in the high areas. The two kame deposits are an exception (see Surficial Geology).

Topography

The topography reflects the glacially smoothed Pre-Cambrian bedrock surface, which has been minimally modified by glacial drift. Terrain is more gentle in the north, with several narrow stream valleys.

Hydrology

The drainage of much of the NSA is poor, being flat and having abundant wetland areas. There are several significant streams that flow into the Sapochi and Odei Rivers. The few lakes within the study area are small. Large lakes (up to 2 km × 15 km) occur to the north and north-west of the NSA. Bog and fen occur on the most low-lying terrain.

	BOREAS region		SSA		NSA	
	Latitude (°N)	Longitude (°W)	Latitude (°N)	Longitude (°W)	Latitude (°N)	Longitude (°W)
Northwest	59.979	111.000	54.319	106.227	56.249	98.824
Northeast	58.844	93.502	54.223	104.236	56.083	97.241
Southwest	51.000	111.000	53.513	106.320	55.542	99.045
Southeast	50.089	96.970	53.419	104.368	55.379	97.489

Table 3.1 North American Datum of 1983 (NAD83) corner co-ordinates of the BOREAS region and study areas.

3.1.4 Climate of the BOREAS region.

Section 2.2.1.2 gave a general introduction to the climatology of boreal forests. However, because climatic factors are the most significant of all environmental variables determining plant growth (under non-limiting conditions), it would be beneficial to detail the recent climate of a few specific sites within the BOREAS region.

Data from the Boreal Forest Transect Case Study (BFTCS), an extension of BOREAS, illustrates clearly the ecoclimatic gradient that exists within the region (Figure 3.6). The boreal region of central Canada is known for minimal variation in elevation, apart from the general decrease north-eastward. A decrease in mean temperature and an increase in annual precipitation mirror this pattern.

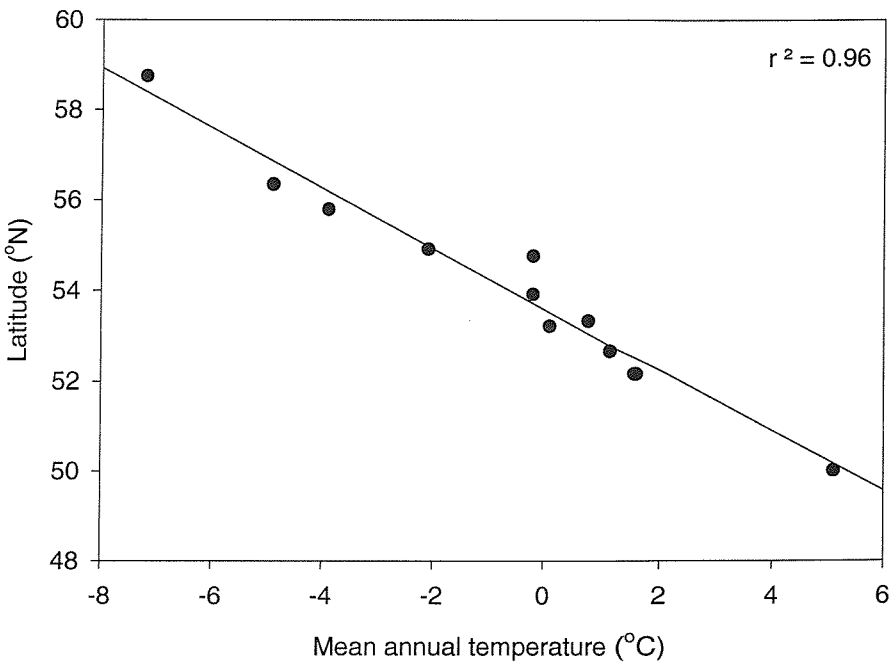

Figure 3.6 Data from the BFTCS illustrating the environmental gradient within the biome.

Winters tend to be less harsh and summers are warmer and drier in the SSA than the NSA (Table 3.2).

Climate characteristic	SSA [a]	NSA [b]
Mean January air temperature (°C)	-19.8	-25.0
Mean July air temperature (°C)	17.6	15.7
Mean annual precipitation (mm)	405	536

[a] data based on a 48 year average from Prince Albert, Saskatchewan
[b] data based on a 23 year average from Thompson, Manitoba

Table 3.2 Selected climate characteristics for the BOREAS SSA and NSA.

More specifically, Figure 3.7 illustrates the tremendous seasonal range of climate (mean daily temperatures) at one TFS (SSA Old jack pine (OJP)) during 1994, with a range of 70.6 °C between mid-January and mid-July!

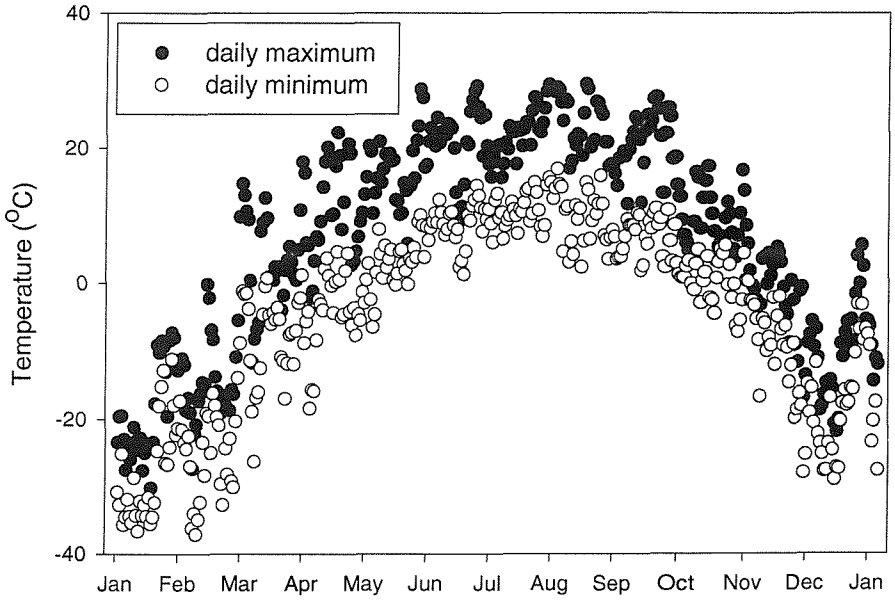

Figure 3.7 Maximum and minimum daily temperatures at SSA OJP during 1994 (data from the BOREAS Information System (BORIS)).

Seasonal patterns of precipitation appear to conform to summer convective activity, hence, variable over space and time. The TFS of the SSA demonstrate the aridity of the region with annual precipitation between 350 - 450 mm, around 50% of which falls between July and August (Figure 3.8) (Larsen 1980).

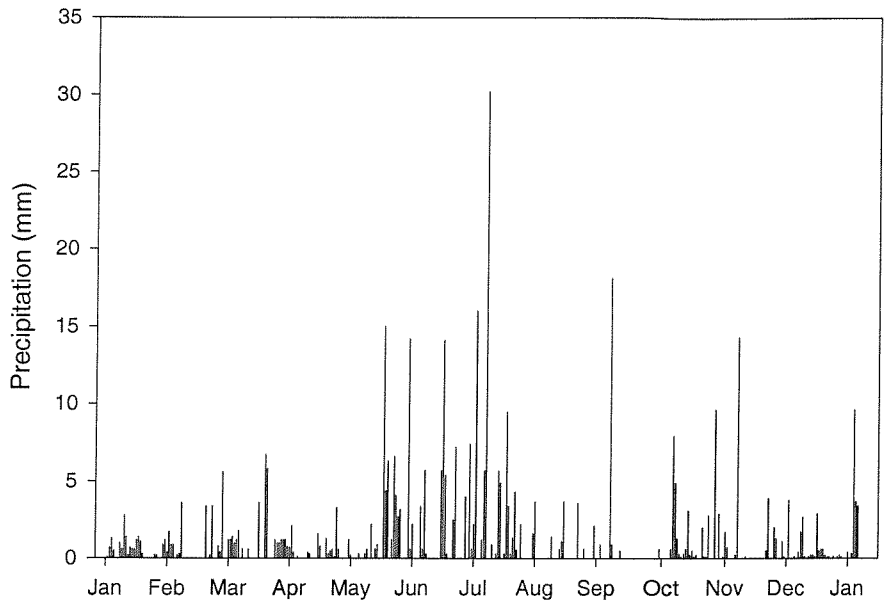

Figure 3.8 Precipitation recorded at SSA OJP during 1994 (data from the BOREAS Information System (BORIS)).

(Note: more detailed site-specific climate data may be found within Chapter 4).

The duration of BOREAS was such that it was impossible to measure global climate change directly. Figure 3.9 gives no indication of obvious trends in key climatic variables at one TFS since 1975.

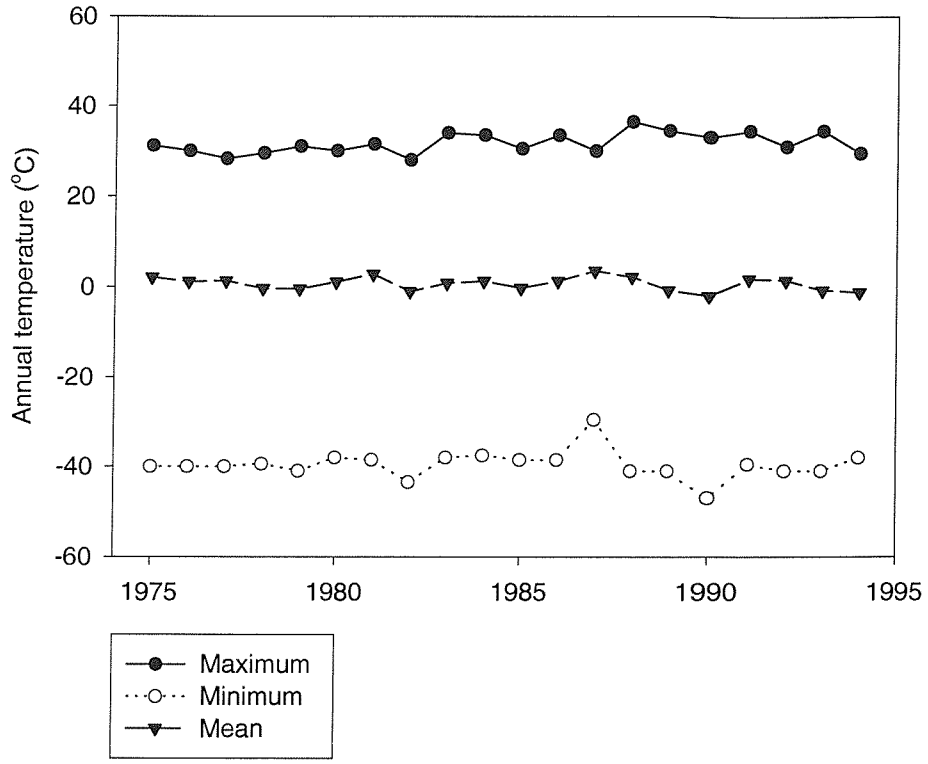

Figure 3.9 Historical Canadian meteorological data (data from the BOREAS Information System (BORIS)).

3.2 Ground Data Acquisition

The multi-disciplinary nature of this investigation is such that a variety of data have been acquired from a range of sources.

3.2.1 BORIS: The BOREAS database

The BOREAS Information System (BORIS) is the single, central collecting and distribution point for data sets and documentation provided by the science investigators of BOREAS. The major purpose of BORIS is to facilitate the integrative science of the project. Hence, BORIS is a service organisation facilitating data exchange, accomplished with intra-disciplinary co-operation. Indeed, it is this integrative nature of BOREAS that has the potential to make the project so valuable. Data have been loaded onto a BORIS on-line facility enabling small data sets to be downloaded by investigators and their associates. A CD-ROM of BOREAS data is soon to be available. The remainder of this sub-section details the ground data obtained through BORIS for this study.

3.2.1.1 LAI ground measurements and estimates

The definition of LAI used within this thesis is the one-sided green leaf area per unit area of ground (Chen and Black 1992a; Fassnacht *et al.* 1994; Gower *et al.* 1999). A number of direct and indirect methods have been used to estimate LAI. Although ideal, direct measurements of LAI in forest stands, derived from destructive sampling, are extremely laborious (e.g., area harvest and leaf litterfall), therefore impractical for many investigations. As a result, indirect methods of LAI estimation have been explored (Gholz *et al.* 1991; Chen and Black 1992b; Nel and Wessman 1995; Vose *et al.* 1994). Spectral methods (Jordan 1969; Holben *et al.* 1980; Asrar *et al.* 1984), hemispherical photographs (Bonhomme and Chartier 1972; Rich *et al.* 1993), bi-directional reflectance distribution function methods (Goel and Thompson 1984; Norman *et al.* 1985), litter-fall extrapolation (Marshall and Waring 1986), allometric equations (Pierce *et al.* 1994), gap-fraction methods (Norman and Campbell 1989; Fassnacht *et al.* 1994; Chen *et al.* 1997; Gower *et al.* 1999) and Global Positioning System (GPS) Position Dilution of Precision (PDOP) (e.g., Sigrist *et al.* 1999) are examples of some indirect techniques!

This section reviews the more common direct and indirect approaches used to estimate LAI, before detailing the methods used to collect ground data used within this investigation.

Direct measurements of LAI

Area harvest involves the periodic destructive sampling of vegetation, in plots located randomly within a single community, during the growing season (Gower *et al.* 1999). The harvested foliage tissue is sub-sampled for specific leaf area (SLA, the ratio of fresh leaf area to dry foliage mass) determination (Landsberg and Gower 1997). This approach is more appropriate for 'short-stature' ecosystems (e.g., grasslands, agricultural crops) than for forests because it is extremely laborious when conducted for an area of sufficient size to characterise the spatial heterogeneity adequately. More appropriate for the estimation of forest LAI is the use of allometric relationships applied to each tree surveyed. Allometry is the relationship between the mass of a part or all of an organism and an independent variable that is difficult and / or laborious to measure. Mass variables used commonly to estimate LAI of forest stands are stem diameter (e.g., Gholz *et al.* 1991; Curran *et al.* 1992) and sapwood cross-sectional area (e.g., Peterson *et al.* 1987; Pierce *et al.* 1994). Direct measurements of biomass and area of plant constituent parts involves harvesting plants that encompass the size range encountered in the survey plots. Gower *et al.* (1992; 1997; 1999) give detailed descriptions of field methods used to harvest trees destructively to determine the mass and area of the biomass components.

Indirect measurements of canopy gap fraction to estimate LAI

Recently, much emphasis has been placed on using indirect optical measurement techniques, particularly suited to measuring the canopy gap fraction, to estimate the LAI of vegetation canopies (e.g., Welles 1990; Welles and Cohen 1996; Gower *et al.* 1999).

> '*There is a probability that a beam of radiation passing through some distance of a vegetative canopy will be intercepted by foliage. The probability of such interception is proportional to the path length, foliage density and foliage orientation. Therefore, if the beam transmittance is known, then it is possible to invert foliage information*' (Welles and Norman 1991, p. 818).

This is the fundamental theory behind the adoption of optical instruments to obtain accurate and quick estimates of LAI. Many optical instruments measure canopy gap fraction based on radiation transmission through the canopy. Assuming a random spatial distribution of leaves, the effective LAI (L_e) can be calculated from the gap fraction, using:

$$L_e = 2\int_0^{\pi/2} \ln\left[\frac{1}{P(\theta)}\right]\cos\theta\sin\theta\, d\theta \qquad (3.1)$$

where, $P(\theta)$ is the gap fraction at the view zenith angle. Although this equation was developed originally for the calculation of LAI (Chen *et al.* 1991), the result from (3.1) should be

regarded as effective LAI because leaves in plant canopies are often not distributed randomly in space. Indeed, equation 3.1 implies that LAI can be calculated without knowledge of foliage angle distribution if the gap fraction is measured at several zenith angles. The LI-COR LAI-2000 is well suited to this purpose because of its ability to measure $P(\theta)$ at five zenith angles simultaneously from diffuse blue light transmission through the canopy (Chen *et al.* 1997). Hemispherical photography can also provide gap fractions in the full zenith angle range, hence can be used to estimate L_e.

Since L_e is obtained from gap fraction measurements and is the quantity that many optical instruments measure, Chen (1996a) used it as a basis for calculating LAI:

$$L = (1-\alpha)\, L_e / \Omega \tag{3.2}$$

where, α is the woody-to-total area ratio (by using the factor $(1 - \alpha)$ the contributions of non-leafy materials are removed). However, this assumes non-leafy materials have a similar spatial distribution pattern to leaves, quantified by a parameter determined by the spatial distribution pattern of leaves (Ω). The Ω value may be separated into two components (Chen 1996a):

$$\Omega = \Omega_E / \gamma_E \tag{3.3}$$

where, γ_E is the needle-to-shoot area ratio quantifying the effect of foliage clumping within a shoot (increases with increasing clumping) and Ω_E is the element clumping index. The final equation for the estimation of LAI then becomes:

$$L = (1-\alpha) L_e \gamma_E / \Omega_E \tag{3.4}$$

Methods

The following three sub-sections describe the use of three pieces of optical equipment: the ceptometer, the LAI-2000 plant canopy analyser and hemispherical photography and detail how they were employed to collect data during the BOREAS.

Ceptometer measurement procedure

The ceptometer is a line quantum sensor consisting of an integrated probe and micro-controller. 80 separate photodiodes (sensitive to radiation at wavelengths between 400-700 nm) are spaced at 1-cm intervals along the 80-cm long probe (Pierce and Running 1988; Welles and Cohen 1996). The micro-controller interprets and stores the signals coming from the probe. Measurements above and below the canopy are made to determine canopy transmittance at a number of solar zenith angles. Further details of specifications and operation of the ceptometer may be found at "Decagon Devices" web site (http://www.decagon.com/).

During BOREAS ceptometers were used to measure total incident photosynthetically active radiation (PAR), diffuse incident PAR, total PAR transmitted through the canopy and diffuse PAR in the canopy for tower flux and auxiliary sites within the SSA (Plummer *et al.* 1997). At each of these sites measurements were taken by BOREAS researchers from group RSS04 at the same ten sampling positions used for hemispherical photography. To avoid inconsistency when comparing LAI estimates, measurements were obtained at several zenith angles. Each site measurement constituted 6400 individual PAR measurements. LAI was calculated subsequently, using:

$$L = \frac{[f_b\,(1-\cos\theta)-1]\ln(E_i / E_a)}{0.72 - 0.337\,f_b} \tag{3.5}$$

where E_a is the total incident PAR above the canopy, E_i is incident PAR beneath the canopy, θ is the solar zenith angle and the beam fraction (f_b) is:

$$f_b = \frac{E_a - E_{ad}}{E_a} \tag{3.6}$$

The ceptometer-derived LAI estimates from BOREAS RSS04 were used in a training capacity within this investigation.

LAI-2000 measurement procedure

The LI-COR LAI-2000 plant canopy analyser is composed of a control unit and an optical sensor head. The sensor head projects an image of its nearly hemispheric field-of-view (148°) onto five photodiodes arranged in concentric rings (at zenith angles of approximately 0, 22.5, 37.5, 52.5, and 67.5 °) which make measurements of the incoming diffuse incident flux above and below the canopy at blue wavelengths (<490 nm) (Welles 1990; Gower and Norman 1991). Further information on the LAI-2000 plant canopy analyser may be found on the LI-COR web site (http://env.licor.com/products/LAI2000/). The LAI-2000 uses the data collected to calculate the gap fraction for the five zenith angle ranges, hence L_e, using (3.1).

Three LAI-2000 units were used during BOREAS, two for in-stand measurements and one for the reference measurements (either at the top of a flux tower or in a nearby clearing). Data were acquired by BOREAS groups RSS07 and RSS04, along three 170 m - 300 m parallel transects separated by 10 m at the tower sites and along two 50 m transects at the auxiliary sites. All measurements were taken near sunset or under overcast conditions to reduce the effect of scattered blue light within the canopy. For this investigation these data were used in a testing capacity.

Hemispherical photography measurement procedure

Hemispherical (fisheye) canopy photography is a technique used to characterise plant canopies using photographs taken through an extreme wide-angle lens (viewing angle approaches or equals 180°) (Anderson 1964; Rich 1990). The images serve as permanent records of the geometry of the canopy openings. The geometric distribution of openings can be measured precisely and used subsequently to estimate LAI via efficient image analysis techniques (e.g., Chazdon and Field 1987; Becker *et al.* 1989). Rich (1990) gives a detailed description of the principles behind LAI estimation from hemispherical photographs.

For BOREAS, hemispherical photographs were acquired in sample arrays at heights of 0.8, 1.5 and 2.5 m for each of the tower flux and auxiliary sites, at 10 m intervals along the central x axis of each plot, by BOREAS researchers from group TE23. The photographs were taken with Kodak TMAX 400 ASA film (pushed to 800 ASA), using a Nikkor 8 mm fisheye lens fitted on a Nikon FM2 body and suspended pointing directly upward in a self-levelling mount on a Bogen professional monopod (Fournier *et al.* 1997). Hemispherical photograph negatives were video digitised at a resolution of 512 (horizontal) × 480 (vertical) × 7 bits using the hemispherical photograph analysis system CANOPY (Rich 1990). L_e and other canopy indices were then calculated using the program LAICALC (Rich *et al.* 1993). Finally, to compare hemispherical photography and LAI-2000 data, the gap fractions from the photographs were separated similarly into five zenith angles from 0 to 75°.

Comparison of LAI estimates

An obvious goal of using indirect techniques and approaches to estimate LAI is to be able to compare favourably with direct, destructive measurements (usually assumed to be more accurate and are typically the standard for comparison) (Chen *et al.* 1997; Gower *et al.* 1999). Chen *et al.* (1997) gave a comprehensive comparison between estimates of LAI from the three methods outlined above. They concluded that (i) each of these optical techniques offers considerable advantages over laborious, destructive sampling and (ii) accurate optical estimates of LAI must consider canopy architecture. Measurement of L_e is, therefore, an important first step in optical measurements, hence the applicability of the LAI-2000 and hemispherical photography. For this investigation, where necessary, values of the woody-to-total area ratio (α), the element clumping index (Ω_E) and the needle-to-shoot area ratio (γ_E) for the BOREAS sites were taken from Gower *et al.* (1997) to standardise estimates obtained via the different methods. Table 3.3 summarises the average values of each component leading to

the LAI estimates based on optical measurements and compares these with allometric estimates for selected BOREAS TFS. Differences (within 25%) are similar in magnitude to those reported by Gower *et al.* (1997; 1999) and are most likely due to underestimates by using optical instruments under clumped foliage canopies (Chen *et al.* 1997). Indeed, for this reason, Gower *et al.* (1999) recommend that direct measurement is the only reliable approach for canopies with a LAI greater than 6. However, as indirect estimates of LAI usually plateau around 5 – 6 (Gower *et al.* 1997) indirect techniques for LAI estimation are suited to this investigation.

TFS [a]	Period	L_e	γ_E	Ω_E	$(1-\alpha)$	Optical LAI	Allometric LAI
SSA OBS	IFC-93	2.27	1.42	0.70	0.84	3.87	-
	IFC-1, 94	2.35	1.30	0.70	0.84	3.67	-
	IFC-2, 94	2.45	1.36	0.70	0.84	4.00	6.3
	IFC-3, 94	2.27	1.42	0.70	0.84	3.87	-
SSA OJP	IFC-93	1.75	1.51	0.71	0.68	2.53	-
	IFC-1, 94	1.77	1.28	0.71	0.68	2.17	-
	IFC-2, 94	1.87	1.46	0.71	0.68	2.61	2.5
	IFC-3, 94	1.76	1.51	0.71	0.68	2.54	-
SSA YJP	IFC-93	1.46	1.37	0.72	0.95	2.64	-
	IFC-1, 94	1.51	1.43	0.72	0.95	2.85	-
	IFC-2, 94	1.55	1.52	0.72	0.95	3.10	2.8
	IFC-3, 94	1.57	1.37	0.72	0.95	2.83	-

[a] OBS is Old black spruce; OJP is Old jack pine and YJP is Young jack pine.

Table 3.3 Summary of optical and allometric LAI measurements for selected BOREAS SSA TFS (Chen *et al.* 1997).

Table 3.4 summarises the three BOREAS data sets of LAI and their use within this thesis.

BOREAS group	**RSS04**	**RSS07**	**TE23**
Measurement procedure	ceptometer	LAI-2000	hemispherical photography
Reference	Plummer *et al.* 1997	Chen *et al.* 1997	Fournier *et al.* 1997
Measurement acquisition	three 300 m parallel transects per TFS and two 50 m parallel transects per AUX (§3.2.1.1 for detail)	three 300 m parallel transects per TFS and two 50 m parallel transects per AUX (§3.2.1.1 for detail)	photos acquired at 10 m intervals along central axis of each site (§3.2.1.1 for detail)
Aggregation	site measurements averaged (n = 9)	site measurements averaged (n = 10)	original data used (n = 235)
Abbreviation	$LAI_{training}$	$LAI_{testing}$	$LAI_{hem\ photo}$
Used in thesis within	§4.3.3.1, §5.2.2, §7.4.1, §7.5.1, §7.5.2	§5.3.3, §7.5.3	§6.2
Location maps	Figure 7.2	Figure 7.2	-

Table 3.4 Summary of BOREAS LAI measurements used within this thesis.

3.2.1.2 NPP ground estimates

NPP, defined here as the annual net production of biomass, comprises approximately 50% of net canopy photosynthesis (Landsberg and Gower 1997) and is an integral component of net ecosystem exchange (NEE). Therefore, given the importance of NPP, there is a great need for process-based models that can produce accurate estimates of NPP. It is essential such model estimates are compared to field measurements of above-ground NPP (NPP_A) for accuracy assessment (Lucas and Curran 1999; Gower *et al.* 1999).

The conceptual definition of NPP is accepted widely as:

$$NPP = GPP - R_A \tag{3.7}$$

where, GPP is gross primary production and R_A is autotrophic respiration. However, GPP cannot be measured directly and R_A is difficult to measure. Alternatively:

$$NPP = \sum Pi + H \tag{3.8}$$

where, P is the net production of dry biomass for each of the plant tissues (i), and H is consumption of organic matter by herbivores (generally less than 10%) (Schowalter *et al.* 1986).

Equation 3.8 is appropriate to estimate NPP for any ecosystem, although, the approach of data collection is dependent on the structure, spatial heterogeneity of the ecosystem. In a similar fashion to LAI (§3.2.1.1), two common approaches to estimating NPP_A are (i) area harvest and (ii) allometry.

Area harvest involves periodic destructive sampling during the growing season of all above-ground living tissue in plots located randomly. The harvested organic matter is dried (or sub-sampled and dried) and statistically significant increments, or production of organic matter are combined to estimate NPP_A. Whilst appropriate for short-stature ecosystems, yet again, this approach is inappropriate for almost all forests because it is so laborious and annual production of organic matter is so small relative to the spatial variability of standing organic matter. The most realistic alternative is to establish permanent plots located randomly within representative stands. By recording the diameter and species of each tree in the plot, annual production of organic matter for each component can be estimated from annual radial increment data in combination with allometric equations (Gower *et al.* 1999).

Confusion surrounding the estimation of NPP can usually be traced to either (i) the lack of strong allometric equations to estimate the production of some tissues and (ii) the simultaneous production and shedding (e.g., mortality) of tissues (Linder *et al.* 1987). However, by measuring leaf litterfall and assuming the foliage mass of the canopy is in equilibrium (i.e., new foliage production approximates leaf litterfall) researchers can use:

$$NPP_A = B + D \tag{3.9}$$

where, B is biomass increment and D is detritus or litterfall production (Grier 1988). One potentially larger source of error relates to the debate over whether tree mortality should be added to estimates of NPP (Binkley and Arthur 1993).
The NPP data sets, used for accuracy assessment within this thesis, were part of the effort by the BOREAS team TE06 to develop carbon budgets for the various Canadian boreal forest types. A brief summary of the operations of the BOREAS TE06 group is given here, with a detailed description in Gower *et al.* (1997).

Measurements were made to best quantify NPP for the BOREAS TFS, Carbon Evaluation (CEV) and auxiliary (AUX) sites in 1993 and 1994: Four replicate plots were established at each site. The plot size varied from 7.5 m × 7.5 m to 30 m × 30 m depending upon tree density.

The number of trees per plot ranged from 60 to 120. It was assumed that the large number of trees and the random location of the four replicate plots were sufficient to characterise the forest stands adequately. In August 1994, two dominant, three co-dominant, three intermediate and two stunted trees were sampled destructively (immediately outside the replicate plots). Data from these trees were used to develop site-specific allometric equations for the dominant overstorey species in each stand. The diameter at breast height (dbh) was measured for all trees within each plot and either a disk or a core removed from trees within variable radius plots

(which provide an unbiased sample of trees). Annual stemwood radial increment for each year between 1986 and 1994 was measured subsequently.

The other component of aboveground NPP, litterfall, was measured at the TFS and CEV sites by placing 1 m × 1 m screens on the forest floor within each plot.

Understorey vegetation was sampled from a 2 m × 2 m subplot located randomly within each plot. All vegetation was clipped and stored in a cold room (3 °C) until processed. Samples were separated into three categories: ephemeral, new foliage and twig from perennial plants and old foliage and twig from perennial plants. Samples were dried and weighed to the nearest 0.1 g. Understorey NPP was calculated as the sum of the ephemeral, new twig, and new foliage tissues. Fine root NPP was also estimated using ingrowth cores. BOREAS researchers from group TE06 then used these measurements in conjunction with the derived site-specific allometric equations to obtain estimates of NPP (§3.2.2.5 details the calculations).

In summary, radial increment cores taken from live trees (e.g., Jozsa 1988; Vogt and Persson 1991; Hendrick and Pregitzer 1993) may be used to calculate annual biomass increment, which when used in combination with allometric equations is essential to the estimation of NPP (Gower *et al.* 1999; Reich *et al.* 1999).

3.2.2 BERMS fieldwork

In addition to data from the BORIS database, it was necessary to obtain further ground estimates of NPP_A to assess the accuracy of NPP estimates produced by driving an ecosystem simulation model with remotely sensed data. Post-BOREAS field research, under the new acronym BERMS (Boreal Ecosystem Research and Monitoring Sites) is an effort by several Canadian agencies and the NASA to maintain the BOREAS infrastructure. The main aim of BERMS is to characterise the impact of inter-annual climatic variability on the carbon, water and energy fluxes of the boreal forest. The Canadian Atmospheric Environment Service (AES) is supporting climatic measurements, while the NASA intends to use the BERMS sites to assess the accuracy of biophysical variable estimates from Terra sensors.

In March 1998 a successful application was made to the BERMS Science Committee to obtain tree cores in order to estimate NPP for accuracy assessment of ecosystem model simulations. Fieldwork was undertaken during September 1998.

3.2.2.1 Work within the field: Extracting and transporting tree cores

120 plots were established (Figure 3.10), many of which coincided with sites where previous allometric measurements had been taken by BOREAS research teams (1994 – 1996). The plots were located in relatively homogeneous areas to provide accurate stand level descriptions. Plot size varied from 7.5 m × 7.5 m to 30 m × 30 m depending upon tree density. A hand-held Global Positioning System (GPS) was used to locate each plot (horizontal accuracy within ± 20 m) (Sigrist *et al.* 1999; Magellan 1999).

The diameters of trees located within a plot were measured and two cores extracted (at 180° to each other) for two representative trees within each plot. Jozsa (1988) showed that two cores taken at 180° give more accurate estimates of annual increment than three or four samples taken randomly. An increment borer starter-aid was made to facilitate core extraction. As well as freeing both hands and maintaining borer alignment, the starter-aid provided a stable pivot point for the core barrel (when used for the first 5cm of penetration), thus minimising 'cork-screwing' (Plate 3.2a).

Figure 3.10 The location of BERMS tree core sites.

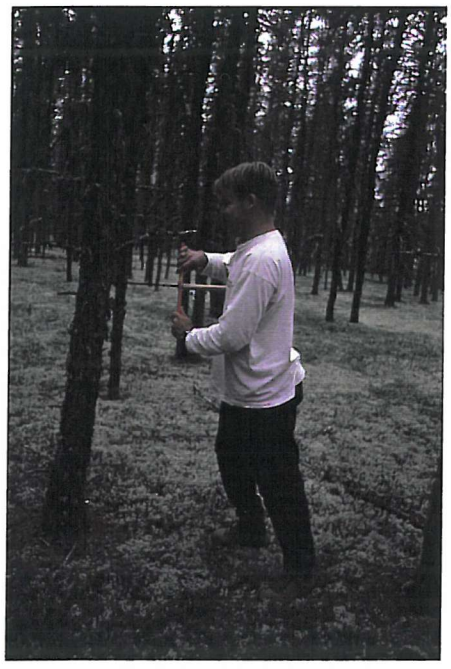

Plate 3.2a Use of an increment borer and starter-aid.

Plate 3.2b Core extraction.

Cores were labelled systematically by writing on the wet sapwood zone using a fine permanent technical drawing pen. Corrugated cardboard and masking tape were used to constrain cores during air-drying whilst in the field to prevent moulding, decay and warping. Once dry, straws were used for long-term storage and transport (Plate 3.3).

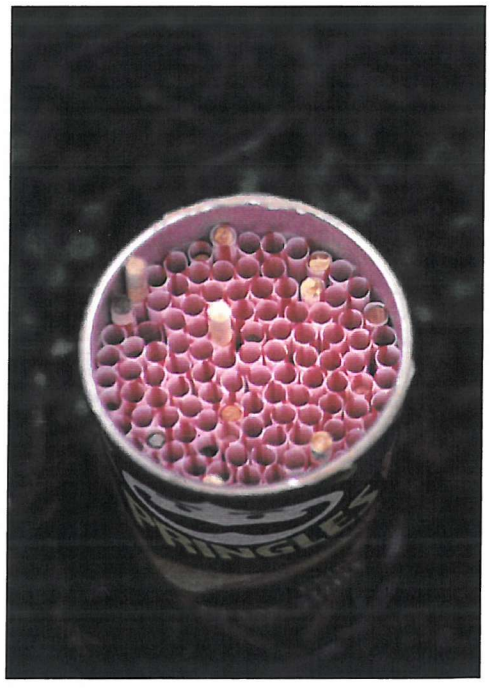

Plate 3.3 Storage of tree cores for transportation.

3.2.2.2 Laboratory analysis: Accurate measurement of annual increment

Cores were further air-dried in laboratory conditions (Phipps 1985), before being mounted onto redwood blocks with polyvinyl acetate (a cold setting resin adhesive). Each core was then planed-off to enhance ring boundaries using a finely set smoothing plane. Certain samples were also stained with tea to increase contrast further.

To measure annual increment accurately it was necessary to design and construct an 'incremental measuring stage' (Plate 3.4) for use with a binocular 'Nikon' microscope. Tree-ring width was measured with a precision of 1 μm using a dial-gauge in combination with a graticule eyepiece. Ring widths for 1988 to 1997 inclusive were measured for the two cores taken from each tree (hence four measurements per year from each tree, which were then averaged).

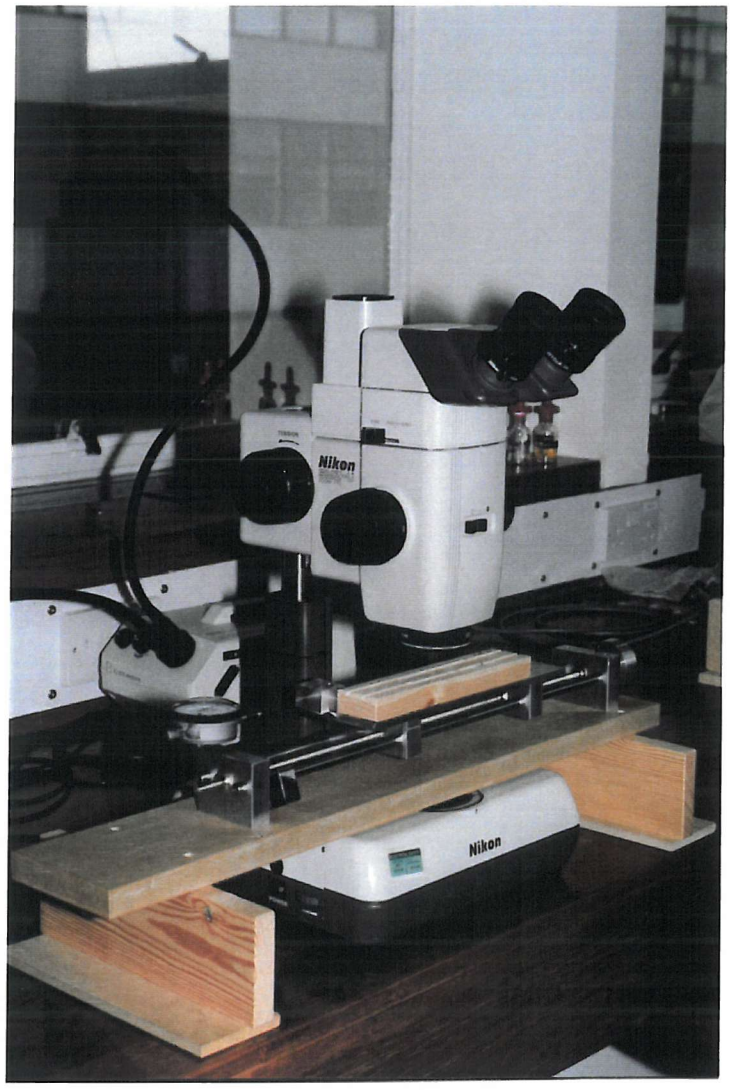

Plate 3.4 The incremental measuring stage.

3.2.2.3 NOAA ITRDB 'VERIFY5' accuracy assessment program

The International Tree-Ring Data Bank (ITRDB) is a professional organisation providing the only world-wide database of dendrochronological data. The ITRDB 'Program Library', a collection of DOS utilities to help the dendrochronological community analyse tree-ring data, is maintained by the National Oceanic and Atmospheric Administration (NOAA) Paleoclimatology Program (Grissino-Mayer 1997).

To check the accuracy of the tree-ring width measurements within this study, 'VERIFY5' was obtained through the NOAA ITRDB library. This accuracy assessment program was designed to assess consistency between two sets of tree-ring width measurements. Detailed information on the program and the measurement process can be found in Grissino-Mayer (1997). The accuracy assessment technique used by the model was adapted from Fritts (1976, p. 250-252).

The program output lists basic statistics associated with the interval of years both input data sets have in common. The assumption used by VERIFY5 is that, if two data sets represent the same distribution, they should have the same descriptive statistics. 'Regression results' are also included and again VERIFY5 assumes that if the two sets of data represent the same distribution, the regression should indicate near perfect agreement (an r-value near 1.0). Finally, the program output indicates whether the measurements should be 'accepted' or 'rejected' based on two levels of confidence, 0.05 (ring-porous or diffuse-porous wood) and 0.01 (conifers) and flags any anomalies (if the absolute difference for any particular year is greater than 2.5 times the average absolute difference, then that year is flagged).

A complete sequence of tree-ring widths was measured for a single core. These measurements were then repeated 10 times and the accuracy/consistency compared using VERIFY5. This was repeated for representative cores for each species. Results indicated that accuracy was high, with the greatest mean square error of 8.97 μm (2.02%) for jack pine (Figure 3.11).

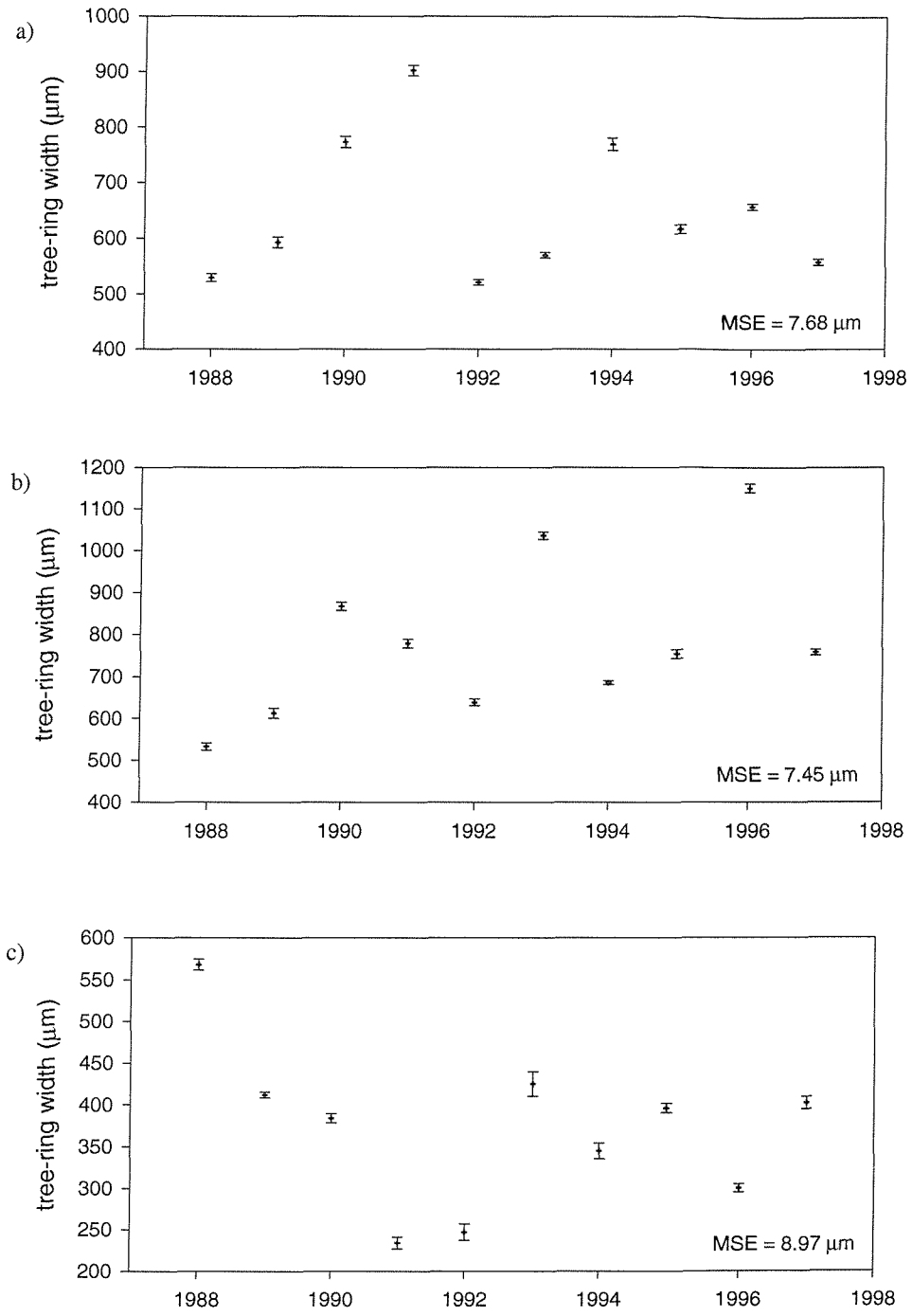

Figure 3.11 Accuracy of tree ring-width measurements for a) aspen, b) black spruce and c) jack pine (MSE is mean square error).

3.2.2.4 Derivation techniques and algorithms

NPP was estimated by inputting the tree-ring width measurements into allometric equations and then scaling to the hectare level using a plot scaling factor that reflects the tree's size in relation to the plot size (Dilworth and Bell 1979). The site-specific allometric equations used within this investigation were developed by BOREAS team TE-06 (§3.2.1.2). Gower *et al.* (1997) gives a detailed description of how the allometric equations were derived. They estimated that the number of human hours needed to take the measurements to develop a single allometric equation was in excess of 1,000 hours per site, per year (Gower *et al.* 1997)! Allometric equations are developed on a log-log basis to correct for non-homogeneous variance:

$$\Delta B = (inv \log(a + b(\log X))) \; PSF \tag{3.10}$$

where, ΔB is biomass by component, a and b are regression coefficients (Table 3.5), X is annual increment (cm) at dbh (1.37 m) and PSF is the plot scaling factor.
Stem, branch and foliage biomass were calculated using:

$$\log_{10} Y_{1,2,3} = a + b \log_{10} X \tag{3.11}$$

where, Y_1 is mass (kg), Y_2 is stem sapwood volume (m^3) and Y_3 is leaf area (m^2)

BOREAS site	Species	dbh range	Tissue [a]	*n*	*a*	*b*	r^2
SSA YJP [b]	jack pine	0.8 – 6.4	S	10	-0.921	1.888	0.994
			SAP	10	-3.695	1.879	0.965
			NF	10	-1.879	1.621	0.917
			OF	10	-1.354	1.592	0.941
			TF	10	-1.239	1.606	0.957
			NT	10	-2.395	1.495	0.884
			BR	10	-1.743	2.277	0.959
			NLA	10	-1.041	1.545	0.901
			OLA	10	-0.597	1.575	0.944
			TLA	10	-0.462	1.575	0.959

[a] Tissue symbols are as follows: S, stem; SAP, stem sapwood volume; NF, new foliage; OF, old foliage; TF, total foliage; NT, new twig; BR, branch; NLA, new leaf area; OLA, old leaf area; TLA, total leaf area.
[b] These data are from the BOREAS SSA young jack pine (SSA YJP) TFS. Complete data from all other sites may be found within Gower *et al.* (1997).

Table 3.5 Regression coefficients and data used by TE06 to develop site-specific allometric equations (Gower *et al.* 1997).

Finally, NPP (kg C ha^{-1} yr^{-1}) for each plot was estimated by combining the vegetation components :

$$NPP = Y_1 + Y_2 + Y_3 + u + D \quad (3.12)$$

where, u is understorey mass (kg).

3.2.2.5 Data quality and potential sources of error

NPP estimates for the BOREAS sites are of good quality because they were derived from site-specific allometric equations and direct measurements of litterfall (§3.2.1.2) (Gower *et al.* 1997). Estimates derived for the additional auxiliary sites may suffer slightly as site-specific allometric equations were not available (Santantonio 1988). In particular, estimating overstorey biomass increment from non-site-specific equations is problematic when the diameters of the trees measured are smaller or larger than the diameters of the trees that were harvested to develop the allometric equation. For this reason, the general equations of Singh (1982) were used for trees at any site that had a diameter that was either too large or small for the BOREAS TE-06 allometric equations.

3.3 Remotely Sensed Data Acquisition

The study of forests using remotely sensed data has focused primarily on the Landsat Thematic Mapper (TM) and National Oceanic and Atmospheric administration (NOAA) Advanced Very High Resolution Radiometer (AVHRR) sensors because of (i) suitability, (ii) availability and (iii) cost. Reflecting this trend and as a pre-cursor to the potential use of data collected by future sensors, this investigation also used data from these sensors. This section describes the characteristics of the TM and AVHRR sensors and the satellites that carry them (Table 3.6).

	Landsat	NOAA
Orbit	Near polar, Sun synchronous	Near polar, Sun synchronous
Altitude (km)	705	833
Inclination (degrees)	98.2	98.7
Orbital period (minutes)	98.9	102
Equator crossing time (LST (hrs))	09.45 (descending node)	07.30 and 19.30 (even satellites) 14.30 and 02.30 (odd satellites)
Repeat cycle (orbits per day)	14.56	14
Global frequency coverage [a] (days)	16	9

[a] The AVHRR viewing angle is wide enough to give daily coverage, albeit with different viewing geometry.

Table 3.6 Characteristics of the Landsat (-4 and -5) and NOAA (-9, -11, -12, and -14) satellites (Avery and Berlin 1985; Cracknell 1997; Lillesand and Kiefer 1999).

3.3.1 Characteristics of the Landsat TM satellite sensor

The first Landsat satellite (ERTS-A) was launched by NASA in 1972, followed by Landsat 2 (ERTS-B), 3, 4 and 5 in 1975, 1978, 1982 and 1984 respectively, of which Landsat 5 is still operating. Landsat 6 was launched in 1993 but did not become operational, unlike Landsat 7 (http://landsat.gsfc.nasa.gov/), launched on 15 April 1999. The Landsat satellites operate in near-polar, sun-synchronous orbits. The altitude of the orbit of the Landsat 5 and 7 satellites is 705 km (Mather 1999). Each orbit takes approximately 99 minutes, with just over 14.5 orbits being completed in one day. The orbit was chosen in such a way that every 16 days the whole Earth surface is covered (Rencz 1999).

The Landsat Multi-Spectral Scanner (MSS) was the primary sensor on the Landsat 1, 2 and 3 satellites, operating in four bands in visible and NIR wavelengths. The second generation of Landsat satellites (4 and 5) marked a significant advance in remote sensing through the addition of the more sophisticated TM sensor, with higher spectral and spatial resolution. The Landsat TM records both reflected and emitted Earth surface radiation from 7 bands in the electromagnetic spectrum (Table 3.7). Referred to as the workhorse of the Earth observation community (Curran 1993b), the characteristics of the TM bands were selected to maximise its capability for detecting and monitoring different types of Earth resources (Gorte 1999). Landsat-7 carries the Enhanced Thematic Mapper-Plus (ETM+) sensor, which extends the capabilities of the TM by providing a 15 m panchromatic band (0.5–0.9 μm) and a spatial resolution for the thermal band (band 6) of 60 m (Mather 1999).

The Landsat TM records radiation in scan-lines that run perpendicular to the ground track of the satellite. An oscillating mirror design acquires data of 16 scan-lines within each forward and reverse sweep, since there are 16 detectors for each band (except the thermal band, which has 4 detectors). During one mirror sweep the satellite advances over a distance that corresponds to 16 scan-lines, such that eventually the entire terrain is covered. This geometry results in an along-track ground resolution of approximately 29.6 m (118.5 m for band 6) (Kruse 1999). The length of each scan-line (i.e., the across-track width of a TM image) is 185 km, which when divided into approximately 6,000 pixels, gives an across-track spatial resolution of approximately 30.8 m. TM digital image data are relayed back to one of more than 14 ground receiving stations on Earth and resampled, usually to a spatial resolution of 30m (or 120 m for band 6), giving scenes that are 32,400 km^2 in area. Smith and Curran (1999) provided details of signal-to-noise ratio (SNR) calculations and estimated a value of 341:1 for the Landsat TM sensor.

Thematic Mapper (TM) sensor

Radiometric resolution: 8 bits (256 level)
Spatial resolution: 30 m (Channels 1– 5 and 7) and 120 m (Channel 6)
View angle: 14.9 degrees
Swath width: 185 km

Channel	Spectral resolution (μm)	Primary uses
1	0.45 – 0.52 (blue)	Coastal water mapping, soil/vegetation differentiation
2	0.52 – 0.61 (green)	Vegetation differentiation and vigour assessment
3	0.62 – 0.69 (red)	Chlorophyll absorption detection, cultural feature identification
4	0.77 – 0.91 (near infrared)	Vegetation biomass surveys, water body delineation
5	1.56 – 1.79 (short middle infrared (1))	Vegetation and soil moisture measurement
6	10.45 – 12.46 (thermal infrared)	Vegetation stress analysis, thermal mapping
7	2.08 – 2.35 (short middle infrared (2))	Mineral and rock discrimination, hydro-thermal mapping

Table 3.7 Characteristics of the TM sensor (Lillesand and Kiefer 1999).

The BOREAS Landsat TM images used in this thesis were acquired through the Canada Centre for Remote Sensing (CCRS). The CCRS receiving station in Prince Albert, Saskatchewan collected the vast majority of the raw data from the Landsat-5 TM. Limited radiometric and geometric corrections were applied to produce the path-oriented level-3a images (§4.2.3.1). Systematically corrected (level-3s) and precision corrected (level-3p) images, processed through the CCRS Geocoded Image Correction System (GICS) (Friedel 1992), were also made available.

3.3.2 Characteristics of the NOAA AVHRR satellite sensor

The AVHRR sensor represents the culmination of a series of advances in NOAA's Polar-orbiting Operational Environmental Satellite (POES) system (Hastings and Emery 1992). Initially designed to assist in weather prediction and monitoring (Rao *et al.* 1990), the sensor has been operating continuously since 1978. It was first launched on the NOAA-6 satellite and has been carried ever since onboard NOAA-7 to NOAA-15 inclusive (Cracknell 1997; Lillesand and Kiefer 1999) (http://poes.gsfc.nasa.gov/history/history_home.htm). The NOAA satellite orbit repeats exactly after 9 days. The orbital height is 833-870 km with an inclination of 98.7° and a period of 102 minutes (Mather 1999).

The AVHRR sensor is an across-track scanning system featuring one visible, one near infrared, one middle-infrared, and two thermal channels (Table 3.8), with a SNR of 33:1 (Smith and Curran 1999). The definitive source of information on the AVHRR sensor is Cracknell (1997). The AVHRR sensor has provided data for investigation of clouds, land-water boundaries, snow and ice extent, ice or snow melt inception, day and night cloud distribution, temperatures of radiating surfaces, and sea surface temperature (SST) (e.g., McClain *et al.* 1985; Sasamal 1999; Schenoi 1999). By virtue of its properties (Table 3.8), however, it has been recognised increasingly that there are many alternative uses for AVHRR data (Hayes 1985; Hastings and Emery 1992; Ehrlich *et al.* 1994; Tucker 1996; Mather 1999). The sensor has evolved consequently into an invaluable data source for coarse scale land-cover studies and ecosystem analysis (Gervin *et al.* 1985; Malingreau and Belward 1994, Kruse 1999) and has been labelled 'the most suitable sensor for observing the Earth at regional to global scales' (Belward 1992, p.206).

There are currently many data sets, derived from the data recorded by the sensor, for studies of the Earth (Malingreau and Belward 1992; Cracknell 1997). The most common of which are the Local Area Coverage (LAC) (approximately 1.1 km spatial resolution and collected routinely for several continents) and the Global Area Coverage (GAC) (a lower-resolution (approximately 4km) sample of the LAC data, providing information at continental and global scales) (Kidwell 1991). Recognising the need for improved, long time-series data, processed with stable calibration and community consensus algorithms, the NOAA and the NASA initiated the Pathfinder Program in 1990 to better assist the global change research community (Cracknell 1997). In particular, the AVHRR Land Pathfinder was entrusted with the task of reprocessing and rehabilitation of the AVHRR records for the period 1981 to date, to produce multi-channel terrestrial data sets. The Goddard Distributed Active Archive Centre (DAAC) (http://daac.gsfc.nasa.gov/) maintains archives of Pathfinder AVHRR Land (PAL) data, including:

- 10-day composited NDVI and AVHRR channel radiance images
  (8 x 8 km and 1 x 1 degree resolutions, binary format)
- Global gridded monthly NDVI
  (1 x 1 degree resolution, binary format)
- Global gridded daily and 10-day full parameter products
  (8 x 8 km resolution)
- Global gridded 10-day NDVI climate product
  (1 x 1 degree resolution)

A complete Overview of AVHRR PAL data sets may be found on the internet at:
http://daac.gsfc.nasa.gov/CAMPAIGN_DOCS/LAND_BIO/GLBDST_Data.html.

Advanced Very High Resolution Radiometer (AVHRR) sensor

Radiometric resolution: 10 bits (1024 level)
Spatial resolution: 1.1 km
View angle: 55.4 degrees (IFOV ≈ 6 km at swath edge)[a]
Swath width: 2,700 km

Channel	Spectral resolution (μm)	Primary uses
1	0.58 – 0.68 (visible)	Daytime cloud and surface mapping, snow and ice extent
2	0.75 – 1.10 (near infrared)	Surface water delineation, snow and ice extent
3	3.55 – 3.93 (middle infrared)	Hot target detection, night-time cloud mapping
4	10.50 – 11.30 (thermal infrared (1))[b]	Cloud and surface temperature determination, cloud mapping
5	11.50 – 12.50 (thermal infrared (2))[c]	Day or night cloud mapping, water vapour correction

[a] The most usable within the swath of 2700 km is the area within ± 15°. At 15° the area covered by a pixel is approximately 1.5 km and repeated coverage for this swath is about 6 days.
[b] For NOAA-7 and -9, channel 4 was 10.3-11.3 μm
[c] Not on NOAA -6, -8, -10.

Table 3.8 Characteristics of the AVHRR sensor (Cracknell 1997; Lillesand and Kiefer 1999).

Data from AVHRR sensors on the NOAA-9, -11, -12, and -14 polar orbiting satellites were acquired by CCRS and provided for use by BOREAS researchers. The BOREAS Level-3b AVHRR-LAC images cover the entire 1,000 km by 1,000 km BOREAS region (containing both the NSA, the SSA and the transect region between them).

3.4 Chapter Summary

This chapter has introduced the study area, emphasising the environmental factors that affect the productivity of the boreal forest species investigated throughout the remainder of this thesis. Ground and remotely sensed data in a range of formats (e.g., measured and estimated biophysical variables, maps of forest age classes, Landsat TM and AVHRR images), collected by a number of investigators from different backgrounds and brought together through the BOREAS, are combined within this study. Indeed, one of the most challenging and rewarding aspects has been the integration of diverse ground and remotely sensed data to achieve the objectives of this thesis (§1.1).

Chapter 4

Driving an ESM with Remotely Sensed Data

Large uncertainties exist in spatial estimates of carbon pools and fluxes in the landscape (Figure 2.1) as spatially extensive measurements of photosynthesis and respiration are not obtained easily because of the need for regular, large area field surveys. Direct measurements of carbon fluxes can be made but only for small portions of space and time. This chapter investigates whether accurate estimates of carbon fixation for 20 km^2 of boreal forest may be obtained by driving the FOREST-BGC ESM with remotely sensed estimates of LAI from the Landsat TM.

4.1 Experimental Design and Objectives

The objectives of this pilot study are threefold. First, to collect and format the data necessary to 'initialise' FOREST-BGC for a specific BOREAS site and to ascertain model sensitivity to input variables. Second, to 'optimise' FOREST-BGC to obtain accurate estimates of NPP for a number of sites throughout the BOREAS SSA. Third and finally, to 'automate' the model using remotely sensed estimates of LAI to produce map of NPP for 20 km^2 of boreal forest. The structure of this chapter reflects the iterative development of the investigation, from initialisation, through optimisation to automation (Figure 4.1).

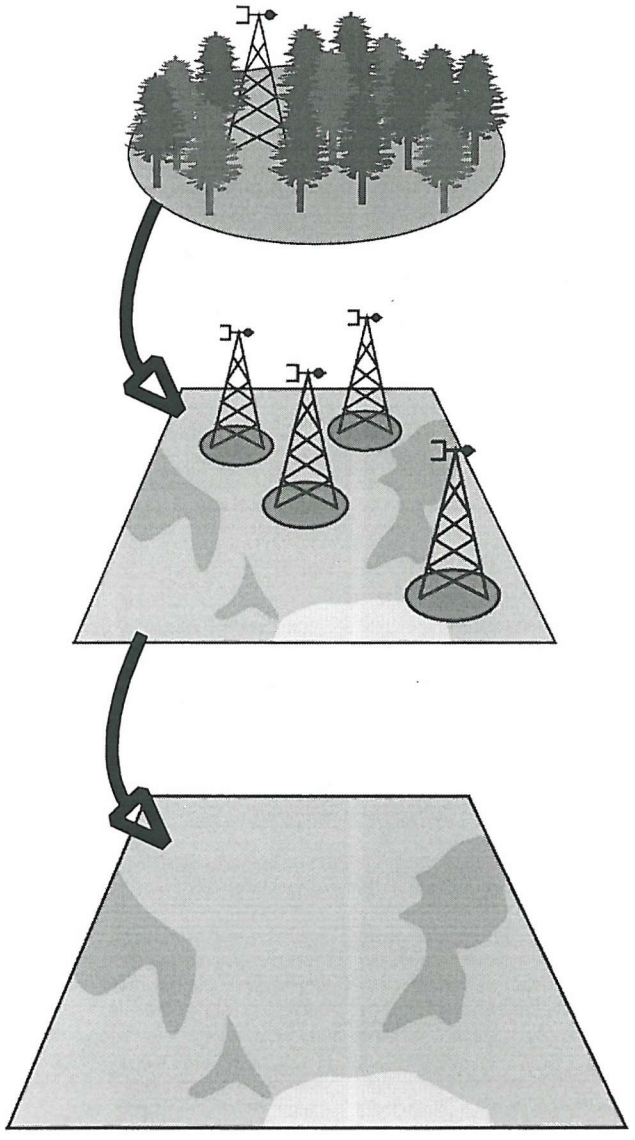

Stage 1: 'Initialisation'

FOREST-BGC run for an individual site. Sensitivity of the model to input variation assessed.

Stage 2: 'Optimisation'

FOREST-BGC run for a series of sites throughout the BOREAS SSA and simulations assessed for accuracy.

Stage 3: 'Automation'

Remotely sensed estimates of LAI used to drive FOREST-BGC for 20 km^2 of boreal forest.

Figure 4.1 Logic and development of the pilot study.

4.2 Providing the Driving Variables

To drive FOREST-BGC for any area, a number of inputs are required (Table 4.2) (Running and Nemani 1991; Running 1994; Waring and Running 1998). The following section describes the inputs used within this pilot study to drive FOREST-BGC: climate data, site-specific input variables and variables derived from remotely sensed data.

4.2.1 Climate data extraction and formatting from BORIS

A number of BOREAS research groups, to include the continual 'Staff Monitoring Program', were aimed at providing researchers with a sufficient record of near-surface meteorological and radiation measurements for several years preceding and throughout the field experiment (Figure 4.2). These data exist in the BOREAS database in a variety of different formats, many of which were appropriate for data extraction to produce the climate data files required to run FOREST-BGC.

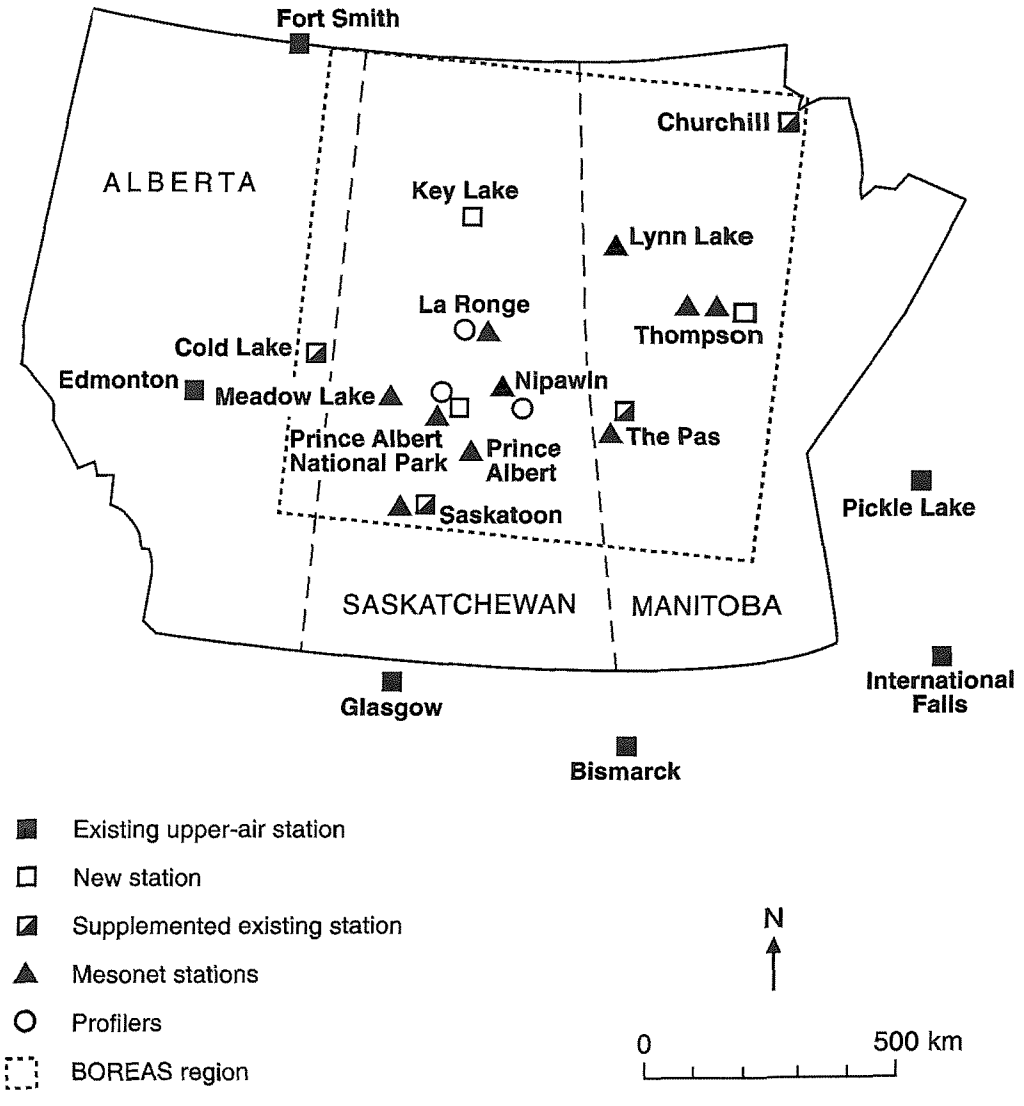

Figure 4.2 BOREAS meteorological measurement sites.

Tower Flux Sites (TFS)

The most comprehensive series of near-surface meteorological and radiation measurements exist for four Tower Flux Sites (TFS). Data for the SSA Old Jack Pine site (SSA OJP), SSA Old Aspen site (SSA OA), NSA Old Jack Pine site (NSA OJP) and NSA Thompson Airport site (NSA YTH) between 1994 and 1996 were extracted from the BOREAS database.

A program was written in *Visual Basic* to:

1. Calculate daily averages of T_{max} (°C), T_{min} (°C), Radiation (Wm^{-2}) and Precipitation (mm) from continuous 15-minute data.
2. Compute daily averages of mean atmospheric temperature (°C) and relative humidity (%)
3. Calculate daily average dew point temperature, T_{dew}, (°C) from 2. using the following:
   Relative humidity is related to vapour pressure and saturation vapour pressure at temperature T:

$$RH = 100x\frac{e_d}{e_s} \tag{4.1}$$

   Therefore,
$$e_d = e_s * RH/100 \tag{4.2}$$

   Saturation vapour pressure is a function of temperature:

$$e_s = 0.6108\exp(\frac{17.27T}{237.3+T}) \tag{4.3}$$

   where, e_d is the actual vapour pressure at temperature T. The dew-point temperature is the temperature at which this vapour pressure would mean the air is saturated. Hence, the temperature at which e_d is the saturation vapour pressure is given by:

$$T_{dew} = \frac{116.96 + 237.3\ln e_d}{16.777 - \ln e_d} \tag{4.4}$$

   where, T_{dew} is dew-point temperature (°C), T is average air temperature (°C), RH is relative humidity (%), e_s is saturation vapour pressure (kPa) and e_d is vapour pressure (kPa).
4. Save the data file in the desired format to run FOREST-BGC (Julian day, T_{max} (°C), T_{min} (°C), T_{dew} (°C), Radiation (W m^{-2}), Precipitation (mm).

Automatic Meteorological Stations (AMS)

The surface network of fourteen Automatic Meteorological Stations (AMS) was established to enhance the record of meteorological measurements within and between the two study areas (Figure 4.2). These AMS collected 15-minute interval data throughout BOREAS for a range of meteorological variables, however, radiation data had to be substituted from TFS records. Hence, using a modified version of the program written for the TFS data, climate files for the SSA Old Black Spruce site (SSA OBS) between 1994 and 1996 were produced from measurements taken at Waskesiu Lake (Figure 3.3).

'Environment Canada' data - Saskatchewan Research Council (SRC) stations

The third (and final) source of meteorological measurements were 'Environment Canada' Saskatchewan Research Council (SRC) historical data sets. In a similar fashion to the AMS data, daily averages of temperature and precipitation were extracted, with radiation data being substituted from the nearest TFS. Measurements from Thompson and Prince Albert airports were used for sites in the NSA and SSA respectively.

4.2.2 Site-specific input variables

Values were obtained from both published literature and unpublished site observations from BOREAS researchers.

Mean daily vegetation solar albedos for snow-free conditions were estimated from site observations reported by Sellers *et al.* (1995a), whereas the mean daily solar albedo for snow was set at 0.8 (Brutsaert 1988). Canopy extinction of solar radiation was set at -0.5 based on data for temperate deciduous and evergreen forests (Jarvis and Leverenz 1984; Hunt and Running 1992).

Mean annual LAI values were derived from overstorey LAI measurements collected over three periods during the 1994 growing season (Chen 1996a). No attempt was made to configure the model to represent the contribution of an understorey canopy (very low productivity mosses) to daily carbon exchange or seasonal changes in LAI. Specific leaf area (SLA) and LNC were estimated from plucked needle and leaf measurements at the black spruce, jack pine and aspen sites (Dang *et al.* 1997). Leaf carbon information was derived from LAI and SLA values:

$$L = \frac{Lc \times \alpha_s}{\alpha_g} \tag{4.5}$$

Therefore, $$L_C = \frac{L \times \alpha_g}{\alpha_s} \quad (4.6)$$

where, L is leaf area index ($m^2\ m^{-2}$), L_C is leaf carbon (kg), α_s specific leaf area ($m^2\ kg\ C^{-1}$) and α_g is ground surface area (m^2).

Leaf, stem and root maintenance respiration coefficients reflect daily rates of carbon respired per unit of carbon in living tissue and were estimated from measured rates for coniferous and deciduous cover types (Sprugel *et al.* 1995; Kimball *et al.* 1997). Leaf cuticular, boundary layer and maximum stomatal conductances were obtained from Nobel (1991) and Waring and Schlesinger (1985). These variables have a wide range of values reported in the literature, however, values used for this study represent the lower end of the range based upon evidence that reduced nutrient availability in boreal regions causes reductions in carbon uptake and stomatal conductances (Schulze *et al.* 1994). Temperature and vapour pressure deficit (VPD) bounds on mesophyll conductance were estimated from values reported in the literature for coniferous and deciduous stands (Waring and Franklin 1979; Waring and Schlesinger 1985; Running 1994; Baldocchi *et al.* 1996; Kimball *et al.* 1997).

The Q_{10} variable quantifies the slope of the relationship between temperature and maintenance respiration. Values of Q_{10} show considerable variation (e.g., between 1.3 and 3) but have an average of approximately 2.0 for most plants (Sprugel *et al.* 1995). A Q_{10} of 2.3 was used for all sites based on observations by Ryan (1991) that the value of Q_{10} may be higher for woody plants than for herbaceous plants and specifically by Baldocchi *et al.* (1996) for the jack pine stand in the SSA.

4.2.3 Remotely sensed data

> '*Any serious quantitative study of a landscape must incorporate some type of remote sensing: There is no other way to obtain consistent measurements across large areas*' (Waring and Running 1998, p. 246).

It is now acknowledged that remotely sensed data provide the only accurate means of deriving the variables needed to drive ecosystem simulation models at regional scales (Aber *et al.* 1993) (§2.3.2). This section describes briefly the pre-processing of the BORIS Landsat TM images (§3.3.1) at the CCRS (§4.3.3.details in-house processing at the University of Southampton).

4.2.3.1 Geometric pre-processing

The data provided to BORIS by CCRS were resampled geometrically using a cubic convolution (CC) algorithm because "It was agreed at the beginning of BOREAS that CC overall is the best compromise, preferable to nearest neighbour (NN), given that all resampling is a trade-off" (Cihlar *pers. comm.*).

NN resampling uses the pixel that has its centre nearest the point located in the image and transfers this pixel to the corresponding location. In comparison, CC resampling uses the surrounding sixteen pixels: Cubic polynomials are fitted along the four lines of four pixels surrounding the point in the image, to form four interpolants. A fifth cubic polynomial is then fitted through these to synthesise a pixel value for the corresponding location (Richards 1993). Therefore, a significant limitation of CC resampling is that the digital number (DN) / radiance relationship is modified irreversibly. It is, therefore, undesirable for further numerical analyses where radiometric accuracy is of prime importance (Schowengerdt 1996). In comparison, NN resampling is 'quicker and retains the radiometric integrity of an image' (Mather 1999, p.85).

Unfortunately, many researchers using BORIS Landsat TM imagery either failed to realise, or chose to ignore the effects of CC resampling and used such imagery 'for numerical analyses where radiometric accuracy is of prime importance' (e.g., Chen and Cihlar 1996; Peddle *et al.* 1997; Middleton *et al.* 1997a; Middleton *et al.* 1997b).

To assess the effect of CC resampling upon the BOREAS imagery, a raw quarter scene (Landsat-5 TM, Path 37, Row 22, acquired on 2 September 1994) was obtained directly from EOSAT. The image was processed in-house at the University of Southampton using NN resampling and compared directly to the same image produced using a CC algorithm by the Canadian Centre for Remote Sensing (CCRS) for BORIS (§3.3.1) (Table 4.1; Plate 4.1).

TM band	Mean radiance (NN)	Maximum difference in radiance	Mean difference in radiance	Mean difference in radiance as % of mean radiance
1	38.12	81	0.207	0.54
2	14.13	110	0.098	0.69
3	12.48	36	0.162	1.30
4	26.96	90	0.514	1.91
5	23.41	122	0.583	2.49
7	6.88	37	0.243	3.53

Table 4.1 Difference in radiance (mW cm^{-2} sr^{-1} μm^{-1}) per band between Landsat TM images resampled with CC and NN algorithms.

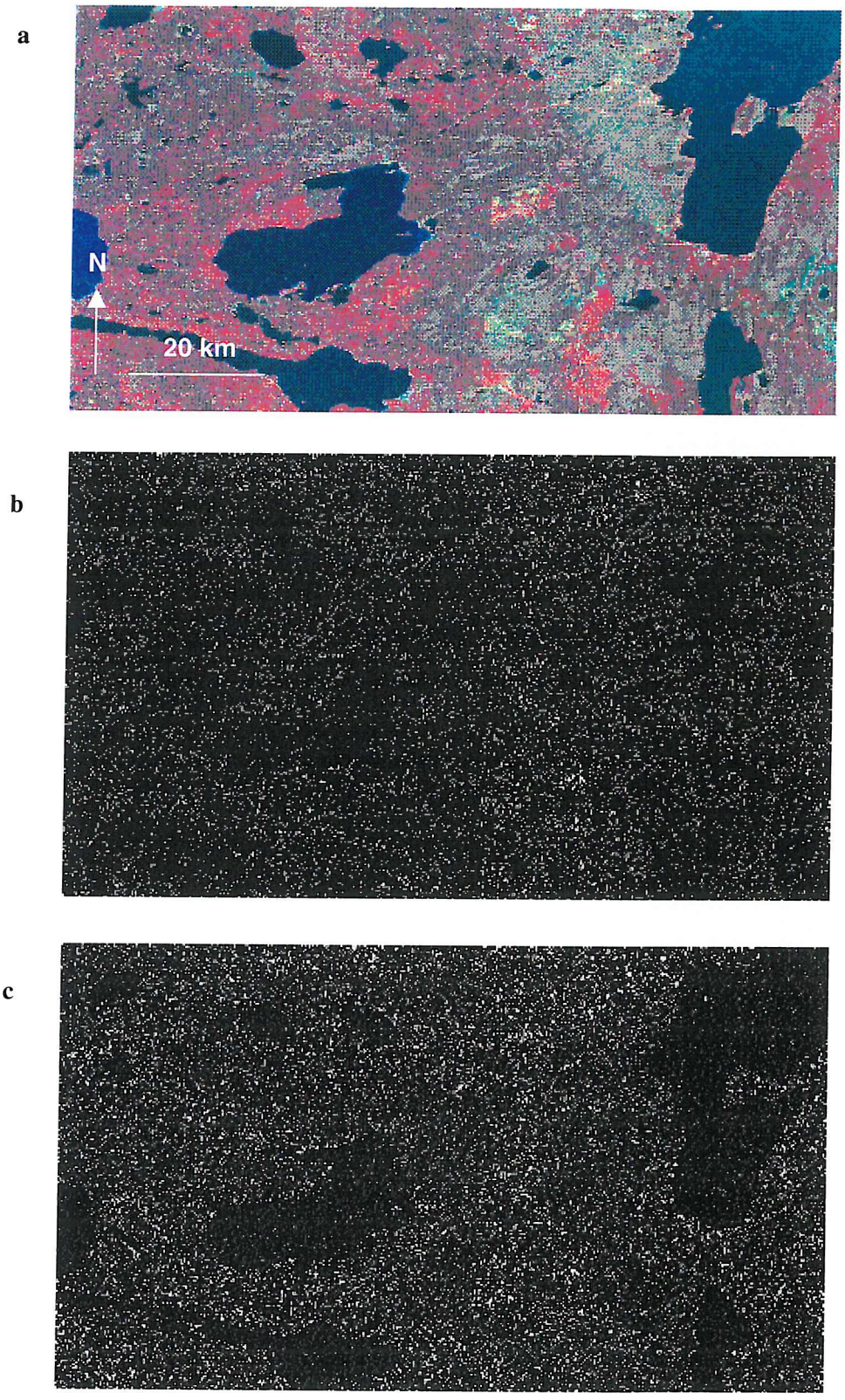

Plate 4.1 A subset of Landsat-5 TM (2 September, 1994). a CC false colour composite RGB (bands 4,3,2 at-sensor radiance) and b and c are radiance difference (CC – NN resampling) bands 3 and 5 respectively.

Table 4.1 shows that mean difference in radiance as a percentage of mean radiance (corresponding to a quantification of introduced error) is small, particularly at shorter wavelengths. An interesting trend is constant increase of mean difference in radiance as a percentage of mean radiance with increasing wavelength. This may be in part a manifestation of signal-to-noise ratio (SNR) (Smith and Curran 1996; 1999). For example, as SNR is related to signal and signal is related to variability (dark surfaces less variable than bright ones), brighter areas, with stronger signal, would be more influenced. However, this is only part of the story as signal (and SNR) peak in NIR, whilst mean difference in radiance between CC and NN increases constantly with wavelength.

Plate 4.1 and Figure 4.3 in particular, illustrate that the greatest difference between the two images was at the boundaries of spectrally distinct features. Fortunately, for this investigation, the choice of resampling algorithm appears negligible as data were used from the shorter wavelengths and the images comprise vast areas of relatively homogeneous forest stands, therefore, the BORIS CC Landsat TM images were used.

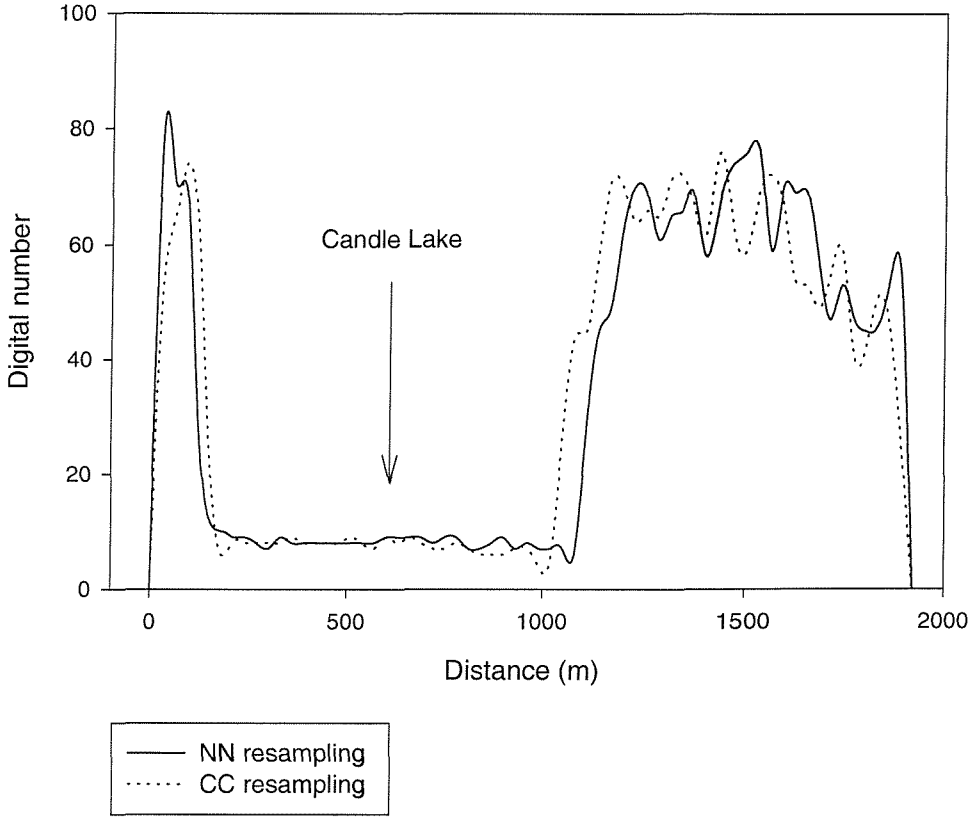

Figure 4.3 Digital number transects across the NN and CC resampled Landsat TM images.

4.3 Methodology

In accordance with the objectives of this pilot study (§4.1), the following section details the methods adopted to initialise (§4.3.1), optimise (§4.3.2) and automate (§4.3.3) FOREST-BGC in order to produce an accurate map of NPP for 20 km^2 of boreal forest.

4.3.1 Stage 1: 'Initialisation'

FOREST-BGC has 20 initial conditions that must be set prior to any simulation, including the initial carbon of the stem, leaves and roots, soil water content and the mass of carbon fixed by photosynthesis in the previous year (Table 4.2) (Korol *et al.* 1991). The model was initialised to estimate NPP for the SSA OJP TFS during 1994. Simulations were compared subsequently to field estimates of Gower *et al.* (1997) (§3.2.1.2).

Input code	Input name (units)	Value
X6	*Start-up mass of carbon fixed by* 'Photosynthesis' (kg)	3200
X8	Leaf carbon (kg)	4033
X9	Stem carbon (kg)	207000
B1	Leaf area index (unitless)	2.42
B2	Canopy light extinction coefficient (unitless)	-0.5
B7	Latitude (°)	53.9163
B8	1 – surface albedo (unitless)	0.8
B11	Maximum canopy leaf conductance (m s^{-1})	0.001
B12	Leaf water potential at stomatal closure (MPa)	2.0
B13	Leaf conductance humidity reduction (ms^{-1} μm^{-1} cm^{-3})	0.05
B15	Photosynthetic response coefficient (kJm^{-2} d^{-1})	9720
B16	Maximum mesophyll conductance (m s^{-1})	0.0008
B17	Minimum photosynthesis temperature (°C)	0
B18	Maximum photosynthesis temperature (°C)	40
B19	Leaf respiration coefficient (kg kg^{-1} $°C^{-1}$ d^{-1})	0.003
B20	Stem respiration coefficient (kg kg^{-1} $°C^{-1}$ d^{-1})	0.002
B23	Temperature coefficient, mesophyll conductance (°C)	4.0
B25	Q_{10} response coefficient for respiration (°C)	2.3
B26	Maximum leaf nitrogen concentration (kg)	0.004
B45	Root growth respiration (kg)	0.35

Table 4.2 Critical input variables for SSA OJP 1994 (§4.2.2 details data acquisition).

Initialisation simulations

Mean daily plots of the FOREST-BGC simulation of the 1994 carbon balance for the SSA OJP site are presented in Figure 4.4. Simulated Gross Primary Production (GPP) was low, ranging from 0 to 3.9 g C ha^{-1} day^{-1} over the year, with mean daily fluxes of 2.39 g C ha^{-1} day^{-1} during the growing season. Simulated maintenance respiration at the site, ranging from 0.7 to 4.9 g C ha^{-1} day^{-1} over the year. GPP exceed respiration over an 83-day period from April 12 to August 13.

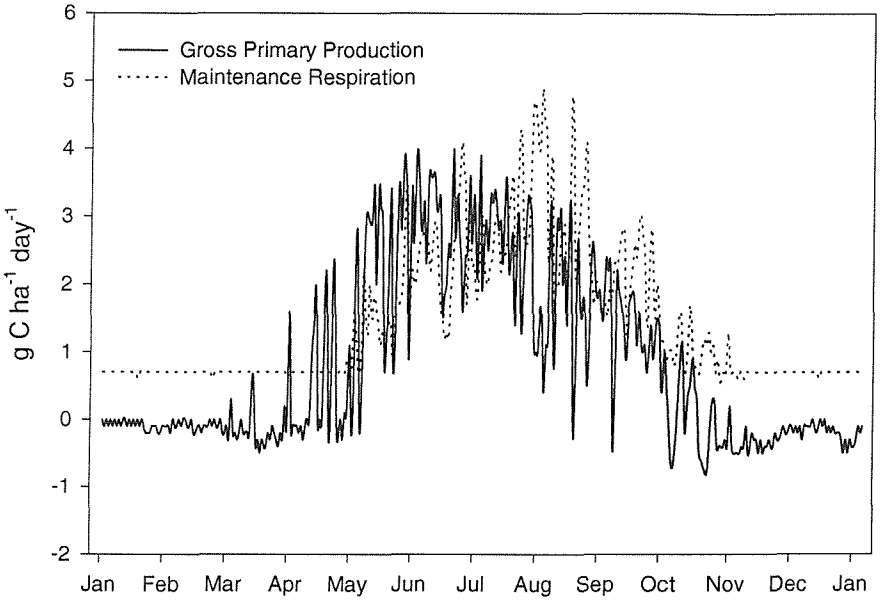

Figure 4.4 Simulated seasonal canopy processes at SSA OJP during 1994.

4.3.1.1 FOREST-BGC sensitivity analysis

An analysis of the sensitivity of FOREST-BGC to its input values was undertaken using 1994 data from the SSA OJP TFS. Determination of the most influential inputs would suggest those that could be explored with the greatest potential in terms of intra-site and species variation (inextricably linked) for development of 'ecophysical' input libraries to facilitate generalisation / spatial scaling. Model sensitivity was examined by running FOREST-BGC with a 'standard' input file the result of initialisation, to generate a 'standard' output file. Subsequent model runs involved varying each input individually by +20% and then -20% of its range, allowing comparison with the 'standard' outputs.

Sensitivity analysis simulations

Simulation differences demonstrate the sensitivity of the model to variation in input values (Table 4.2) and emphasise model assumptions about how the system functions (Dewar and Cannell 1992). Table 4.3 shows the twenty most influential inputs upon the simulation result.

Input code	Input name	Rank
B1	Leaf area index (unitless)	1
X6	*Start-up mass of carbon fixed by* 'Photosynthesis' (kg)	2
B7	Latitude (°)	3
B16	Maximum mesophyll conductance (m s^{-1})	4=
B23	Temperature coefficient, mesophyll conductance (°C)	4=
X8	Leaf carbon (kg)	6
B25	Q_{10} response coefficient for respiration (°C)	7
B19	Leaf respiration coefficient (kg kg^{-1} $°C^{-1}$ d^{-1})	8
B11	Maximum canopy leaf conductance (m s^{-1})	9
B13	Leaf conductance humidity reduction (m s^{-1} μm^{-1} cm^{-3})	10
B8	1 – surface albedo (unitless)	11
B15	Photosynthetic response coefficient (kJ m^{-2} d^{-1})	12
B26	Maximum leaf nitrogen concentration (kg)	13
B17	Minimum photosynthesis temperature (°C)	14=
B18	Maximum photosynthesis temperature (°C)	14=
B20	Stem respiration coefficient (kg kg^{-1} $°C^{-1}$ d^{-1})	16
B45	Root growth respiration (kg)	17
X9	Stem carbon (kg)	18
B2	Canopy light extinction coefficient (unitless)	19
B12	Leaf water potential at stomatal closure (MPa)	20

Table 4.3 Rank of input value influence upon simulation result.

The sensitivity analysis of FOREST-BGC was instructive in distinguishing input values that:

1. have a major impact on productivity (photosynthesis, mesophyll conductance, respiration coefficients and the restrictions on photosynthetic temperature).
2. have a relatively small impact on productivity (soil water content, canopy light extinction coefficient, leaf water potential, nitrogen availability and photosynthetic compensation point).

Although, Table 4.3 shows the rank of the twenty most influential inputs to FOREST-BGC it is not until these are classified and plotted that their influence becomes apparent (Figure 4.5). The prominence of groups of inputs may be distinguished clearly, for example, the over-riding importance of 'respiration' and 'photosynthetic' inputs as opposed to those of the 'soil' group.

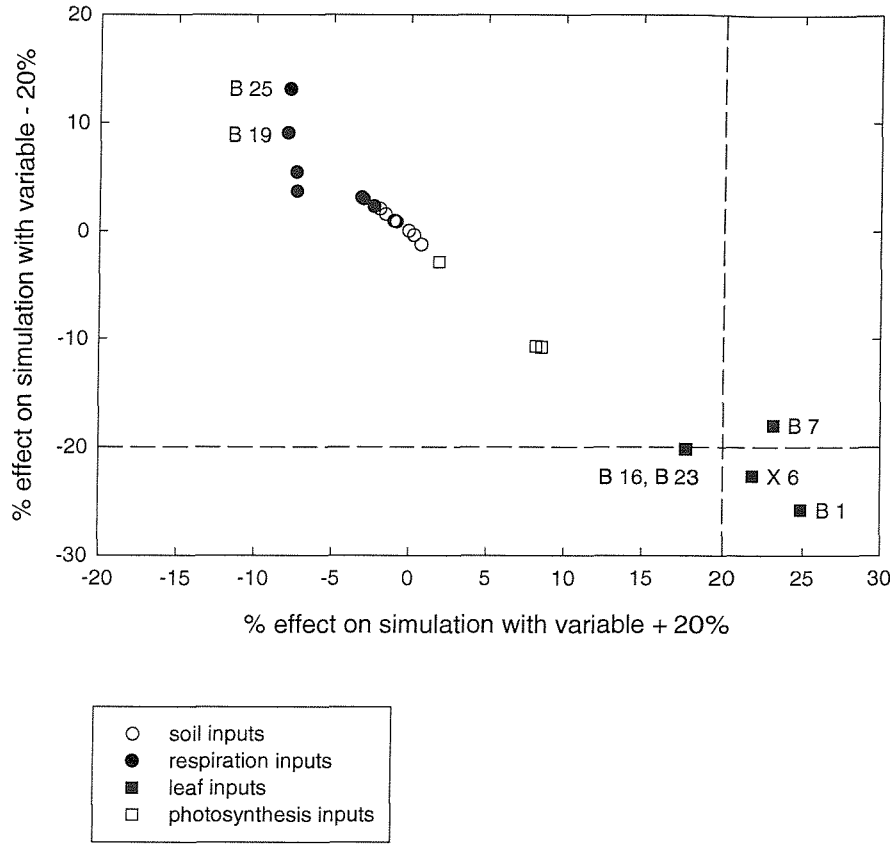

Figure 4.5 The influence of individual inputs upon the simulation result.
(Some input codes are included for illustration, see Table 4.3 for all input codes).

Hence, the model was run for a single site and its sensitivity to individual inputs established. The next step, towards regional estimates of NPP, was to ascertain whether the model could be run to estimate NPP accurately for a number of sites.

4.3.2 Stage 2: 'Optimisation'

In this instance, 'optimisation' is taken to mean running the model for a number of sites and assessing simulations for accuracy.

Climate data files were generated for several other sites of varying species type (including, aspen and black spruce) (§4.2.1). FOREST-BGC was then run for 11 sites within the BOREAS SSA, incorporating ecophysical input libraries (Table 4.4), to increase the accuracy of simulations.

4.3.2.1 Simulation accuracy assessment

When driving a forest ecosystem simulation model it is necessary to determine how close model simulations are to the observed state of the real system (Running 1994; Lucas and Curran 1999). Hence, accuracy assessment may be defined as the comparison of model simulations with observations from the real world, together with an assessment of model performance. To date, ecological modelling has been criticised for its lack of such accuracy assessment (Running 1994). Hence, if ecological modelling is to gain credibility as a research tool for spatial and temporal extrapolation, a measure of 'quality control' is essential (Burke *et al.* 1990; Lucas and Curran 1999). For example, Aber *et al.* (1993) recommended a comparison of model 'predictions' with data not used in the construction or calibration of the model.

According to Running (1994), it is not possible, practically, to determine the accuracy of models of systems as complex as an ecosystem. However, it is practical to determine the accuracy of certain model outputs as a measure of the model's function, in the same way that temperature and blood chemistry are used as a measure of bodily function (Lucas and Curran 1999). Hence, for this investigation, emphasis was placed upon model outputs (as opposed to structure) because although the model is being used to explore the workings of the system and increase understanding, the ultimate aim of the pilot study is to make simulations that will replace observations.

Little guidance has been published regarding accuracy assessment (e.g., Thornley and Johnson 1990; Trenberth 1992; Mitchell 1997). Hence, accuracy is often presented as scatter graphs of prediction against observation (e.g., Aber and Federer 1992; Warnant *et al.* 1994), sometimes analysed using regression, which is intended to be an objective and quantitative measure of model accuracy (e.g., Reckhow *et al.* 1990; Flavelle 1992; Parton *et al.* 1993; Mayer *et al.* 1994; Paruelo and Sala 1995; Woodward *et al.* 1995; Coops 1999). However, given that accuracy comprises both precision and bias (Figure 4.6) (Webster and Oliver 1990), the value of regression is limited as it fails to give information on individual deviations (i.e., quantitatively for each simulation, how far the model fails to simulate the natural system). Therefore, in addition to regression, the method of Mitchell and Sheehy (1997) was adopted. Deviations (prediction minus observation) are displayed graphically along the range of model operation, enabling evaluation of the uniformity of model performance. The criteria for adequacy are defined, prior to model simulations, as (i) the envelope of acceptable error and (ii) the proportion of points that must lie within it.

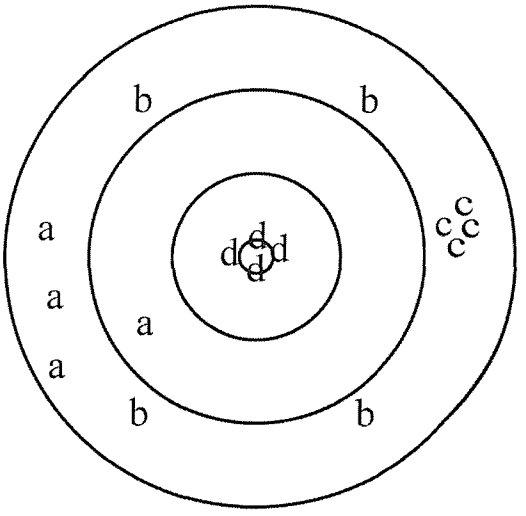

Figure 4.6 Using a target to define accuracy: **a** are imprecise and biased, **b** are imprecise and unbiased, **c** are precise and biased and **d** are precise and unbiased = accurate.

Optimisation simulations

Determination of the most influential inputs (Table 4.3) assisted with the development of ecophysical libraries. Only seven of the 'critical input variables' (Table 4.2) needed updating for these optimisation simulations (Table 4.4).

Input code	Input name (units)	sensitivity rank	jack pine	black spruce	aspen
B1	Leaf area index (m^2 m^{-2})	1	(2.39) [a]	(1.67)	(2.94)
X8	Leaf carbon (kg)	6	4033	6400	1200
B22	Specific leaf area (m^2 kg C)	-	6	6	22.5
B7	Latitude (°)	3	(53.9163)	(53.9987)	(53.6293)
X6	Photosynthesis (kg)	2	3900	4500	3200
B19	Leaf respiration coefficient (kg kg^{-1} $°C^{-1}$ d^{-1})	8	0.0003	0.0003	0.0004
B20	Stem respiration coefficient (kg kg^{-1} $°C^{-1}$ d^{-1})	16	0.013	0.012	0.01
B21	Root respiration coefficient (kg kg^{-1} $°C^{-1}$ d^{-1})	-	0.0005	0.0005	0.0003
B45	Root growth respiration (kg)	17	0.35	0.35	0.5

[a] values shown in brackets are specific to the TFS of the SSA
[b] all remaining FOREST-BGC inputs were held constant for simulations

Table 4.4 Ecophysical input libraries for FOREST-BGC (§4.2.2 details data acquisition).

Black spruce and old jack pine sites had generally low rates of GPP ranging from 0 to 5.7 and 0 to 3.9 g C m^{-2} day^{-1}, respectively, over the year. Maintenance respiration rates for these sites were relatively high: GPP exceed maintenance respiration for only 108 (SSA OBS) and 83 (SSA OJP) days (Figure 4.7). Such low productivity may be attributed to high respiration costs and a lack of soil water towards the end of the growing season. In contrast, simulations of annual NPP at aspen and young jack pine sites were considerably greater, due primarily to lower maintenance respiration costs.

Simulations were compared to field estimates of Gower *et al.* (1997) (§3.2.1.2). As models are simplifications of reality, they are rarely perfect (Mitchell 1997). Therefore, it seems reasonable to suggest that the degree of acceptable error may be defined with respect to the purpose of the model. With respect to this investigation, 90% of simulations fell within the degree of acceptable error (+/- 0.3 kg C ha^{-1} yr^{-1}) (Aber *et al.* 1993; Lucas and Curran 1999; Gu *et al.* 1999), defined prior to optimisation (Figure 4.8a). An r^2 of 0.86 between simulated NPP and the field estimates of Gower *et al.* (1997) confirmed the strong relation (Figure 4.8b). The one anomaly was an auxiliary site and the apparent model overestimate may be a manifestation of using a non-site-specific allometric equation (§3.2.2.5) (Santantonio 1988; Gower *et al.* 1997).

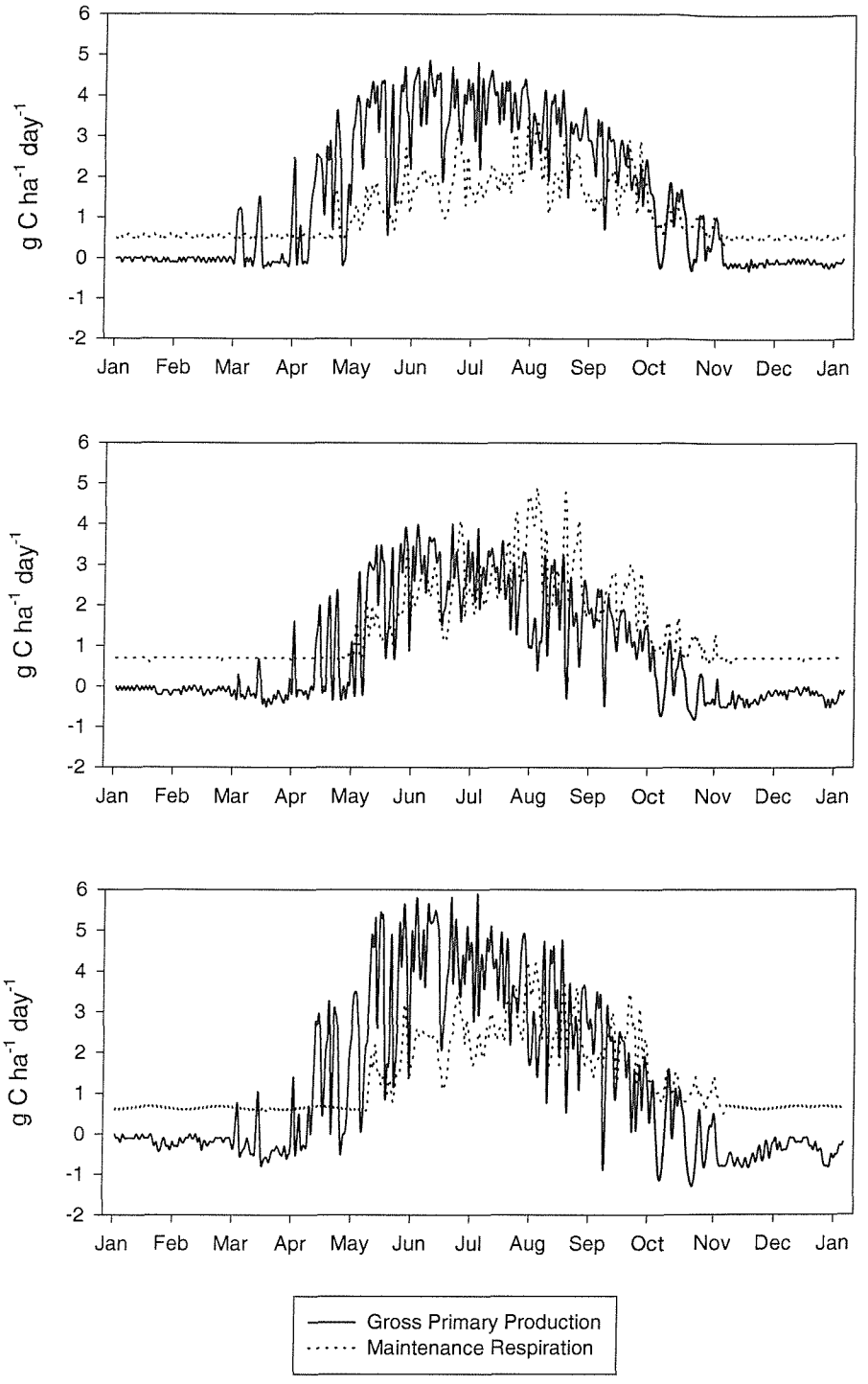

Figure 4.7 Simulated seasonal canopy processes at three SSA TFS during 1994.

a

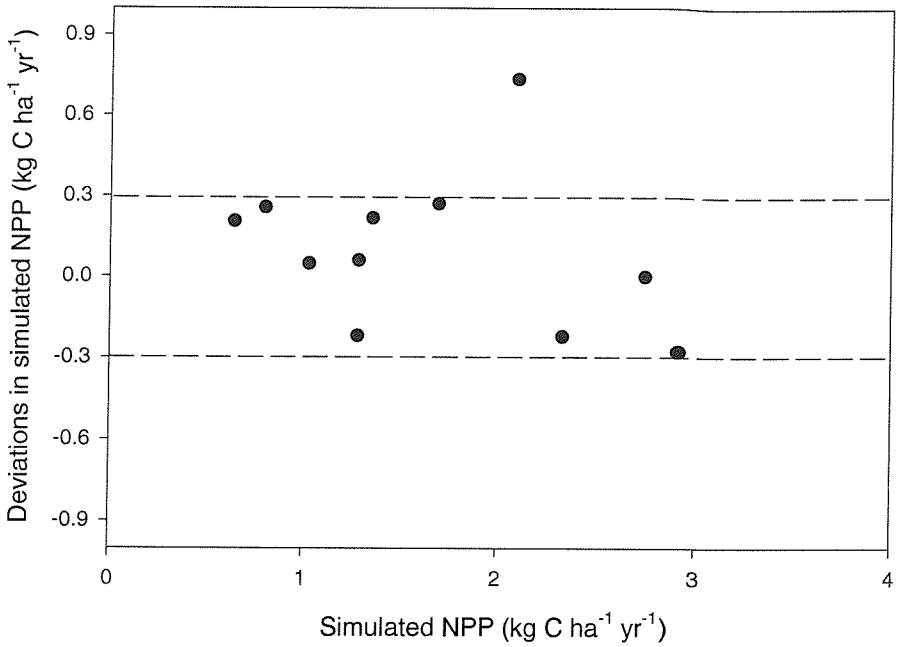

b

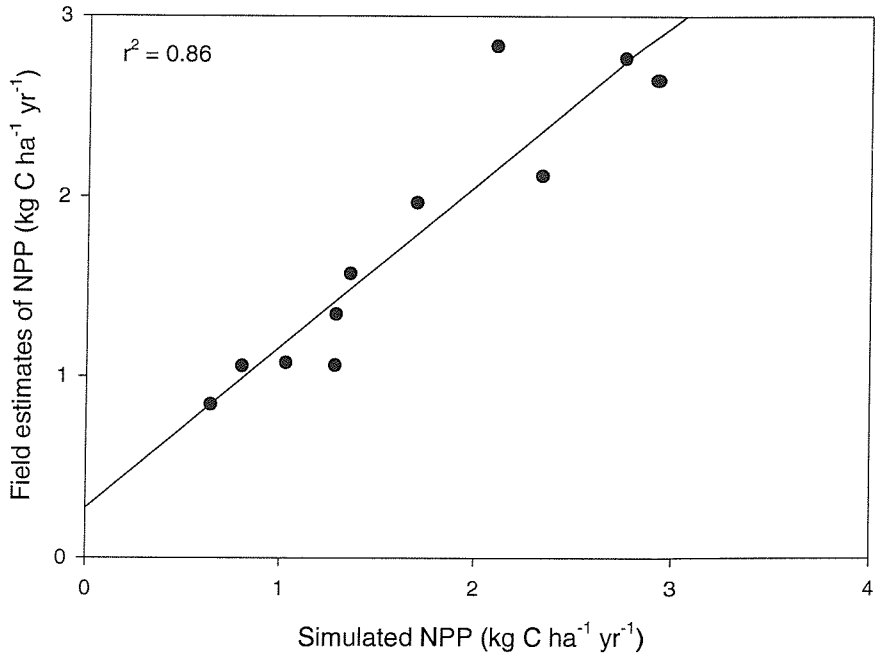

Figure 4.8 Results of accuracy assessment: **a** deviations, **b** regression.

Variables for the simulation of various boreal species were chosen as a consequence of two processes: First, an intensive study of published data appropriate for ecosystems with a boreal climate; and second, the sensitivity analysis, which illustrated those inputs with the greatest potential to influence the simulation result.

Climate and LAI alone can account for much of the productivity of ecosystems (Running and Coughlan 1988). Unsurprisingly fundamental life-form variables of specific leaf area, leaf carbon, respiration, etc., appear to be of greatest importance. Of less importance it would appear are soil moisture status and nitrogen availability. Such conclusions, however, could be dismissed as circular logic since this is precisely the hierarchy incorporated into the model structure (Running and Hunt 1993). However, of particular interest is how well the model simulates spatial variability of ecosystem-level processes. Recognition of those inputs left unchanged for simulations is also crucial: reliance upon variables of western conifers (for which FOREST-BGC was developed initially) to represent the range of boreal species encountered within this study is acknowledged.

4.3.3 Stage 3: 'Automation'

Accuracy assessment of the optimisation simulations demonstrated that FOREST-BGC can be run to simulate NPP accurately for a number of sites within a region (Figure 4.8). The next step was to run the model over the entire region to generate a map of NPP.

4.3.3.1 Estimation of LAI for boreal forests using Landsat TM imagery

Remote sensing provides a means of obtaining the distribution of LAI over large areas (§2.3.2). Green leaves absorb solar radiation selectively in comparison to non-vegetative surfaces. At visible wavelengths, green leaves have strong absorption with little reflectance or transmission, whereas at NIR wavelengths reflectance is high (due to scattering) with little absorption but medium transmission. Radiation from visible and NIR wavelengths have, therefore, been used to formulate various vegetation indices as indicators of LAI (Jordan 1969; Deering 1978; Qi *et al.* 1994; Turner *et al.* 1999). Among the various vegetation indices, the normalised difference vegetation index (NDVI) (Deering 1978):

$$NDVI = \frac{NIR\ radiance - Visible\ radiance}{NIR\ radiance + Visible\ radiance} \tag{4.7}$$

and the simple ratio (SR) (Jordan 1969):

$$SR = \frac{NIR\ radiance}{Visible\ radiance} \tag{4.8}$$

Both have been used to estimate LAI and other biophysical variables accurately from remotely sensed data (e.g., Sellers *et al.* 1994; Chen and Cihlar 1997; McMichael *et al.* 1999; Ikeda *et al.* 1999; Lymburner *et al.* 2000). Recent studies have revealed that the addition of radiation from MIR wavelengths (3.0 - 5.0 μm), where necessary, may increase the accuracy of estimates even further (Laporte *et al.* 1995; Foody *et al.* 1996; Boyd 1996; DeFries *et al.* 1997; Mantovani *et al.* 1997; Boyd *et al.* 1999).

In this instance, the method for producing a LAI map consisted of four stages:

1. collection and processing of a Landsat TM scene of the BOREAS region that had been recorded during the 1994 growing season;
2. extraction of radiance values for areas that concurrent field estimates of LAI had been obtained;
3. determination of the relationship between a vegetation index and LAI and
4. use of this relationship and values of the vegetation index to estimate LAI for other areas.

Landsat TM processing

A cloud free scene of the BOREAS SSA (2 September 1994, path 37 row 22) was chosen for the purpose of this study (Plate 4.1a). The scene was acquired at a solar zenith angle of 40.10°. The image had limited pre-processing at the CCRS (§4.2.3). Radiometric corrections (DN to radiance) were made using coefficients (gains and offsets) provided in the image header information. Thirty ground control points were used to geometrically correct the image to an accuracy of less than ± one pixel (root-mean-square error (RMSE) of ± 9.2 m).

Relations between ground and remotely sensed data

Concurrent ground based estimates of LAI taken by researchers affiliated to BOREAS RSS04 ($LAI_{training}$) (§3.2.1.1) were regressed against TM radiance data at nine plots (Wülder *et al.* 1996; Cusack *et al.* 1999). The TM derived values were computed initially using single TM pixels at the specific plot geometric locations. This was followed by using mean values from 3 by 3 TM pixel windows to reduce the possible influence of the geometric error and the chance variability due to the location of the centre pixel (Ahern *et al.* 1991; Franklin *et al.* 1997; Atkinson and Emery 1999). However, no difference in results were found (at the 95% significance level) compared to the single pixel analysis (Figure 4.9).

There have been numerous studies on the relationship between derived vegetation indices and LAI in forest stands (e.g., Foody *et al.* 1996; Chen and Cihlar 1997; Franklin *et al.* 1997; Chen *et al.* 1997; Cihlar *et al.* 1998; Cusack *et al.* 1999). However, the continuing lack of

understanding behind the interaction of radiation with structurally complex forest stands and the difficulty of obtaining quality ground-based measurements have plagued such investigations (Nemani *et al.* 1993; Spanner *et al.* 1994; Peddle *et al.* 1996; Jasinski 1996). In particular, research based on the relations of NDVI with biophysical variables has recently come under intense scrutiny within the remote sensing community because of a lack of robust relationships (Dawson *et al.* 1999a). The nature and strength of NDVI – LAI relationship is explored in greater detail within Chapter 7 of this thesis. For the purpose of this pilot study, however, it was decided that the linear relation (in this particular case) between LAI and NDVI, in conjunction with other NDVI values, was adequate for generating a map of LAI to drive FOREST-BGC. The coefficient of determination (r^2) was 0.92 between NDVI and LAI (Figure 4.10).

In accordance with Cusack *et al.* (1999), values of NDVI obtained from the Landsat TM were estimated with ground estimates of LAI (§3.2.1.1) using the derived linear predictive regression relation:

$$LAI = 13.687 NDVI - 1.411 \tag{4.9}$$

The choice of a mapping method for a biophysical variable has critical implications for accuracy, representation of spatial pattern and scale and for correlation of the biophysical variable with other spatial variables (Dungan *et al.* 1994). As the relation was between LAI and NDVI was strong, aspatial regression was considered appropriate for the purpose of this pilot study (Dungan 2000). However, two alternatives to aspatial regression for producing spatially extensive estimates of LAI (cokriging and conditional simulation) are explored within Chapter 6.

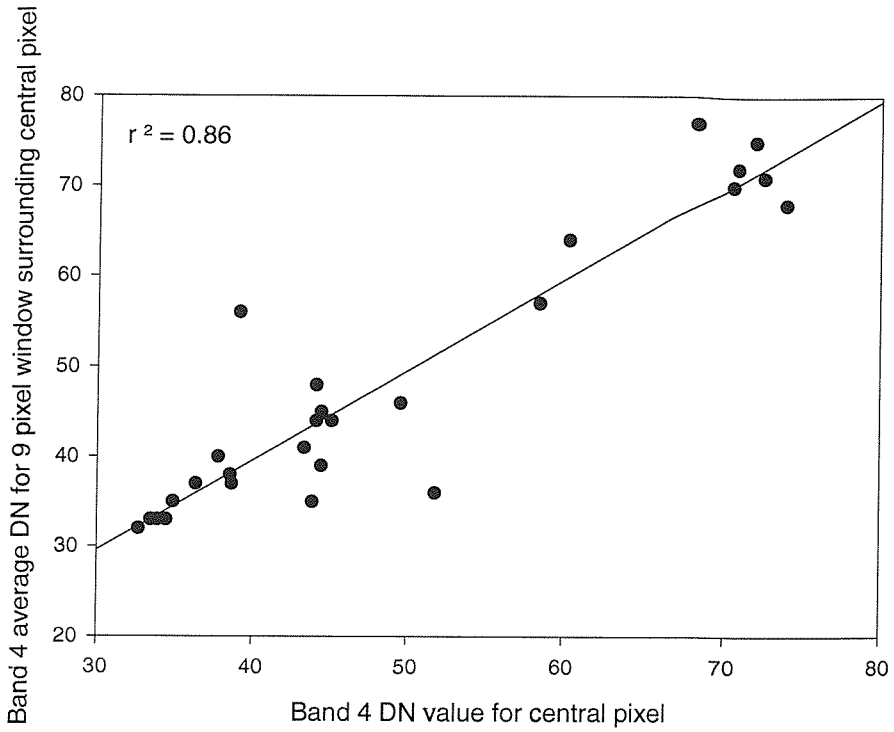

Figure 4.9 Comparison of using a single pixel and 3 by 3 pixel window for extraction of remotely sensed data values (Landsat TM Band 4).

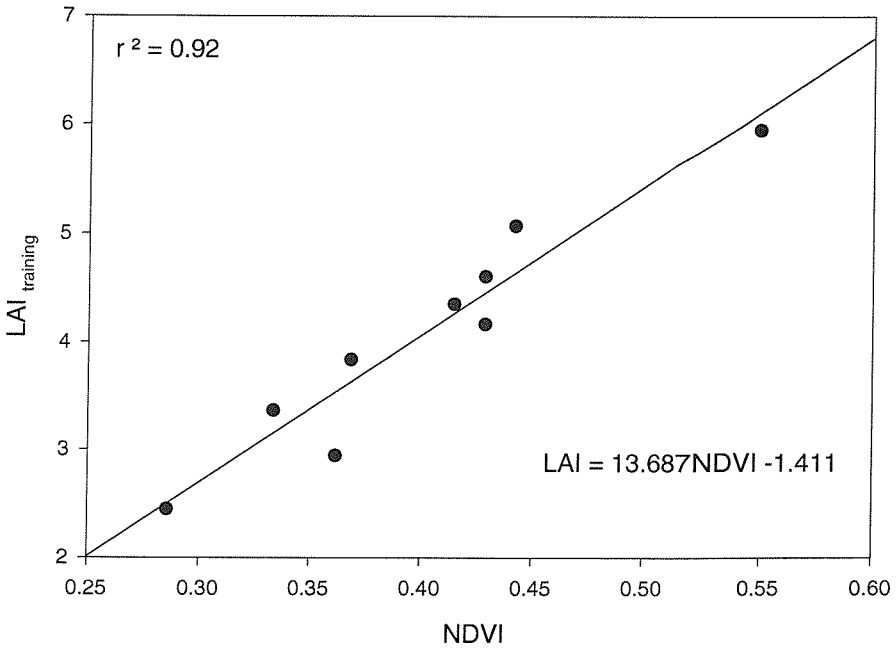

Figure 4.10 Relationship between NDVI and $LAI_{training}$.

4.3.3.2 Spatial estimates of NPP

Having produced spatial estimates of LAI, the main variable which drives FOREST-BGC, the aim was to run the ecosystem simulation model on a per-pixel basis in order to produce a map of NPP for 20 km^2 of boreal forest.

The generation of a look-up-table

The generation of a look-up-table (LUT) made the task of running FOREST-BGC on a per-pixel basis considerably more efficient. The model was run to encompass the range of data within the LAI map and values plotted against simulated NPP (Figure 4.11). The reduction in NPP above LAI values of 5 may be attributed to increased autotrophic respiration and decomposition (Ryan *et al.* 1997; Calow 1998) and reduced photosynthesis (Drake *et al.* 1997), a manifestation of less sunlight penetrating the canopy. This is supported by logic incorporated into the FOREST-BGC code (§2.4).

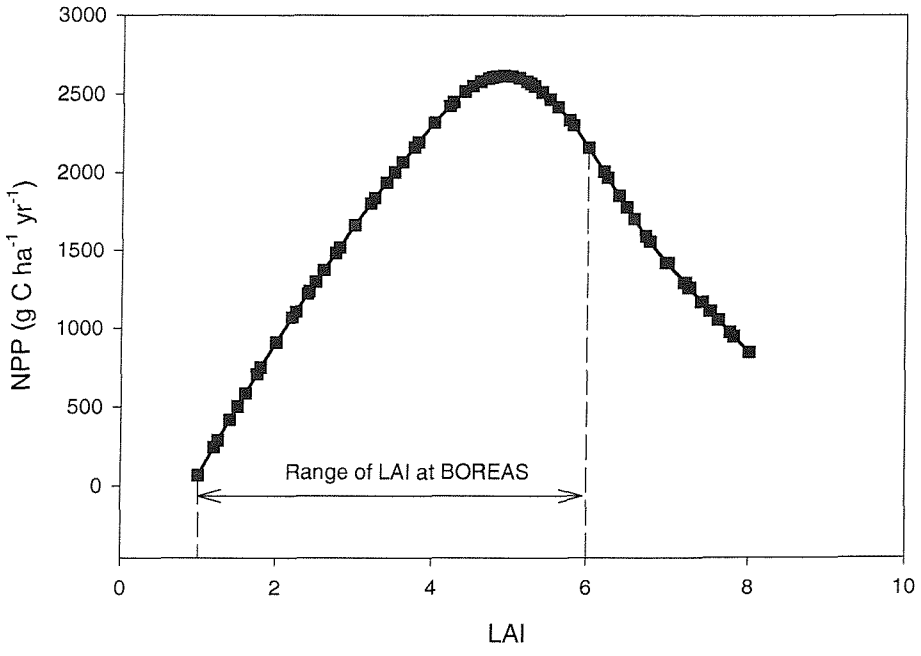

Figure 4.11 The curve produced from FOREST-BGC simulations used for the generation of a look-up-table.

Within Microsoft Excel, a second order polynomial was used to describe the LUT data:

$$NPP = 177.05\ LAI^2 + 1708\ LAI - 1693.2 \qquad (4.10)$$

The LUT was used to produce of a map of NPP for 20 km^2 of boreal forest (Plate 4.2).

Automation simulations

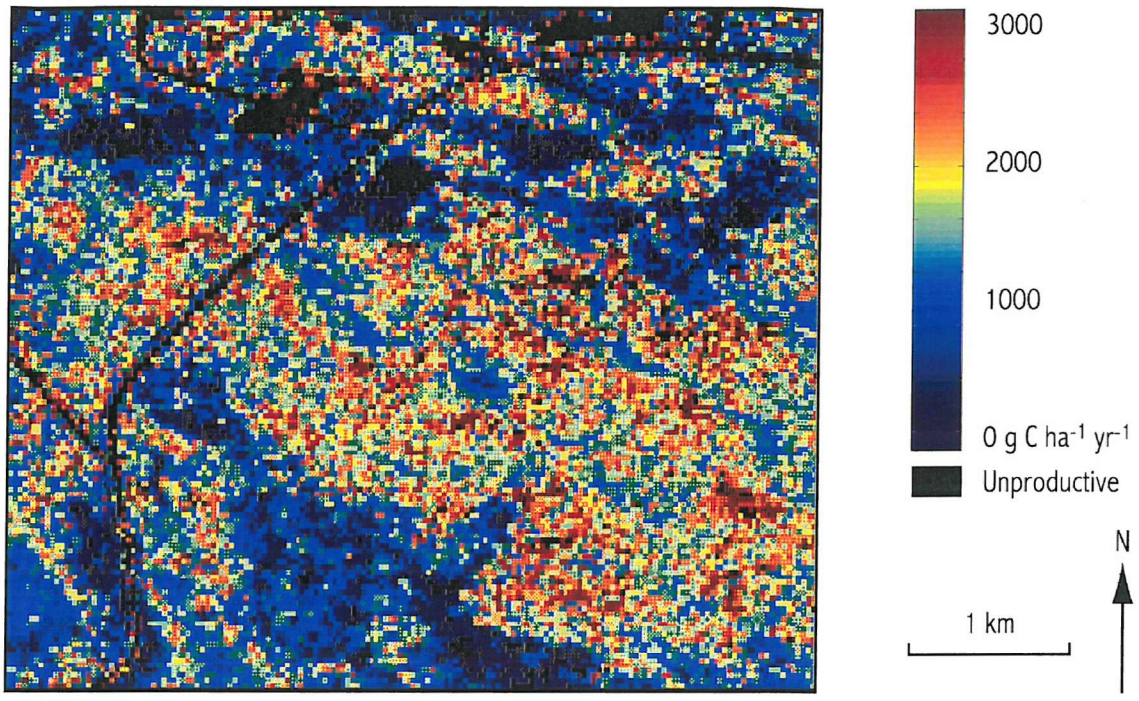

Plate 4.2 A map of NPP for a 20 km^2 subset of the SSA.

Accuracy assessment with BERMS field estimates (§3.2.2) was essential to ensure the credibility of such a map. Model simulation accuracy was very similar to the optimisation stage of the pilot study, with 88% of estimates within ± 0.3 kg C ha^{-1} yr^{-1} (Figure 4.12).

According to Curran and Atkinson (1999, p.17), 'the challenge of spatial dependence is that of choosing a spatial dimension best suited to a specific application'. As large areas of relatively homogeneous forest stands may be distinguished within Plate 4.2, this may lead to questioning whether the 30 m pixel size of Landsat TM images is the 'best suited' for estimating boreal forest characteristics at regional scales, particularly in the context of Figure 4.9.
Also, there is an obvious degree of inflexibility associated with the adoption of a global LUT, in that local adaptation is not possible. Much could be achieved by automation of the stages of the spatial estimation of NPP presented within this pilot study. Rather surprisingly, automation may offer a degree of flexibility, in that by adapting progressively a number of inputs to FOREST-BGC, assumptions made concerning their spatial variation are minimised. Indeed, within this pilot study it is only the biophysical data derived from remote sensing which give a spatial context to the ecosystem simulation model. The incorporation of a fine resolution (100 m pixel size or finer) digital elevation model (DEM) and additional topographic variables, such as slope and aspect would be a significant development.

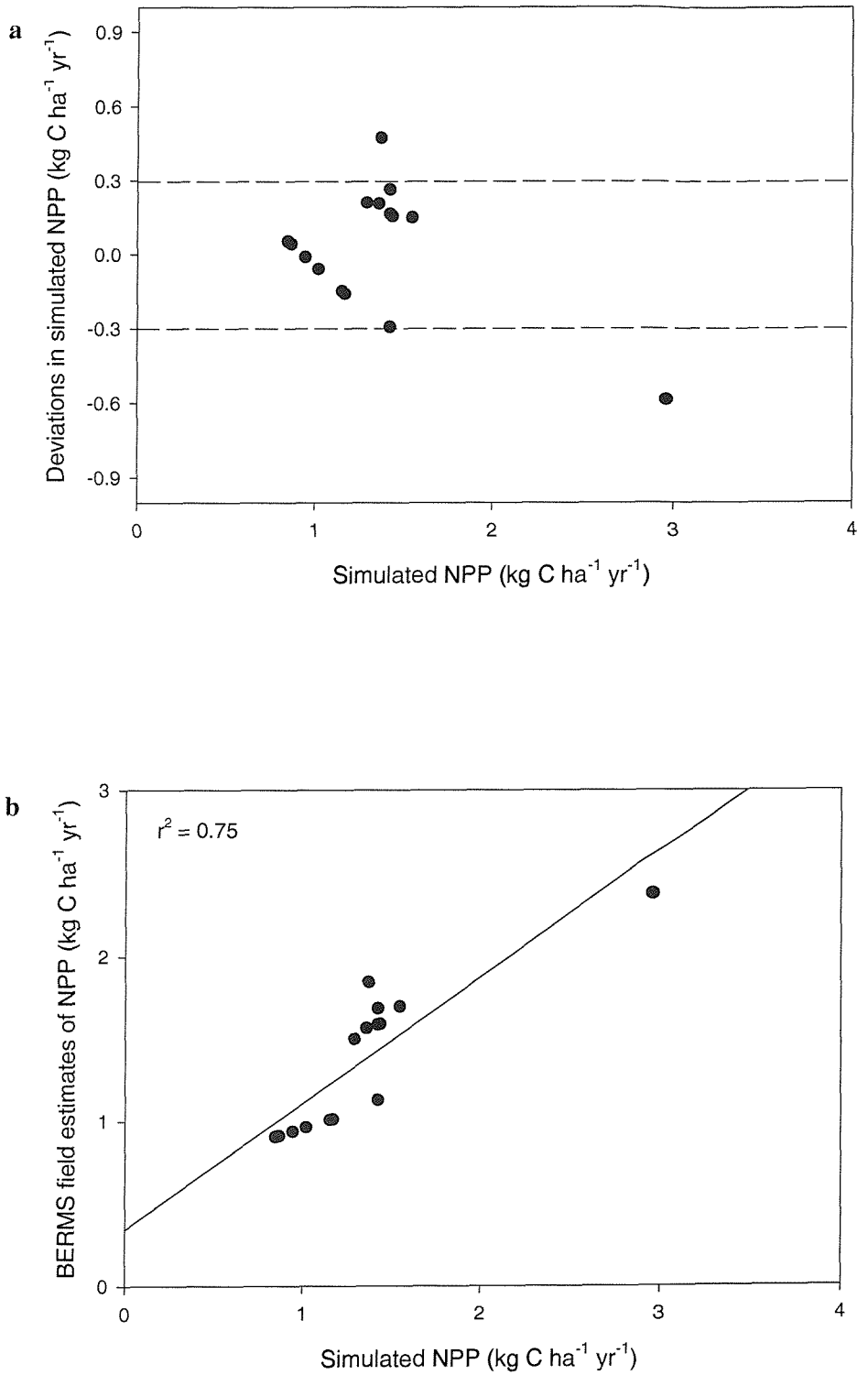

Figure 4.12 Accuracy assessment for 20 km^2 map of NPP: **a** deviations, **b** regression.

4.4 Conclusion

FOREST-BGC was initialised and optimised with a range of data from the BORIS as well as species-specific data from unpublished site observations and detailed literature searches. Comparisons between model simulations and ground estimates of NPP were extremely encouraging, especially given the general nature of FOREST-BGC with regard to stand morphology (§2.4.3). Running and Coughlan's (1988) observations that climate and LAI alone can represent much of the productivity of ecosystems were confirmed. However, by testing the sensitivity of the ecosystem simulation model to its inputs, those variables that have a major impact upon the storage of carbon in boreal forests and are likely to be sensitive to climate change were distinguished.

Realisation of the third objective of this pilot study: To produce an accurate map of NPP for 20 km^2 of boreal forest, highlighted several avenues for further research (Chapter 4A, p. 110). The general correspondence between predicted values of NPP and observed ground estimates indicated that driving FOREST-BGC with data derived from remote sensing provides a sound framework for modelling at regional scales.

Chapter 4A

The Way Forward

A review of the literature, study area selection, data acquisition and completion of the pilot study emphasised four key areas for further investigation (Figure 4A.1). Given the importance which FOREST-BGC assigns to LAI (§2.4; §4.3.1), the ability to maximise the accuracy of spatial estimates of LAI from remotely sensed data was particularly evident:

1. The Landsat TM 30 m pixel may be an inappropriate unit for the spatial representation of boreal forest biophysical variables at regional scales. **Chapter 5** investigates the choice of an *optimum* sampling unit for such investigations.
2. Although appropriate for the pilot study, with a coefficient of determination of 0.92 over 20 km^2 of relatively homogeneous forest stands, global aspatial regression fails to account for spatial configuration of the data. **Chapter 6** explores whether geostatistical prediction methods offer increases in accuracy for regional scale studies.

Data considerations, in particular, a lack of cloud- and haze-free Landsat TM imagery, combined with 'scaling-up' to produce accurate spatial estimates of NPP at regional scales prompted a switch to coarse spatial resolution satellite sensors. Therefore, NOAA AVHRR imagery was adopted to maximise the accuracy with which LAI could be estimated:

3. The use of NDVI only makes use of radiation from the visible and near-infrared wavelengths of the electromagnetic spectrum. **Chapter 7** assesses the potential of using MIR (3.0-5.0 μm) radiation acquired by the AVHRR.
4. Uncertainties still exist surrounding the nature and magnitude of various feedbacks and the total response of the boreal forest ecosystem to the effects of climate change (Coops 1999). For example, warmer air temperatures and longer growing seasons may enhance evapotranspiration rates, whilst lower humidity and reduced soil water levels could minimise evapotranspiration by inducing water stress (§2.2.2). Such issues require further investigation and are explored in greater detail within **Chapter 8**. Because the southern portion of the boreal forest appears more sensitive to warmer drier conditions than more northerly regions due to the longer growing season (Kimball *et al.* 1997), the remainder of this thesis concentrates attention on the BOREAS SSA.

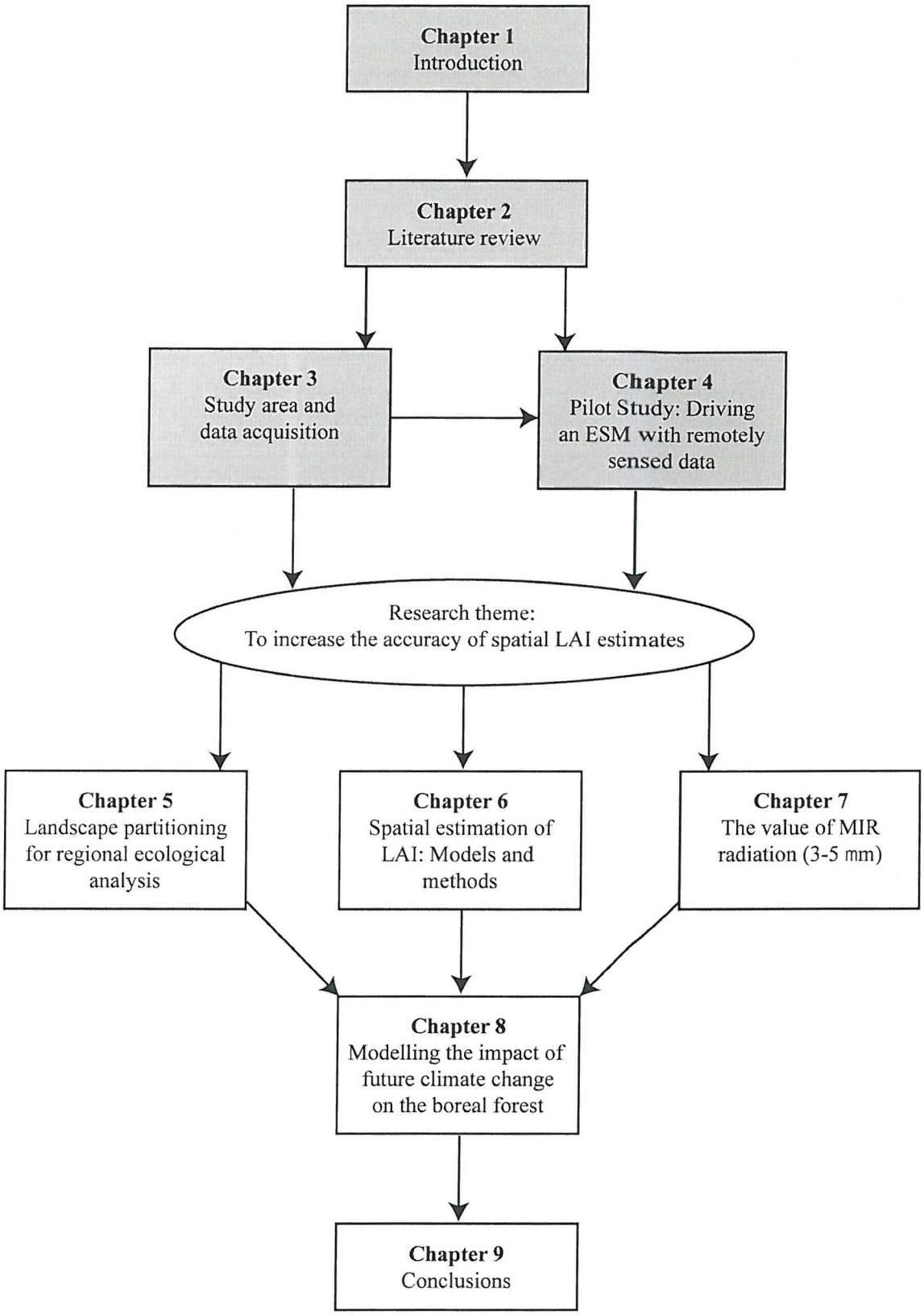

Figure 4A.1 Progression through the thesis structure.

Chapter 5

Landscape Partitioning for Regional Ecological Analysis

This chapter addresses the issues of scale and the choice of an *optimum* sampling unit for the study of forested landscapes using remotely sensed data. Scale and scaling-up were investigated through (i) determining if there is a spatial resolution above which information loss increases rapidly and (ii) developing a technique to partition remotely sensed images into relatively homogeneous 'areal sampling units' (ASU) in order to optimise estimates of biophysical variables for subsequent input to ecosystem simulation models.

5.1 Introduction

Over the past few hundred years researchers have developed a reasonably sound understanding of how Earth system processes operate at the local scale (i.e., a scale somewhere between cells/leaves and fields/trees) (Curran and Atkinson 1999). However, the problem of estimating carbon pools and fluxes requires an understanding at regional to global scales (Foody and Curran 1994b). Researchers have tried to address such regional to global scale problems by scaling-up local understanding (e.g., Aber and Federer 1992; Reich *et al.* 1999). However, in reality because components of the environment interact (Grace *et al.* 1997) such scaling attempts may be inappropriate / inaccurate. Indeed, representing the variability of forest systems quantitatively is a daunting task, given that there is no single approach 'appropriate' for the ecological analysis of landscapes (Waring and Running 1998).

5.1.1 Aims of investigation

Points in a landscape that are near to each other are more alike than those that are further away and the degree of dissimilarity depends on both spatial autocorrelation in the landscape and the sample unit size of the remotely sensed observations (Curran and Atkinson 1998). The 'challenge' of spatial dependence is that of choosing a spatial dimension best suited to a specific application (Curran and Atkinson 1999).

The objective of this chapter is to present one such example, resulting in a dynamic technique for partitioning a forested region into ASU. The ASU can be used subsequently to derive biophysical variables for use within regional scale modelling studies, solving several inadequacies of current estimates of NPP at regional scales. This objective may be broken down into three aims:

1. define the most appropriate pixel size for estimating LAI at regional scales;
2. investigate techniques for partitioning LAI images into relatively homogeneous ASU and
3. assess the influence of boundary pixels on LAI estimates per-ASU.

5.1.2 Driving ecosystem simulation models with remotely sensed data

Ecosystem simulation modelling allows investigation of responses and feedbacks of processes operating at a range of spatial and temporal scales, with the ultimate objectives of increasing (i) the accuracy of estimates and (ii) the understanding of biosphere-atmosphere interactions. The spatial nature of ecosystem simulation models is often implicit (aspatial), i.e., they are run for discrete points within a landscape (e.g., Friend *et al.* 1993; Curran 1994a; Kimball *et al.* 1997) and demand detailed input data (van Rompaey *et al.* 1999). Indeed, it is often technically and financially impossible to acquire the necessary input data with the precision required by a model at regional scales (§2.2.1). A few researchers have driven ecosystem simulation models using per-pixel inputs derived from remotely sensed images to estimate NPP (e.g., Running *et al.* 1989; Dungan 1998; Running *et al.* 1999) although, the error due to coarse spatial resolution, low accuracy input data is not quantified in most cases (van Rompaey *et al.* 1999).

To estimate accurately carbon pools and fluxes at regional scales, first accurate spatial estimates of biophysical variables (e.g., LAI) are required to drive ecosystem models that can output estimates of NPP (§2.2.2). Traditionally, estimates of LAI have been acquired *in-situ* using extremely labour-intensive sampling techniques (§3.2.1.1) (e.g., Franklin *et al.* 1997a; Chen *et al.* 1997; Wülder 1998b; Gower *et al.* 1999). For regional scale studies, however, remotely sensed observations provide the only practical means of collecting the inputs necessary to drive ecosystem simulation models (Aber and Federer 1992).

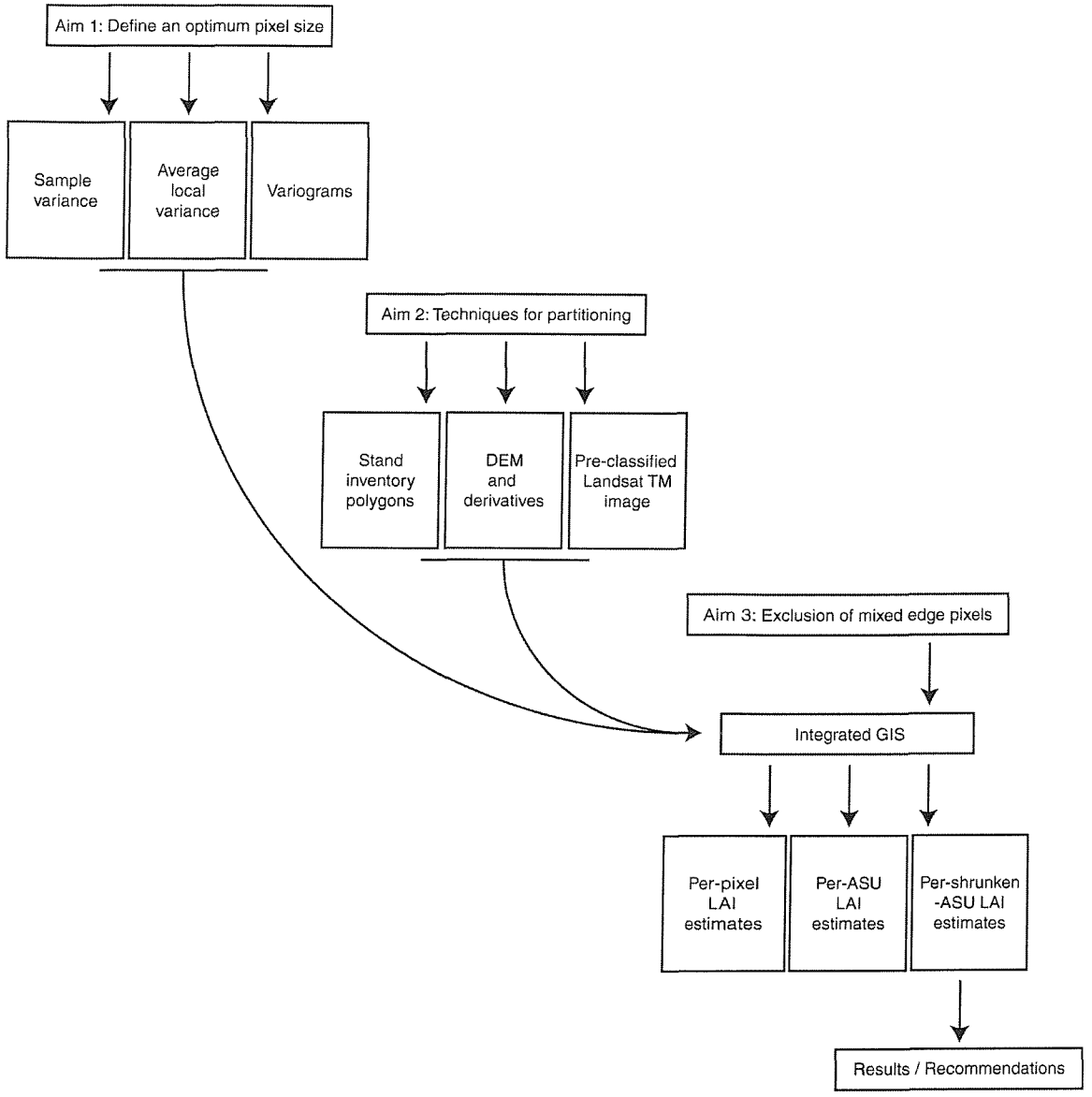

Figure 5.1 Diagrammatic representation of the aims and structure of this chapter.

5.1.3 Principles of geographic representation and implications for accuracy

> *'It is a geographical fact of life that the results of spatial study will always depend on the areal units that are being studied'* (Openshaw 1984, p.37).

The realisation that changing the shape and / or size of the units on which data are mapped can change correlations and statistical models generated on multivariate data was identified in the geography literature as the modifiable areal unit problem (MAUP) (Openshaw 1984; Fotheringham and Wong 1991; van Beurden *et al.* 1999). Hence, the choice of unit used to partition a landscape may have considerable implications (Reich *et al.* 1999).

The simplest mathematical representation of a landscape is obtained using a grid of square cells with equal dimensions, in a *raster* format. Any cell may be defined by its x and y co-ordinates. For example, in remote sensing, the observed areas are defined, to a first approximation, by the pixel size of the resultant image (Atkinson and Curran 1995). Alternatively, polygons of any shape can serve to define a landscape, in a *vector* format. Cell identification within a vector coverage is more difficult but vectors may represent complex landscape patterns, at a range of scales, more realistically. Regardless of the spatial representation, the aim is to partition the landscape into units that maximise both the within-unit homogeneity and between-unit heterogeneity.

The properties most useful for landscape partitioning are site variables (e.g., topography and vegetation type). However, in reality such clear representation is challenging as transitional situations are the norm (Edwards and Lowell 1996). The implications of this observation can be visualised easily by considering the remote sensing of categorical variables (Welch 1982; Townshend and Justice 1988). When classifying a remotely sensed image, if the sampling unit is much smaller than the 'dominant spatial frequency' (Woodcock and Strahler 1987), too much variability is captured, thus leading to a potential decrease in classification accuracy. Conversely, high local variance may be subsumed if the sampling units are too large, giving sample units of mixed composition, which also could result in a decrease in classification accuracy (Franklin *et al.* 1997b; Curran and Atkinson 1999). Hence, the choice of sample unit size is dependent upon the degree of spatial autocorrelation (a measure of the degree of similarity between neighbouring areas) within a landscape, with obvious implications for landscape partitioning.

5.1.4 The current situation in forestry

Forested landscapes are partitioned traditionally, either by calculating the commercial potential to grow trees (Franklin *et al.* 1997b), or by defining vegetation within *stand inventory polygons* (Edwards and Lowell 1996), derived via photo-interpretation (Biging *et al.* 1992). Such stand polygons have been used successfully to organise the landscape for many management activities, including silvicultural operations (Wülder 1998b; Dick and Jordan 1990) (Figure 5.2).

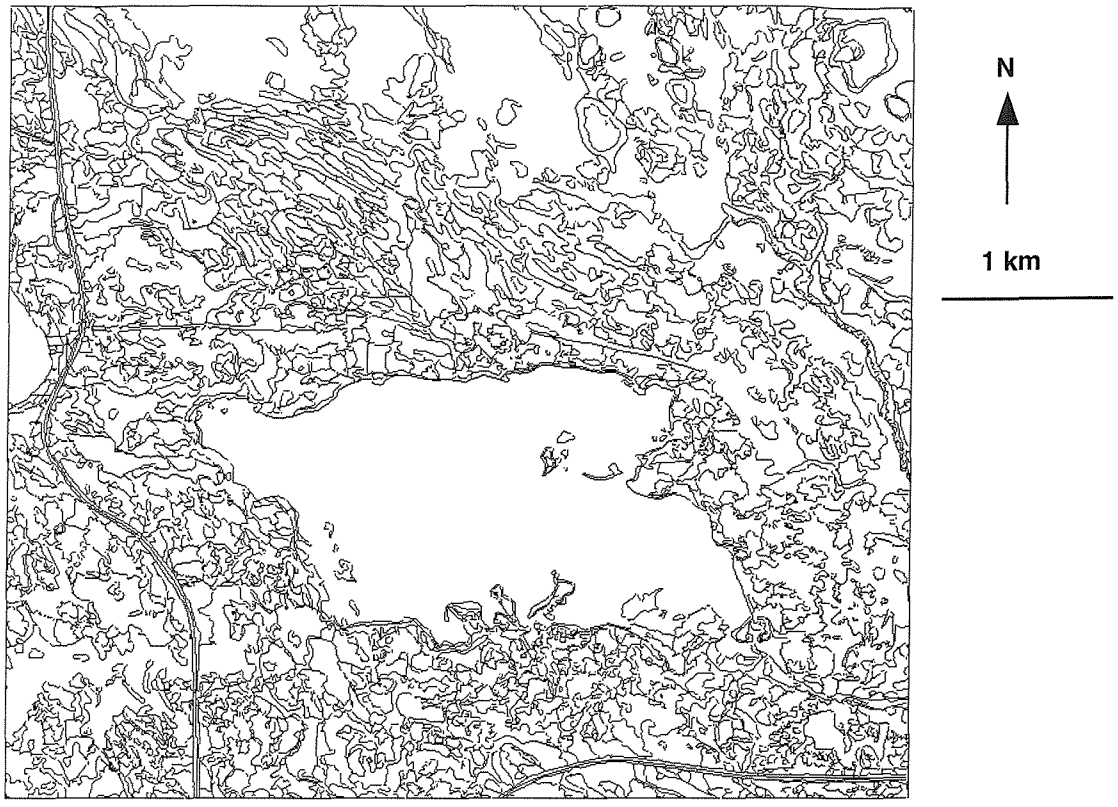

Figure 5.2 Stand inventory polygons of the Whitegull lake catchment, BOREAS SSA.

5.1.5 Issues of scaling-up

The objective of scaling is to use the information at one scale to make estimations / predictions about processes at another scale (§5.1). However, heterogeneity in properties that determine the rates of processes as well as non-linearity in the functional relationships between processes and variables, often result in scaling attempts being of questionable accuracy. Indeed, error propagation over several orders of magnitude of organisation and structure (Figure 5.3) may produce serious deviation from reality (Jarvis 1995b).

Explicit examination of scaling from field measurements to coarse (1 km) spatial resolution surfaces is a central theme of BigFoot (a NASA funded terrestrial ecology initiative to characterise land cover for Terra MODIS accuracy assessment) (§2.3) (Reich *et al.* 1999). One specific aim is to characterise error due to scaling differences versus error due to algorithm definitions by aggregating the fine resolution surfaces to resolutions up to 1 km to determine if there is a resolution above which information loss increases rapidly. More information is available on the internet from: http://www.fsl.orst.edu/larse/bigfoot.

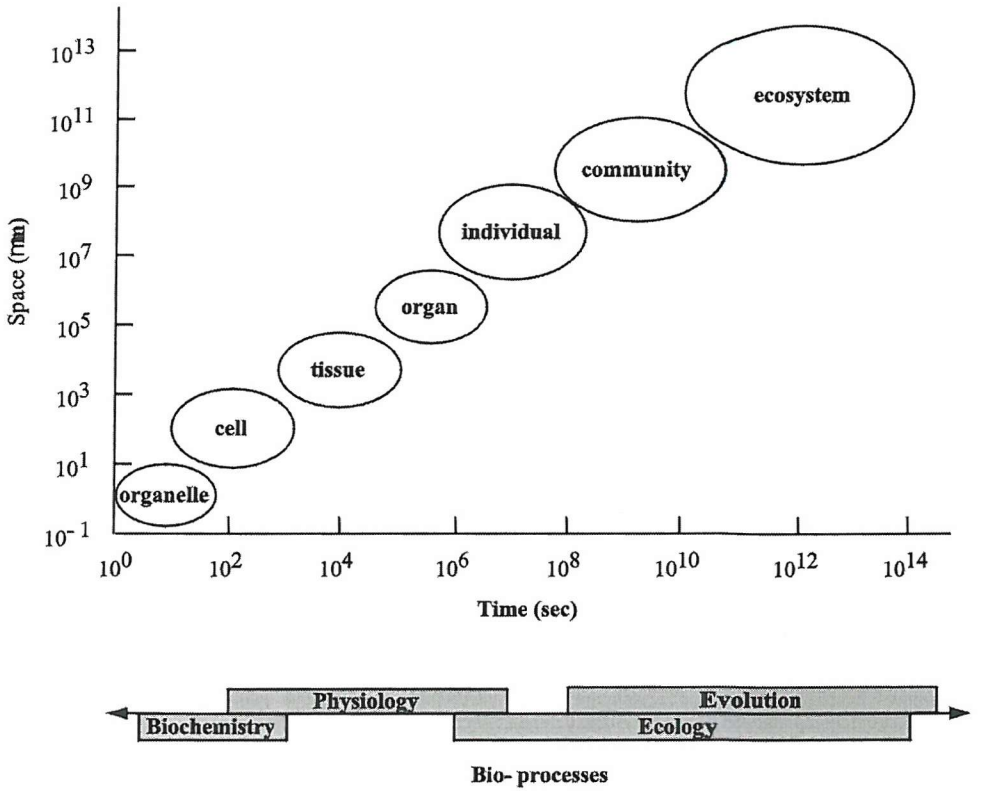

Figure 5.3 Range of spatial scales defining the state of a system and temporal scales defining the processes within the system over 14 orders of magnitude ranging from organelle to ecosystem (from Jarvis 1995b).

For many processes related to global environmental change, information on plant and vegetation processes is scaled-up and information on climate is scaled down to match, as far as possible, the spatial and temporal scales of the processes of interest (Figure 5.4).

Recently, there has been an emphasis on identifying phenomena that operate over a wide range of spatial scales, e.g., the absorption of photosynthetically-active radiation (PAR) (Dang *et al.* 1997). Such 'fractal' phenomena possess spatial dependence, such that areas near to each other tend to be more similar than those further apart (Curran and Atkinson 1998). Therefore, there is usually a relationship between the characteristics of an environmental phenomenon and the area over which it is observed. Because scaling-up is the only way of analysing ecosystem function and processes at regional scales, it is important that 'we get it right' (Jarvis 1995b, p.1088). However, since the process is essentially open-ended, there is a major danger that 'we may get it wrong'! Therefore, it is imperative that the accuracy of model predictions is increased steadily and that they are assessed at each transverse of scale.

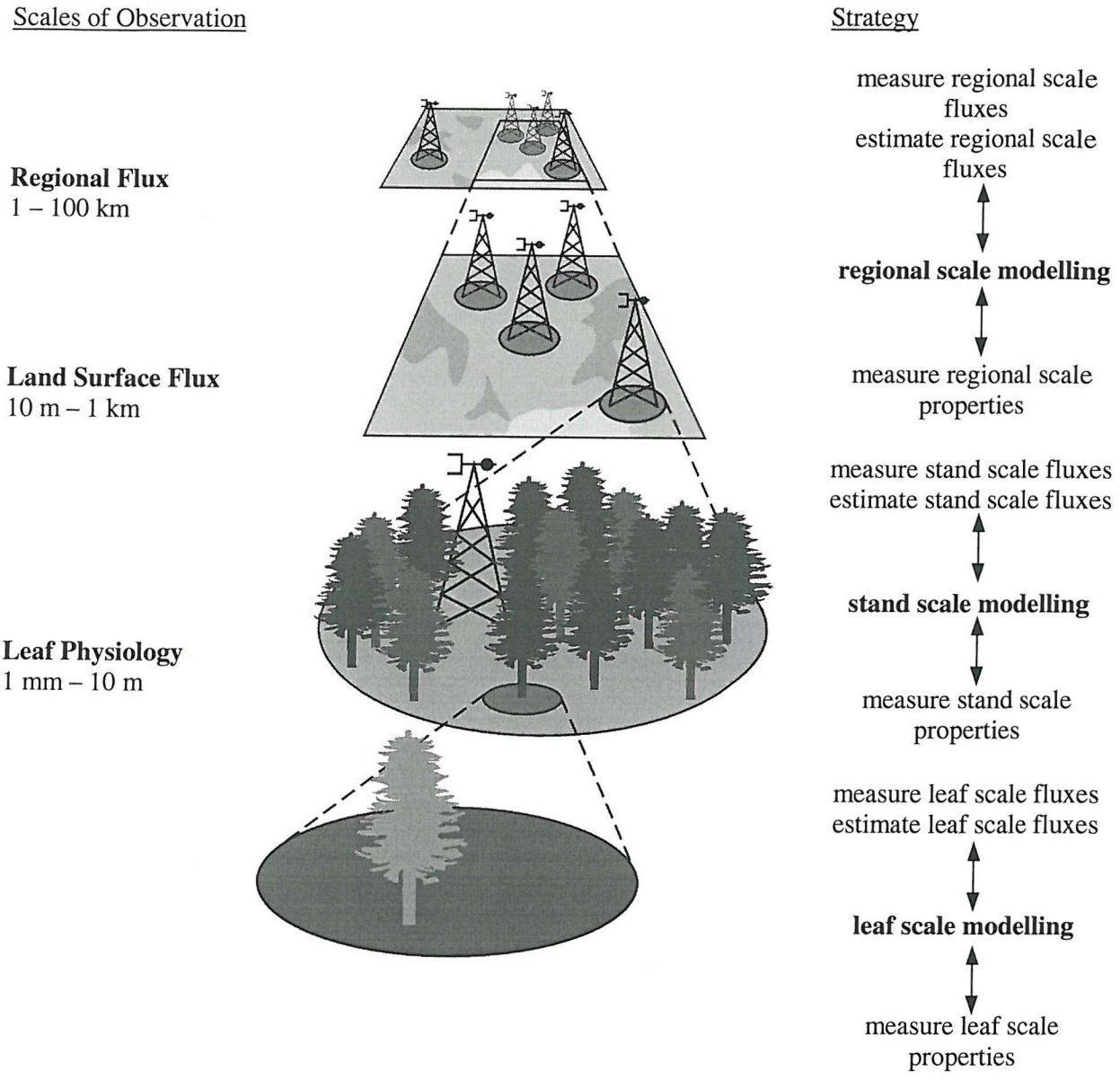

Figure 5.4 The strategy of up- and downscaling across the spatial scales of primary interest in relation to global environmental change (adapted from Jarvis 1995b).

5.2 Study Area and Data Acquisition

The research reported in this chapter focuses on the SSA of the BOREAS study region, situated on the southern edge of the Canadian boreal forest, 40 km north of Prince Albert, Saskatchewan (§3.1.2).

During BOREAS, two independent ground data sets of estimated forest LAI were obtained using LI-COR LAI-2000 Plant Canopy Analyser and ceptometer instruments and made available through the BORIS. The first data set from Plummer *et al.* (1997) provided LAI estimates for 9 sites across the SSA (herein known as $LAI_{training}$). The second, collected concurrently by Chen *et al.* (1998), provided further LAI estimates for 10 sites (herein known as $LAI_{testing}$). In both cases, the LAI estimates for each site were made along transects 50 m to 300 m long (§3.2.1.1).

A cloud-free Landsat-5 TM image of the BOREAS SSA (path 37 row 22), acquired on 2nd September 1994, was also obtained through BORIS (Plate 4.1). Image acquisition was near coincident with the collection of LAI ground data (1994 BOREAS IFC-3). All LAI estimates along transects at each site were assumed to fall into the area represented by a single 30m TM pixel. Therefore, mean LAI estimates for each site (and pixel) were used in the analyses.

5.2.1 Preliminary data processing

The Landsat TM image had undergone limited geometric pre-processing at the CCRS through the GICS (§4.2.3.1) (Cihlar and Teillet 1995; Friedel 1992).

Radiometric corrections (DN to radiance) were made using coefficients (gains and offsets) provided in the image header. A sub-scene of the image was registered to the Universal Transverse Mercator (UTM) Grid using 30 ground control points, with a registration accuracy of less than one pixel (RMSE ±9.2 m).

5.2.2 Generation of a LAI 'reference raster'

The at-sensor radiances ($W\ m^{-2}\ sr^{-1}\ \mu m^{-1}$) recorded by the TM sensor in channels 3 and 4 (§5.2.1) were used to derive the NDVI (§4.3.3) (Rouse *et al.* 1973) for each pixel of the sub-scene.

The $LAI_{training}$ data were then used to develop a predictive regression relationship between NDVI and $LAI_{training}$ (Figure 5.5), with a coefficient of determination (r^2) of 0.92:

$$LAI = 13.687NDVI - 1.411 \quad (5.1)$$

Previous investigations for forests have shown that the NDVI has considerable sensitivity to LAI, especially at low values of LAI (Running *et al.* 1986; Spanner *et al.* 1994; Chen and Cihlar 1996; Turner *et al.* 1999). Typically, the NDVI increases over a LAI range from 0 to 3 – 5 before an asymptote is reached. The upper limit of sensitivity (and the relative importance of visible and NIR radiation in determining this limit) differ among vegetation types (Yoder and Waring 1994; Turner *et al.* 1999). Figure 5.5 would suggest that the asymptote has yet to be reached, hence the use of a linear regression relation. This was applied globally to the sub-scene to generate a LAI 'reference raster' (Figure 5.6).

5.3 Methodology

For clarity of argument, this section is organised according to investigation of the specific aims (§5.1.1) as the iterative development of the methodology dictated.

5.3.1 Aim 1: Defining an optimum sampling pixel size

One of the most fundamental characteristics of a remotely sensed image is its spatial resolution: The size of the area on the Earth's surface from which the measurements that comprise the image are derived (§2.3.1.3) (Townshend 1981). Spatial resolution, therefore, is analogous to the scale of the observations (herein termed pixel size). Avoidance of the significant influence on pixel-level reflectance created by factors such as background soil and understorey vegetation, variability in canopy geometry and the optical properties of canopy constituents (all of which often occur at sub-pixel scales) resulted in a series of investigations using spectral mixture analysis to derive sub-pixel scale scene fractions (e.g., Hall *et al.* 1995a; Peddle *et al.* 1997; Csillag *et al.* 1996). However, of greater relevance to this investigation, with its necessary shift to regional scale processes, is the provision of accurate spatial information from remotely sensed data for direct model input (Running and Hunt 1993), especially given that a remotely sensed observation depends on the pixel size.

Indeed, variability in the brightness of a surface is dependent on pixel size (smaller pixels capture more variability and have a larger range) and the degree of this dependency is related to the spatial properties of the surface (Curran and Atkinson 1999 p. 116).

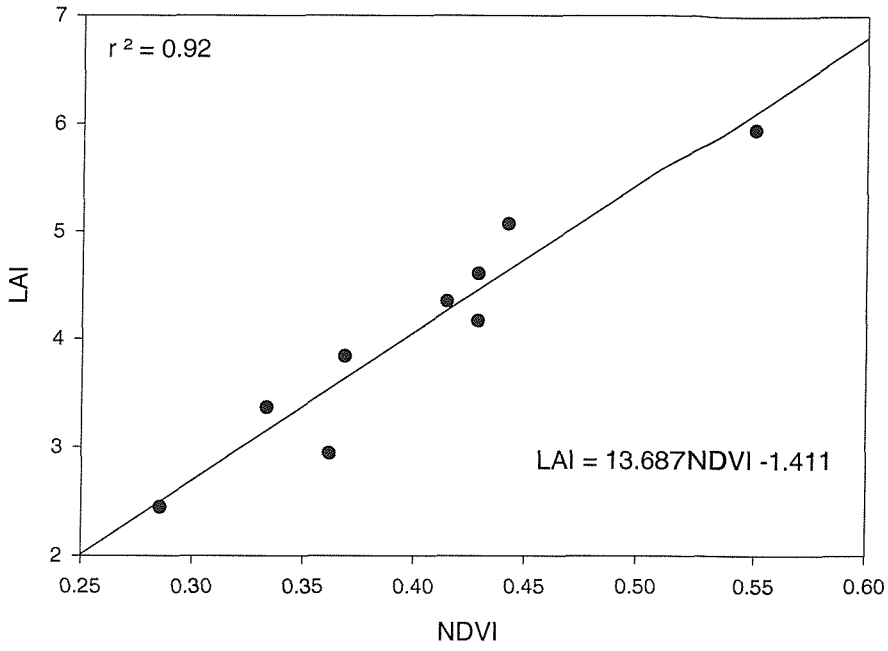

Figure 5.5 Regression relationship used to generate LAI reference raster.

Satellite sensors now exist with many different spatial resolutions, from over one kilometre (NOAA AVHRR) to 1 m (panchromatic Ikonos 2 imagery) and finer spatial resolutions are in prospect from satellite sensors such as QuickBird and OrbView-3 (Aplin *et al.* 1999). To select an appropriate scale of data for this investigation, first the spatial structure of the remotely sensed imagery must be understood. In particular, the manner in which elements of the scene change as a function of spatial resolution. Several authors have investigated the spatial structure of images, usually at one or two discrete spatial resolutions (e.g., Craig and Labovitz 1980; Woodcock and Strahler 1985; Cihlar *et al.* 1998). These investigations demonstrated that the number of pixels containing more than one land-cover type was a function of both the complexity of the scene and the spatial resolution of the sensor (§5.1.3). Hence, the spatial structure of images is related primarily to the relationship between the size of objects in the scene and spatial resolution (Pierce and Running 1995; Reich *et al.* 1999). To investigate the spatial scale of LAI variation within the study area, three descriptors of spatial variation were calculated using the LAI reference raster: i) sample variance, ii) average local variance and iii) variograms.

5.3.1.1 Spatial degradation of imagery

A simple method was employed to degrade the LAI reference raster (§5.2.2) with an original pixel size of 30 m. The algorithm used (taken from ERDAS Imagine software) averages pixel radiance values to be combined into a single, larger pixel. Such image degradation has been practised widely (e.g., Heric *et al.* 1996; Cutler 1998; Aplin 1999; Bian and Butler, 1999), although certain limitations must be acknowledged:

Signal-to-noise ratio (SNR)

When designing a sensor an inevitable trade-off must be made: Given a number of photons being reflected per unit area (i.e., the signal) and the need to record sufficient to overcome the background 'noise' of the sensor, three options are available: (i) increase pixel size, (ii) increase bandwidth and (iii) increase dwell time (stay longer over target). The majority of the noise is, to a first approximation, constant and independent of pixel size. Therefore, by degrading imagery artificially to larger pixel sizes (with constant bandwidth and dwell time), the signal increases as does the SNR, to an artificially high value when compared to imagery with an identical pixel size acquired directly by a sensor (Smith and Curran 1996; 1999).

Point spread function (PSF)

The averaging degradation algorithm retains the point spread function (PSF) of the original image, rather than increasing the PSF in proportion to the degree of degradation. Therefore, the pixels of degraded imagery will approximate more closely a square-wave response than those of original satellite sensor imagery (Townshend 1981; Townshend and Justice 1988).

These assumptions, integral to the degradation algorithm, are unrealistic. However, the aim of this particular investigation is to study the basic relationship between pixel size and LAI estimation and not to simulate the response of a particular satellite sensor. Therefore, the influence of these two factors (SNR and PSF) on the degradation procedure was of relatively minor significance, hence, the omission of measures to account for them here. Also, by using pixel size the controversies over the exact definition of spatial resolution and how it should be measured were avoided (Townshend 1981).

The reference LAI raster (§5.2.2), with an original pixel size of 30 m, was degraded progressively by a factor of 2 in x and y directions to generate images with pixel sizes of 60, 120, 240, 480, 960, 1920 and 3840 m (Figure 5.6). A subset of relatively homogeneous forest (measuring 256 by 256 pixels) was taken from the initial LAI reference raster and also degraded successively to the same pixel sizes.

5.3.1.2 Image and sample variance

Image variance was calculated as the square of the standard deviation of the LAI reference raster, forested subset and subsequently for each of the degraded derivatives (Figure 5.7). Sample variance (i.e., change in image variance) was plotted against degradation of pixel size for both the entire image and the forested subset (Figure 5.8).

Image variances of the entire LAI raster for the BOREAS SSA as well as the forested subset decreased, as expected, with an increasing pixel size. The only observable difference between the subset derived variances are that the relation is smoother, particularly at the larger pixel sizes (480 m and greater). This may demonstrate the contribution of the lakes to the spatial structure of the original LAI reference raster.

The sample variance of the entire LAI raster increased as pixel size increased up to 3840 m. The trough and subsequent peak (to over 70 %) may demonstrate that the scene is dominated by relatively large objects, such as lakes. In contrast, for the forested subset area, sample variance decreased up to a pixel size of 120m, followed by a gentle increase throughout subsequent stages of degradation. This would suggest the absence of such 'dominating large objects'. It is also possible, however, that such patterns may be an artefact of the accuracy of any variance measure being much greater for finer spatial resolutions (n decreases by over a thousand-fold from 30 to 960 m for this example)!

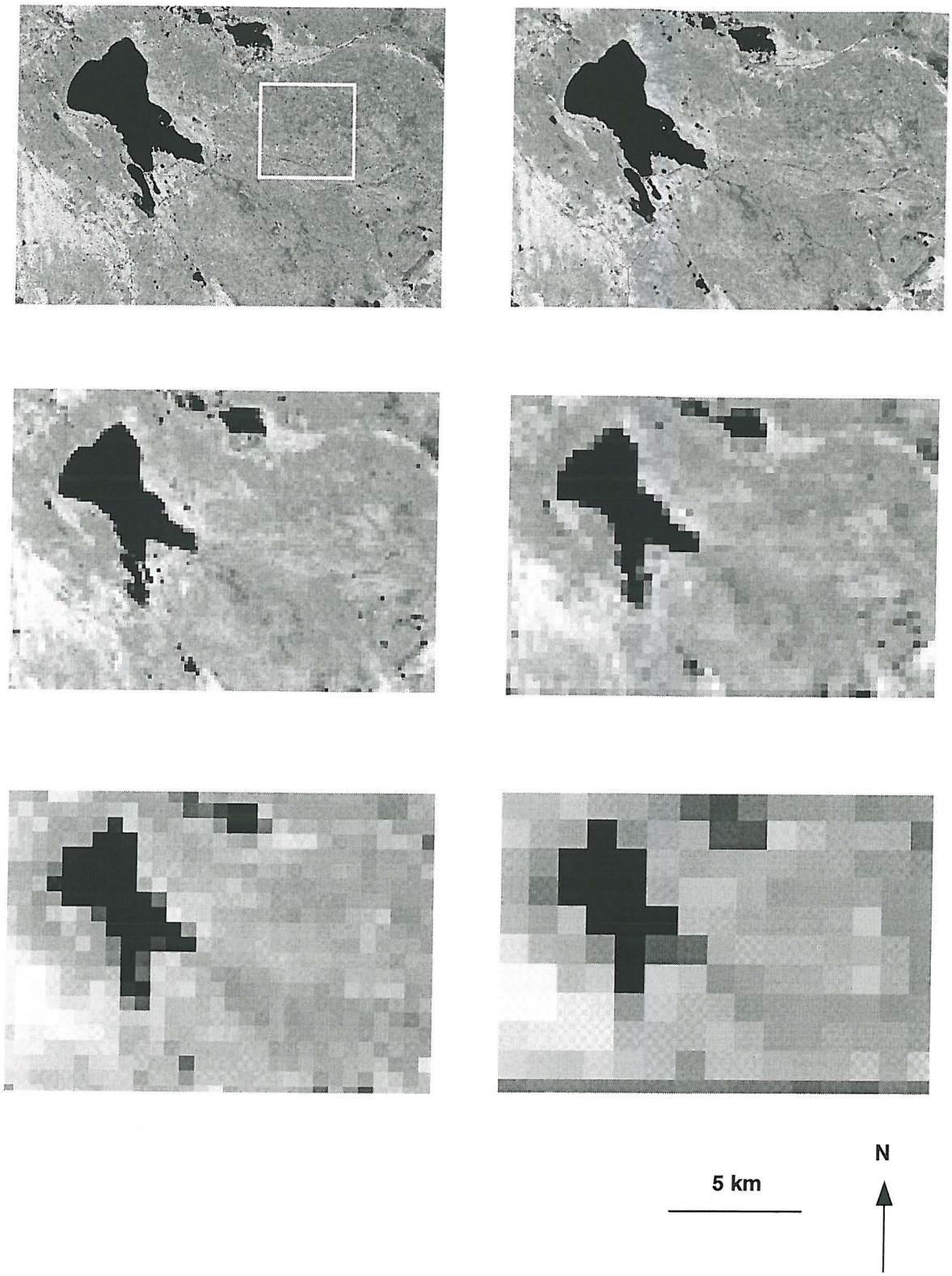

Figure 5.6 LAI raster subset images with (top left to bottom right) 30, 60, 120, 240, 480 and 960 m pixel sizes. (Forest subset (§5.3.1.1) defined by white box on top left image).

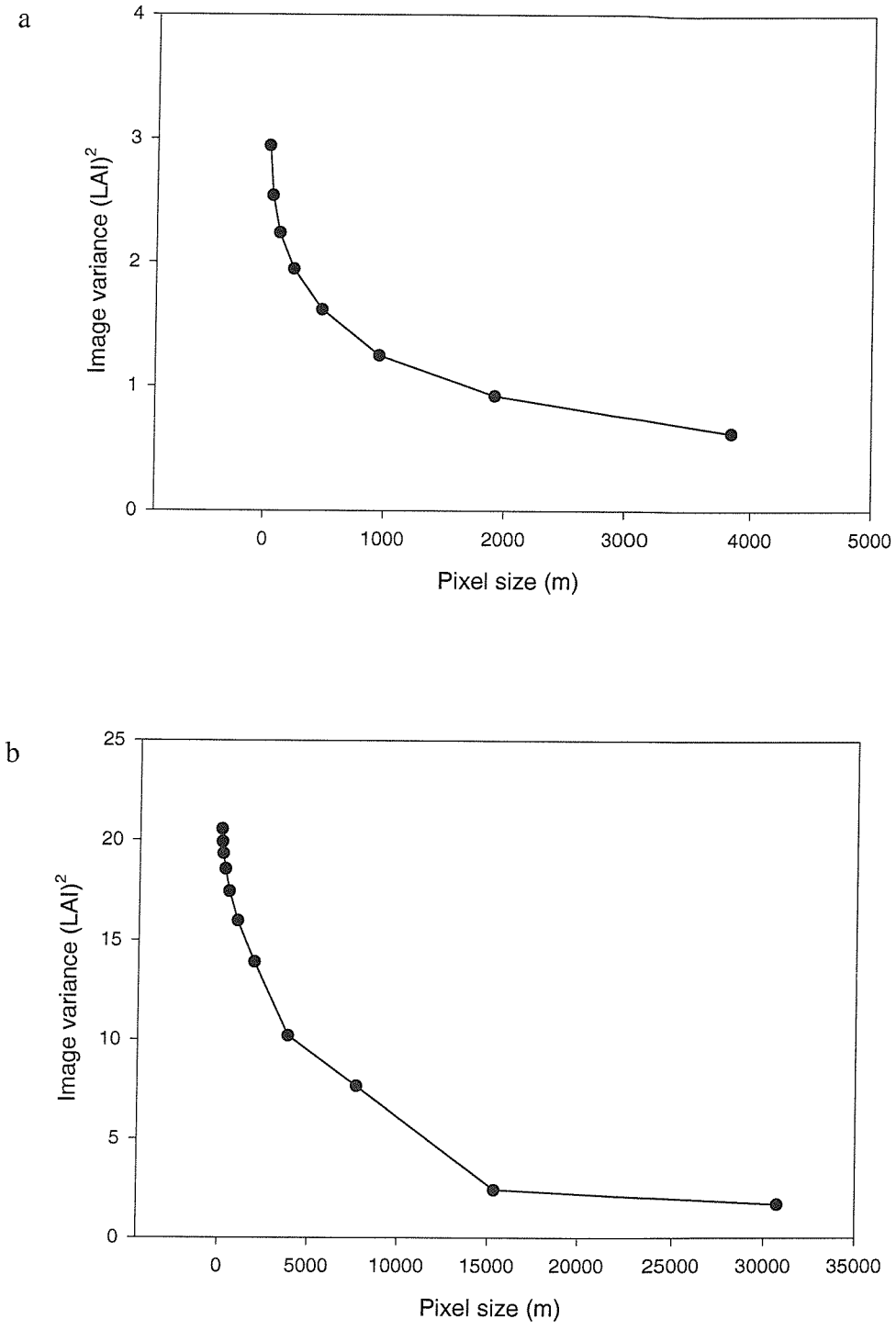

Figure 5.7 Image variance (square of standard deviation) against pixel size for (a) forest subset and (b) entire BOREAS SSA.

a

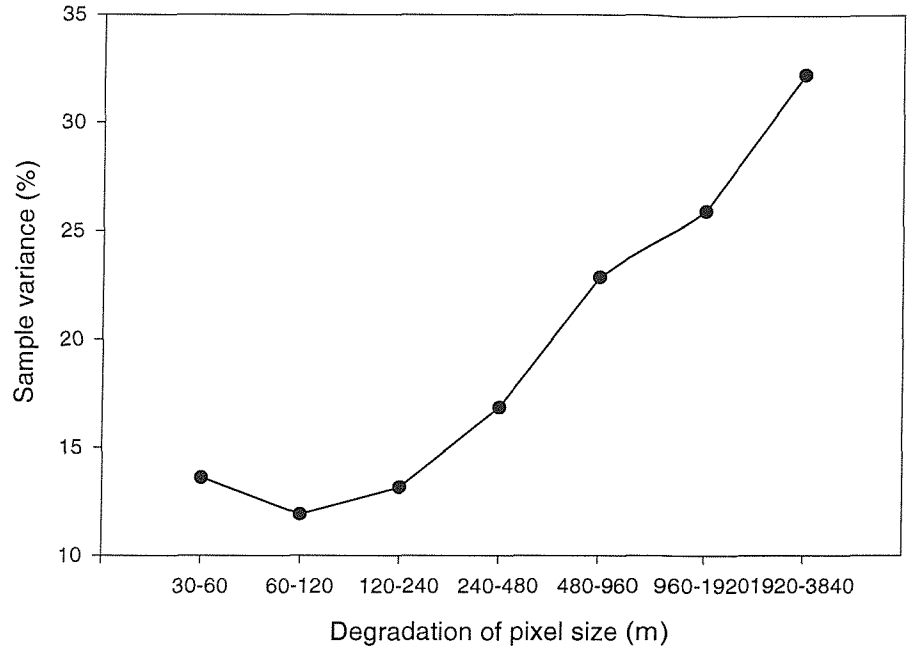

b

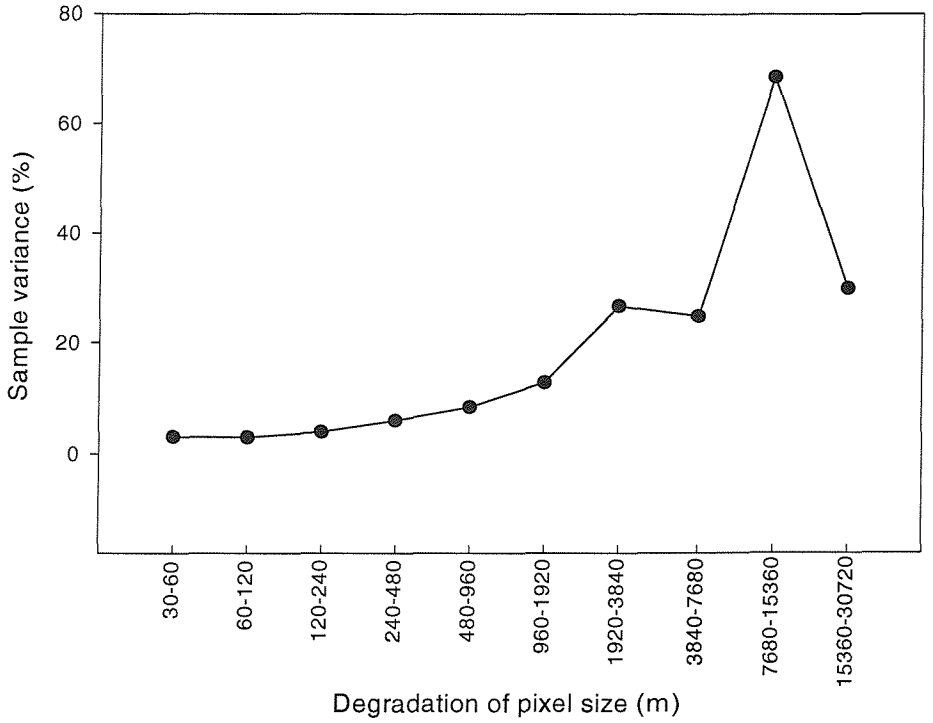

Figure 5.8 Sample variance (change in image variance) against pixel size degradation for (a) forest subset and (b) entire BOREAS SSA.

5.3.1.3 Average local variance

Graphs of average local variance in an image as a function of spatial resolution may also be used to measure / infer spatial structure in images (Woodcock and Strahler 1987). The reasoning behind this relates very much to the earlier example of remote sensing of categorical variables (§5.1.3): As the pixel size increases and many scene objects are subsumed within a single pixel, the average local variance decreases.

There is some dispute as to the method of calculating average local variance so two methods were adopted and results compared. Woodcock and Strahler (1987) calculated average local variance as the mean value of the standard deviation of a moving 3 x 3 pixel window. The standard deviation of the nine pixels was calculated and the mean of these values over the entire image was taken as the average local variance (Figure 5.9). However, according to geostatisticians, average local variance σ_{vw}^2, may be estimated from the same moving 3 x 3 pixel window w, applied to an image of L rows by M columns of pixels with support v, using:

$$\bar{\sigma}_{vw}^{\,2} = \frac{1}{L.M}\sum_{l=1}^{L}\sum_{m=1}^{M}\frac{1}{9}\sum_{j=-1}^{+1}\sum_{k=-1}^{+1}[\bar{z}_v(l+j,m+k) - \bar{z}_v(l+j,m+k)]^2 \qquad (5.2)$$

where, it is assumed there is a buffer of one pixel surrounding the image to be analysed (Atkinson 1999). Hence, two estimates of average local variance were obtained for the original LAI reference raster, the forest subset and their degraded derivatives (Figure 5.10).

Comparison of Figures 5.9 and 5.10 indicates that there is little difference between the two methods for the estimation of average local variance for an image. Both plots for the forest subset (Figures 5.9a and 5.10a) show a peculiar peak at the original pixel size (30 m), perhaps suggesting the presence of scene elements smaller than the pixel size (e.g., individual trees) with a second peak (around 1200 m), possibly corresponding to forest stands.

However, plots of average local variance estimated for the entire BOREAS subset and its degraded derivatives, were very much as expected, rising to a peak (around 10,000 m) and thereafter decreasing with an increase in pixel size (Figure 5.9b, 5.10b).

a

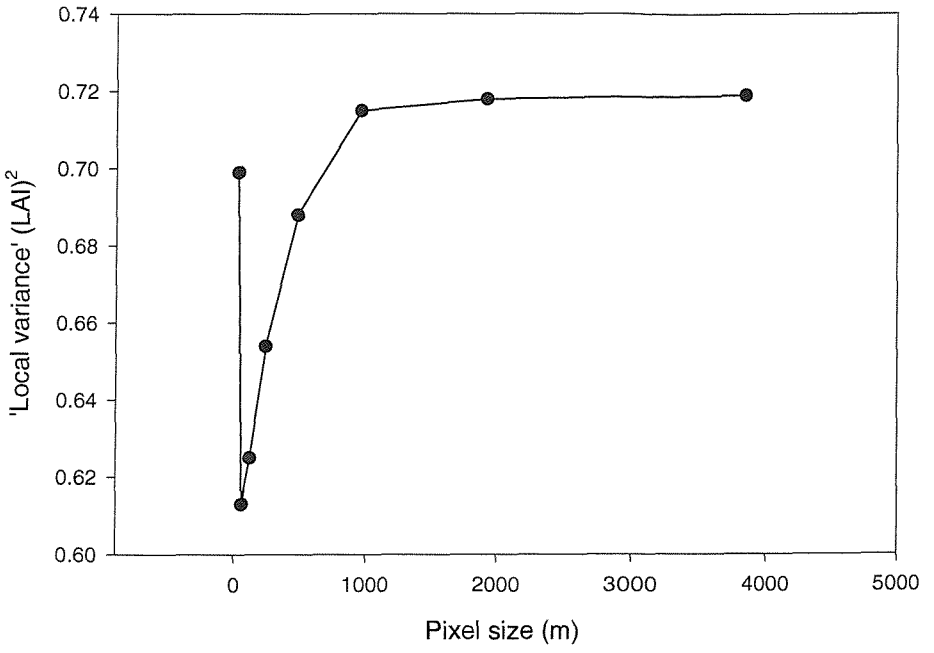

b

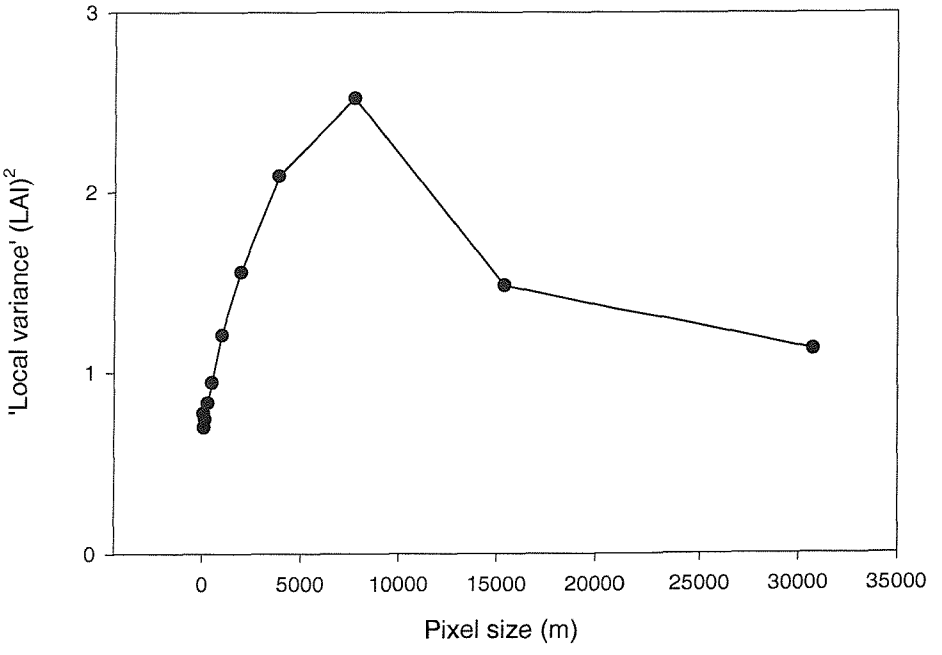

Figure 5.9 Woodcock and Strahler method of 'average local variance' for (a) forest subset and (b) entire BOREAS SSA.

a

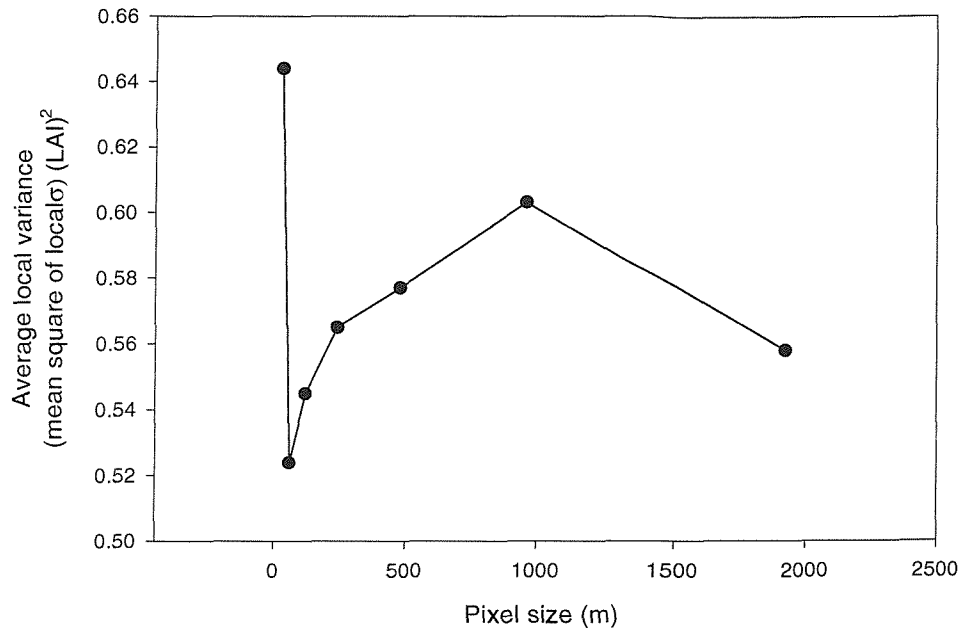

b

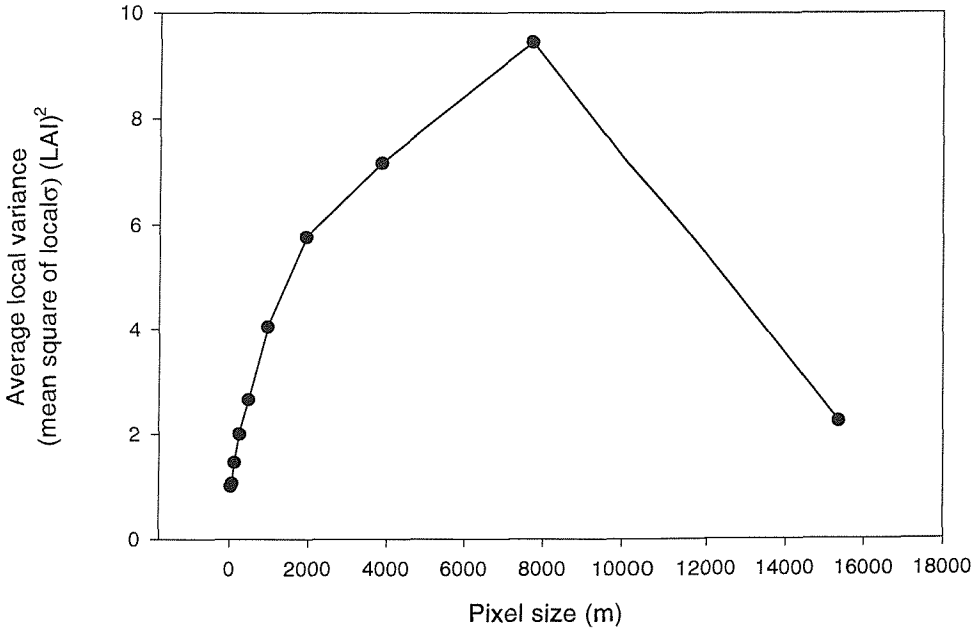

Figure 5.10 Average local variance for (a) forest subset and (b) entire BOREAS SSA.

5.3.1.4 Variograms

In remote sensing pixels have a constant size, shape and meaning. As a result, geostatistical techniques (Webster and Oliver 1990; Curran and Atkinson 1999) that utilise spatial autocorrelation can be used to model, understand and predict the influence of pixel size on remotely sensed observations and the environment they represent (Zhang *et al.* 1990; Rossi 2000).

Variograms were computed for the LAI reference raster, forested subset and subsequently for each of the degraded derivatives using the GSTAT software package (Pebesma 1997; Pebesma and Wesseling 1998).

Figure 5.11 shows the 6 variograms computed for the forest subset and its degraded derivatives. This variogram sequence illustrates two trends. The first effect of coarsening the pixel size is to remove short-range variation from the images so that generally semivariance decreases (e.g., a pixel size of 4 km for the forest subset would give virtually no spatial information)! Second, the nugget variance (the sill of the nugget component) also decreases. Nugget variance is related to both spatial variation which exists at a micro-scale (a shorter interval than that of the sampling frame) and measurement error (Curran and Dungan 1989). Such *noise* tends to be 'smoothed out' by the degrading algorithm (§5.3.1.1) hence, the reduction of nugget variance (Figure 5.11). Further analysis of the variograms computed for the forest subset showed two distinct scales of variation, one below the pixel size and one above the image size (as a distinct sill is never reached). The latter suggests that there is a trend across the image, perhaps due to an increase in path length with scan angle across the sensor. To check for this, separate directional variograms were computed (across the rows and down the columns) (Figure 5.12). Although the form of these variograms appears similar, the semi-variance is greater east-west, as would be expected if there was a trend present due to scan angle effects. Following computation, the north-south (along-track) directional variogram was modelled using a semi-automated technique: approximate model parameters were input initially by the operator and subsequently adjusted automatically using a weighted least squares (WLS) algorithm to provide a better fit (Figure 5.12b).

Variograms computed for the entire BOREAS subset and its degraded derivatives (Figure 5.13) display the same trends as the forest subset (decreases in semi-variance and nugget variance with coarsening pixel size), although, these variograms have a definite range, around 12,000 m, corresponding with peaks in average local variance (Figures 5.9 and 5.10).

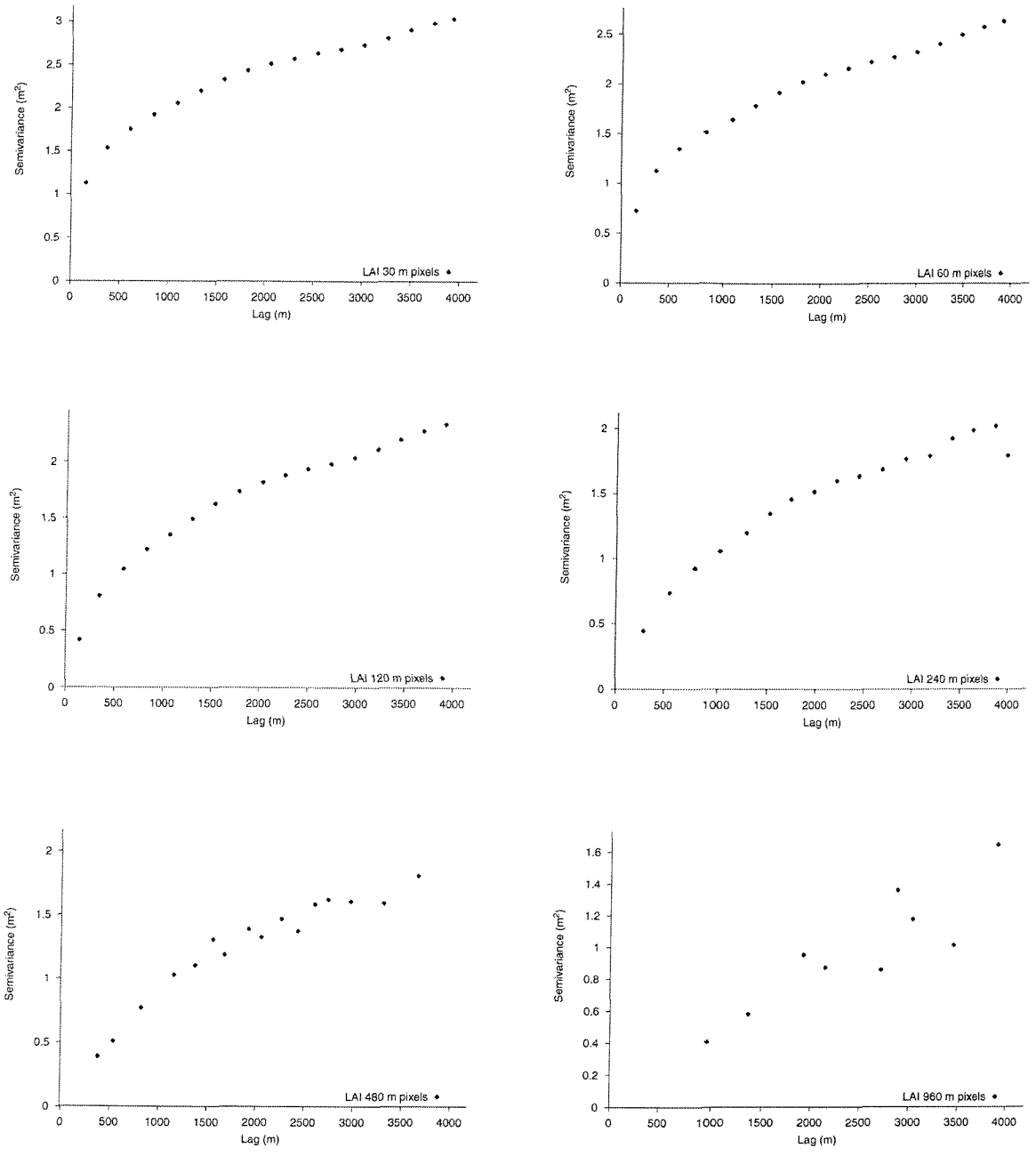

Figure 5.11 Variograms for LAI forest subset images for (top left to bottom right) 30, 60, 120, 240, 480 and 960 m pixel sizes.

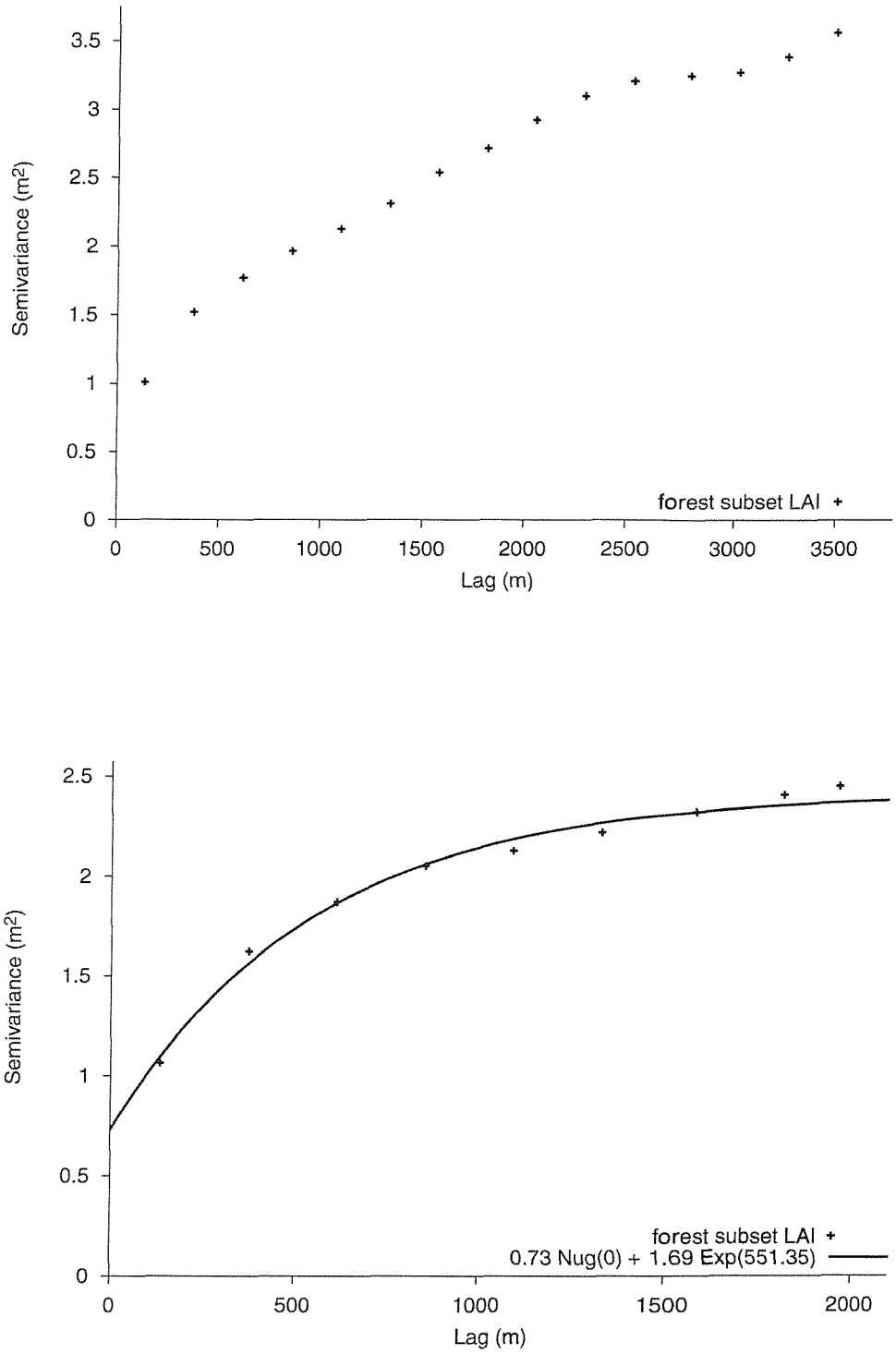

Figure 5.12 Directional variograms for the forest subset LAI images (pixel size 30 m) (a) east-west and (b) north-south.

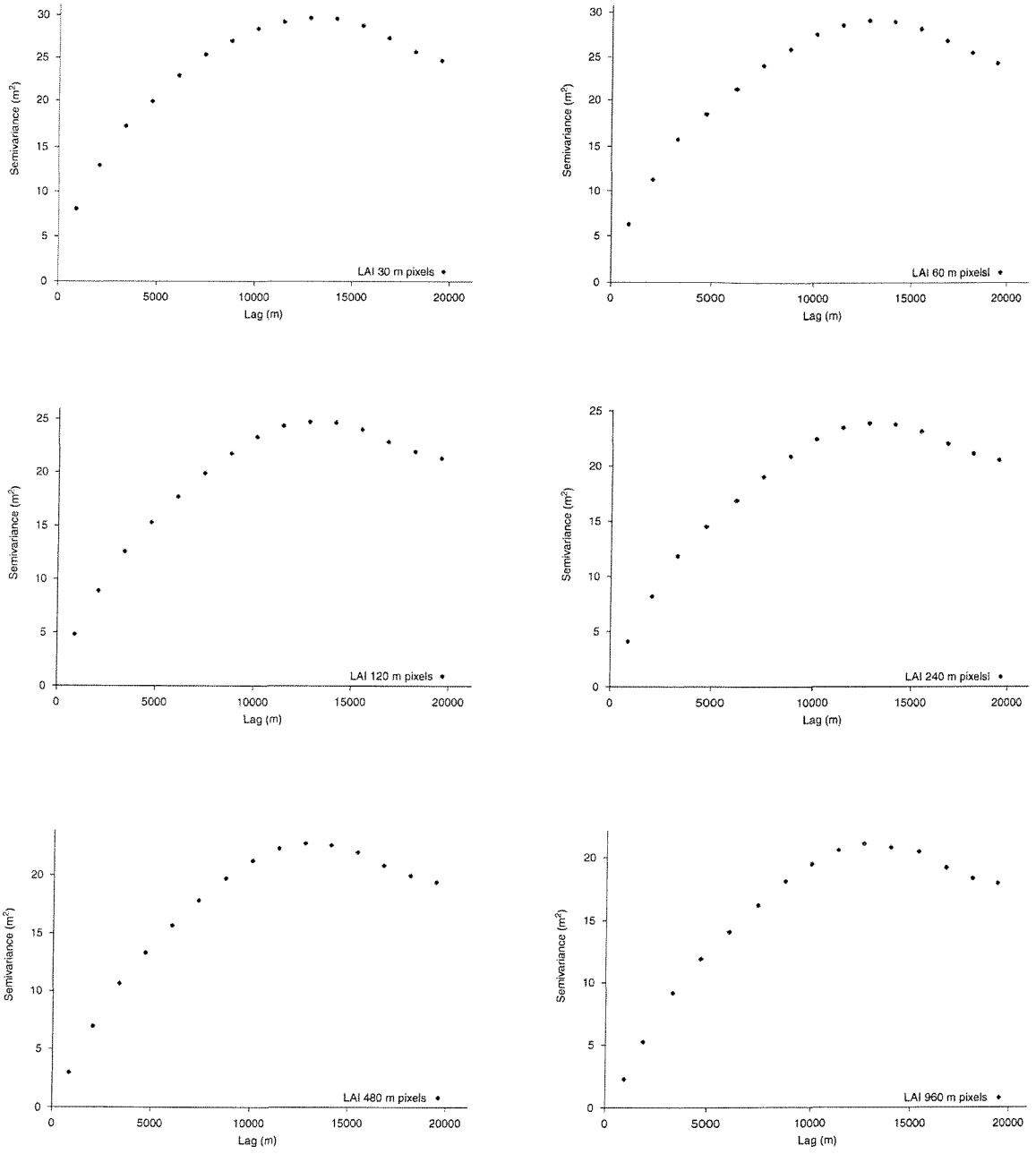

Figure 5.13 Variograms of the entire BOREAS SSA LAI images for (top left to bottom right) 30, 60, 120, 240, 480 and 960 m pixel sizes.

5.3.1.5 Discussion

Table 5.1 summarises the findings of the analyses conducted to define the most appropriate pixel size for estimating LAI at regional scales (aim 1, § 5.1.1).

	Pixel size above which there is little spatial information (m)	
	Forest subset	BOREAS SSA
1. Sample variance (§5.3.1.2)	960	7680
2. Average local variance (§5.3.1.3)	1000	8000
3. Variograms (§5.3.1.4)	960	> 960

Table 5.1 Summary of analyses to determine most appropriate pixel size.

Although this investigation has shown that statistical analysis may be used successfully to infer spatial structure within remotely sensed images, attempts to define an optimum pixel size (above which information loss increases rapidly) for the estimation of LAI, proved extremely difficult. Especially considering that for many applications the potential increase in accuracy of estimates from fine spatial resolution imagery may be offset by the regional coverage, which is possible with coarse spatial resolution sensors. Each technique was, however, useful for determining that ideally, a pixel size of much less than 1 km should be chosen. Indeed, if a pixel size much greater were used, most of the variation of interest would be encompassed within the support, therefore, not detectable by analysis (Atkinson and Curran 1995).

Whatever the spatial resolution of the sensor, investigators tend to try and extract information for areas smaller than the size of the pixel, whether they contain:

- boundaries between two or more mapping units (e.g., stand-clear cut boundary),
- the intergrade between central concepts of mappable phenomena (e.g., ecotone),
- linear sub-pixel objects (e.g., a road), or
- small sub-pixel objects (e.g., a house).

These lead to the 'mixed pixel problem' (Foody 1997; Petrou and Foschi 1999; Chen 1999; Brumbley and Chang 1999). Indeed, no matter what the spatial resolution, the often unstated implication is that the Earth's surface fits conveniently into multiples of rectangular units and that such small areas are homogeneous and conveniently homogeneous up to the coarsest pixel! Natural landscape patterns do not fit into these 'imposed elemental squares' (Fisher 1997, p.679) which suggests the need for another way in which to partition forested landscapes for regional modelling studies.

5.3.2 Aim 2: Techniques for Partitioning LAI Images

> *'There is no unique spatial resolution appropriate for the detection and discrimination of all geographical entities composing a complex natural scene such as a forested environment'* (Marceau *et al.* 1994, p.103).

The objective was to partition the forested landscape using a technique, the key features of which were:

1. based on simple characteristics of forest structure which can be measured in the field;
2. these forest structural characteristics can be estimated using remote sensing to enable study at regional scales (Running *et al.* 1995);
3. the partitioned units translate directly into the inputs for ecosystem simulation models.

Three possibilities were evident from data available. The first was to use traditional forest stand inventory polygons (§5.1.4) derived from photo-interpretation and digitising. However, photo-interpretation accuracy is never very high (Biging *et al.* 1992; Edwards and Lowell 1996). Indeed, a single interpreter may produce significantly different results from the same scene (Figure 5.14) (Edwards and Lowell 1996). Also, this approach does not usually provide the biophysical state and rate variables (e.g., LAI, LNC, PAR) needed for ecological analysis (Waring and Running 1998; Franklin *et al.* 1997b; Hay *et al.* 1997). However, when used previously for this purpose, stand polygons have been assigned a biophysical variable value derived from species-specific equations (e.g., Lavigne *et al.* 1996), which is likely to be unrepresentative if the stand comprises more than one species (Wülder 1998a).

In addition, stand polygons are constructed generally with reference to infrequent ground sampling of stand attributes (e.g., species, age, basal area and density) over relatively small areas (Waring and Running 1998). For precise and consistent monitoring of landscape properties, therefore, more frequent sampling over large areas is required (Atkinson and Curran 1995).

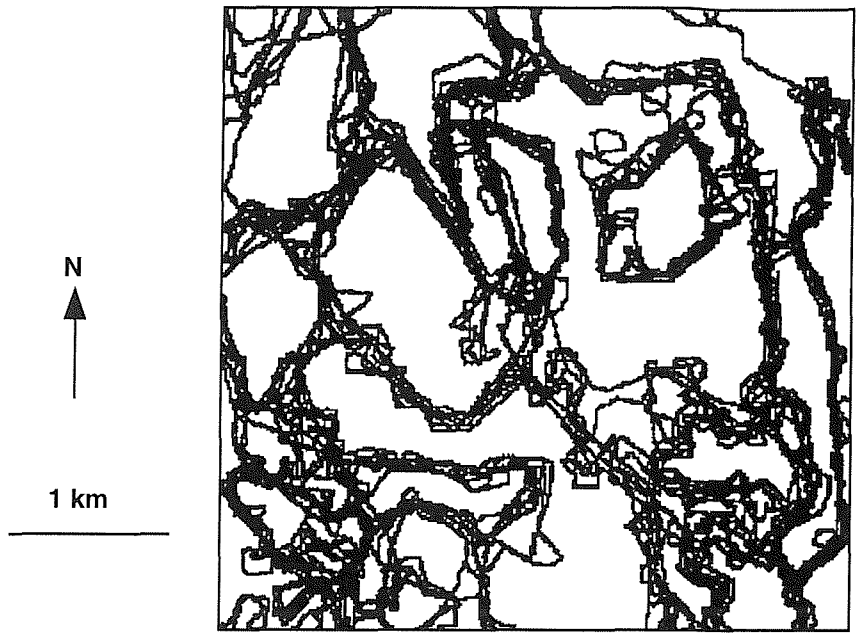

Figure 5.14 Nine interpretations of stand inventory polygons derived (digitised) by the same researcher from a single air photograph (Edwards and Lowell 1996).

This prompted the investigation of elevation, often used for hydrological routing / modelling, for landscape partitioning (Band *et al.* 1993; Michaud and Sorooshain 1994; Wigmosta *et al.* 1994; Moore and Thompson 1996; Harding *et al.* 1996). For example, Nemani *et al.* (1993b) represented the 1,200 km^2 Seeley-Swan basin in Montana at varying degrees of topographic complexity, from 170 land units aggregated to only 6 land units. They concluded that, generally, the more heterogeneous a landscape, the greater is the number of cells required to provide an accurate assessment of variation.

A DEM of the study area was obtained through the BORIS. These data were in the UTM projection, with a pixel size of 100 m (appropriate for the 1:50,000 scale contours from which the DEM was derived). Images of slope and aspect were derived subsequently from the DEM within the GRASS (v. 4.1) software package (Shapiro and Waupotitsch 1993) (Figure 5.14).

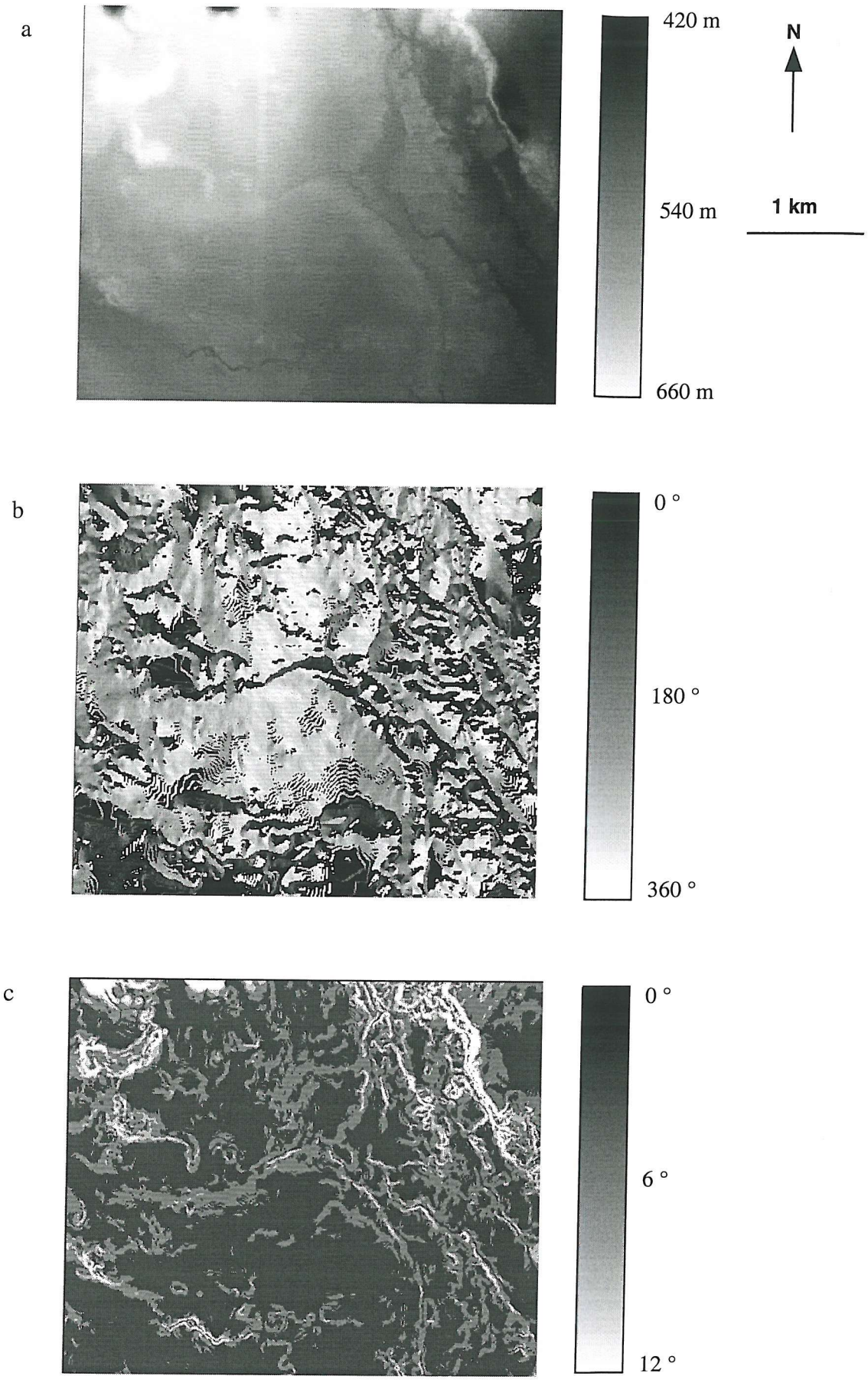

Figure 5.15 Subset images of a) elevation, b) aspect and c) slope for the BOREAS SSA.

Linear regression analysis between elevation (and its derivatives: slope and aspect) and LAI ground data (§3.2.1.1; §5.2) were weak, with coefficients of determination (r^2) of 0.14, 0.09 and 0.27 respectively. This is in stark contrast to previous research (Dungan 1998). There are, however, many possibilities to explain the lack of any relationship. First, and the principal reason, is LAI varies little over the small elevation range in the BOREAS SSA. Second, the algorithm (Horn's formula) used to determine slope and aspect from the DEM within GRASS is biased in 0, 45, 90, 180, 225, 270, 315 and 360 directions. Hence, the distribution of aspect categories is uneven and by using a 3 by 3 pixel neighbourhood window, (which equates to 300 m by 300 m) the accuracy of the aspect decreases dramatically for slopes less than 5 % (3 degrees) (Shapiro and Waupotitsch 1993).

The inadequacies of traditional forest inventory polygons and the lack of a meaningful relationship between elevation (or any of its derivatives) and LAI meant that an original approach was required to partition LAI images into homogeneous ASU. Considering the interest in landscape partitioning to facilitate LAI estimation at regional scales, the potential for remote sensing to provide the necessary ASU coverage seemed a suitable alternative, worth investigating.

A second, older (acquired on 6 August 1990) and pre-classified Landsat TM image was obtained through BORIS (Plate 5.1). A standard supervised maximum likelihood classification approach had been used on the raw digital numbers of bands 1-5 and 7 of the image to produce 11 land cover classes (Peddle *et al.* 1997). Classification accuracies are presented in Table 5.2. The image chosen contained clear topography / vegetation units and had been used by other researchers in BOREAS (e.g., Peddle *et al.* 1997; Steyaert *et al.* 1997; Ranson *et al.* 1997). The classified image was converted subsequently to a vector coverage within ERDAS IMAGINE to generate an ASU coverage for this investigation (Figure 5.16).

Class Reference [a] / Predicted	Unclassified	Black spruce	Jack pine	Mixed	Aspen	Fen	Total
Unclassified	0	0	0	0	0	0	0
Black spruce	0	114	3	14	0	1	132
Jack pine	0	3	18	0	0	0	21
Mixed	0	2	0	4	0	0	6
Aspen	0	0	0	9	54	0	63
Fen	0	2	2	0	0	0	4
Total	0	121	23	27	54	1	226
Producer's accuracy (%)		90.5	66.7	14.8	100	0	
Overall classification accuracy (%) = 78.0 (kappa = 0.660 or 66%)							

[a] No auxiliary reference sites available for other classes.

Table 5.2 Confusion matrix of the pre-classified BOREAS TM image (Peddle *et al.* 1997).

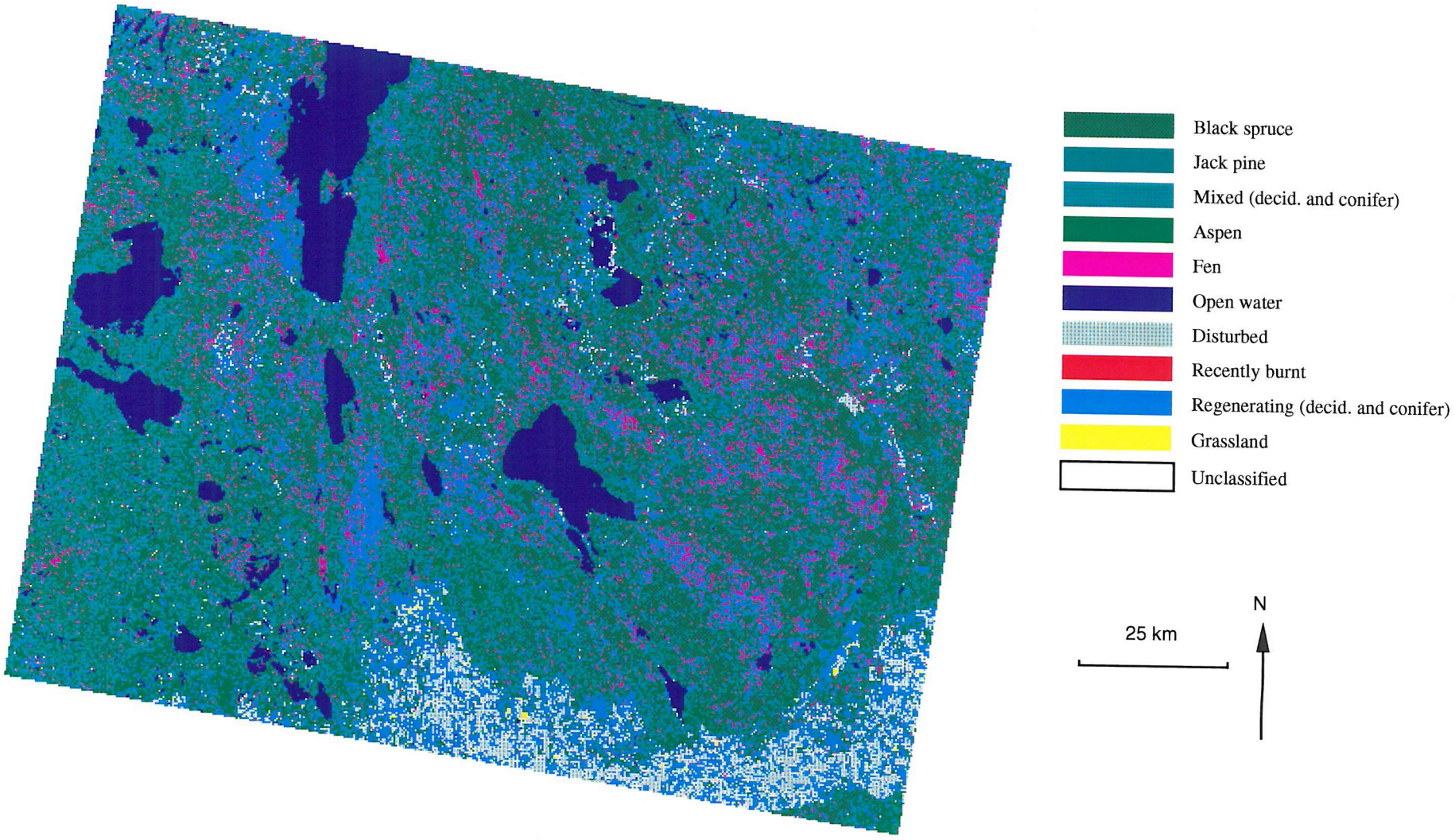

Plate 5.1 Landsat TM classified image of the BOREAS SSA (6 August 1990).

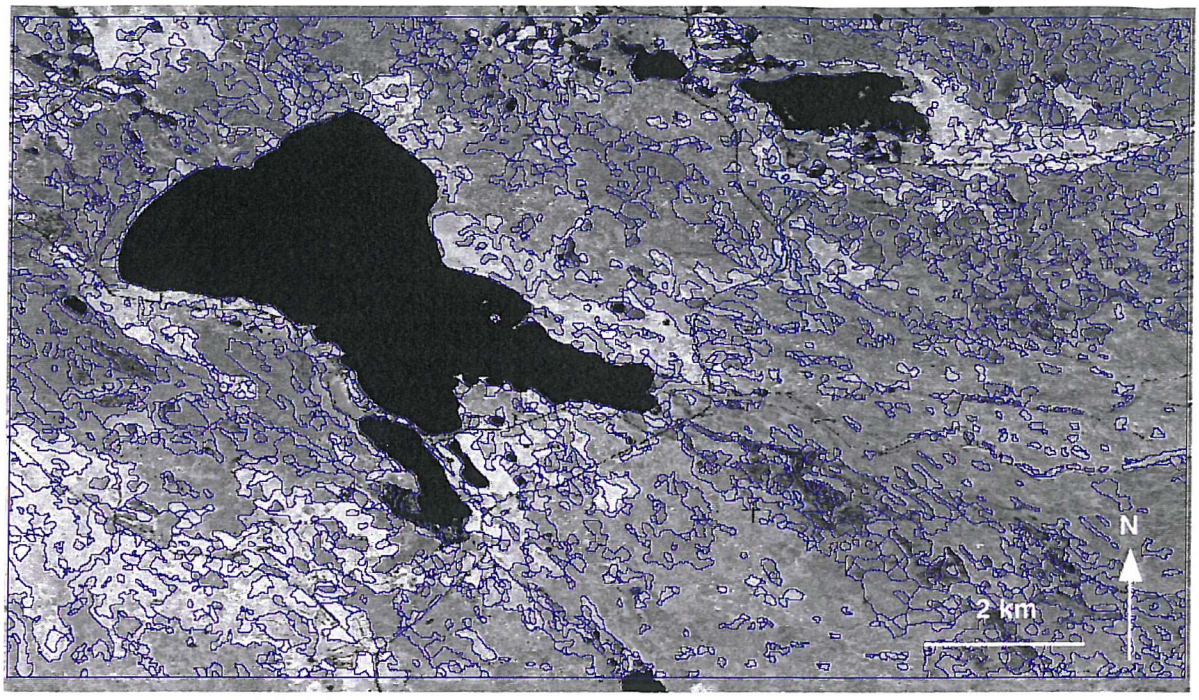

Figure 5.16 The ASU coverage (blue) derived from a pre-classified Landsat TM image and overlaid on the LAI reference raster.

Per-ASU aggregation

A procedure devised to extract raster data for per-parcel land cover mapping (Smith *et al.* 1997; 1998) was adjusted for the extraction and aggregation of LAI estimates per ASU. Figure 5.17 illustrates the procedures that were incorporated into the 'object-oriented' Laser-Scan Integrated Geographical Information System (IGIS) designed initially to bring together raster, vector and ancillary data (Hinton 1996).

The ASU coverage was 'cleaned' within IGIS: Small parcels (containing less than 9 pixels) were removed by merging pixels on a pixel-by-pixel basis to the nearest ASU. The vector polygon of each ASU was used subsequently to identify the pixels in the LAI image that fell within it. These pixels were extracted and their mean and standard deviation calculated. The results were attached as attributes to the ASU polygon. This procedure was repeated for each ASU in turn.

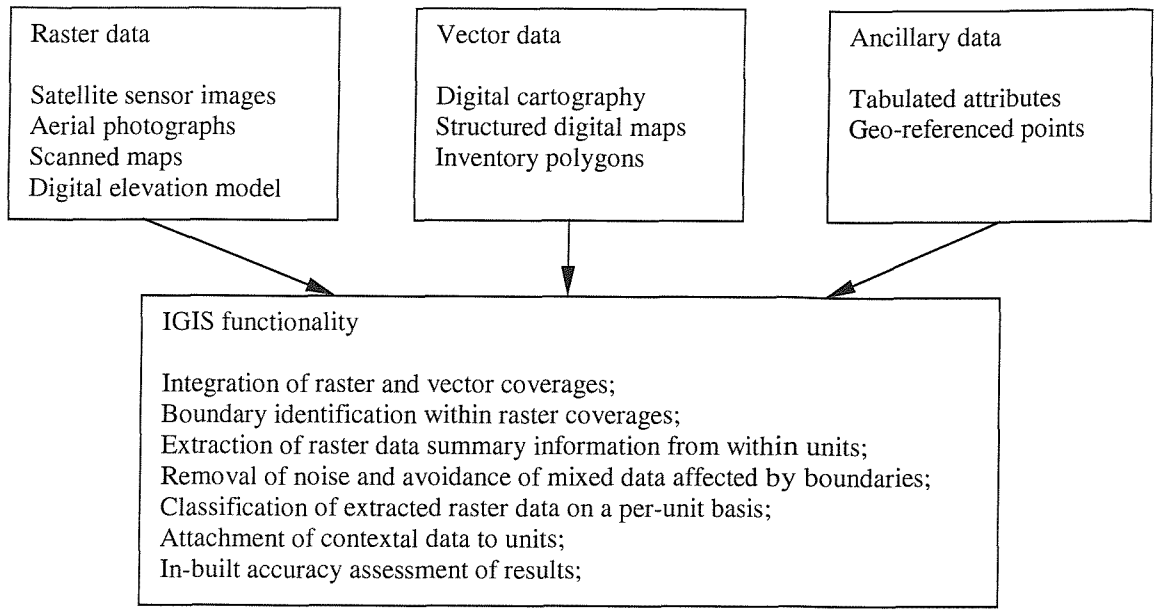

Figure 5.17 Examples of data types that can be integrated and the available per-unit procedures.

Problems of integration

Despite the benefits of combining remotely sensed data and GIS (§2.5.1.1) (e.g., Ehlers *et al.* 1989; Hinton 1996), there are problems associated with such integration. Most obviously, these concern the different data models of remotely sensed raster imagery and vector data (Ehlers *et al.* 1989; Hinton 1996; Wilkinson 1996; Aplin 1999). Indeed, integration is limited by our inability to understand and implement fully a transformation between these two representations of spatial data (Ehlers 1990; Davis *et al.* 1991; Congalton 1997; van Rompaey *et al.* 1999).

Ehlers *et al.* (1989) identified three stages of integrated remote sensing and GIS analysis:

1. separate database, cartographic and image processing systems, each with facilities to transfer data between them
2. two software packages (image processing and GIS) with a shared user interface and simultaneous display
3. a single software package with shared processing (full integration).

To date, several systems have achieved stage two (Hinton 1996; Aplin 1999). However, although stage two integration enables the incorporation of both raster and vector data, it is still necessary to convert one of these forms of data to enable joint analysis. There are numerous examples of the conversion of vector to the raster data model (e.g., Gastellu-Etchegorry *et al.* 1993; Sader *et al.* 1995; Tripathy *et al.* 1996), but fewer exist for conversion of raster to the

vector model (e.g., Mattikali *et al.* 1995; McClean *et al.* 1995). The conversion of data between these spatial models does have associated problems, for example, little is known of the geometric accuracy, which 'questions the validity of projects involving such conversion' (Wilkinson 1996, p. 97). Secondly, where errors exist in the original data, these will be propagated through conversion (Davis *et al.* 1991). Several researchers have attempted to quantify geometric accuracy following conversion and the affect of size and shape of pixels and polygons on the geometric accuracy of conversion (Carver and Brunsdon 1994; Hinton 1996; Congalton 1997). Only a very few systems have achieved the third stage (complete integration), including Laser Scan's IGIS, used within this investigation (Ehlers *et al.* 1989; Smith *et al.* 1997).

5.3.3 Aim 3: Assess the Influence of Boundary Pixels

The estimates of LAI for the boundary pixels at the edges of ASUs may be distorted by the mixing of spectral signatures from adjacent areas. The number of boundary pixels present is related to the actual thickness of the boundary between ASUs on the surface and the pixel size of the image. The problem of boundary pixels is increased by the occurrence of transition zones which effectively broaden the boundary feature and are more common in natural environments.

Methodology

To avoid the inclusion of boundary pixels in the calculation of mean and standard deviation of LAI within each ASU, the ASU polygons were shrunk prior to raster data extraction, so that only core areas were used (Figures 5.18 and 5.19). Indeed, this was the main advantage of using the aggregation technique within an integrated GIS package (Figure 5.17). Shrinkage was dynamic and controllable, with the results being reported back to the ASU to assess accuracy / legitimacy of the extracted raster data.

Accuracy assessment of LAI estimates

Figures 5.20 and 5.21 illustrate the results of regression between the $LAI_{testing}$ ground data (Chen *et al.* 1997) and estimates of LAI from the three sampling units (per-pixel, per-ASU and per-shrunken ASU). Two trends of increasing accuracy of estimates can be seen. First, by matching the sampling unit to spatial structural characteristics within the image (i.e., per-ASU) and second, by excluding mixed boundary pixels (i.e., per-shrunken ASU). This second result is particularly exciting and raises several issues for further research (§5.5). Figure 5.22 demonstrates that mixed edge pixels result in overestimates at low LAI values and underestimates at high LAI values, therefore, are most probably from paths and clear-cuts (of low LAI).

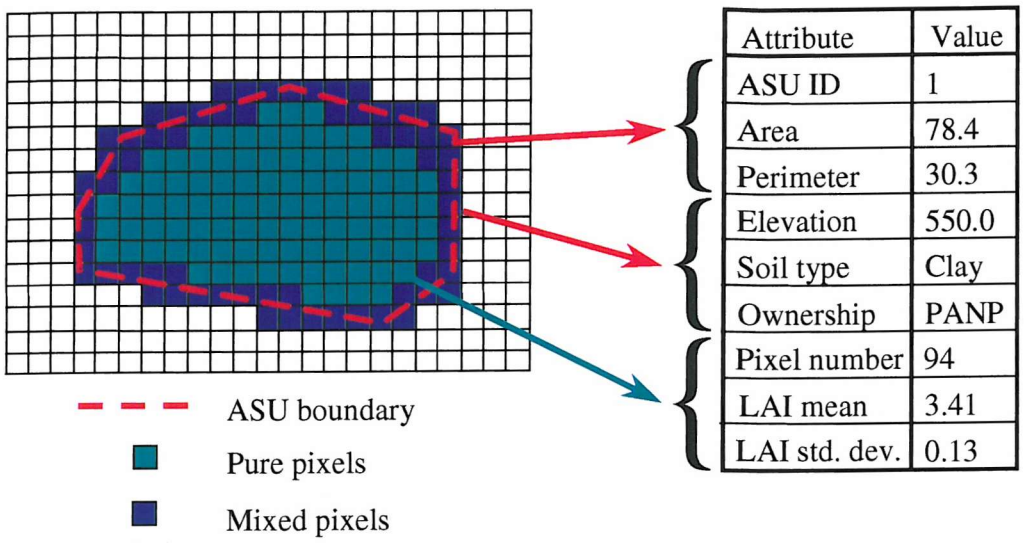

Figure 5.18 Diagrammatic representation of ASU shrinkage to exclude mixed pixels.

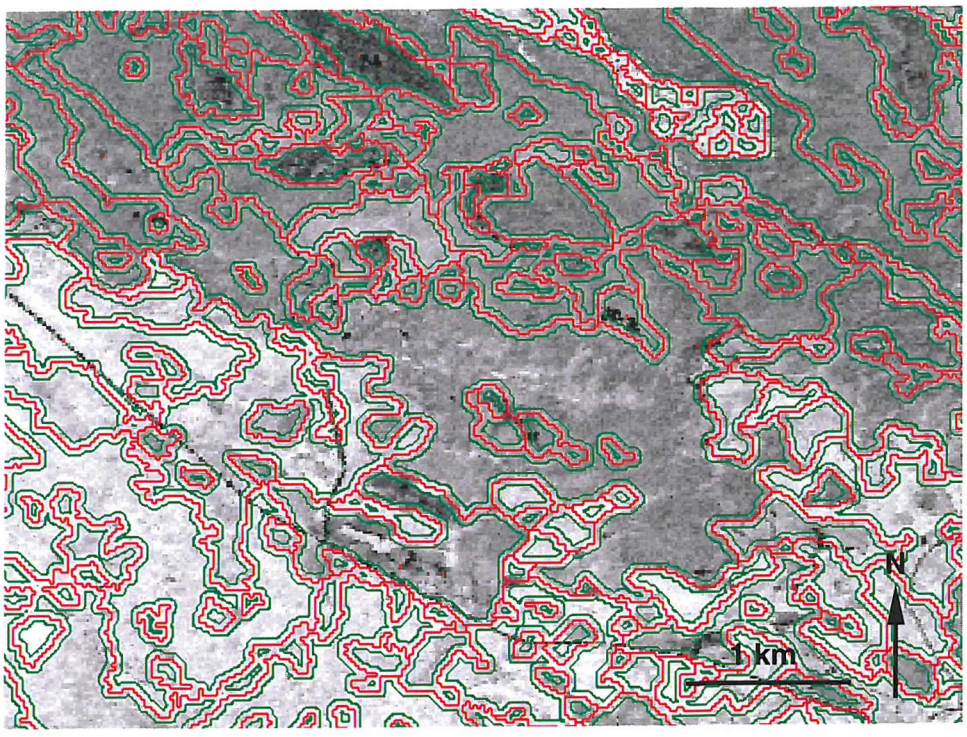

Figure 5.19 A subset of the LAI reference raster with ASU polygons (red) and shrunken ASU polygons (green) overlaid.

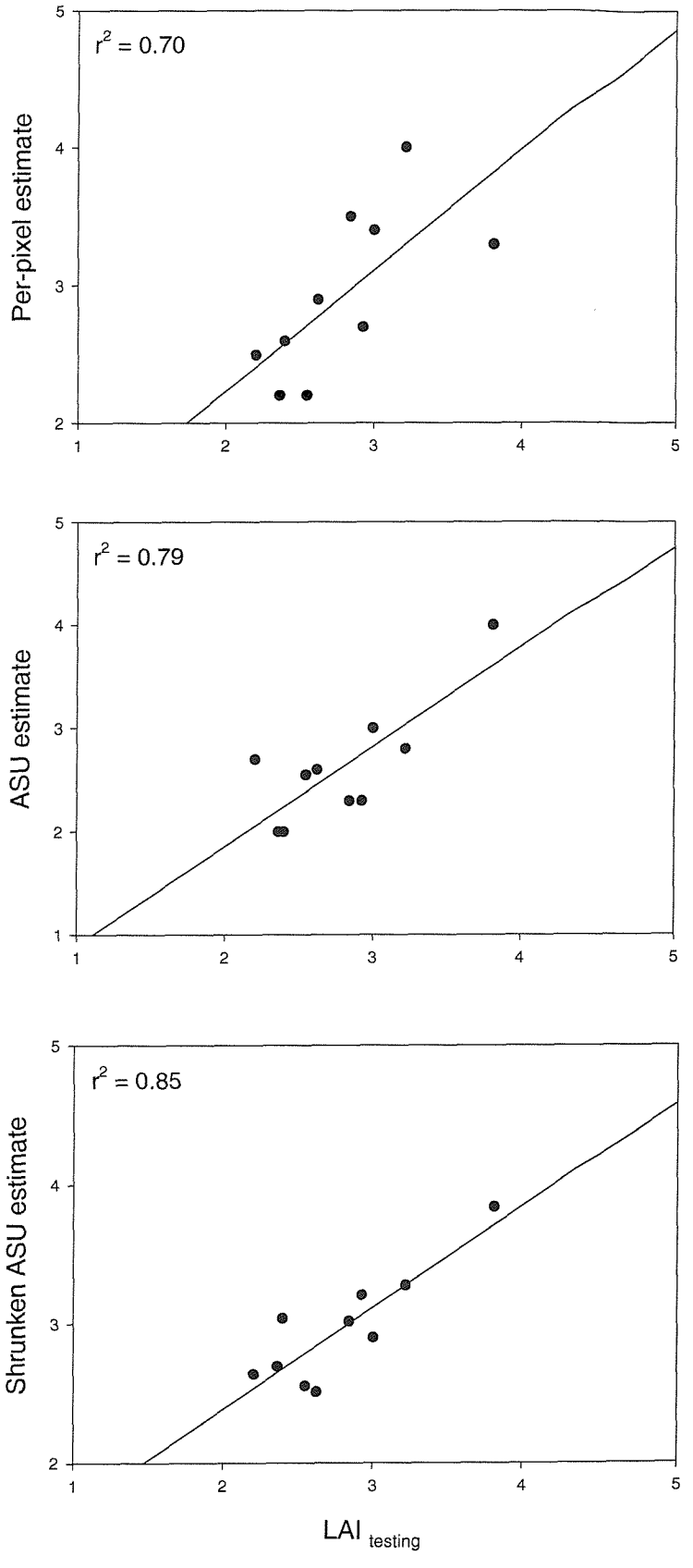

Figure 5.20 Relations between $LAI_{testing}$ data and per-pixel, ASU and shrunken-ASU LAI estimates.

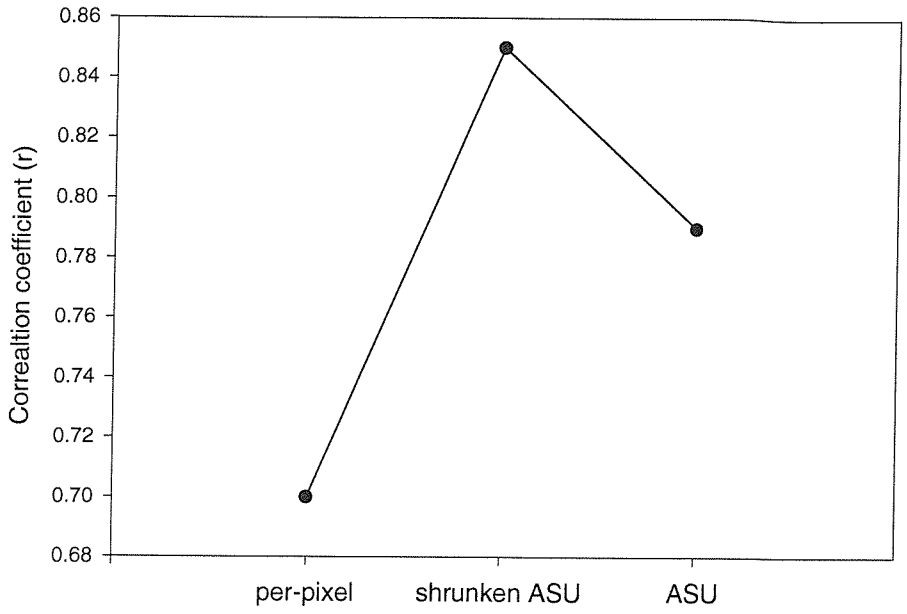

Figure 5.21 Correlation coefficients (r) between estimated and observed LAI for three spatial sampling units.

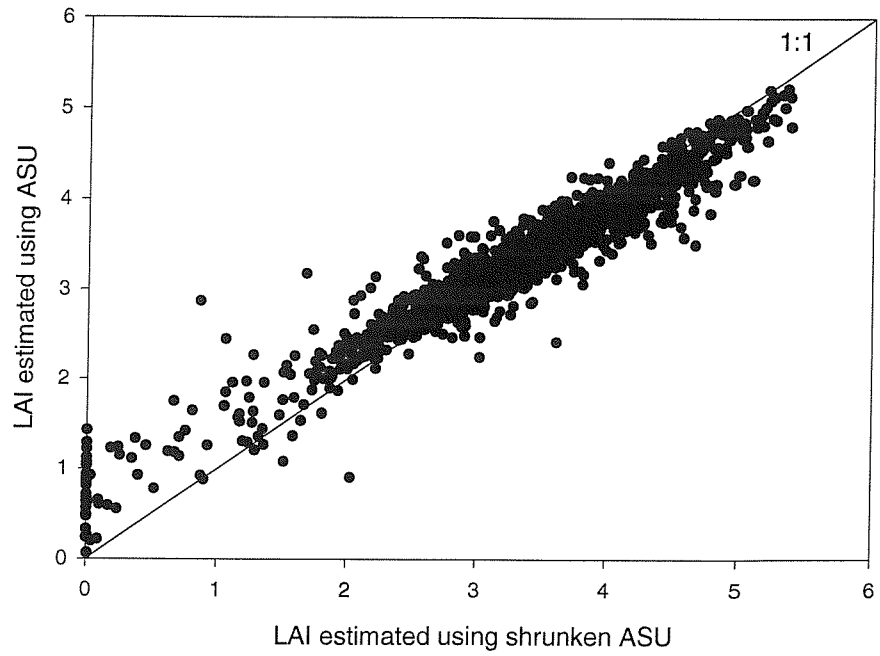

Figure 5.22 Comparison between LAI estimates per ASU and per shrunken ASU.

Therefore, within ASU aggregation offers many advantages:

1. each unit has lower variability than the threshold sensitivity of a model as ascertained by an earlier sensitivity analysis (§4.3.1.1) (Wicks and Curran 1998);
2. fewer model runs are required for regional scale applications (Csillag 1997);
3. by matching sampling unit to 'natural' unit high spatial frequencies removed, therefore,
4. analysis of data at the scale of the ASU offers increased accuracy of LAI estimation and
5. further increases in accuracy attained by excluding edge pixels from ASU analyses.

5.4 Summary and Recommendations

The 'challenge' of spatial dependence (Curran and Atkinson 1999, p.17) is that of choosing a spatial dimension best suited to a specific application. This chapter has presented one such example, resulting in a technique of landscape partitioning for use within ecosystem simulation modelling.

Results confirmed the potential of ASU aggregation for increasing the accuracy of biophysical variable estimation at regional scales. The sampling units captured spatial variation of the landscape, while high spatial frequency features, (some associated with noise in the data), were removed, hence, more representative estimates of LAI (for input to ecosystem models) were attained. Excluding the edge pixels of each ASU from the aggregation procedure attained further increases in estimation accuracy per ASU (relative to per-pixel). Such landscape partitioning may also facilitate model implementation for regional scale investigations as fewer model runs are required and each ASU can have a lower variability than the threshold sensitivity of the ecosystem model employed.

To conclude, the adoption of ASUs for estimating spatial biophysical inputs to ecosystem models, in contrast to traditional stand polygons or '*arbitrary pixels*' (Fisher 1997, p. 680), has the potential to increase the accuracy of NPP estimation at regional scales.

Although this work has focussed specifically on the problems of discriminating homogeneous units within forested landscapes, the main ideas of choice of scale, scaling-up and the discrimination of boundaries are applicable to any domain where raster and / or vector data are employed. Indeed, mapping of soils, coastlines, watercourses, water sediments and pollution, geological features, etc. may all benefit from this kind of analysis. In particular, the interpretation of noisy imagery (such as radar) is also likely to profit, as is the interpretation of the results of more automated image analysis techniques, used widely in remote sensing applications.

Potential for future research

The research within this chapter has highlighted several areas for future research. First, although elevation and its derivatives did not prove useful for landscape partitioning, it may be possible that in combination with a classified image they may add additional information to the ASU coverage. For example, one would expect LAI to vary within a single species forest stand with physical characteristics that affect, for example, the radiation regime. Potential further increases in accuracy of using the ASU to estimate LAI may be achieved by dividing them further according to classes of aspect, slope and elevation.

Second, a current issue within the GIS research community is the representation of transitional boundaries as having a 'fuzzy' width (e.g., van Beurden *et al.* 1999; Zhang and Kirby 1999). Existing work on representing boundaries as having width (e.g., "epsilon bands") includes that of Goodchild (1977), Blakemore (1984), Chrisman (1987) and Dunn *et al.* (1990). However, in all these examples a single width has been employed for all boundaries (i.e., 'global epsilon band width' (Dunn *et al.* 1990)). Such work has concentrated on boundary 'error' as a probability distribution function of possible boundaries around the '*true*' boundary location, hence focussed largely on digitising error. In contrast, the possibility of using a variable boundary width, which is in some way dependent on the characteristics of the two units on each side (e.g., texture variability or discrimination) would seem much more appropriate for the characterisation of boundaries within natural ecosystems and may be worth further investigation. Representing each ASU as a central homogeneous core with an outer boundary that delimits the region of maximum likelihood, hence forming a 'fuzzy' content map would be an extremely useful development. There also exists the potential to model the temporal persistence of these 'homogeneous cores'.

Chapter 6

Spatial Estimation of LAI: Models and Methods

> '*A major challenge facing ecologists studying the Earth as a system is the mapping of vegetation quantities over large areas.*' (Dungan *et al.* 1994, p.237).

Accurate spatial estimates of continuous biophysical variables, such as LAI, are required to drive ecosystem simulation models over large areas (Avissar and Verstraete 1990; Henderson-Sellers 1991). Such maps may also be useful for monitoring regional or global status and changes in vegetation quantities (Dungan *et al.* 1994). Burrough (1987) identified two approaches to create maps of biophysical variables. First, whole-area or exhaustive approaches, using inexpensive, plentiful data (e.g., climate) and applying a transform that relates these data to sparse data on the biophysical variable. Second, point-based approaches, sampling the biophysical variable to be mapped and using an interpolation scheme to create a map. Both approaches have been used to map biophysical variables over large areas (Lieth 1975; Merrill *et al.* 1993; Rasmussen 1998a). Whichever approach is adopted, both models and data are needed to obtain these spatially exhaustive biophysical variable estimates. The models are either statistical or deterministic. Statistical models use mathematics to achieve results with certain statistical properties, whereas deterministic models use mathematics to represent processes presumed to be important in the physical system (Dungan 2000). Biophysical data may be obtained directly (e.g., destructive sampling of trees to estimate leaf area) or indirectly (e.g., light transmittance measurements to estimate leaf area). In practice, most measurements, especially associated with vegetation canopies, are indirect (§3.3.1). These measurements may be sparse spatially, for example, when a canopy is sampled at a few locations on the ground, or

exhaustive, when a remote imaging system records values for overlapping fields of view that, when combined, cover a region completely. A somewhat misguided expectation is that remote sensing ultimately should remove the need for ground data (Steven 1987). In fact, the opposite is true. The demand for good quality ground data, required to utilise remotely sensed data in all except a very limited range of applications, has never been so great! Given the need for spatially exhaustive biophysical variable estimates, therefore, both accurate ground data and robust models are essential. The models can link direct and indirect information, enabling estimation of values at locations where no direct measurements have been made.

The choice of a mapping method has critical implications for accuracy, representation of spatial pattern and scale and for correlation with other spatial variables (Dungan *et al.* 1994). Therefore, this chapter presents three alternative methods for producing spatially extensive estimates of LAI: aspatial regression, cokriging and conditional simulation. The theory behind each is described briefly, before exploring the most appropriate method.

6.1 Theory Behind Models of Estimation

When a variable is distributed in space, it is said to be regionalised (this investigation is concerned with two-dimensional space). Given that a random variable, RV, can take any value within a defined probability density function, a regionalised variable ReV, z(x) may be defined as a particular realisation of the set of RVs {Z(x)} distributed spatially and known as a random function, RF. Therefore, a raster image may be modelled as a realisation of a RF (a spatial set of RVs) (Atkinson and Martin 1999). However, since only a small portion of a RF is represented by data on the Earth's surface, which is just one realisation, important assumptions must be made to construct statistical estimation methods. Some of these assumptions are various forms of stationarity (or consistency) which declare certain characteristics of RFs to be invariant (Dungan 2000). The objective of this chapter is to determine the best method to predict values of LAI across a region. Hence, LAI is the *primary* variable and can be modelled as a RF. Other variables used in the estimation of the primary variable, for example, spectral variables derived from remotely sensed images, are called *secondary* variables and may also be considered RFs. The RFs are used subsequently to construct estimation methods that have the highest possible accuracy.

Across the literature relevant to this subject, many terms are used to describe the type of variable in different contexts, which often leads to confusion! For clarity, in accordance with Atkinson (1999), the combination of terms response / explanatory and primary / secondary variables will be used in conjunction with regression and cokriging respectively.

For regression methods without regard for location (i.e., aspatial) the response variable is estimated in a linear or non-linear combination with an explanatory variable(s).

Rather than using purely RFs, using intrinsic or other RFs that include spatial dependence leads to a group of geostatistical estimators called kriging estimators (Journel and Huijbregts 1978). The most simple forms of kriging use only primary variables (using values at measurement locations to estimate those at unsampled locations), whilst, multi-variable kriging, called cokriging, adds a secondary variable(s) to the estimation equations to increase interpolation precision (Myers 1983).

Such 'optimal predictors' (Goovaerts and Journel 1995) whilst having maximum determinable accuracy, lead to single spatial fields of estimated values that have no guarantee of representing the spatial variability of the actual '*true*' field. In contrast, conditional simulation methods (Journel and Alabert 1989; Journel 1996a) are designed on the same RF foundations but generate multiple spatial fields of the primary variable that reproduce the global (or aggregate) statistics.

The following section describes the three methods and by drawing on recent published examples of their use, demonstrates their applicability to the estimation of boreal forest LAI.

6.1.1 Aspatial regression

Regression analysis is a valuable technique, although abused frequently (Webster 1989). There are three forms of regression model, which may be used to:

1. estimate values of one variable, knowing those of one or more others;
2. calibrate data or
3. describe functional relations.

Choice of which form of regression model to adopt relates to measurement error. The 'proper use' of regression is that of estimation. Only in limited circumstances (where there is no error in one of the variables) should regression be used for calibration (e.g., Smith and Milton 1999). Whereas regression should only be used to describe the functional relation between variables when there is no error in either variable. This sub-section describes the use of regression for estimation.

Aspatial regression is a statistical method used commonly to explore the dependence of one variable on another, describing the form of the relationship by way of an equation (6.1).

Regression may be bi- or multi-variate: the explanatory variable, $X_{(i)}$ (e.g., NDVI) is used to estimate values of the response variable, Y (e.g., LAI):

$$Y = a + \sum_{i=1}^{k} b_i X_i + u \qquad (6.1)$$

where, Y is the response variable; $X_1, X_2, \ldots X_i \ldots X_k$ are k explanatory variables; a and b_i are the regression coefficients, representing the parameters of the model for a specific population (a is the intercept of the line of best fit with the y-axis and b is the gradient of the line); and u is a stochastic disturbance-term which may be interpreted as resulting from the effect of unspecified independent variables and / or a totally random element in the relationship specified (Poole and O'Farrell 1971). Figure 6.1 shows an example of a regression model. Applying this function to all the explanatory data produces a map of estimates of the response variable.

Before linear regression can be applied confidently to a set of data, however, it should be ascertained whether the data satisfy "the seven assumptions" of the model (Poole and O'Farrell 1971, p.148; Webster 1989). These assumptions, listed briefly below, have been variously defined (e.g., Matthews 1981; Ebdon 1985; Shaw and Wheeler 1985; Brunsden *et al.* 1999) and are dependent on the form / use of the regression model (i.e., functional realtions, calibration or estimation):

1. Each value of X_i and of Y is observed without measurement error
2. Relationships between Y and each of the explanatory variables, X_i are linear in the parameters of the specific functional form chosen
3. Each conditional distribution of u has a mean of zero
4. Variance of the conditional distribution of u is constant for all distributions
5. No spatial or temporal autocorrelation exists between Y and X_i
6. Explanatory variables, X_i, are linearly independent of each other
7. The fitted X model requires that the conditional distribution of the disturbance term must be normal in form, which implies clearly that the independent variable, Y, has a normal conditional distribution. The random X model requires that both the conditional and marginal distributions of each variable are normal.

Hill (1995) details a specific example of how data for a tree species / area relationship satisfy these assumptions.

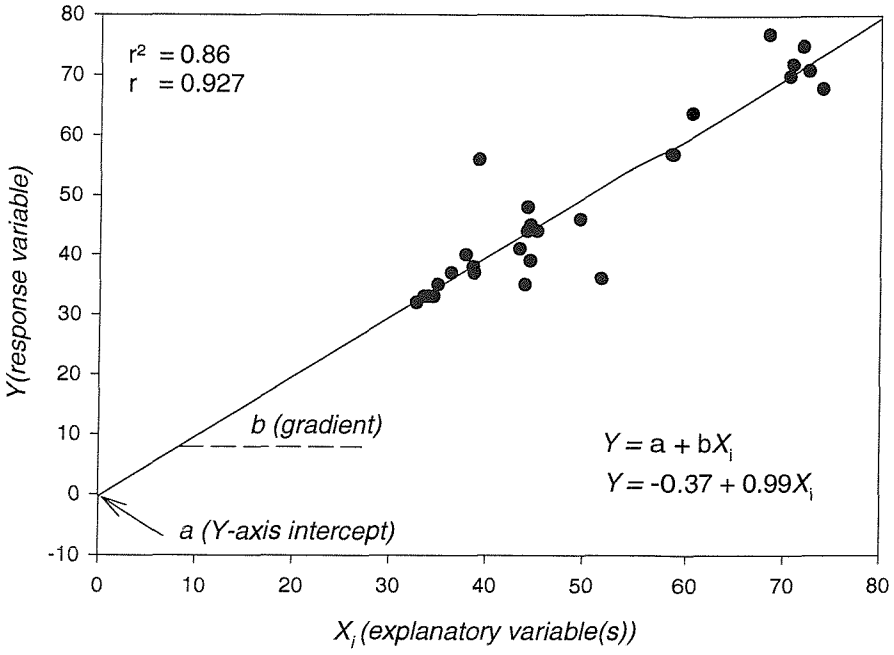

Figure 6.1 Scatter plot illustrating a regression model.

Remote sensing literature is replete with investigations where radiance measures of selected pixels are compared with ground measurements / estimates of some attribute of vegetation (Asrar *et al.* 1985; Peterson *et al.* 1987; Curran *et al.* 1992; Fransson and Israelsson 1999; Dawson *et al.* 1999b). Although, correlation coefficients and regression equations describing the relationships are often reported, only occasionally have these relations been used for direct estimation or mapping (e.g., Curran and Williamson 1987; Running *et al.* 1989; Rasmussen 1998b; Briggs *et al.* 1999). The regression equation is applied to all appropriate pixels to produce a map of the variable (Dungan *et al.* 1994). For example, Cusack *et al.* (1999), used values of airborne NDVI, obtained with the Compact Airborne Spectrographic Imager (CASI) and point-based ground biomass samples to produce a map of above-ground biomass for a 27 km^2 catchment in West Bengal. The largest exponential coefficient of determination (r^2) they obtained was 0.62. This approach appears extremely simple to perform and therefore, to misuse out of context (Webster and Oliver 1990)! Inversion of physically based models, in comparison, may be more realistic for mapping biophysical variables on the Earth's surface but because input variables vary spatially the inversion problem could be ill-posed (Dungan 2000).

The use of regression for mapping is dependent upon a close relationship between the remotely sensed data and the variable of interest (Dawson *et al.* 1999a) as well as the stationarity of the

relationship across the area being mapped (Brunsdon *et al.* 1999). Finally, this method is *aspatial*: all pixels are taken to be independent of their neighbours. This assumption unfortunately implies that the number of ground samples required becomes undesirably large (Curran and Williamson 1986; Cusack *et al.* 1999).

6.1.2 Cokriging

Spatial autocorrelation (dependence) in geographical data can have a large impact in typical applications of aspatial regression (Anselin and Griffith 1988; Haining 1990). Unlike aspatial regression, the main characteristic of geostatistical methods is that they exploit spatial autocorrelation in the data, instead of assuming it does not exist. Indeed, places that are near to each other are more alike than those that are further apart and the degree of dissimilarity depends on both the environment and the nature of the observations (Curran and Atkinson 1998). As such, cokriging estimates values at unsampled locations using a linear combination of values from sampled locations (primary data) and values of another related variable (spatially exhaustive secondary data). Cokriging is the direct geostatistical counterpart to aspatial regression, in that it considers primary and secondary variables (Dungan 2000). The method constructs the estimation *problem* as a weighting of nearby samples of co-located primary and secondary data. At an unsampled location, the cokriging predictor is:

$$p(x_o) = \sum_{j=1}^{N1} \lambda_j p(x_j) + \sum_{k=1}^{N2} \omega_k a(x_k) \qquad (6.2)$$

where, $p(x_0)$ is estimation at location x_0; $p(x_j)$ are N_1 nearby sample values at locations x_j, weighted with factors λ_j and $a(x_k)$ are N_2 nearby secondary values at locations x_k weighted with factors ω_k.

Cokriging is an 'optimal predictor' – a point-based interpolator, except in cases where the secondary variable is spatially exhaustive, when cokriging may be considered a hybrid of point-based and whole-area methods. The appeal of cokriging lies in its potential to incorporate plentiful secondary variables, such as remotely sensed data, to increase the accuracy of estimation at locations where the primary variable has not been measured. However, this potential increase in accuracy comes at the cost of collecting sufficient ground data to enable modelling of the primary variable as well as more time-consuming modelling. Whether this additional effort is worthwhile depends on the strength of the relationship and the spatial cross-correlation between the variables (Dungan *et al.* 1994).

To date, cokriging has been used in several studies in which one variable has been interpolated using sparse measurements of that variable and a second more thoroughly sampled variable (e.g., Leenaers *et al.* 1990; Nash *et al.* 1992). However, it is only comparatively recently that cokriging has been investigated for combining ground measurements and remotely sensed data (e.g., Atkinson *et al.* 1992, 1994; Rossi *et al.* 1994). Ishida and Ando (1999) used soil organic matter samples from the Aidu Basin, Northern Japan in conjunction with remotely sensed data from the Landsat TM to demonstrate that cokriging provided more accurate estimates of soil organic matter than regression. The mean square error (MSE) they obtained using regression was 33% greater than that of the cokriging estimates. However, as yet, cokriging has very rarely been used to produce spatial estimates of continuous vegetation variables (Dungan 2000).

6.1.3 Conditional simulation

Conditional simulation is a geostatistical method that involves a stochastic (random) component, resulting in many 'equally probable' maps (simulations). Each unsampled location is not, therefore, described by its expected value but by a distribution created from information about the neighbouring samples and the spatial covariance. Simulations are 'conditional' to the data (Dungan *et al.* 1994) – they come from a probability model of the variable at an unsampled location 'given' the surrounding data:

$$prob(A_1 \text{ I } A_2) = prob(A_2)prob(A_1|A_2) \tag{6.3}$$

where, A_1 and A_2 are events, such that, the joint probability of A_1 and A_2 is equal to the probability that event A_1 will occur, given A_2 has occurred multiplied by the probability of A_2. This can be extended to n events.

Monte Carlo selections from each distribution at every point produce an arbitrary number of maps that each reproduce the sample data at their measured locations and spatial covariance deemed representative of the region. One of the main features of conditional simulation is its attempt to reproduce spatial patterns as well as characterising the uncertainty about the spatial distribution of the primary variable (Journel and Alabert 1989).

Given sparse data for the primary variable and the many ways in which aggregate statistics can be represented in a spatial field, there is no single solution for a conditional simulation. In fact, simulations are 'multiple alternative fields' (Dungan 1998). Each map produced by conditional simulation is said to be as probable as any other, given the sample. Therefore, the set of all simulations, taken jointly, describes the uncertainty arising from the interpolation /

extrapolation of the sample. The set may be summarised to provide, for example, mean or median estimates. These summaries may be used in risk assessment, sample design or any other applications where spatial estimates of uncertainty are required (Journel and Alabert 1989).

The incorporation of a secondary variable in a conditional simulation method has the potential to provide more information, as in cokriging. However, this information must be accompanied by the modelling of secondary and cross-covariances.

6.1.4 Summary

This section has outlined briefly the theory behind three potential methods for the spatial estimation of biophysical variables. Christakos' (1992) suggested spatial estimation methods should be judged on their ability to incorporate six physical realities: (i) measurement error, (ii) measurement support (support is a geostatistical term used to describe the size, geometry and orientation of the space on which an observation is defined, for example, in remote sensing, the size of support is equivalent to the spatial resolution or pixel size), (iii) sample geometry, (iv) relative locations of the measurements, (v) spatial variability and (vi) spatial correlation. These 'realities' relate to the need for a means of collecting data that are a reliable description of a region. Other distinguishing features of the methods are whether they honour known measurement values and are optimal (i.e., unbiased, with minimum error) (Cressie 1990). In combination these characteristics and properties provide a useful framework for comparing the methods presented in this chapter for the production of a map of boreal forest LAI (Table 6.1). Other practical differences exist, with increasing complexity in procedures, decreasing availability of software for implementation and decreasing speed of computation in the progression from aspatial regression to cokriging to conditional simulation (Dungan, 2000).

		Regression	Cokriging	Conditional simulation
honours known measurement values		✔	✔	
optimal (unbiased, with minimum error)		✔	✔	
provides a measure of 'error'		✔	✔	✔
may use sparse data for primary variable		✔	✔	✔
reproduces of fine scale features		✔		
incorporates measurement support			✔	✔
exploits spatial autocorrelation			✔	✔
	rank	2	1	3

Table 6.1 General properties and characteristics taken into account by each estimation method. ✔ indicates that the method has or preserves the property / characteristic in the spatial estimates.

In an investigation using synthetic data, consisting 300 surrogate 'ground measurements' on a 100 × 100 cell grid, Dungan (2000) found that for a range of correlations between primary and secondary data, cokriging usually produced more accurate maps. It was only when the correlation coefficient (r) was greater than 0.89 that aspatial regression became the most accurate estimator (Figure 6.2).

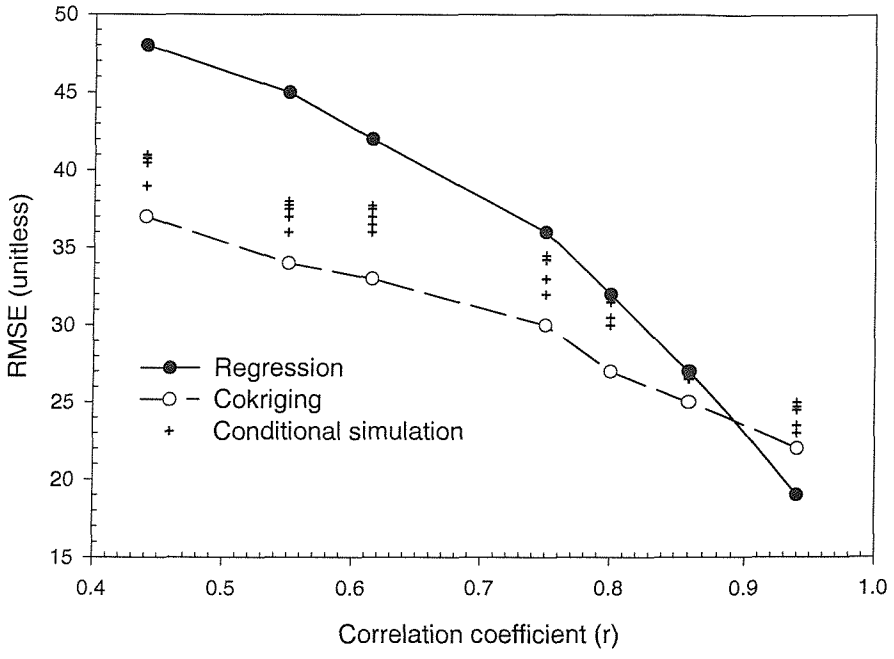

Figure 6.2 The trend in root-mean-square error (RMSE) amongst images mapped with aspatial regression, cokriging and conditional simulation as a function of the correlation between the primary and secondary data in one example with synthetic data (from Dungan 2000).

To reinforce this, Atkinson *et al.* (1994) stated four reasons (both theoretical and practical) why researchers should consider the use of cokriging for estimation:

1. takes account of the spatial autocorrelation in a scene, therefore makes full use of the data available (Webster and Oliver 1990).
2. provides a measure of the minimum estimation or cokriging variance as a by-product (Rossi *et al.* 1994)
3. may be used to determine optimal strategies for sampling the primary variable at the ground prior to the actual field survey (e.g., Atkinson 1991; Hedger *et al.* 1996).
4. redundant information in an image may be excluded without compromising the accuracy of estimates (Atkinson *et al.* 1990).

In addition, cokriging is an 'exact estimator' so ground measurement values are honoured in the estimated map, however, the result is smoothed so one limitation of this estimation method is that will not reproduce fine spatial scale features.

Issues of complexity in procedures, availability of software for implementation and speed of computation detract from conditional simulation in favour of cokriging and aspatial regression. Indeed, from this theoretical review, the spatial estimation method of cokriging has the greatest potential for producing accurate spatial estimates of boreal forest LAI at regional scales. The next section details the data available for use with this method.

6.2 Primary and Secondary Data Sets

The BORIS database contains a plentiful supply of biophysical variable ground measurements taken by a number of researchers (§3.2.1). Potential data sets to be used as a primary variable were extracted. In particular, several research teams from the BOREAS were involved with estimating LAI for the boreal forest (§3.2.1.1). Each LAI data set was obtained through BORIS and examined for its appropriateness for this investigation. The data collected by BOREAS researchers from group TE23 ($LAI_{hem\ photo}$) (§3.2.1.1) was chosen eventually for the sheer number of measurements (n = 235). Data sets of diameter at breast height (dbh), tree density, basal area, crown closure, tree age and tree height were also obtained for potential use as primary variables.

Spatially exhaustive secondary data were available in two forms. First, remotely sensed data and second, a DEM. A cloud free scene of the BOREAS SSA (2 September 1994, path 37 row 22) was chosen for the purpose of this study (Plate 4.1a). At-sensor radiance values for the entire image were converted to produce a NDVI coverage, suitable for use as an secondary variable. The DEM of the study area was also obtained through BORIS. These data were in the UTM projection, with a pixel size of 100 m (appropriate for the 1:50,000 scale contours from which the DEM was derived). Images of slope and aspect were derived subsequently from the DEM within the GRASS (v. 4.1) software package (USACECERL 1993) (§5.3.2).

The results of linear regression analyses between all possible combinations of primary and secondary data are shown in Table 6.2. Relationships between remotely sensed variables and ground measurements of biophysical variables are often statistically significant but not strong (e.g., Friedl *et al.* 1994; Lambert *et al.* 1995; Holmgren and Thuresson 1998). This was reflected in this investigation: weak correlations between the majority of possible primary and secondary variables were found. The only exception being the relation between hemispherical photo derived estimates of LAI and NDVI (r = 0.61) (Figure 6.3).

		Secondary variable (exhaustive)		
		$LAI_{hem\ photo}$ (n=124)	NDVI	Elevation
Primary variable	$LAI_{hem\ photo}$	-	0.61	0.01
	Elevation	0.07	0.003	-
	Slope	0.08	0.004	0.37
	Aspect	0.21	0.06	0.05
	DBH	0.46	0.20	0.42
	Crown closure	0.30	0.55	0.28
	Tree age	0.31	0.56	0.12
	Tree height	0.27	0.41	0.51
	Tree density	0.22	0.43	0.18
	Basal area	0.54	0.32	0.39

Table 6.2 Summary of variable relations. Values are correlation coefficients (r).

To implement cokriging, the first step is the description of spatial dependence of the primary and secondary variables. The omnidirectional semivariograms ($\gamma_p(h)$) for the LAI estimates (n = 235) (Figure 6.4a) and the secondary variable image (i.e., NDVI) (Figure 6.4b), were fitted well by the spherical model with a nugget variance:

$$\gamma_p(h) = c_0 + c_1\left\{\frac{3h}{2a} - \frac{1}{2}\left(\frac{h}{a}\right)^3\right\} \qquad (6.4)$$

where, c_0 is the intercept of the model on the ordinate (the nugget variance), c_1 is the sill of the spatially correlated variance and a is the range of the model (Webster and Oliver 1990; Atkinson *et al.* 1994).

The models of the semivariograms illustrate that the primary and secondary variable are spatially dependent over the same range and in particular, the model for the secondary variable has a low nugget variance (which equates to small error) (Table 6.3).

Variable	Model	c_0	c_1	a (m)	Maximum lag (m)
LAI	spherical	0.420	0.367	511	800
NDVI	spherical	0.004	0.005	531	800

Table 6.3 Coefficients of the models that provided the best fit to the variograms (Figure 6.4).

Next, a cross variogram was produced between the primary sample data and the co-located secondary data in order to form a linear model of co-regionalisation (Isaaks and Srivastava 1989). An attempt was made to fit a model to the cross variogram (Figure 6.5). However, insufficient co-located pairs of data were available to produce a stable cross variogram, a most likely manifestation of biased distribution of the primary data. Hence, as the estimation of spatial covariance was not robust, cokriging could not be used in this instance.

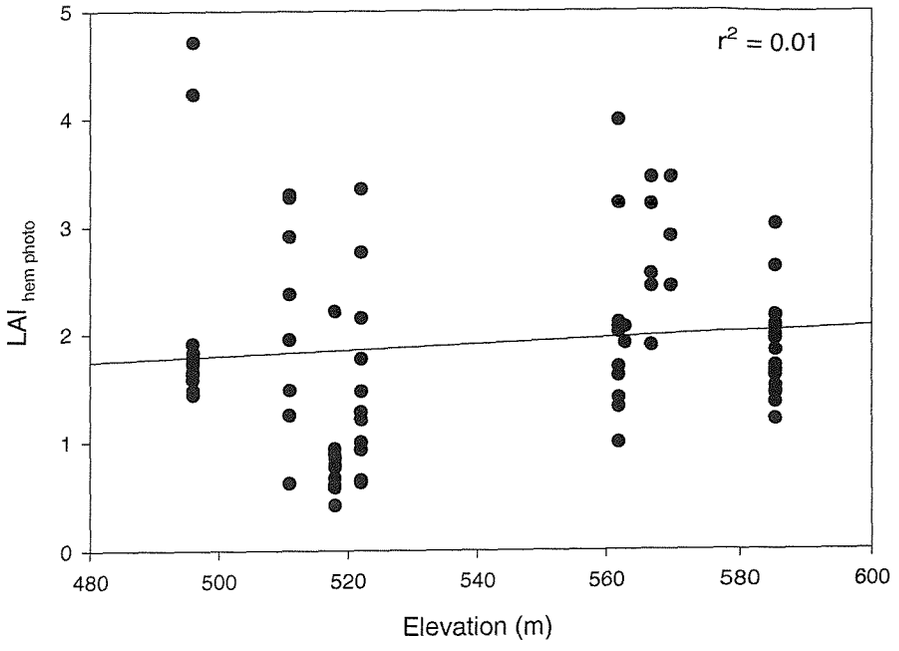

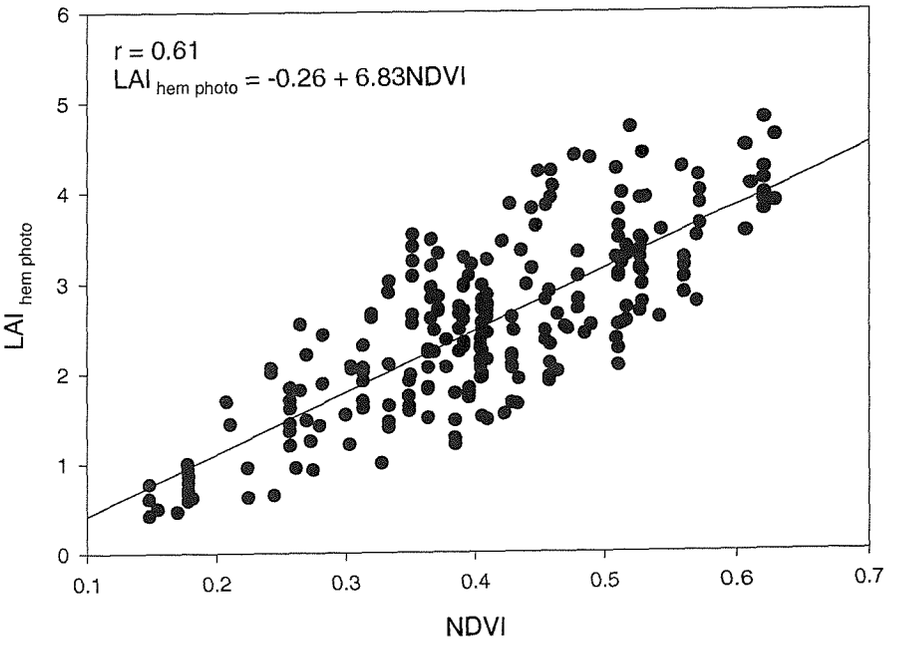

Figure 6.3 Relations between possible primary and secondary variables.

a

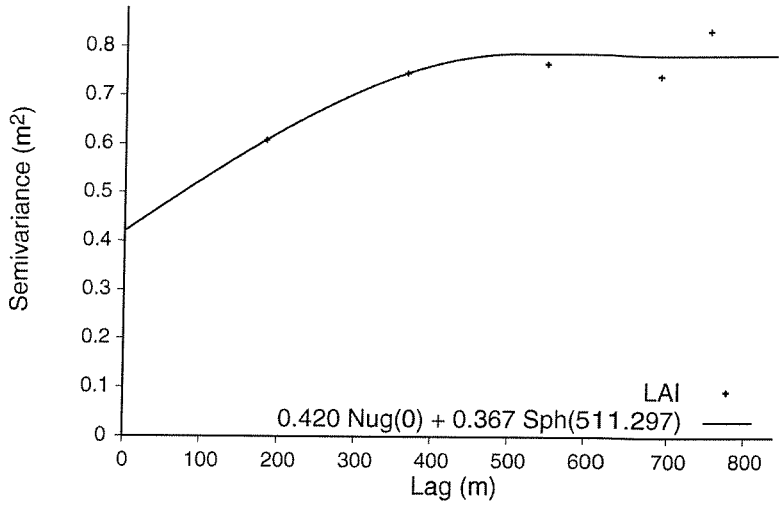

b

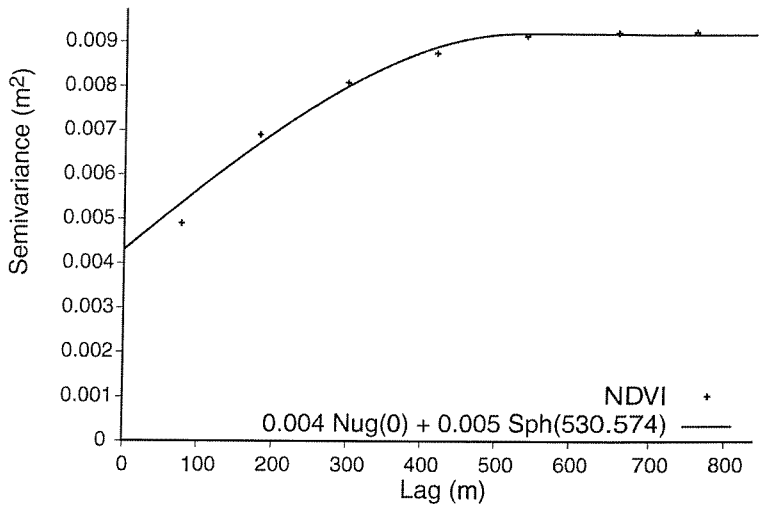

Figure 6.4 Semivariograms computed and modelled for (a) primary and (b) secondary variables.

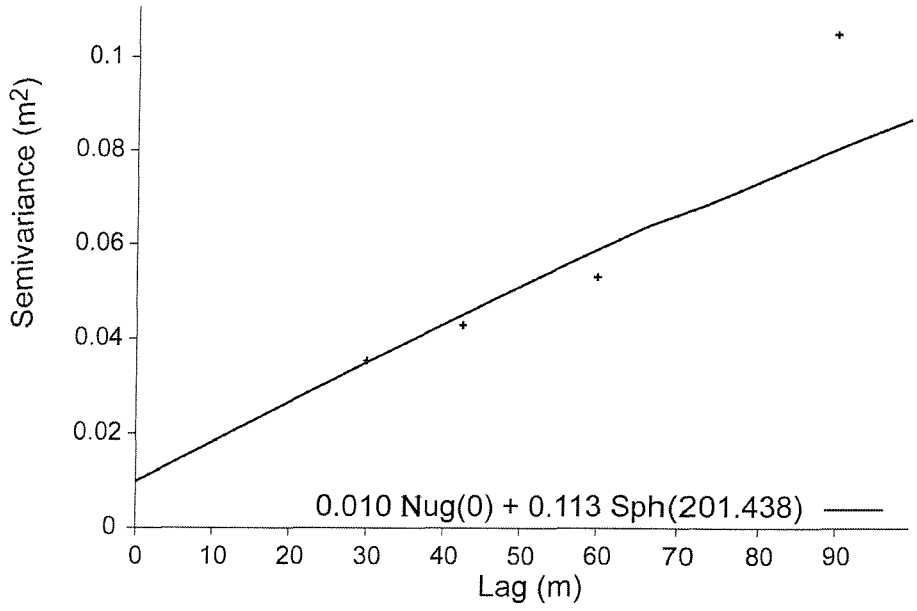

Figure 6.5 Cross variogram of LAI and NDVI.

6.3 Discussion and Conclusions

Theoretical differences among the methods of estimation presented within this chapter may have less to do with their relative frequency in the research literature than practical considerations. Indeed, the dominance of the aspatial regression estimation model in the remote sensing literature may be explained by its simplicity and the wide availability of software for implementation. However, these practical advantages can be outweighed by the need for spatial estimation methods that exploit the information content of remotely sensed secondary data fully. Other advantages of geostatistical methods are the inclusion of measurement error for the secondary data, the consideration of measurement location and sample arrangement and the exploitation (instead of the neglect) of spatial autocorrealtion (Dungan 2000). Indeed, the variogram is clearly a useful tool, allowing the characterisation of the spatial variation of variables (Atkinson and Martin 1999). The accuracy of estimation certainly has the potential to be increased by using spatial information in addition to the correlation information. However, as shown by the example within this chapter, the quality of results is sensitive to the adequacy of the variogram models, stationarity assumptions and the strength of the relationship between primary and secondary variables.

Although geostatistical methods have been cited as reducing the number of samples required to achieve a required level of accuracy (e.g., Webster and Burgess 1984; Dungan *et al.* 1994), they do need robust estimation of spatial covariance, which in turn require, at the very minimum, 100 sample measurements of the primary variable (Webster and Oliver 1990; Cusack *et al.* 1999; Dungan 2000). However, sample sizes as large as this may even be insufficient for an aspatial regression estimation of the regional mean (Curran and Williamson 1986). Dungan *et al.* (1994) used simulated primary and secondary data – in that their 'ground data' was, in fact, radiance from a second spectral region of the same remotely sensed image comprising the primary data!

Regardless of the method used, if researchers require accurate spatial estimates, increasing sample size will be an important factor (Curran and Atkinson 1998). Sampling design is also a particularly important consideration if bias in the primary variable measurements is to be avoided (Atkinson and Martin 1999). Indeed, usually, samples are not located to represent complete spatial randomness but are chosen for logistical or historical reasons. Such subjectivity can result in statistics that are unrepresentative of the whole region (Steven 1987) but the cost of obtaining spatially random plentiful primary variable data may be excessive (Curran and Atkinson 1998).

Ultimately, the best choice of mapping approach is dependent on the purpose for which the map is intended and should be governed by both theoretical and practical considerations (Dungan *et al.* 1994; Brunsdon *et al.* 1999).

To conclude, although the review at the beginning of this chapter suggested cokriging may produce the most accurate spatial estimates of boreal forest LAI, because of the lack of a robust estimation of spatial covariance the aspatial regression approach (the next best option, §6.1.4) will be adopted for the remainder of this thesis. Most recently, several researchers are 'revisiting aspatial regression', having recognised the importance of spatial autocorrelation of continuous variables, to promote techniques that exploit geographical location, such as geographically weighted regression (GWR) (e.g., Brunsdon *et al.* 1996; Brunsdon *et al.* 1999; Fotheringham 1999).

Indeed, provided measurement error in both primary and secondary variables (especially their relative magnitude) are addressed so as to make an informed choice of explanatory (and response) variables, estimation using regression is straightforward (Webster 1989). Reduction in the error of spectrally derived variables may be achieved by minimising sources of error and inconsistency caused by:

1. spatial and temporal misregistration;
2. different supports between ground measurements and pixels;
3. imprecise radiometric calibration (Atkinson and Emery 1999);
4. atmospheric contribution to the remotely sensed signal and
5. variation of reflectance with direction caused by terrain and / or non-Lambertian properties of vegetation.

It is anticipated that such sources of error will be reduced greatly in those sensors launched recently or planned for the near future, for example, the Moderate Resolution Imaging Spectroradiometer (MODIS) and the Medium Resolution Imaging Spectrometer (MERIS), each of which have considerable potential for the mapping / estimation of biophysical variables, such as LAI (§2.3) (Justice *et al.* 1998; Gobron *et al.* 1999).

Chapter 7

The Value of Middle Infrared Radiation (3-5 μm)

To maximise the accuracy with which remotely sensed data can be used to estimate boreal forest LAI, the potential of using radiation acquired by the NOAA AVHRR satellite sensor was explored. Particular attention was given to reflected radiation acquired in MIR wavelengths (3.0-5.0 μm) because it is (i) more sensitive to water content (indirectly related to LAI) and (ii) less influenced by molecular and aerosol scattering, than radiation acquired at shorter wavelengths. The relationship between LAI and several spectral vegetation indices (some incorporating MIR radiation) were assessed and the strongest relationship used to produce a LAI map.

7.1 Introduction

Regional scale LAI can be estimated using coarse spatial resolution sensors mounted on satellite platforms (Running 1990). One suitable sensor is the NOAA AVHRR, which measures radiation from the Earth's surface in five spectral channels (Table 7.1), at a nominal spatial resolution of 1.1 km across a swath width of 2,700 km (Cracknell 1997).

Following correction for atmospheric effects, the radiation reflected from a vegetation canopy and measured by the AVHRR is related causally to LAI. These causal links include a negative relationship between LAI and visible radiation (0.4 - 0.7 μm), due to absorption by leaf pigments and a positive relationship between LAI and NIR radiation (0.7 - 1.5 μm), due to within-leaf scattering (Jensen 1983; Danson and Curran 1993).

Channel number, name and spectral resolution (μm)	Primary uses
1. Visible (0.58-0.68)	Daytime cloud and surface mapping
2. Near Infrared (0.75-1.10)	Surface water delineation, snow and ice
3. Middle Infrared (3.55-3.93)	Hot target detection, night-time cloud
4. Thermal Infrared 1 (10.50-11.30)	Determining cloud and surface temp.
5. Thermal Infrared 2 [a] (11.50-12.30)	Cloud mapping, water vapour correction

Table 7.1 Spectral characteristics of the AVHRR (Cracknell 1997). [a] Not on NOAA -6, -8, -10.

AVHRR measurements of visible and NIR radiation may be employed in combination, within vegetation indices such as the NDVI. The positive, strong relationship between LAI and NDVI, at least up to the reflectance asymptote of the canopy (Tucker 1977a; Curran 1985), has been used to estimate the LAI, or its surrogate, for a number of forest ecosystems (Nemani and Running 1989b; Foody and Curran 1994c; Running *et al.* 1995; Fazakas and Nilsson 1996; Wellens 1997). As such, the use of the NDVI to estimate LAI represents a well-rehearsed approach within remote sensing. Indeed, current literature is replete with examples where remotely sensed radiation and this relationship have been used to obtain estimates of boreal forest LAI (e.g., Chen *et al.* 1997; Cihlar *et al.* 1998; Turner *et al.* 1999).

However, the use of radiation acquired at only visible and NIR wavelengths for LAI estimation does not exploit fully the information provided by the five channel AVHRR satellite sensor (Table 7.1). Recent studies have revealed the value of MIR radiation (3.0 - 5.0 μm) for the study of ecosystems (particularly those with high-LAI) (Laporte *et al.* 1995; Foody *et al.* 1996; Boyd 1996; Boyd and Ripple 1997; DeFries *et al.* 1997; Mantovani and Setzer 1997). MIR radiation has proved to be more accurate for the estimation of biophysical properties related to LAI and less influenced by atmospheric or scan angle effects than visible or NIR radiation (Kaufman and Remer 1994; França and Setzer 1998).

The use of MIR radiation for the estimation of LAI at and beyond regional scales may, however, be unreliable (Kaufman and Remer 1994) as it comprises a mix of reflected and emitted radiation. At regional to global scales, the emitted radiation may be influenced more by confounding variables (e.g., localised atmospheric conditions, such as wind speed and air vapour conductance, or site specific factors, such as topography, aspect and soil moisture conditions) than those biophysical properties that relate to LAI (such as basal area and tree density) (Price 1989; Luvall *et al.* 1990; Nemani *et al.* 1993a; Florinsky *et al.* 1994; Nichol 1995).

It is necessary, therefore, to remove emittance from the total MIR radiation flux and use only the reflected MIR radiation (Kaufman and Remer 1994) for the estimation of regional LAI. MIR radiation reflected from a vegetation canopy is thought to be related to liquid water content of that canopy (primary factor) and canopy structure (secondary factor) (Boyd *et al.* 2000). For example, an increase in LAI will be accompanied by an increase in the amount of liquid water in the canopy and thereby the ability of the canopy to absorb the incident radiant component of MIR radiation (Kaufman and Remer 1994; Boyd and Curran 1998). Also, as LAI increases the structure of the canopy may become more complex, trapping more incoming photons thereby producing shadows, which will also decrease reflected MIR radiation (Figure 7.1).

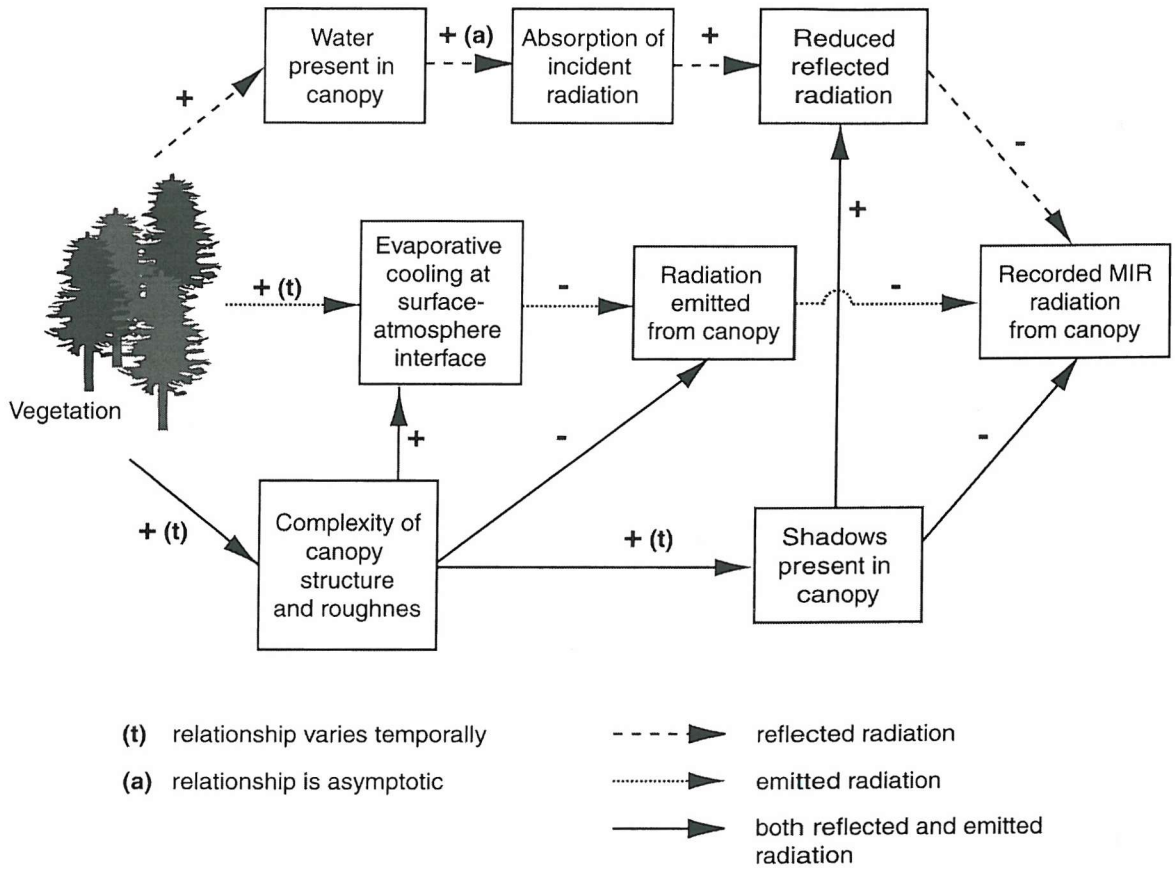

Figure 7.1 Schematic representation of the radiation recorded by the NOAA AVHRR at MIR wavelengths (adapted from Boyd and Curran 1998).

Information provided by reflected MIR radiation has been used in number of recent studies (e.g., Shimabukuro *et al.* 1994; Lambin and Erhlich 1996; Boyd *et al.* 1999), generally, in conjunction with radiation acquired in other wavebands. For example, the Vegetation Index 3 (VI3), which combines the information on canopy properties provided by reflected radiation at NIR and MIR wavelengths, has proved to be more accurate than the NDVI for the estimation of

biophysical properties in a wide range of environments (Kaufman and Remer 1994; Kaufman and Tanré 1996; Boyd *et al.* 1999; Pereira 1999).

Finally, the AVHRR sensor also records radiation at thermal infrared (TIR) wavelengths (channels 4 and 5, Table 7.1). Although radiation acquired at these wavelengths has been employed successfully to estimate crop water stress at local to regional scales (e.g., Goward *et al.* 1985; Seguin *et al.* 1989) it is inherently unstable temporally and spatially (i.e., influenced strongly by (i) terrain, (ii) local variability in wind speed and (iii) cloud shadow) (Rencz 1999). As such, the use of TIR radiation has, to date, received minimal attention for the estimation of LAI. The advent of new multi-spectral, fine spatial resolution sensors (e.g., MODIS) in combination with real-time processing (e.g., Lang *et al.* 1994; Brass *et al.* 1996) may promote the use of TIR. Although, its application will remain more suited to monitoring weather patterns and natural disasters (e.g., wildfire temperature and spread) than more temporally persistent features of the Earth's surface (Rencz 1999).

Therefore, in an effort to maximise the accuracy with which the LAI of boreal forests may be estimated, this chapter explored the potential of several vegetation indices, some incorporating radiation from MIR wavelengths.

7.1.1 Aims of investigation

The three aims of this investigation were to:

1. establish the nature and strength of the relationships between data acquired by the NOAA AVHRR satellite sensor and boreal forest LAI;
2. assess the accuracy of several spectral vegetation indices for the estimation of boreal forest LAI and
3. produce a map of boreal forest LAI using NOAA AVHRR data and the most robust relationship found between remotely sensed radiation and LAI.

7.2 Study Area and Data Acquisition

This research focused on the SSA of the BOREAS study region (§3.2).

During BOREAS, two independent data sets of estimated LAI (one-sided leaf area per unit ground area) were obtained using LI-COR LAI-2000 and ceptometer instruments and made available through the BORIS (§3.2.1.1). The first data set from Plummer *et al.* (1997) provided LAI estimates for 9 sites across the SSA (herein known as $LAI_{training}$). The second, collected concurrently by Chen *et al.* (1998), provided LAI estimates for 10 sites (herein known as $LAI_{testing}$) (Figure 7.2). In both cases the LAI estimates were made along 50 m to 300 m transects of relatively homogeneous forest cover that were representative of each site and were calibrated to allow both inter-comparison and comparison with other LAI data sets (Chen and Cihlar 1995b).

A NOAA-9 satellite AVHRR LAC image was acquired in the satellite's afternoon ascending mode on 21st July 1994. This was near-coincident with the LAI estimation and at a time of year when the contribution of understorey vegetation to the remotely sensed signal would have been negligible (i.e., the canopy cover is complete). All LAI estimates along the transects at each at site were assumed to fall into the area represented by an AVHRR pixel. Therefore, a mean LAI estimate for each site and thereby AVHRR pixel was used in the analyses.

7.3 Processing of Remotely Sensed Data

The NOAA AVHRR image had undergone limited geometric pre-processing at the CCRS (Cihlar and Teillet 1995). The distortions due to spacecraft orbit, altitude and velocity as well as the Earth's rotation and curvature had been corrected using the geocoding and compositing system (GEOCOMP) (Robertson *et al.* 1992).

7.3.1 Radiometric processing to radiance

For the entire image the DN of each of the five channels were converted to spectral radiance using published correction coefficients and constants appended to the image. Radiometric correction for data acquired in visible and NIR channels was different to that for MIR and TIR channels and this is discussed in detail in the following sub-sections.

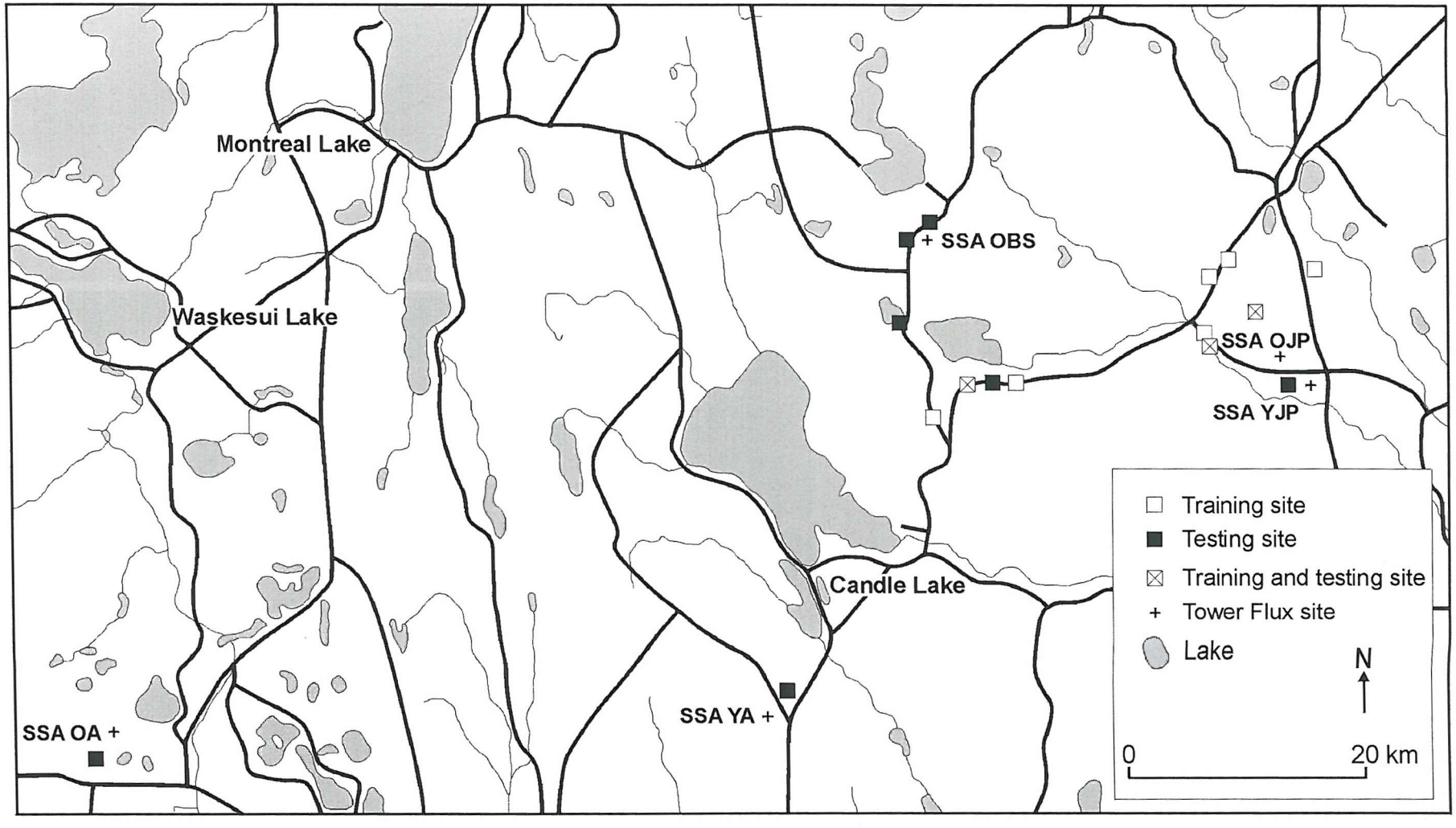

Figure 7.2 Location of LAI $_{training}$ (Plummer *et al.* 1997) and LAI $_{testing}$ (Chen *et al.* 1997) plots.

7.3.1.1 Correction of data from visible and NIR channels

The relationship between at-sensor radiance and recorded DN in both visible and NIR channels is known to alter whilst the AVHRR sensors are in orbit. This is due to launch-associated contamination and continual exposure to the harsh space environment (Brest and Rossow 1992; Kaufman and Holben 1993). Therefore, the use of pre-launch coefficients (Kidwell 1991) for the radiometric correction of these channels will be inaccurate. Several researchers have investigated these 'degradation' effects and the most effective ways in which to remove them from the measured signal in visible and NIR channels (e.g., Che and Price 1992; Teillet and Holben 1994; Rao 1995). It was decided to adopt the procedure outlined within Rao *et al.* (1996) as this not only ensured removal of spurious temporal trends but also established continuity between satellite sensors (Table 7.2).

Satellite (launch date)	Channel	Radiometric correction algorithm
NOAA-9	Visible	L = (C10-37) * 0.5465 * exp (1.66*10^{-4} * d-65)
(12/12/1984)	NIR	L = (C10-39.6) * 0.3832 * exp (0.98*10^{-4} * d-65)
NOAA-11	Visible	L = (C10-40) * 0.5496 * exp (0.33*10^{-4} * d)
(24/09/1988)	NIR	L = (C10-40) * 0.3680 * exp (0.55*10^{-4} * d)
NOAA-14	Visible	L = (C10-41) * 0.5604 * exp (0.35*10^{-4} * d)
(30/12/1994)	NIR	L = (C10-41) * 0.3527 * exp (0.51*10^{-4} * d)

C10 is the extracted DN value, d is the time elapsed in days since launch and L is spectral radiance (W m^{-2} sr^{-1} mm^{-1}).

Table 7.2 Radiometric correction algorithms for the AVHRR sensors on NOAA polar orbiting platforms (from Rao *et al.* 1996) from which AVHRR LAC data were acquired for BOREAS.

7.3.1.2 Correction of data from MIR and TIR channels

Onboard calibration coefficients maintain consistency and precision over long time intervals within these channels (Gutman *et al.* 1996). Therefore, the original procedure (Kidwell 1991) was considered appropriate for correction:

$$L = c \times \mathrm{DN} + d \tag{7.1}$$

where, L is the at-sensor radiance (mWm^{-2} sr cm^{-1}); and c and d are constants extracted from the header file of the AVHRR image (Di and Rundquist 1994).

7.3.2 Radiometric processing to reflectance

For this investigation, the conversion of AVHRR channel 1 and 2 radiance values (§7.3.1.1) to reflectance was relatively straightforward. However, data from channels 3, 4 and 5 (§7.3.1.2) needed considerable processing to derive surface temperature at TIR wavelengths and emitted and reflected radiation at MIR wavelengths.

7.3.2.1 Deriving visible and NIR reflectance

The top of atmosphere (TOA) radiances recorded by the AVHRR image in channels 1 and 2 (W m^{-2} sr^{-1} μm^{-1}) were converted to TOA reflectance using the methodology outlined within Kidwell (1991):

$$\text{Channel 1 reflectane} = \frac{L_1}{191.3/(100\pi \times 0.117)} \tag{7.2}$$

$$\text{Channel 2 reflectane} = \frac{L_2}{251.8/(100\pi \times 0.239)} \tag{7.3}$$

where, L_1 and L_2 are radiance values in channels 1 and 2 respectively (§7.3.1.2).

7.3.2.2 Deriving surface temperature

Following the work of Boyd (1996), the radiation acquired in channels 4 and 5 was used to derive the land surface temperature of the boreal forest. To calculate land surface temperature for each pixel, channel radiance values were converted initially to brightness temperatures, using the inverted Planck function:

$$BT\lambda = C_2 v / \ln(1 + C_1 v^3 / L) \tag{7.4}$$

where, $BT\lambda$ is the surface brightness temperature (K) at a particular wavelength; v is the central wavenumber of the channel filter (cm^{-1}) at the wavelength derived by Wooster *et al.* (1995), C_1 and C_2 are constants (1.191064×10^{-5} mW m^{-2} sr^{-1} $(cm^{-1})^{-4}$ and 1.43883 $(cm^{-1})^{-1}$) and L is the radiance value (§7.3.1.2) (Kidwell 1991; Di and Rundquist 1994).

Brown *et al.* (1985; 1993) questioned the accuracy of brightness temperature values due to a range of factors, including non-linear errors associated with variations in the AVHRR sensor's internal temperature and the effects of ageing on radiometer performance. Although the effect of ageing is not known accurately, the non-linearities of the system can be compensated for using the look-up tables of Weinreb *et al.* (1990) (Boyd 1996).

The corrected brightness temperature values were used subsequently to derive surface temperatures through the split window algorithm, using:

$$T_s = T\lambda_{11} + 3.33(T\lambda_{11} - T\lambda_{12}) - 273 \quad (7.5)$$

where, $T\lambda_{11}$ and $T\lambda_{12}$ are the non-linearity corrected brightness temperatures (K) in AVHRR channels 4 and 5 respectively and T_s is the surface temperature (°C) (Price 1984). The emissivity was assumed to be 0.98, the modelled value for spherical canopies at a LAI of approximately 2 (Guoquan and Zhengzhi 1992; Olioso 1995), a considerable assumption when estimating LAI![†]

7.3.2.3 Splitting MIR radiation into emitted and reflected components

Following the methodology of Kaufman and Remer (1994), reflected MIR radiation was derived using the assumption that:

$$L_{3.75} = \rho_{3.75} + E_{3.75} \quad (7.6)$$

where, $L_{3.75}$ is total radiant energy measured in AVHRR channel 3 (MIR radiance from §7.3.1.2); $\rho_{3.75}$ is reflected energy (reflected component of AVHRR channel 3) and $E_{3.75}$ is emitted energy (emitted component of AVHRR channel 3). The reflected energy, $\rho_{3.75}$, herein known as reflected MIR, was calculated by assuming that the emitted energy from the 10.5-11.3 μm spectral region (i.e., the brightness temperature calculated from the radiance in channels 4 and 5, §7.3.2.1) is related to $E_{3.75}$ through Planck's function. This information was used subsequently within:

$$L_{3.75} = t'_{3.75}\ \rho_{3.75}\left(\left(\frac{F_0}{\pi}\right)\mu_0\right) + t_{3.75}\ \varepsilon_{3.75}\ B_{3.75}\ (T) \quad (7.7)$$

where, $B_{3.75}$ is the Planck function in AVHRR channel 3; F_0 is the incident solar radiance at top of atmosphere (TOA) in AVHRR channel 3; μ_0 is the cosine of the solar zenith angle; $\varepsilon_{3.75}$ is the emissivity of the target in AVHRR channel 3; $t_{3.75}$ and $t'_{3.75}$ are respectively the one- and two-way atmospheric transmission of radiation in AVHRR channel 3. For this investigation, transmissivities were assumed to be of the mid-latitude atmosphere type and constant across the SSA (Kaufman and Remer 1994) (Appendix A gives a full worked example of 'splitting').

[†] Subsequent to the completion of this research Goetz *et al.* (1999) produced an 'emissivity surface' from interpolated field measurements for the entire BOREAS region (with data in the range of 0.9 to 1). In the future, incorporation of such a surface into the method for deriving surface temperature would be advantageous.

7.3.3 Geometric processing

A subscene of the AVHRR image, covering the SSA, was registered (using NN resampling) to a geocoded (Friedel 1992) Landsat TM image using 63 ground control points, with a registration accuracy (RMSE) of less than one pixel (±0.59 of a pixel). As well as compensating for distortions so that the corrected imagery had the geometric integrity of a map, geometric correction enabled the location of the sites for which mean LAI had been estimated on the ground.

7.4 Methodology

Figure 7.3 is a schematic representation of the estimation of LAI from remotely sensed data. The first stage is the conversion of raw satellite sensor data into radiance (and if required, reflectance) so that it represents the signal just after leaving the target of interest. LAI may then be estimated from these data using an algorithm (or model) derived usually from field or laboratory measurements, computer simulation, or a combination of both. The final stage is accuracy assessment, where the LAI estimates are compared with an independent data set (not used in the algorithm development).

Initial attention was placed on the determination of the nature and strength of the relationships between the $LAI_{training}$ data (Plummer *et al.* 1997) and radiated and reflected radiation acquired in each AVHRR channel. Linear correlation (r) analysis was used to investigate these relationships.

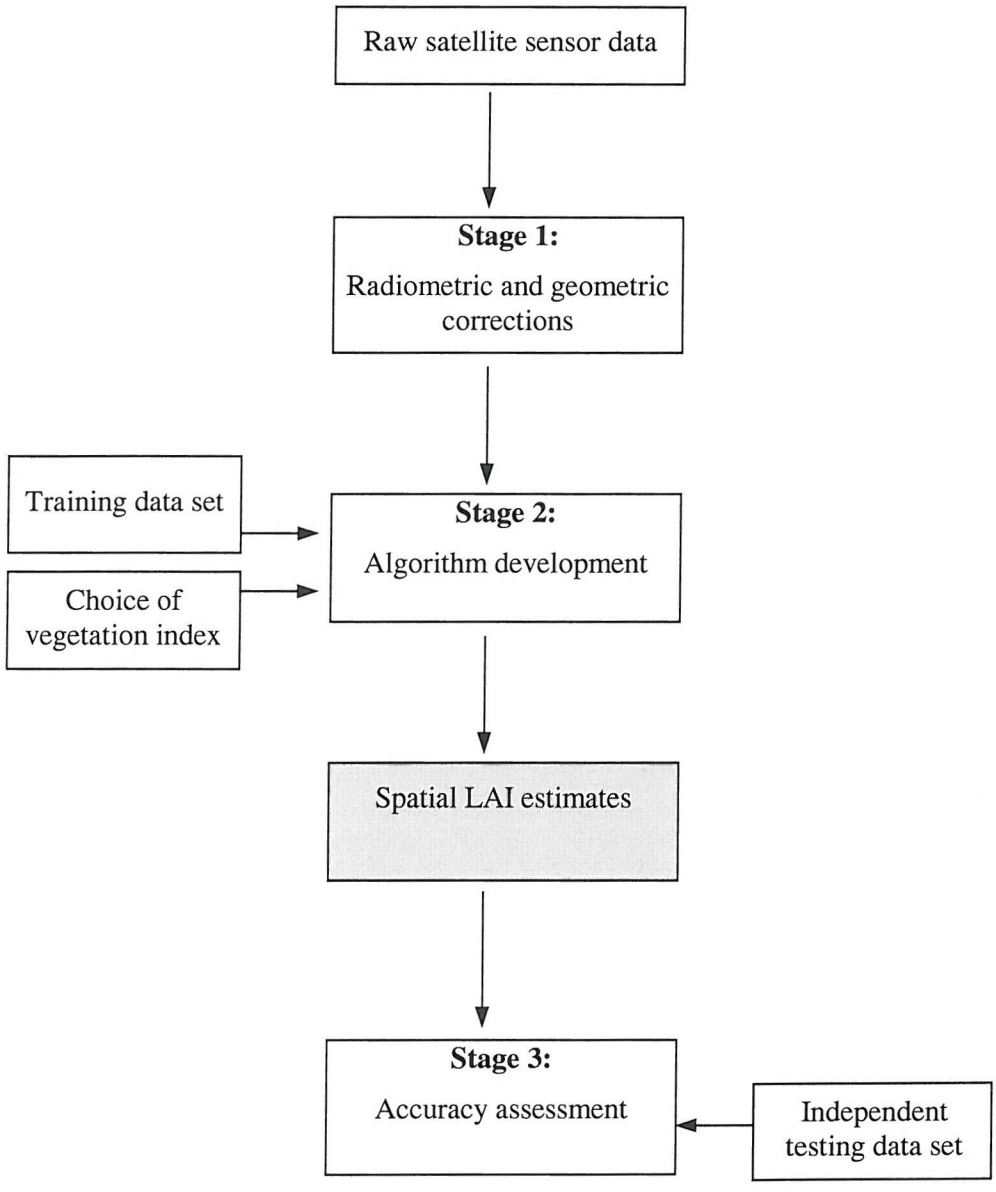

Figure 7.3 Schematic representation of the spatial estimation of LAI from remotely sensed data.

7.4.1 Use of vegetation indices

Early spectroradiometer measurements of visible and NIR energy identified a strong relationship between a visible and NIR transmittance ratio and measured LAI (Jordan 1969). At visible wavelengths, the high absorption by photosynthetic pigments in plant foliage results in relatively low transmittance and reflectance. In contrast, at NIR wavelengths, plant cell walls (especially the lignin component) cause scattering, resulting in relatively high NIR transmittance and reflectance (Gates *et al.* 1965). These observations suggested that spectral reflectance measurements in visible and NIR wavelengths that are related strongly to vegetation amount or LAI (Tucker 1977b) offered the opportunity for 'scaling-up' from the plot level to regional scales (Foody and Curran 1994a). This recognition has sustained interest, over the last three decades, in the development of empirical algorithms relating LAI to surface reflectance and vegetation indices derived from remotely sensed observations (Turner *et al.* 1999).

Furthermore, two recent developments provide a new impetus in this field of remote sensing. First, a new generation of advanced satellite sensors will be launched over the next few years, which will offer much improved performance over existing sensors. For example, the Medium Resolution Imaging Spectrometer (MERIS) sensor (Rast *et al.* 1999). Although designed to address open ocean and coastal zone environmental issues, MERIS will also offer new opportunities for the observation of land surfaces (Verstraete and Pinty 1999). Second, significant advances have been achieved in the understanding and interpretation of vegetation indices (e.g., Pinty *et al.* 1993; Myneni *et al.* 1995).

For LAI mapping, vegetation indices are simple, convenient and effective tools to extract useful information from remotely sensed data, provided they are designed to address the needs of specific applications and take advantage of the characteristics of particular instruments (Govaerts *et al.* 1999; Gobron *et al.* 1999). Numerous ratio-based vegetation indices have been related statistically to LAI, the most common being the SR (Jordan 1969):

$$SR = \frac{\text{NIR reflectance}}{\text{Visible reflectance}} \tag{7.8}$$

and NDVI (Rouse *et al.* 1973),

$$NDVI = \frac{(\text{NIR reflectance} - \text{Visible reflectance})}{(\text{NIR reflectance} + \text{Visible reflectance})} \tag{7.9}$$

(e.g., Goward *et al.* 1991; Barret and Guyot 1991; Huete *et al.* 1994; Chen 1996b; Teillet *et al.* 1997; Gemmell and Varjo 1999; Turner *et al.* 1999).

The appeal of these indices is rooted strongly in the complementary response of visible and NIR reflectance to increases in LAI from a non-vegetated condition and their independence from soil type variation and solar illumination (Curran 1980; Hall *et al.* 1995b) (with the exception of wavelength dependent variation on wet, red soils; Colwell 1974).

In addition, measurement errors in remotely sensed data due to, for example, changes in solar zenith angle, sub-pixel contamination of cloud, or dissimilar surface features, variation in local topography and other environmental factors can cause simultaneous increases or decreases in visible and NIR reflectance (Chen 1996b; Chen and Cihlar 1996). Ratio-based indices reduce such effects. Indeed, other indices, involving mathematical operations other than ratioing, could retain the errors or even amplify them (Curran 1980; Turner *et al.* 1999). Therefore, the optimum ratio-based index for a particular application is dependent on the data available, its mode of collection, statistical properties and the degree of standardisation required (Curran 1980; Chen 1996b; Turner *et al.* 1999).

Variation in background (soil and litter) reflectance can affect visible-NIR vegetation indices (Tucker 1977b; Peddle *et al.* 1999). This led to the development of alternative indices, which include correction factors or constants, to account for (or minimise) variation in background reflectance, for example, the soil adjusted vegetation index (SAVI) (Huete 1988; Huete *et al.* 1994),

$$\text{SAVI} = \frac{(\text{NIR reflectance} - \text{Visible reflectance})(1+L)}{(\text{NIR reflectance} + \text{Visible reflectance} + L)} \tag{7.10}$$

where, L is an adjustment factor related to background reflectance. Such indices, developed to minimise the effect of the background may, however, also reduce the sensitivity to changes in canopy conditions (Gemmell and Varjo 1999; Turner *et al.* 1999).

In applications focussed on canopy LAI, variability in reflectance from understorey vegetation can likewise be problematical (Spanner *et al.* 1990) and inspired alternative indices incorporating reflected MIR (Nemani *et al.* 1993b). Indeed, reflected MIR has been shown to be less affected by understorey reflectance, atmospheric and scan angle effects than either visible or NIR reflectance (Kaufman and Remer 1994; França and Setzer 1998). This prompted Kaufman and Tanré (1992; 1996) to develop the VI3.

$$\text{VI3} = \frac{(\text{NIR reflectance} - \text{reflected MIR})}{(\text{NIR reflectance} + \text{reflected MIR})} \tag{7.11}$$

Numerous studies have examined the relative merits of vegetation indices (§2.3.2). A general conclusion from these studies is that there is considerable sensitivity to LAI but more so at relatively low LAI values (Turner *et al.* 1999; Pereira 1999). Typically, visible-NIR vegetation indices increase over a LAI range from 0 to between 3 and 5, before an asymptote is reached (Tucker 1977a). The upper limit of sensitivity and the relative importance of visible and NIR reflectance in determining this limit differ among vegetation types (e.g., White *et al.* 1997; Turner *et al.* 1999).

To compare these four vegetation indices, spectra from three of the BOREAS TFS, (covering the range of LAI for the region) were extracted from BORIS and each index calculated (Table 7.3). Interesting features of Table 7.3 are the small range in VI3 values yet it is the only index to preserve the order of LAI values and has the strongest correlation with LAI. Table 7.4 illustrates the strengths of each index for boreal forest applications.

TFS	$LAI_{training}$	SR	NDVI	SAVI	VI3
SSA YJP	1.767	1.759	0.275	0.407	0.562
SSA OJP	2.405	1.595	0.229	0.338	0.650
SSA OBS	3.658	2.844	0.480	0.710	0.824
correlation (r) with $LAI_{training}$		0.896	0.872	0.871	0.998

Table 7.3 $LAI_{training}$ (Plummer *et al.* 1997) and the four vegetation indices calculated from BORIS reflectance spectra for three BOREAS TFS (YJP is young jack pine, OJP is old jack pine and OBS is old black spruce).

Advantage	SR	NDVI	SAVI	VI3	Reference
Use a ratio	✔	✔		✔	Cihlar *et al.* 1997; Turner *et al.* 1999
Linearity with biophysical variables	x	x		✔	Baret and Guyot 1991; Chen 1996b; França and Setzer 1998
Ease of computation	✔	✔			Verstraete and Pinty 1996; Gemmell and Varjo 1999
Less sensitive to soil	x	x	✔	✔	Huete 1988; Qi *et al.* 1994; Chen 1996b
Less sensitive to atmospheric effects	x	x		✔	Pinty and Verstraete 1992; Kaufman and Tanré 1992, 1996
Less sensitive to understorey				✔	McDonald *et al.* 1998; Turner *et al.* 1999
Sensitive to canopy water content				✔	Boyd and Curran 1998; Pereira 1999

Table 7.4 Strengths of the vegetation indices for boreal forest applications (✔ indicates reference corroborates advantage, whereas x indicates reference disproves advantage).

Processed remotely sensed radiation values (§7.3) were used to derive the indices presented above for each AVHRR pixel covering the SSA subscene. As for the initial individual channel analyses, the nature and strength of the relationships between the $LAI_{training}$ data (Plummer *et al.* 1997) and the resultant vegetation index images of the SSA were determined.

To test the relative ability of the vegetation indices to estimate boreal forest LAI at regional scales, the predictive regression relationships developed between each index and the $LAI_{training}$ data set were applied to the SSA vegetation index images to provide remotely sensed estimates of LAI. These estimates were assessed for accuracy using the second independent field $LAI_{testing}$ data set (Chen *et al.* 1997).

7.5 Data Analysis and Results

The following three sub-sections document and offer explanations for the results obtained through the processing and analysis of the data. As noted in §7.2, the field estimates of LAI were taken, as far as possible, from sample plots within areas of relatively homogeneous canopies in order to represent the surrounding forest. The following analyses, therefore, rely on the assumption that the LAI estimates at each sample plot may be related directly to the remotely sensed response derived from the pixel in which they were recorded. Relations were derived for each individual AVHRR channel as well as vegetation indices (§7.4.1).

7.5.1 Assessment of individual channels

Initial emphasis was placed on the determination of the nature and strength of the relationship between the $LAI_{training}$ data and the radiation acquired in each AVHRR channel for the study area. Examination of scatterplots (Figure 7.4) revealed that near-linear relationships existed, hence linear correlation analyses were performed. From the correlation coefficients (r) computed (Table 7.5) it was apparent that the relationships between visible and NIR radiance and $LAI_{training}$ were weak. The MIR and TIR channels, in comparison, exhibited strong, inverse and significant (95 % level of confidence) relationships with $LAI_{training}$ data. Molecular and aerosol scattering (stronger at shorter wavelengths where the particle size is similar to the radiation wavelength) may account for this trend (Kaufman and Tanré 1996).

Channel	Correlation coefficient (r)
Visible radiance	+ 0.28
Near Infrared radiance	+ 0.56
Middle Infrared radiance	- 0.91
Reflected Middle Infrared	- 0.82
Thermal Infrared (1) radiance	- 0.88
Thermal Infrared (2) radiance	- 0.86

Table 7.5 Relations between the $LAI_{training}$ data (Plummer *et al.* 1997) and radiation acquired in all five AVHRR channels.

The strength of the relationship between the reflected component of MIR and $LAI_{training}$ was less than that of MIR radiance (correlation coefficients (r) of -0.91 and -0.82 respectively). This corresponds well with previous research undertaken at tropical latitudes (e.g., Sader *et al.* 1989; Vanclay and Preston 1990; Boyd 1996). However, reflected MIR should be more robust for regional scale applications, due to the removal of the emitted portion of the MIR signal, which is influenced by localised confounding variables, for example, atmospheric conditions, such as wind speed and air vapour conductance, or site specific factors, such as topography, aspect and soil moisture conditions (§7.1).

In summary, given a fairly dark canopy (LAI in the range of 2-3), sensitivity to variation in LAI of visible radiation is low (Baret and Guyot 1991; McDonald *et al.* 1998), whereas, in contrast, MIR radiation (highly sensitive to water; Kaufmann and Tanre 1996; Periera 1999) has greater sensitivity to LAI variation because canopy water content is related indirectly to LAI. Hence, these results indicated that data acquired at MIR wavelengths (in comparison to visible radiation) may have a rôle to play in the estimation of boreal forest LAI (Boyd *et al.* 2000).

The next step was to investigate whether accurate and robust relationships for estimation of LAI could be derived with the incorporation of the radiation acquired at MIR wavelengths into vegetation indices.

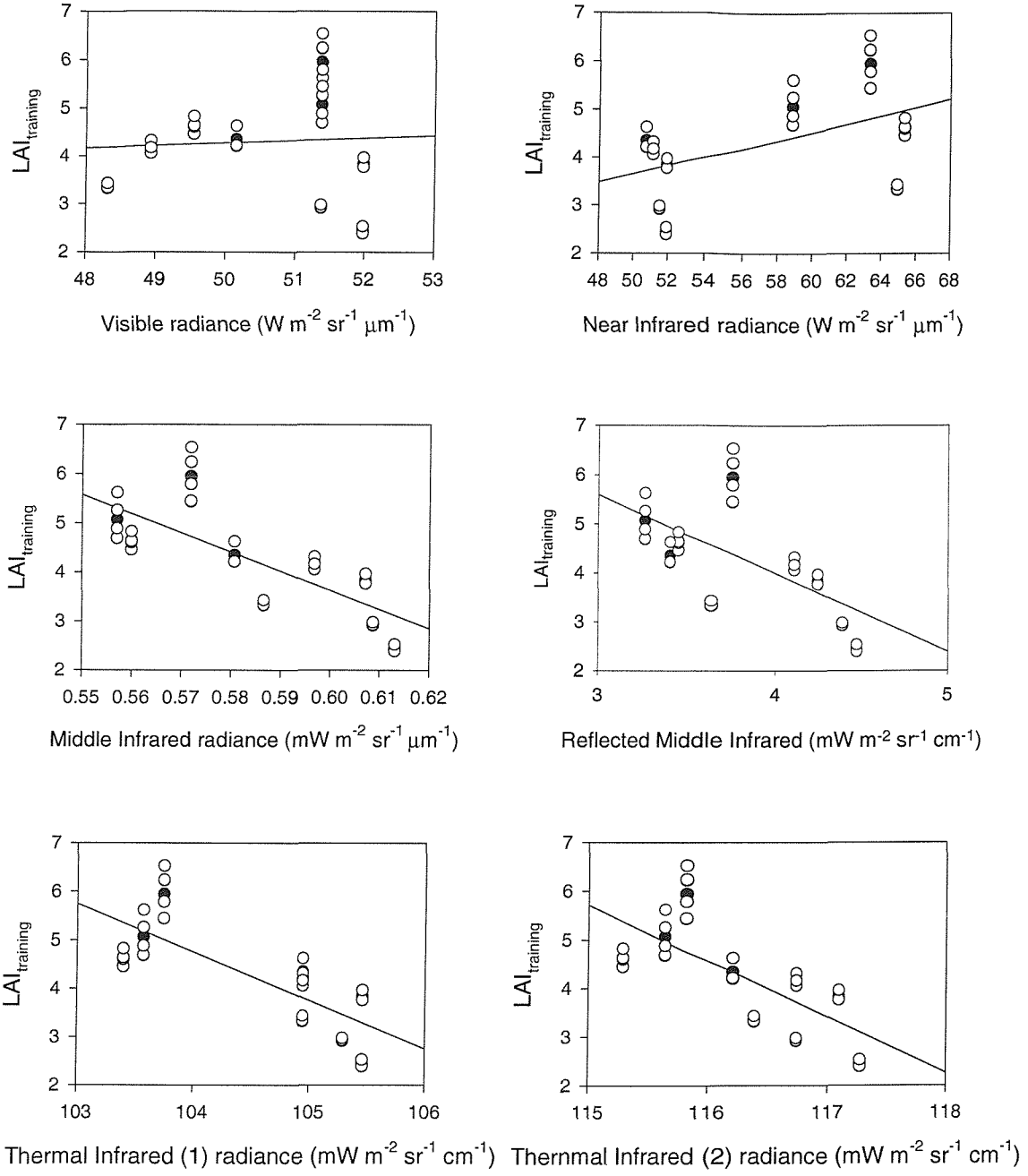

Figure 7.4 Relations between $LAI_{training}$ data and radiation acquired in each AVHRR channel. For illustrative purposes, the LAI estimates for each transect are shown (O). The regression was developed for a mean LAI estimate for each site (●) because all transects were assumed to fall into the area covered by an AVHRR pixel.

7.5.2 Assessment of vegetation indices

The relations between the four vegetation indices and $LAI_{training}$ data were investigated (Figure 7.5). Visible reflectance appears insensitive to the changes in LAI of boreal forest stands (Figure 7.4). Therefore, those vegetation indices designed to maximise the information content in visible wavelengths are affected adversely (Figure 7.5). The major drawback of SAVI is its reduction in sensitivity to Earth surface conditions because of the use of the adjustment factor, *L* in the denominator, making it "inappropriate for boreal ecosystem applications" (Chen 1996b, p. 241). *L* prevents the exact ratioing and dampens the background effect at the expense of the sensitivity. The VI3 was better correlated to the field data than all other indices.

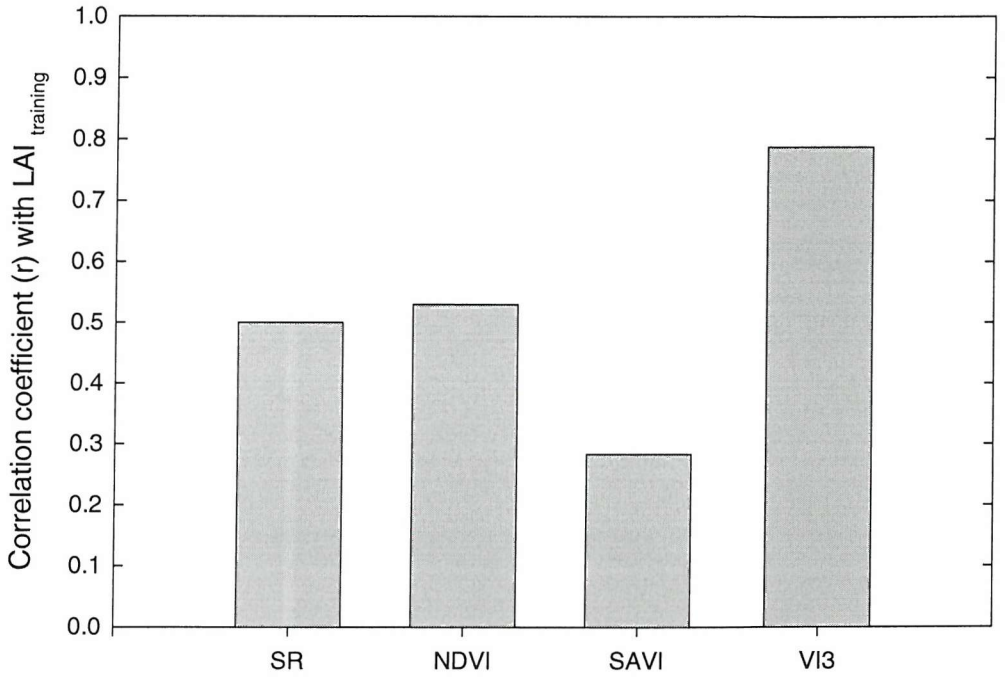

Figure 7.5 Correlation coefficients (r) between vegetation indices and $LAI_{training}$ (Plummer *et al.* 1997).

Therefore, employing the VI3 for estimation of boreal forest LAI has several advantages:

- MIR radiation has greater sensitivity to LAI variation than visible radiation because it is highly sensitive to canopy water content (§7.5.1) (Periera 1999);
- at regional scales emitted MIR radiation may be influenced by confounding variables so its removal is advantageous (§ 7.1);
- rather than using reflected MIR alone, it is more robust within a ratio index (Chen 1996b). Also, given the complementary responses of NIR and MIR with increasing LAI additive constants may be removed and
- little is known about interaction of TIR with forest canopies (Rencz 1999) and its temporal instability detract further from its use (§7.1).

Predictive regression relationships were derived (hence useful to switch from r to r^2) for both NDVI and VI3 (Table 7.5; Figure 7.6).

Vegetation Index	Coefficient of determination (r^2)	Predictive relation
SR	0.27	-
NDVI	0.28	LAI = 5.237NDVI + 0.8219
SAVI	0.08	-
VI3	0.62	LAI = 7.2357VI3 - 2.3009

Table 7.5 Coefficients of determination (r^2) between vegetation indices and $LAI_{training}$ data.

A shortcoming of the predictive relationships between $LAI_{training}$ and vegetation indices is their small sample size (n=9). Nevertheless, the relationships concur with those observed in previous studies (e.g., Boyd *et al.* 1999), where the negative relationship between LAI and VI3 (r^2 = 0.62), was stronger than the relationship between LAI and NDVI (r^2 = 0.28). The scatter exhibited in both these relationships can be attributed to i) the limited range of LAI in the boreal forest, ii) the asymptotic nature of the relationships, iii) variability in the reflectance of understorey vegetation and iv) atmospheric attenuation. The first three factors would have had similar effects on both vegetation indices. This is the case, even for iii), where the low solar angle and resultant shadow would have masked the effect of variability in understorey vegetation at all wavelengths (Boyd *et al.* 2000). However, atmospheric scattering is much greater in visible than in MIR wavelengths. Replacement of the visible reflectance component of the NDVI with reflected MIR, to form the VI3, would have reduced atmospheric attenuation effects and consequently strengthened the relationship between remotely sensed data and LAI. Furthermore, water content of leaves (particularly for crops) is usually less variable than their chlorophyll content (Malthus *et al.* 1993). Consequently, the scatter in the relationship between remotely sensed data and LAI would be reduced if the VI3 were used instead of the NDVI.

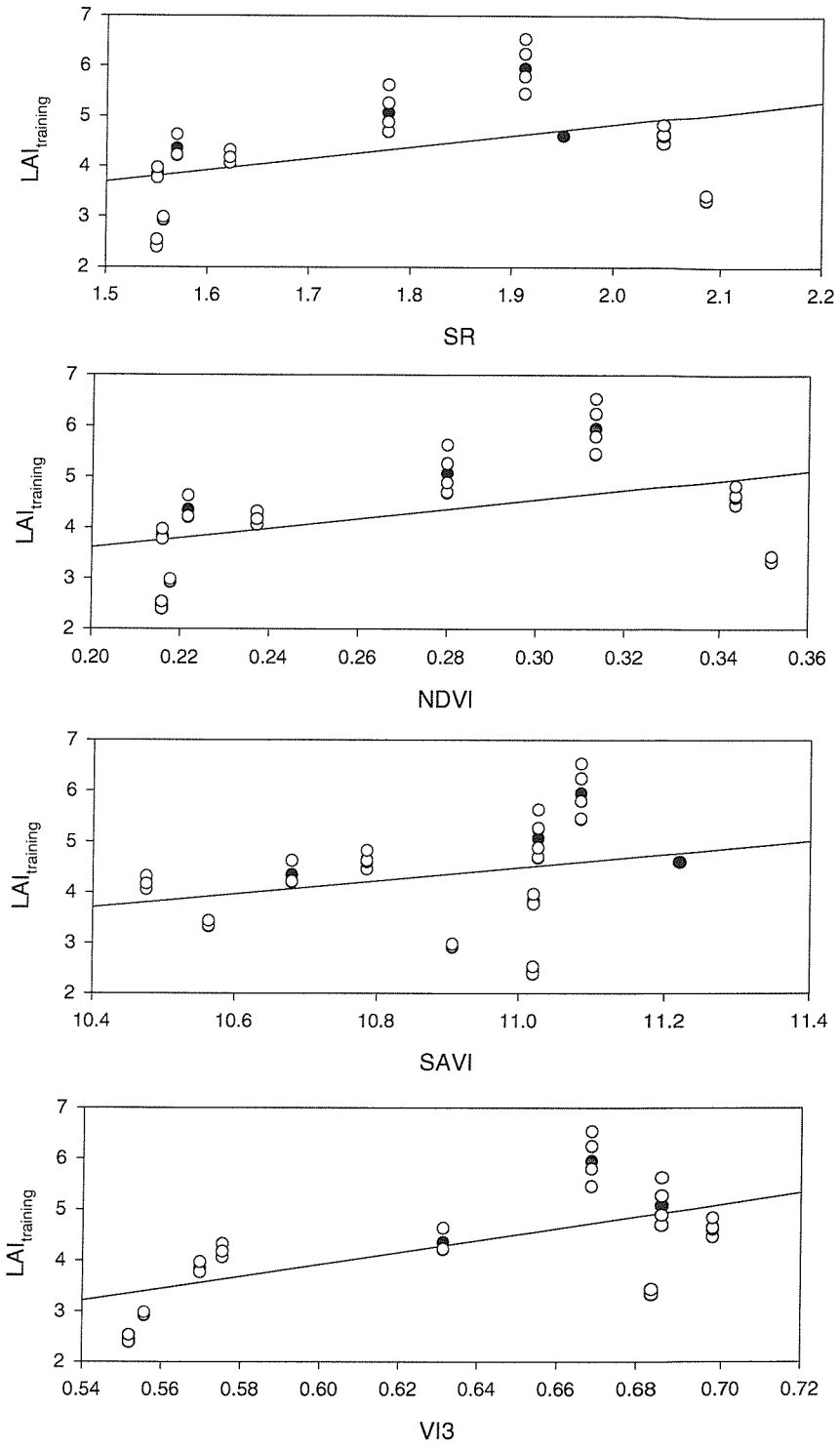

Figure 7.6 Predictive relationship between SR, NDVI, SAVI, VI3 and $LAI_{training}$.
For illustrative purposes, the LAI estimates for each transect are shown (O). The regression was developed for a mean LAI estimate for each site (●) because all transects were assumed to fall into the area covered by an AVHRR pixel.

7.5.3 Accuracy assessment

To determine the relative ability of the two vegetation indices (NDVI and VI3) to estimate boreal forest LAI, the predictive regression relationships (Table 7.5, Figure 7.5) were applied to both the NDVI and VI3 images produced for the AVHRR subscene (§7.3.2). Hence, remotely sensed estimates of LAI were obtained for the entire BOREAS SSA (including those sites for which $LAI_{testing}$ data had been estimated in the field, Figure 7.2). The coefficients of determination (r^2) derived for the relationships between $LAI_{testing}$ and LAI estimated by the NDVI and VI3 were 0.46 and 0.76 respectively (significantly different at the 95% confidence level; $P = 0.1$).

These findings suggest that the NDVI is considerably less precise than the VI3 for estimating the LAI of boreal forests. The lakes (Plate 7.1) appear to be the only anomaly, when using the VI3 predictive regression relationship, with exceptionally high estimates of LAI! This is attributable to the failure of reflected MIR to delineate water bodies (a most likely manifestation of inadequacies in the 'splitting procedure'). To avoid these anomalies the NDVI predictive regression relationship could be used to generate a 'water body mask' for subsequent use with a LAI surface estimated from the VI3.

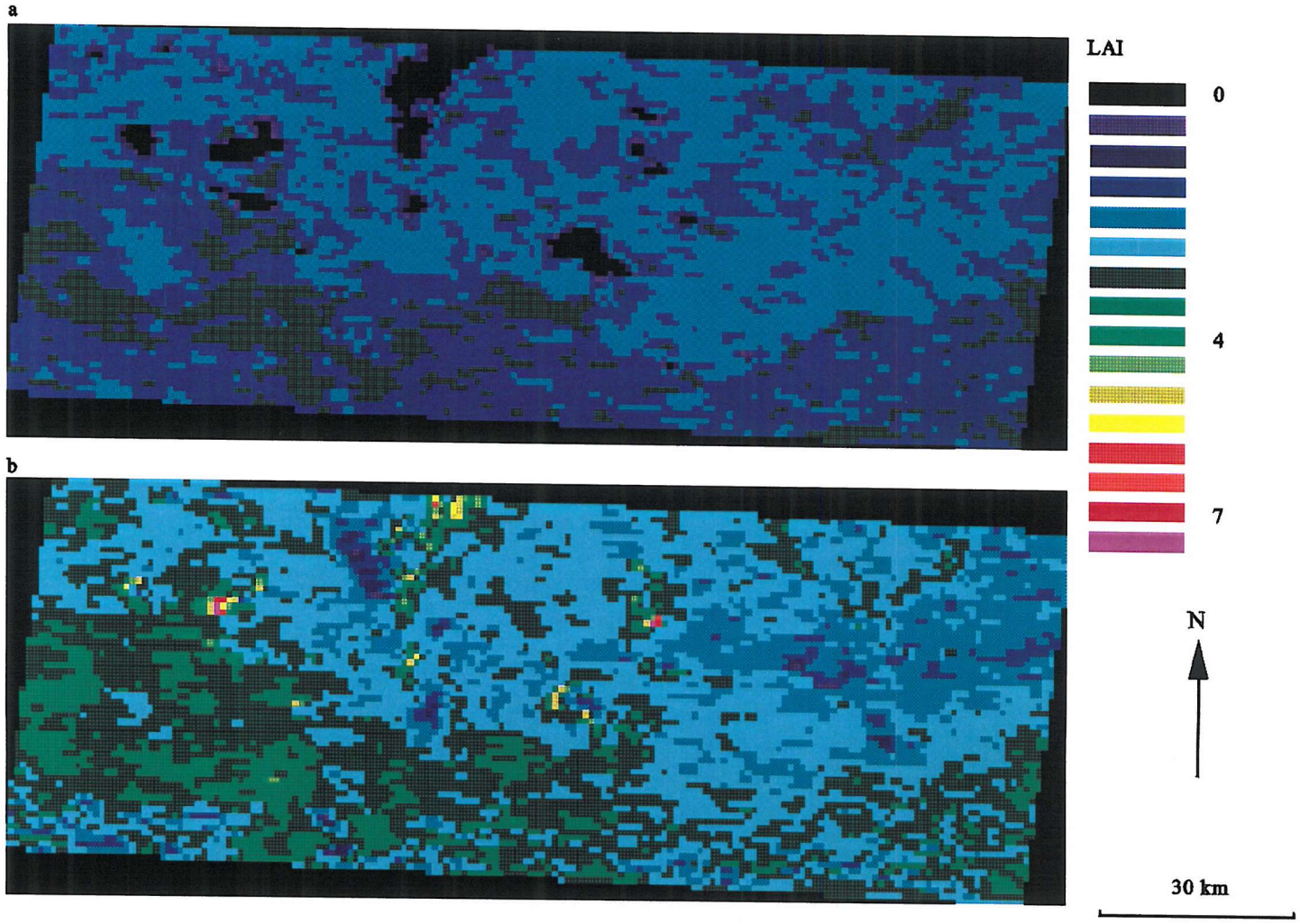

Plate 7.1 Maps of NPP produced from a) NDVI and b) VI3.

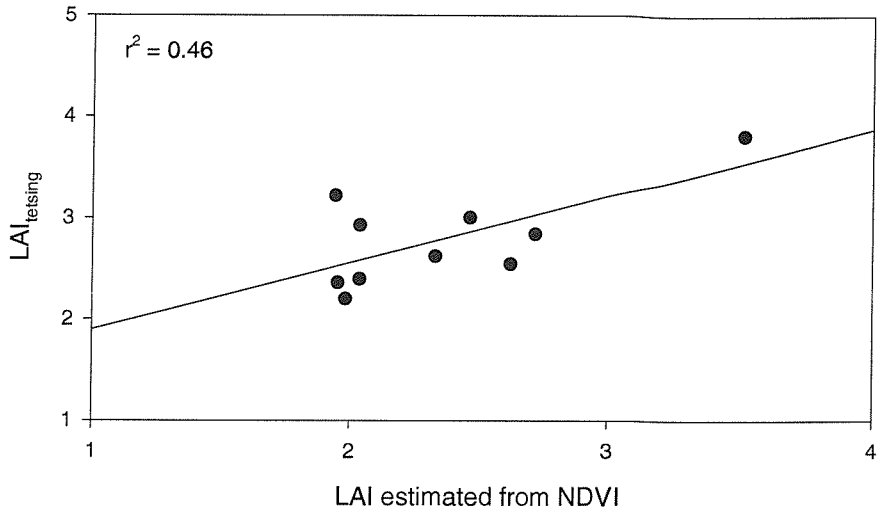

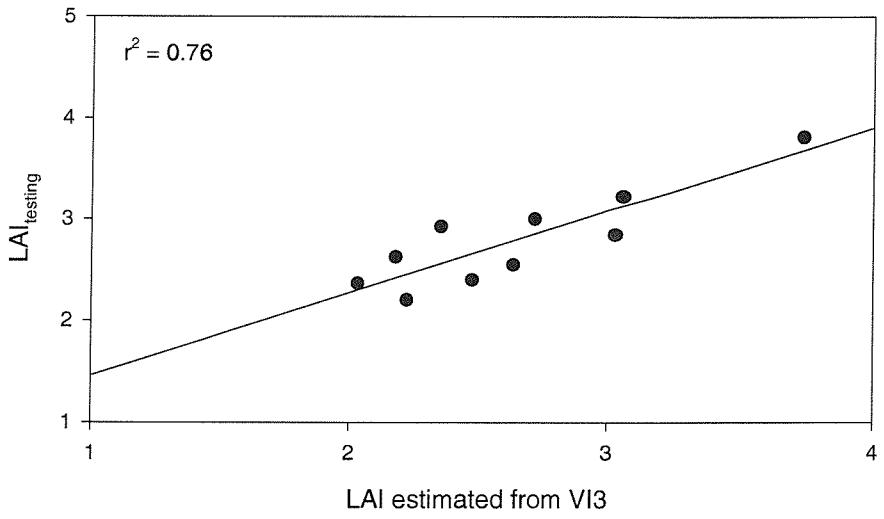

Figure 7.7 Accuracy assessment for the NDVI and VI3 with LAI $_{testing}$ data.

7.6 Discussion

The three objectives of this chapter (§7.1.1) have been met. In addition, by demonstrating the value of remotely sensed radiation reflected at MIR wavelengths this chapter has highlighted three issues that require attention before these data can be used with confidence at regional to global scales:

1. To date, research exploring the success of reflected MIR for LAI estimation has focused only on a limited number of biome types, therefore, research needs to be replicated in other biome types where LAI magnitude and range, canopy structure and soil and understorey are different.
2. The real success of using remote sensing within ecosystem process research at regional to global scales is the ability to monitor over time and scale-up between imagery acquired at different spatial resolutions (Cihlar *et al.* 1998, Reich *et al.* 1999). However, relative to the radiation acquired in visible and NIR wavelengths, understanding of the interactions of MIR radiation with vegetation is poor; little is known of temporal variability and effects of the growing season on reflected MIR and furthermore, the MIR channel of the NOAA AVHRR sensor is not complimentary to that of other satellite sensors currently in operation with different spatial resolutions (e.g., Satellite Pour l'Observation de la Terre (SPOT) High Resolution Visible (HRV), Landsat TM).
3. The method for deriving reflected MIR from total radiant energy measured in AVHRR channel 3 is still evolving and dependent heavily upon assumptions made (e.g., emissivity) (§7.3.2.2) (Nerry *et al.* 1998; Roger and Vermote 1998).

Resolving these issues would further enhance the potential of reflected MIR to increase the accuracy with which LAI of ecosystems may be estimated. Such optimisation of remotely sensed data, acquired by a number of sensors operating currently (e.g., NOAA AVHRR, European Remote sensing Satellite (ERS) (ATSR) and Terra MODIS) and in the future (Envisat Advanced Along-Track Scanning Radiometer (AATSR)), with complimentary MIR channels to the AVHRR sensor, has wide implications for regional to global scale ecological modelling (Cohen and Justice 1999, Verstraete and Pinty 1999).

7.7 Conclusions and Future Research

Vegetation indices provide a simple approach to the analysis of remotely sensed data. Interpretation of these indices, however, requires understanding of their nature, properties and characteristics. Recent advances in index design and evaluation, together with the upcoming advent of new space sensors, have stimulated the development of optimal vegetation indices (Govaerts *et al.* 1999).

To conclude, four main observations were drawn from this investigation:

1. MIR radiation contains valuable information for estimating boreal forest LAI at regional scales and with an increased understanding of the interaction between MIR radiation and forest canopies, reflected MIR should be adopted more widely for ecological applications of remote sensing at and beyond regional scales.
2. The 'splitting' technique to obtain reflected MIR is still evolving and is particularly dependent upon the assumption of constant emissivity.
3. The VI3 (incorporating reflected MIR) was identified as being more strongly related to boreal forest LAI than the more widely used NDVI. Indeed, the NDVI may be considered a sub-optimal index for the estimation of boreal forest LAI.
4. The lack of understanding of the interaction between radiation acquired at MIR wavelengths and forest biophysical variables, such as LAI (particularly at higher latitudes) is acknowledged.

Future research could highlight how the NDVI is less accurate than the VI3 by producing a spatial difference map of the two LAI estimation techniques and cross-correlating with other spatial data (e.g., site-specific variables, such as, vegetation type, soil characteristics, etc.). Secondly, exploration of seasonal effects upon the stability of the relation between reflected MIR and boreal forest LAI found within this investigation would be advantageous.

Chapter 8

Modelling the Impact of Future Climate Change on the Boreal Forest

Climate change is one of the most significant global scale environmental issues facing the world today (Parry *et al.* 1999). To begin to consider global response to climate change, the United Nations Framework Convention on Climate Change (UNFCCC) was signed by over 150 countries in June 1992. 'Article 2' of the UNFCCC, which details the ultimate objectives, considered climate change '*dangerous*' and to be avoided if irreversible damage to global ecosystems is to be prevented.

The circumpolar boreal region (Figure 2.2) is one of the largest biomes in the world and contains significant pools of carbon that are sensitive to changes in global climate. This chapter investigates the impact of future climate on the carbon budget of the boreal forest. The FOREST-BGC ecosystem simulation model was run with climate change predictions (derived from three different scenarios of CO_2 emissions) as well as input data that were a result of the preceding research chapters of this thesis (Figure 1.1, p.6). Results of the different scenarios were compared. Particular attention was given to whether the boreal forest, which currently sequesters approximately 15 % of anthropogenic carbon emissions (DETR 1999), would remain a terrestrial carbon sink under different scenarios of climate change. To conclude, the mechanisms likely to control the future carbon budget of the boreal forest are discussed.

8.1 Introduction

Atmospheric CO_2 concentration increased from 290 to 378 ppm from 1880 to 1999 (Keeling *et al.* 1996a; Schimel *et al.* 1996; DETR 1999), accompanied by a mean global increase in near-surface air-temperature of approximately 0.8 °C (Nicholls *et al.* 1996; Beerling 1999). The increase in atmospheric CO_2 concentration has been caused mainly by anthropogenically-controlled combustion of fossil fuels and land use changes in the tropics (Brown *et al.* 1993; Houghton 1999; Houghton *et al.* 2000). According to current estimates, these sources amount to approximately 7.1 Pg C yr^{-1} (1 Pg = 10^{15} g) (Chen *et al.* 1999), of which, approximately 3.2 Pg C yr^{-1} (45 %) and 2.0 ± 0.9 Pg C yr^{-1} (28 %) accumulate in the atmosphere and oceans respectively (Keeling *et al.* 1996b; Schimel *et al.* 1996; Beerling 1999). The remaining 1.9 Pg C yr^{-1} (27 %), the so-called 'missing carbon sink', is probably sequestered by the terrestrial biosphere (Ciais *et al.* 1995; Bender *et al.* 1996; Keeling *et al.* 1996a; Houghton *et al.* 1998).

Many researchers have suggested that this putative sink might be found in "pristine undisturbed terrestrial ecosystems" (Beerling 1999, p.55) in which carbon sequestration has increased as a result of increasing atmospheric CO_2 concentration (i.e., CO_2 fertilisation) and nutrients in soils (e.g., Houghton, 1995; Drake *et al.* 1997). The fertilisation effect due to CO_2 and nitrogen has been estimated as 0.5-2.0 Pg C yr^{-1} and 0.5-1 Pg C yr^{-1} respectively, for the 1980s (Tans *et al.* 1990; Melillo *et al.* 1996).

Although forest ecosystems are estimated to contain approximately 80% of all global aboveground carbon (Dixon *et al.* 1994), determining their rôle in the global carbon cycle is particularly difficult (Waring and Running 1998). This is because the magnitude of forest carbon stores, let alone fluxes, continue to be a matter of great uncertainty (Dixon *et al.* 1994; Houghton *et al.* 2000) (§2.1). Storage estimates range from 380 Pg in biomass with 770 Pg in forest soils (Dixon *et al.* 1994), to 458 Pg in biomass and 1200 Pg in the soil (Hunt *et al.* 1996)! Also, while forest ecosystems in lower latitude areas are releasing carbon (primarily due to deforestation) (Brown *et al.* 1993; Lal *et al.* 1995; Houghton *et al.* 2000), northern ecosystems (arctic tundra, temperate forest, boreal forest and northern bogs) have been net sinks for carbon (Post 1990; Klinger *et al.* 1996; Waddington and Roulet 2000). For example, using $\delta^{13}C$ measurements in atmospheric CO_2 from a global air-sampling network, Ciais *et al.* (1995) found northern temperate and boreal ecosystems between 35° and 65°N to be major carbon sinks of 3.5 ± 1.0 Pg C yr^{-1} in 1992. In addition, based on multiyear continuous CO_2 eddy flux measurements, boreal evergreen conifer stands in central Sweden and Manitoba, Canada were shown to be weak sources of atmospheric CO_2, (Lindroth *et al.* 1998; Goulden *et al.* 1998).

Today, boreal forests are believed to sequester approximately 0.7 Pg C yr^{-1} (Houghton *et al.* 1998; White *et al.* 1999), contributing significantly to reducing the rate at which atmospheric CO_2 concentration is increasing. However, they are not static ecosystems and cannot be assumed to be in equilibrium in terms of carbon exchange (Hulme *et al.* 1999a). The current carbon budget of the boreal forests is influenced strongly by their past history. In particular, continuing responses to recent environmental fluctuations have shaped the structure and function of the contemporary boreal forests over a relatively short time and fine spatial scales (Apps *et al.* 1993; Kurz and Apps 1994). Hence, the mechanisms responsible for the boreal forests acting presently as a net sink of carbon are most likely adjustments to:

- recovery from climate perturbations / post-glacial warming (e.g., little ice-age, 1250-1850);
- increased forest disturbance over the past two centuries (Dirks *et al.* 2000)
- recent nutrient inputs associated with atmospheric pollution and
- CO_2 fertilisation effects

Apps *et al.* (1993) suggested, however, that the impact of these mechanisms is unlikely to be sustained, even in the absence of climate change so the magnitude of the carbon sink is likely to be reduced. One of the principal mechanisms appears to be an ageing and aggrading boreal forest, primarily due to changes in past and present disturbance regimes, a structural phenomenon that cannot be maintained indefinitely.

When combined with the effects of climate change, therefore, the transient response of the boreal forest over the next century will likely be accompanied by large carbon exchanges within the atmosphere, although the long-term (equilibrium) changes in terrestrial carbon storage in future vegetation complexes remain uncertain. Such a transient response results from the interaction of many (often non-linear) processes whose impacts on future carbon cycles remain poorly quantified.

Of greater certainty, however, is that should the disappearance, or worse, reversal of the boreal forest carbon sink be a direct consequence of climate change, this would constitute a dangerous positive feedback to the climate system (Houghton *et al.* 1998; Kabat 1999; White *et al.* 1999).

Therefore, to investigate the impact of future climate change on the carbon budget of the boreal forest, the objectives of this chapter were fourfold:

1. choose and implement realistic future climate change scenarios;
2. automate fully FOREST-BGC for regional scale applications;
3. estimate the future carbon budget for the BOREAS SSA and

4. discuss mechanisms that may be responsible for future changes in the boreal forest carbon budget and suggest implications that these may have on future global climate.

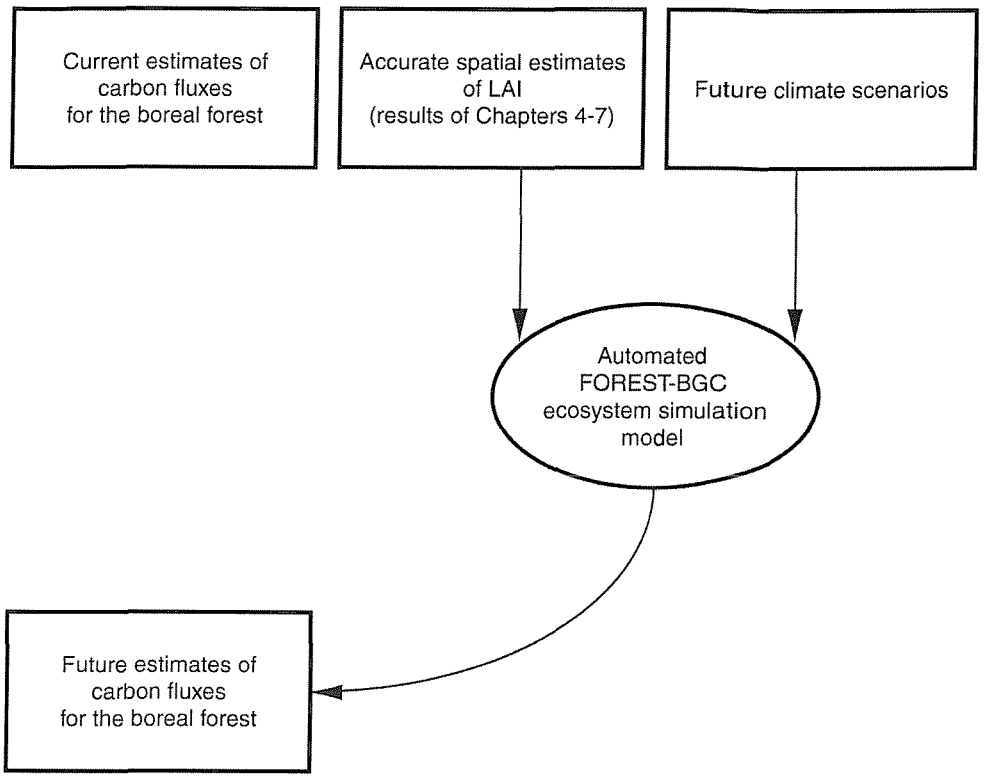

Figure 8.1 Simplified diagrammatic representation of the structure of this chapter.

8.2 Data and Methodology

To estimate the impact of future climate on the boreal forest, FOREST-BGC was driven with climate change predictions (derived from three different scenarios of CO_2 emissions) and input data that were a result of the preceding chapters (Figure 8.1). This section describes the choice of realistic climate scenarios and the automation of FOREST-BGC, before detailing how the simulations were implemented.

8.2.1 The choice of realistic future climate scenarios

> '*Any assessment of the possible impacts of future climate change requires descriptions of possible future climates on appropriate spatial and temporal scales*' (Hulme *et al.* 1999b, p.3).

These 'descriptions' (herein scenarios) originate most commonly from climate change experiments made using global climate models (GCMs) (Riedo *et al.* 1999). However, to date,

impact assessments have not been well co-ordinated (Parry *et al.* 1999). They have been based on different assessment methods and on a wide variety of climate change scenarios, which result in analyses that are difficult to compare. To overcome such inconsistencies, researchers are attempting to standardise the climate scenarios that are adopted for impact investigations.

Hulme *et al.* (1999b) described a set of climate change scenarios that have been used in a series of recent studies investigating the impacts of climate change on several environmental systems and resources. The scenarios derive from modelling experiments completed by the UK's Hadley Centre over the last four years, using successive versions of their coupled ocean-atmosphere global climate model (HadCM2) (Viner and Hulme 1997; Hulme *et al.* 1999b). These scenarios were adopted for this investigation because of their 'fast-track' development (Parry *et al.* 1999): Until very recently, the lag between the publication of climate change scenarios and that of the impact assessments that use these scenarios averaged about three years (e.g., Beerling 1999; Riedo *et al.* 1999). This gap has been reduced to six months by the rapid preparation and transfer of climate change data through the UK's Climate Impacts LINK Project (see http://ipcc-ddc.cru.uea.ac.uk) and by funding from the UK's Department of Environment, Transport and the Regions (DETR). The remainder of this section (§8.2.1) describes briefly the development of the Hadley Centre modelling experiments and subsequent implementation of the resulting scenarios.

8.2.1.1 Observations and predictions of climate change

There are two broad methodologies available for climate change scenario construction: empirical methods and process-based models. Empirical methods include instrumental analogues, palaeo-analogues (e.g., Gorham 1991; Klinger *et al.* 1996) or spatial analogues for climate change. While process-based models (deemed "the most suitable methodology for the construction of climate change scenarios" by the Intergovernmental Panel on Climate Change (IPCC) (DETR 1997, p. 7)) consist of a hierarchy of mathematical models that represent the climate system. GCMs are the most complex of climate models, since they attempt to represent the main components of the climate system in three-dimensions (Viner and Hulme 1997). Coupled ocean-atmosphere GCMs combine three-dimensional representations of the atmosphere, cryosphere and ocean components of the climate system.

The Hadley Centre's experiments explore future changes in climate by driving a climate model, first with an observed climate data set that describes recent climate conditions and trends (e.g., increasing atmospheric CO_2 from 1860 to 1995). The model used to generate scenarios used in

this study, was the second generation Hadley Centre Coupled Model (HadCM2) (Johns *et al.* 1997; Viner and Hulme 1997).

Once observed climate can be modelled reliably and consistently, projected increases in concentrations of greenhouse gases can be introduced in order to predict future climates (DETR 1997; Riedo *et al.* 1999).

However, confidence in predictions from climate models continues to be limited by imperfect understanding of processes that control climate; the Earth system may respond to increasing greenhouse gas concentration in a very different way to a climate model. As an extreme example, it has been suggested that the intense deep-water currents that are responsible for re-distributing heat between the equator and the poles could decrease or even 'switch-off' as a direct consequence of greenhouse gas concentrations (Wood *et al.* 1999). The severity of change in these currents could depend crucially on the rate of build-up of greenhouse gases (Tett *et al.* 1997).

Despite such limitations, climate models remain essential tools for developing future climate scenarios that incorporate active anthropogenic reduction in emissions. The Hadley Centre experiments that produced the scenarios used for this research, were driven with the mean monthly terrestrial climate data set of New *et al.* (1999) (created specifically to support climate change impact assessments). Simulations were started from 1860 to allow the full effect of pre-1990 emissions to be taken into account (i.e., "warm-start experiments" (Viner and Hulme 1997, p.9)) and run to 2250 as stabilisation of CO_2 at 750 ppm is not achieved until approximately 2225 (Figure 8.2) (DETR 1999). The experiments showed that long-term (i.e., in the region of 100 years) climate predictions using HadCM2 were relatively insensitive to different initial climate conditions that spanned the range of natural variability (Hulme *et al.* 1999b).

8.2.1.2 Creating and applying the scenarios

To assess the scientific understanding of climate change, the World Meteorological Organisation (WMO) and the United Nations Environment Programme (UNEP) established the IPCC in 1988. In particular, the IPCC's 1998 annual assessment report focussed on the socio-economic impacts resulting from global climate change according to a 'business as usual' (herein unmitigated) emissions scenario (DETR 1999).

For comparison and to contribute to the discussion on interpreting Annex 2 of the UNFCCC, in addition to the IPCC's 1998 unmitigated emissions scenario, three further scenarios were adopted for this investigation. Two of these, produced from the experiments conducted at the Hadley Centre (§8.2.1), related to reduced emissions, leading to a stabilisation of the concentration of atmospheric CO_2 at 550 and 750 ppm (approximately twice and three times pre-industrial concentrations respectively) (herein stabilisation at 550 ppm and stabilisation at 750 ppm). The final scenario (unrealistic but useful for comparison) was that of atmospheric CO_2 remaining constant at the 1994 concentration (herein constant (358 ppm)) (Schimel *et al.* 1996).

Figure 8.2 illustrates the profiles of anthropogenic emissions and the resulting CO_2 concentration profiles for each of the scenarios used in this investigation (IPCC 1996; DETR 1999). The data were obtained on-line from the Climate Impacts LINK project (http://www.cru.uea.ac.uk/link).

8.2.1.3 Climate change under stabilisation scenarios

The changes in global mean annual surface temperature for the stabilisation scenarios compared to the unmitigated scenario are shown in Figure 8.3. A global average temperature rise of 2 °C, which would occur by the 2050s with unmitigated emissions, would be delayed by approximately 50 years under 750 ppm stabilisation and by over 100 years under 550 ppm stabilisation (DETR 1999).

a

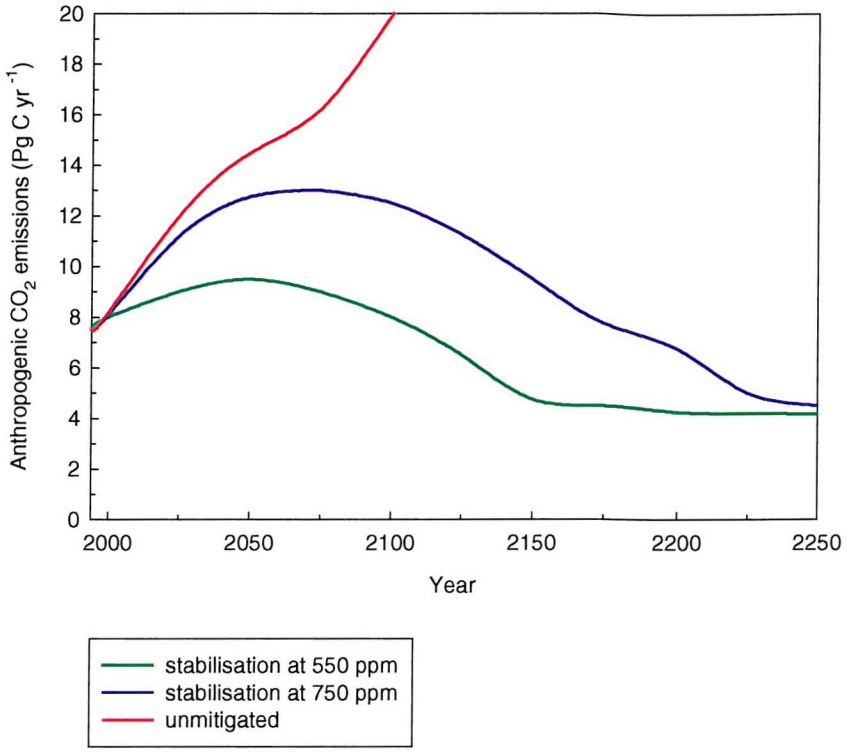

b

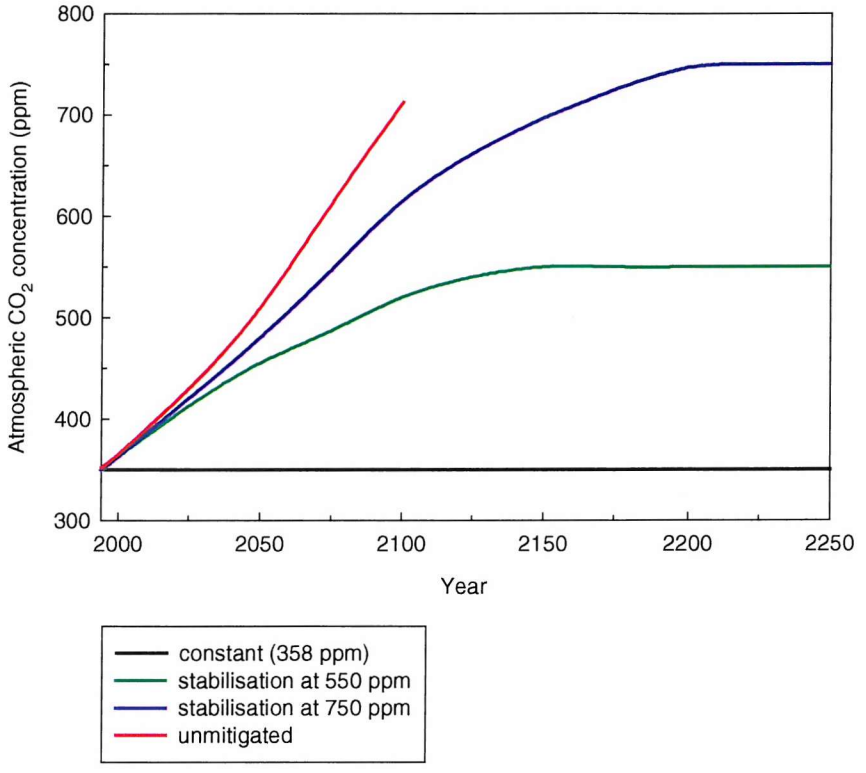

Figure 8.2 a Profiles of future anthropogenic emissions of CO_2 (IPCC 1996).
b Atmospheric CO_2 concentrations resulting from a (DETR 1999).

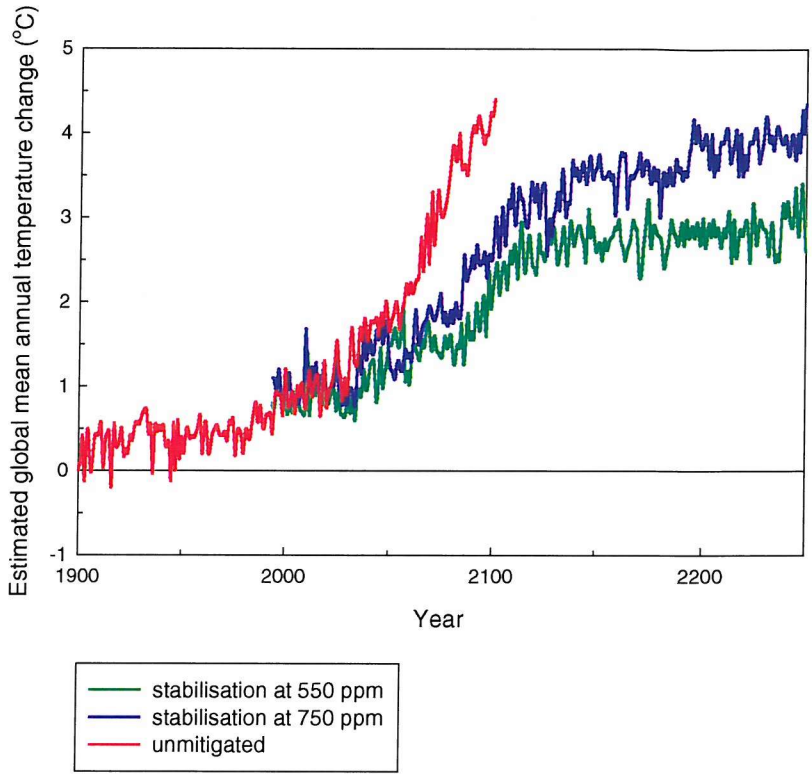

Figure 8.3 The global mean temperature rise resulting from the emission scenarios (DETR 1999).

In fact, these scenarios may well be conservative estimates for this investigation: While mean global warming is expected to amount to between 1 and 3.5 °C (Figure 8.3), this will not be uniform around the globe (Hasenauer *et al.* 1999; O'Riordan 2000). High latitudes are expected to experience levels of warming greater than the global average (IPCC 1996; Sellers *et al.* 1996b) partly due to projected changes in the polar sea ice climatology and snow-albedo feedbacks (Sellers *et al.* 1997). For Canada, annual mean temperatures may increase between 5 and 10 °C (approximately 3 times the global mean) over the next century (Environment Canada 1997).

The remainder of this chapter explores the impact of these global scenarios on the future productivity of the boreal forest.

8.2.2 FOREST-BGC simulations

This section describes the automation of FOREST-BGC and outlines the input data used to run the model over a 106 year period (1994 to 2100). Simulations were run on two LAI surfaces. First, the spatial LAI estimates from the VI3 applied to AVHRR imagery (§7.5.3, Plate 7.1 b) approximately 12,000 km^2 (herein VI3 LAI estimates) and second, LAI estimates from the shrunken-ASU aggregation technique on Landsat TM imagery (§5.5, Figure 5.19) approximately 150 km^2 (herein ASU LAI estimates).

8.2.2.1 The automation of FOREST-BGC

The generation of a look-up-table (LUT) made the task of running FOREST-BGC on a per-pixel basis considerably more efficient for the pilot study (§4.3.3). However, more flexible automation was necessary to model the impact of future climate change scenarios for larger areas of the boreal forest (Figure 8.4).

Initially, it was necessary to write a small program, 'RUN CODE' (Appendix B), to collect the data required by FOREST-BGC for each model simulation. By reading values from a LAI surface (§8.2.2), classified image (§5.4, Plate 5.1) and DEM (§5.4, Figure 5.15 a), RUN CODE updated a template 'initialisation file'. Each initialisation file contained general variables (§4.2.2, Table 4.2), climate scenario manipulation variables as well as pixel-/ASU -specific information: latitude, longitude and elevation (taken directly from the DEM), LAI and leaf carbon (taken from the LAI coverage) and a species flag (taken from the classified image).

Second, the original FOREST-BGC code used for the pilot study (§4.3.1) (written in Turbo Pascal for the DOS environment) was translated into the C programming language and re-compiled to run within the UNIX environment. In addition, two significant alterations were made:

1. The code was adjusted so that the initialisation file was read-in before each simulation. As well as updating LAI values, the initialisation file pointed to the relevant input 'ecophysical variable input file' and 'climate variable input file' for each simulation. The model used one of four ecophysical variable input files (the result of species-specific variable libraries (§ 4.3.2.1)), depending on the species flag from the classified image. Given latitude and longitude, the model used the climate variable input file derived from the station nearest to the location (Figure 4.2).
2. The code was adjusted to enable one output file to be written per-pixel (-ASU), containing each output variable for each simulation year.

A single FOREST-BGC simulation consisted of running the model for each pixel (or ASU) for the 106 years for which climate data were available.

Third, a second small program, 'PROCESS' (Appendix B), was written to combine the output files. PROCESS produced one 'annual output' ASCII file per simulation year. Annual maps of each output variable were produced by importing each annual output file into an image processing software package (e.g., ERDAS Imagine). Further analyses, to include generation of descriptive statistics and accuracy assessment, were then possible.

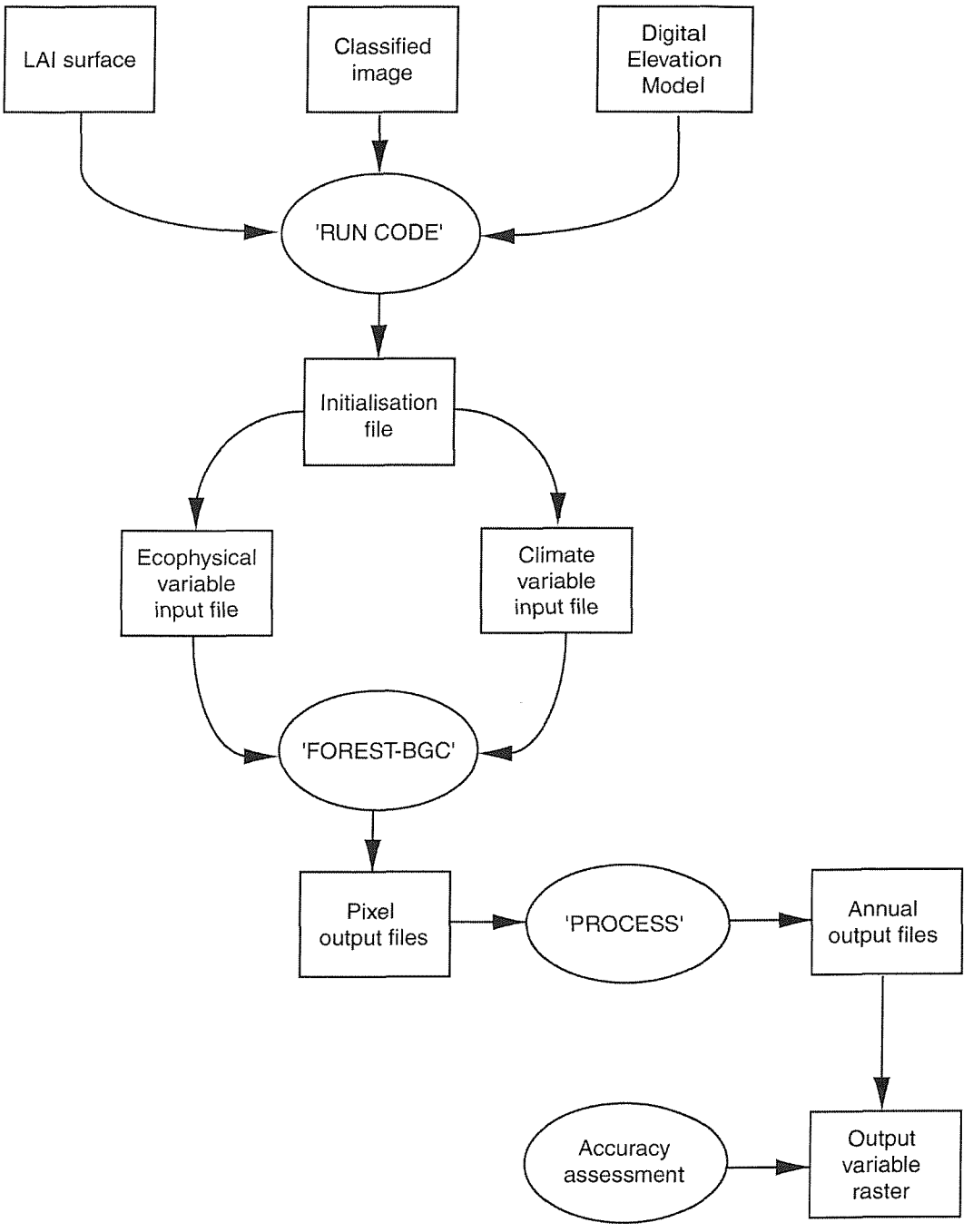

Figure 8.4 Stages in the automation of FOREST-BGC.

8.2.2.2 Creation of modified climate files: Application of change fields

To create modified climates for a given climate scenario (§8.2.1), the annual 1994 FOREST-BGC climate input files (i.e., the *base climate*) used for the pilot study (§4.2.1) were modified using annual scenario change fields (within a spreadsheet), according to the following:

1. For maximum, minimum and mean temperature and for relative humidity:
   addition of the corresponding temperature or relative humidity difference to the base climate daily values.
2. For precipitation and incident solar radiation:
   multiplication of base climate daily values by the corresponding annual change ratios.

To avoid confusion, the following modified climate input file naming protocol was adopted:

sss_styr-enyr_ccs.mtc

where, **sss** is a three letter site code; **styr** is the start year; **enyr** is the end year and **ccs** is the three letter code of the climate change scenario (e.g., ojp_1994-2100_358.mtc)

To limit physical inconsistencies arising from the generation of modified climates the following two basic rules (VEMAP 2000) were applied to each prepared climate input file:

1. For solar radiation: New values of total incident solar radiation were limited so as not to exceed potential solar input at the Earth's surface;
2. For relative humidity: Any values greater than 100% were set to 100% and negative values to 0%.

Although, this "minimum set of checks for any constructed climate" (VEMAP 2000, p.28) does not cover all possible physical inconsistencies, it was comforting that none of the climate files generated for this investigation (up to the year 2100) violated these rules and so no adjustments were necessary.

8.2.2.3 Simulation outputs

A total of 8 modelling experiments were conducted (i.e., four future climate scenarios run on two LAI input surfaces, Table 8.1) for the 106 year period from 1994 to 2100. Although several output variables are available from FOREST-BGC (§2.5.6.1), Net Ecosystem Production (NEP) (i.e., annual carbon sequestration) was chosen as the most useful to address the third objective of this chapter (§8.1): to estimate the future carbon budget for the BOREAS SSA:

$$\text{Net Ecosystem Production} = \text{Net Primary Production} - \text{Heterotrophic respiration} \qquad (8.1)$$

Scenario	VI3 LAI surface	ASU LAI surface
constant (358 ppm)	1	5
stabilisation at 550 ppm	2	6
stabilisation at 750 ppm	3	7
unmitigated	4	8

Table 8.1 The order of modelling experiments.

8.3 Data Analysis and Results

First, descriptive temporal statistics for NEP were calculated from the annual output variable files, before maps of annual NEP were produced (within ERDAS Imagine).

8.3.1 VI3 LAI future climate scenario estimates of NEP

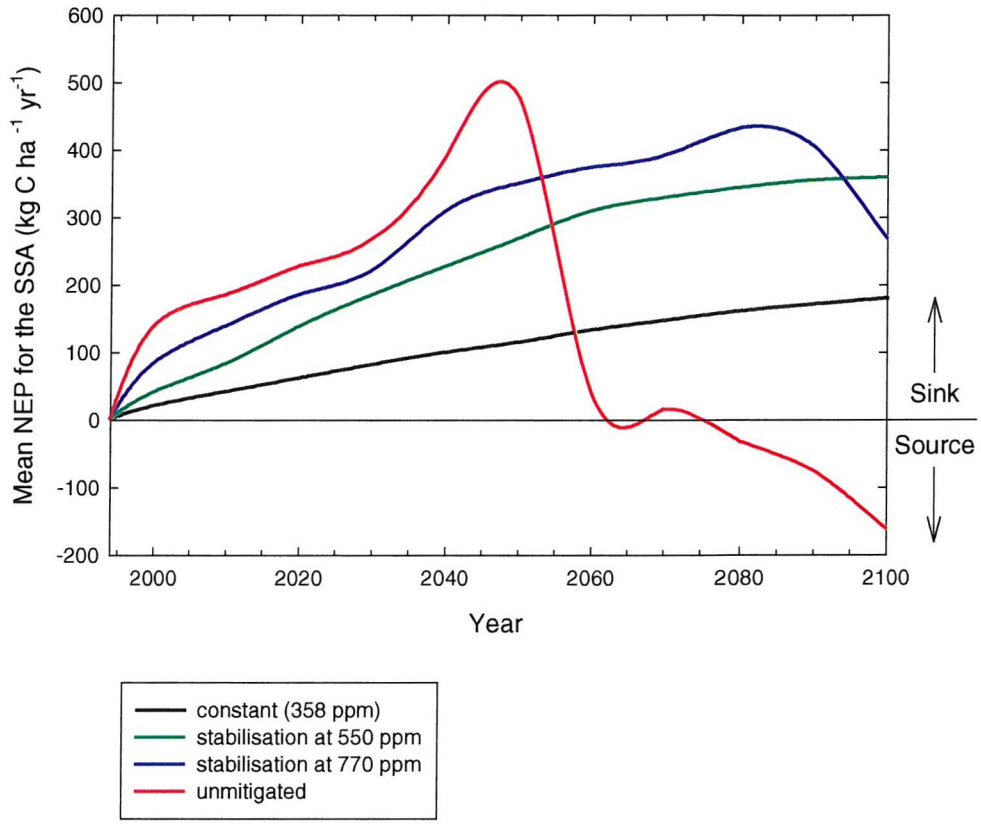

Figure 8.5 Mean annual NEP (kg C ha^{-1} yr^{-1}) for the SSA from the VI3 LAI input surface.

Figure 8.5 shows the net carbon sequestration of the SSA (i.e. the rate of increase as a carbon sink) in response to the climate change scenarios using the VI3 LAI surface. Given the unrealistic, constant (358 ppm) scenario, simulations showed a steady continual increase in mean annual NEP of the SSA, possibly just reaching an asymptote of approximately 180 kg C ha^{-1} yr^{-1} by 2100 (black line on Figure 8.5). This is useful, if only for comparison because (i) it shows the system to be relatively stable, given constant inputs and (ii) the difference between NEP in a given year under different scenarios gives an indication of how different the future will be to that expected if atmospheric CO_2 were to remain constant.

Reducing anthropogenic emissions to attain a stable concentration of atmospheric CO_2 of 550 ppm also resulted in increased carbon sequestration (a strengthening of the SSA as a sink of carbon), to approximately 380 kg C ha^{-1} yr^{-1} by 2100 (green line on Figure 8.5), more than double that of the constant atmospheric CO_2 scenario.

The more lax (but more realistic) third scenario, to attain a stable concentration of atmospheric CO_2 of 750 ppm, exaggerated this trend further, to a maximum carbon sink in excess of 420 kg C ha^{-1} yr^{-1} by 2080 (blue line on Figure 8.5). The NEP of the SSA decreased steadily over the subsequent years up to 2100, although, by 2100 the SSA was still sequestering approximately 280 kg C ha^{-1} yr^{-1}.

Under the unmitigated scenario, results suggested that the SSA strengthened as a carbon sink to in excess of 500 kg C ha^{-1} yr^{-1} by 2050 (red line on Figure 8.5). However, after 2050 the carbon sink weakened dramatically and disappeared by 2080, becoming a net source of approximately 170 kg C ha^{-1} yr^{-1} by 2100.

Rather than display maps of annual NEP here, it is more appropriate to illustrate the magnitude of difference between the unmitigated emissions scenario and constant (358 ppm) scenario by generating a time series of difference maps (Plate 8.1). Unsurprisingly, the form of Figure 8.5 was replicated in these maps. In 1994 the mean difference between the unmitigated and constant (358 ppm) scenarios was slightly positive 71 kg C ha^{-1} yr^{-1} (Table 8.2). This difference increased to a maximum mean difference of 382 kg C ha^{-1} yr^{-1} by 2050 (Plate 8.1, Table 8.2) as the annual sequestration of carbon by the SSA reached its maximum under the unmitigated scenario. By 2100 the SSA weakened as a carbon sink given the unmitigated scenario, hence the negative difference map (mean difference -176 kg C ha^{-1} yr^{-1}).

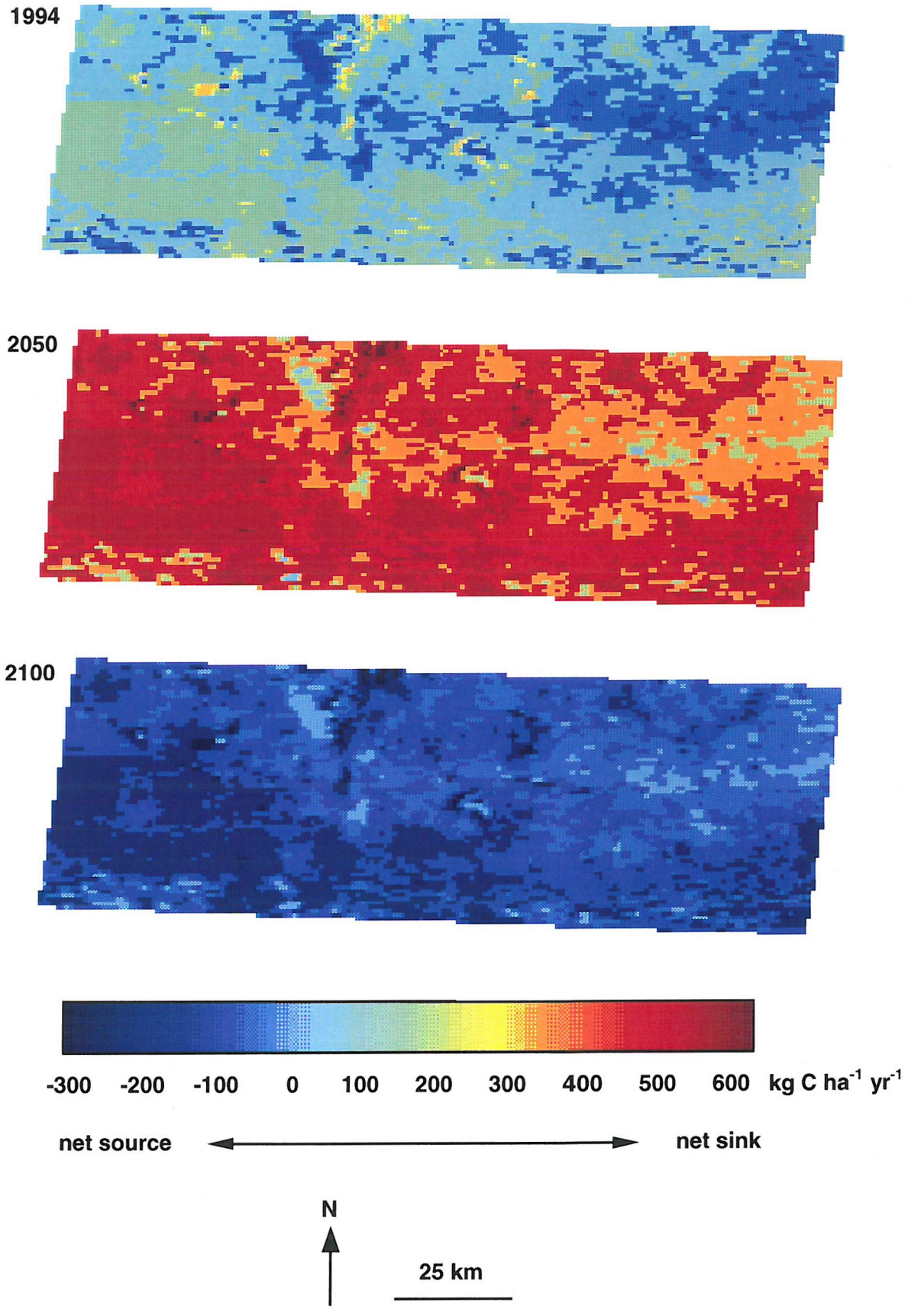

Plate 8.1 Mean difference in annual NEP (kg C ha^{-1} yr^{-1}) for the SSA from the VI3 LAI input surface (unmitigated - constant (358ppm)).

8.3.2 ASU LAI future climate scenario estimates of NEP

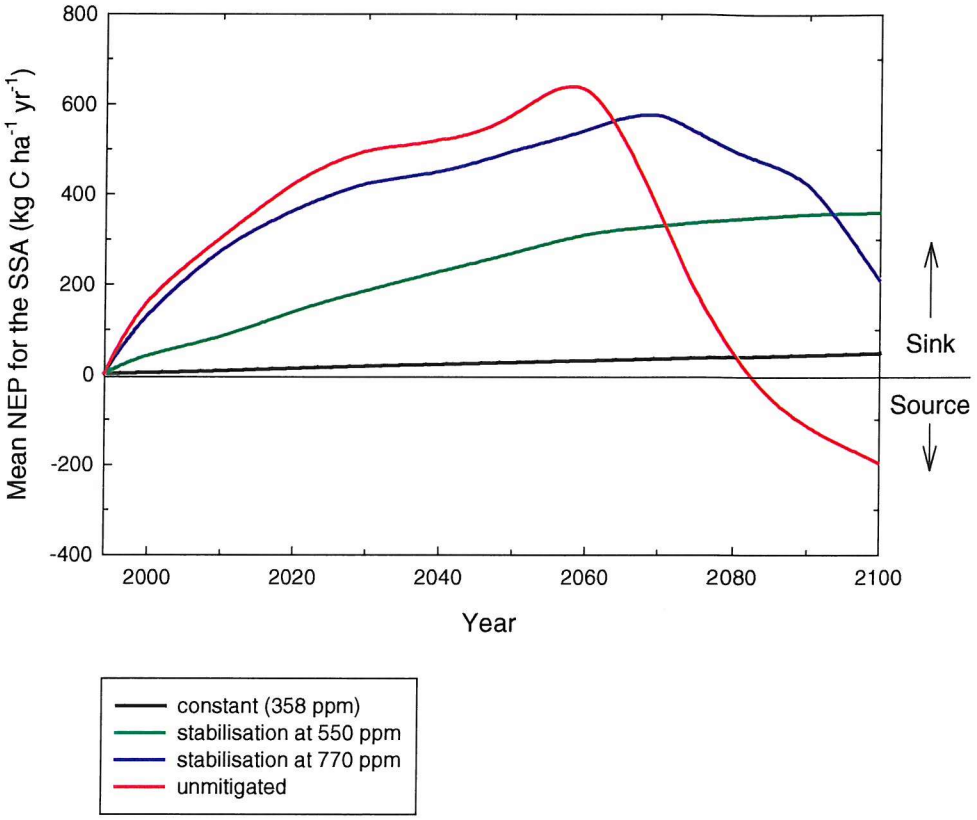

Figure 8.6 Mean annual NEP (kg C ha^{-1} yr^{-1}) for the SSA from the ASU LAI input surface.

In general, the net carbon sequestration of the SSA simulation results from the ASU LAI surface (Figure 8.6) followed very similar patterns to those from the VI3 LAI surface (Figure 8.5). Although, one noticeable difference was the magnitude of difference: NEP calculated from the ASU LAI surface was on average 19% greater than for simulations on the VI3 LAI surface. This can be attributed to the areas covered. The ASU LAI surface was approximately 150 km^2 of relatively homogeneous forest cover, whilst the VI3 LAI surface was 12,000 km^2, encompassing the entire BOREAS SSA. Because of the shrinkage technique (§5.5) mixed boundary pixels (primarily due to forest tracks / paths) were excluded from the ASU estimates of LAI. This would have resulted in slightly higher estimates of LAI, than for the VI3 LAI surface. Consequently, NEP estimates were higher.

The slight but continual increase in mean annual NEP under the constant (358 ppm) scenario, had a similar form to the results on the VI3 LAI surface, reaching approximately 50 kg C ha^{-1} yr^{-1} before 2100.

The second climate scenario, by reducing anthropogenic emissions to attain a stable concentration of atmospheric CO_2 of 550 ppm also resulted in a strengthening of the SSA as a sink of carbon, to approximately 250 kg C ha^{-1} yr^{-1}. Similarly, this trend was replicated further by following the stabilisation at 750 ppm scenario to a maximum carbon sink in excess of 420 kg C ha^{-1} yr^{-1} by 2080. The subsequent years up to 2100 saw the NEP of the SSA steadily decrease, although, by 2100 the SSA still remained a considerable sink of approximately 220 kg C ha^{-1} yr^{-1}. Under the unmitigated scenario, results suggested that the SSA strengthened as a carbon sink to in excess of 600 kg C ha^{-1} yr^{-1} by 2050. However, after 2050 the carbon sink weakened dramatically and disappeared by 2080.

Therefore, emissions scenarios that stabilised the atmospheric CO_2 concentration delayed considerably the loss of the SSA as a sink of carbon. However, they did not prevent this loss from occurring: The form of the stabilisation at 750 ppm curves (blue line) in Figures 8.5 and 8.6 suggested that positive annual carbon sequestration would be lost within the first quarter of the twenty second century. The form of the stabilisation at 550 ppm curves were, however, more encouraging as they appeared to reach an asymptote towards 2100. With unmitigated emissions the loss of the carbon sink occurred when the atmospheric CO_2 concentration was still rising (Figure 8.2 b).

In a similar fashion to the estimates of NEP made using the VI3 LAI surface, difference maps were produced for the same dates for these scenarios run on the ASU LAI surface (Plate 8.2, Table 8.2). Yet again, there was consistency between the results: The mean difference between the unmitigated and constant (358 ppm) scenarios increased to a maximum mean difference of 551 kg C ha^{-1} yr^{-1} by 2050 (Plate 8.2, Table 8.2). By 2100 the SSA had weakened as a carbon sink following the unmitigated scenario, to approximately the same value as for the VI3 LAI surface inputs. The greater mean difference in net carbon sequestration can be explained by the low value of the constant (358 ppm) scenario, hence the negative difference map (mean difference -244 kg C ha^{-1} yr^{-1}).

	VI3 LAI estimates				ASU LAI estimates			
year	mean	maximum	minimum	standard deviation	mean	maximum	minimum	standard deviation
1994	+71	+156	0	33	-76	+7	-124	16
2050	+382	+458	0	160	+551	+897	0	191
2100	-176	0	-210	74	-244	0	-312	52

Table 8.2 Mean difference in NEP (kg C ha^{-1} yr^{-1}) between unmitigated and constant climate scenarios (- shows a net source difference and + shows a net sink difference).

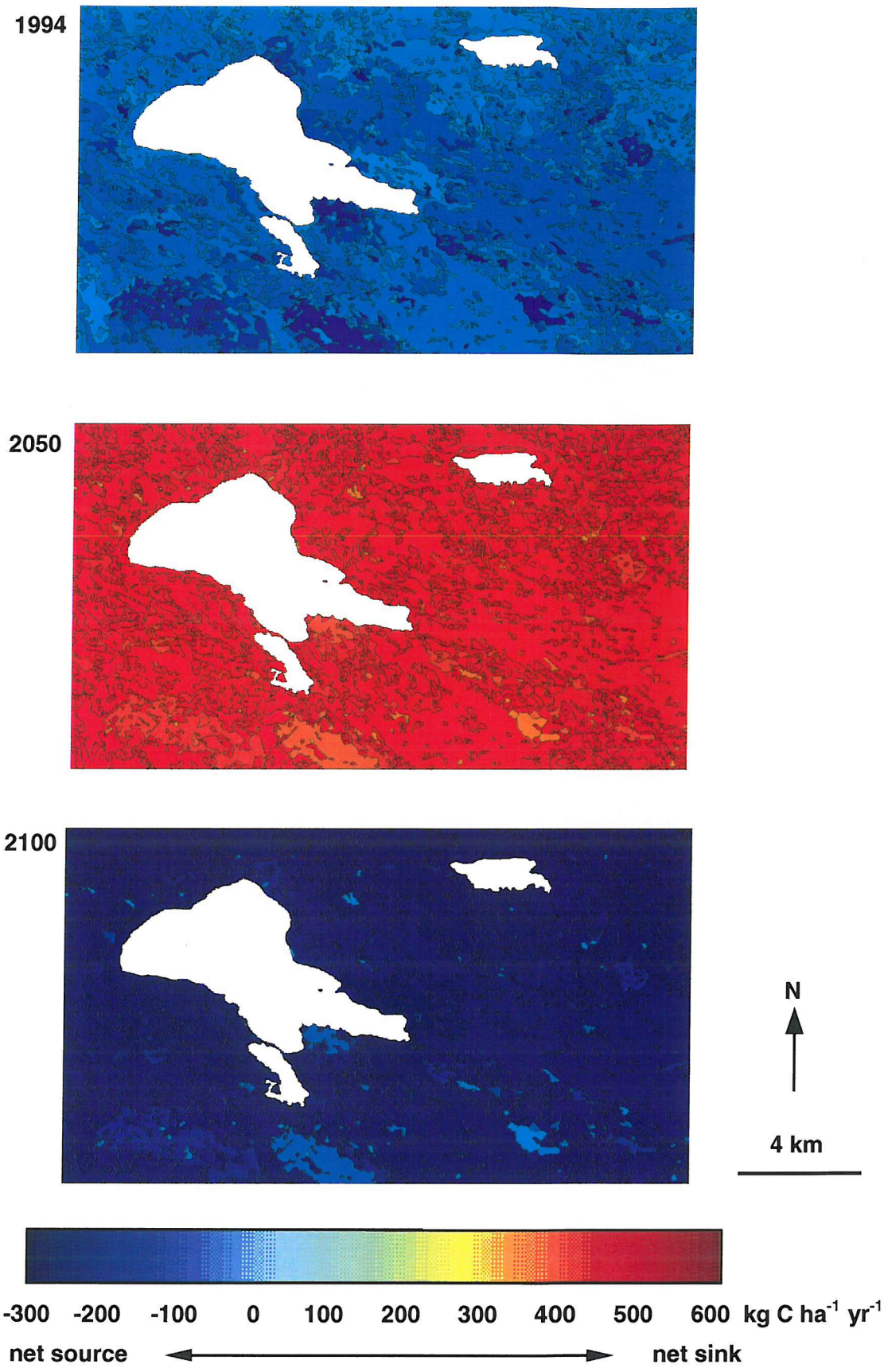

Plate 8.2 Mean difference in annual NEP (kg C ha^{-1} yr^{-1}) for the SSA from the ASU LAI input coverage (unmitigated - constant (358ppm)).

8.4 Discussion

Boreal forests may continue to provide a substantial 'brake' on the rate of increase in atmospheric CO_2 until well into the twenty second century, provided anthropogenic emissions of CO_2 are dramatically reduced to within the limits shown by Figure 8.2a. However, if the unmitigated scenario is followed, this experimental modelling investigation suggests that the boreal forest carbon sink strengthens until 2050, but thereafter collapse is likely, resulting in a disappearance of the carbon sink by 2080. Such collapse could have serious implications on the physical climate system and ecosystems (Figure 2.7). The following sub-sections offer explanations for the results obtained from the modelling experiments and subsequent analyses of this chapter. Mechanisms that may be responsible for future changes in the boreal forest carbon budget are suggested.

8.4.1 Initialising and driving mechanisms

Although the circumpolar boreal forest is presently a sink for atmospheric carbon (Lindroth *et al.* 1998; Goulden *et al.* 1998; Chen *et al.* 1999; Houghton *et al.* 2000), it is extremely unlikely that the mechanisms believed responsible for this sink (§8.1) will be sustained as they are principally continuing responses to recent environmental fluctuations (Apps *et al.* 1993). In addition, given the results of modelling experiments within this chapter based on predictions of future climate, Figure 8.7 depicts a hypothetical mechanism behind the future collapse of the BOREAS SSA as a carbon sink under the unmitigated and stabilisation at 750 ppm emissions scenarios.

The main reason for the collapse of the carbon sink, it is suggested, is an unsustainable increase in standing biomass and LAI of the boreal forest stands within the SSA. Initially carbon sequestration increases as a result of increasing atmospheric CO_2 concentration, most probably due to CO_2 fertilisation (Tans *et al.* 1990; Melillo *et al.* 1996), increased nutrient use and increased water use (Houghton, 1995; Drake *et al.* 1997). Apps *et al.* (1993) suggested nutrient inputs associated with low-level but wide-spread atmospheric pollution may yield short-term increased carbon uptake but more likely will lead to future forest decline. By 2050 (unmitigated) and 2080 (stabilisation at 750 ppm) a threshold is reached whereby increases in biomass and LAI can no longer be sustained, initiating increased autotrophic respiration and decomposition (Ryan *et al.* 1997; Calow 1998) and reductions in the rate of photosynthesis (Drake *et al.* 1997), a manifestation of less sunlight penetrating the canopy (Figure 8.7). This is supported by logic incorporated into the FOREST-BGC code (Figure 4.11, §4.3.3) such that the allocation of available carbon (primarily above-ground) is assessed on the basis of daily GPP and maintenance respiration costs.

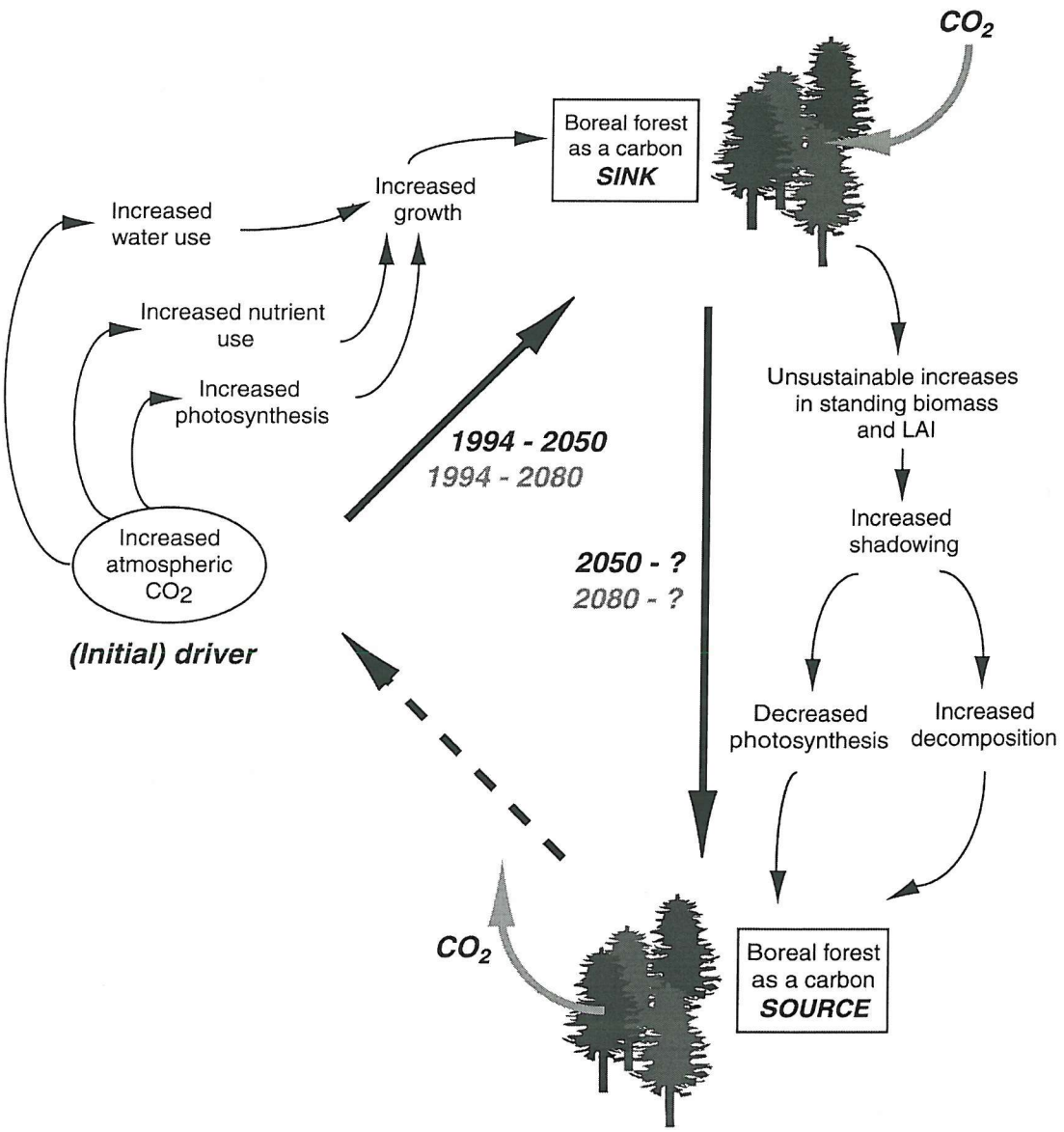

Figure 8.7 Schematic representation of a hypothesised mechanism that may result in the boreal forest as a source of carbon. Time-scales are shown for both unmitigated (black) and stabilisation at 750 ppm (grey) emissions scenarios.

The mechanism depicted within Figure 8.7 may be explained by the fundamental principle of plant responses to environment, in that plants usually respond to virtually any environmental variable according to a common pattern (Figure 8.8) (Oliver and Larson 1996). Different variables, such as atmospheric CO_2 concentration and light intensity, interact and can be limiting at the same time, although one is often the major factor (Blackman 1905). As the limiting variable increases, a *threshold* is reached above which the variable begins to have an effect: The response (e.g., carbon sequestration) increases until the system becomes *saturated* by the variable (Lawlor 1993). Then, as the variable's concentration continues to increase, response remains constant (long dashed curve, Figure 8.8) or begins to decrease if at such high concentrations that the variable inhibits.

Such effects may be indirect as suggested by Figure 8.7: Unsustainable increases in standing biomass and LAI (as a consequence of increasing atmospheric CO_2) result in decreased rates of photosynthesis and increased decomposition from increased shadowing (i.e., light becomes a limiting factor).

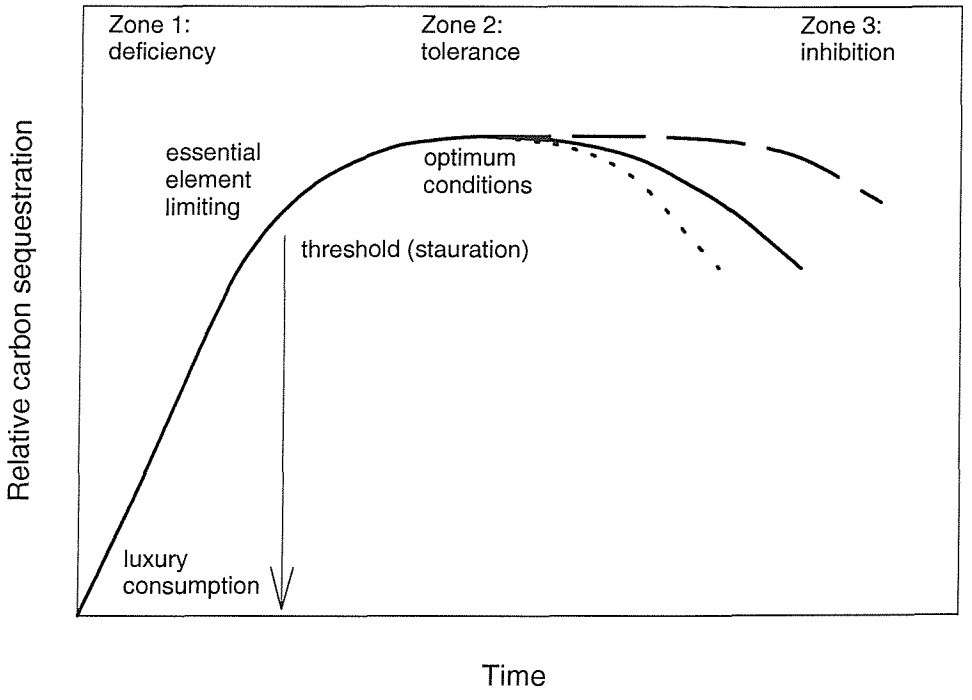

'Luxury consumption' refers to unrestricted growth and the 'threshold' is the point at which the 'essential element' (i.e., limiting factor) becomes limiting.

Figure 8.8 Theoretical representation of limiting factors (adapted from Salisbury and Ross 1992).

Whether 'check-back' to a homeostatic system or initiation of positive feedback causing the system to spiral out of control, such a proposed mechanism would have wide-reaching implications for the boreal forest ecosystem and the inextricably linked physical climate system.

Indeed, the pervasive influence of climate on vegetation is obvious but vegetation also exerts influences back on local and regional climate. Bonan *et al.* (1992, 1995) simulated the influence of a major deforestation in the boreal forest zone on climate and concluded that removal of forest cover would expose the snowpack, increasing surface albedo between January and April and result in a 2 to 5 °C mean annual temperature decrease at high latitudes!

8.5 Implications of Chapter Findings: Impacts, Adaptation and Mitigation

The findings of this chapter have serious implications, particularly when viewed in combination with the responses of other terrestrial biomes to future climate change. A direct consequence of the disappearance and worse, reversal of the boreal forest carbon sink is that more of the anthropogenic emissions of CO_2 will remain in the atmosphere. Thus atmospheric CO_2 concentration, that has already increased by approximately 25 ppm (from 355 ppm) since the start of the BOREAS project in 1993 (O'Riordan 2000) will be exacerbated. The following section addresses the implications of the findings of this chapter by describing future impacts and required changes in mitigation and adaptation. First, the results obtained for the BOREAS SSA are extrapolated to larger areas.

8.5.1 Extrapolation to larger areas

Table 8.3 gives estimates of present and future NEP for the BOREAS SSA, the Canadian boreal forest and the global boreal forest. The NEP estimates from the VI3 LAI input surface experiments under the constant (358 ppm) and unmitigated scenarios were assumed to be representative of all boreal forests! Hence, although these values must be considered very uncertain (Apps *et al.* 1993; Curran *et al.* 1997), this exercise indicated the considerable potential future rôle of the boreal forests in the global carbon cycle.

	Scenario	BOREAS SSA 1.1 million ha [a]	Canadian boreal forest 417.6 million ha [b]	Global boreal forest 1249 million ha [c]
1994	Constant	0	0	0
	unmitigated	8.80×10^{-5}	0.033	0.10
2050	Constant	1.08×10^{-4}	0.041	0.12
	unmitigated	5.72×10^{-4}	0.22	0.65
2100	Constant	1.98×10^{-4}	0.075	0.22
	unmitigated	-1.87×10^{-4}	-0.071	-0.21

[a] Halliwell and Apps 1997a; [b] Canadian Forest Service 1999; [c] Apps *et al.* 1993.

Table 8.3 Extrapolated NEP (Pg C yr^{-1}) based on the VI3 LAI surface.

Chen *et al.* (1999) extrapolated CO_2 fluxes, measured using the continuous eddy covariance technique of Goulden *et al.* (1998), assuming these rates of carbon sequestration to be representative of all Canadian boreal forests. Their estimate of NEP for 1994 was 0.038 - 0.05 Pg C yr^{-1}. Given the difficulties and approximations involved with such extrapolation (§5.1.5,

Figure 5.4), it is remarkable and extremely encouraging that the extrapolated value of NEP for the Canadian boreal forests in 1994 from these experiments was 0.033 Pg C yr^{-1} (within 0.005 Pg C yr^{-1} of Chen *et al.* (1999)) (Table 8.3). Such carbon sequestration equates to approximately 3% of the current global missing carbon sink.

8.5.2 Adaptation to the inevitable

Given the history of past emissions from industrialised nations and the inertia of the climate system, considerable further climate change will be experienced (Figure 8.3) even if substantial reductions in anthropogenic CO_2 emissions are made (Figure 8.2 b) (Parry *et al.* 1998).

Options for boreal forest nations to mitigate against increasing atmospheric carbon are limited because, apart from Northern Europe, much of the circumpolar boreal forest remains in a wilderness state. Indeed, only a small fraction of the boreal biome is affected directly by forest management (e.g., approximately 28% of Canada's forests) (Canadian Forest Service 1999) (Figure 8.9).

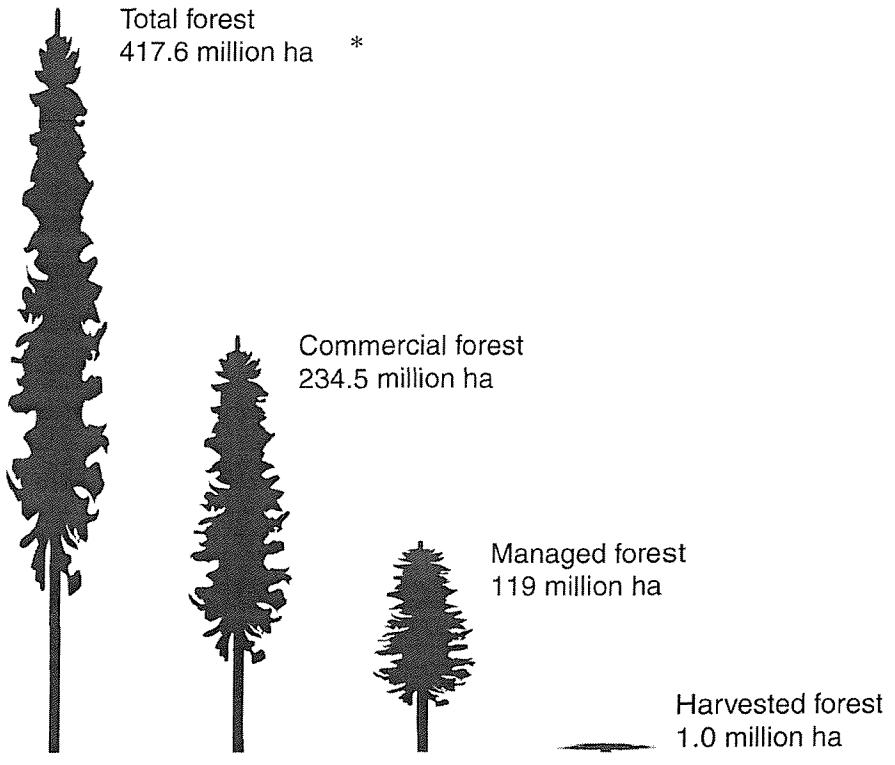

* total land area of Canada is 921 million ha.

Figure 8.9 The area of Canada's forests (Canadian Forest Service 1999).

Improved management practices have the potential to increase biomass yields at local scales (Apps *et al.* 1993) but it is difficult to see how these could be applied effectively at regional

scales because of prohibitive costs. Non-sustainable development practices, however, can adversely affect carbon storage capacity. Even in the absence of such human intervention, transient response of the boreal forest to climate change has the potential to initiate significant positive feedbacks to the climate system, by releasing large quantities of carbon to the atmosphere because of the inertia of the system (Figure 8.7). Therefore, adaptation rather than mitigation would seem appropriate. To date, however, adaptation has received little attention compared with mitigation (Parry *et al.* 1998). This may be because admitting the need to adapt is defeatist to negotiators and adaptation is more complicated than mitigation (O'Riordan 2000). For example, emissions sources are relatively few but the array of adaptations is vast. Therefore, to ignore adaptation is "unrealistic and perilous" (Parry *et al.* 1998, p. 741).

8.5.3 Awareness of limitations and implications for methodological research

Researchers are gaining confidence that the results from climate models do represent the way in which climate will change over future decades at continental to global scales. However, detailed impact assessments demand information at regional scales and predictions not just of mean changes but changes in the variability and extremes of climate both temporally and spatially. The provision of this level of detail continues to present climate researchers with a considerable challenge.

This investigation considered the joint impact of climate change (e.g., elevated temperature and altered precipitation patterns) and elevated CO_2 on the future carbon budget of the boreal forests. However, to increase our understanding of the mechanisms involved, differentiation between the effects of climate change and elevated CO_2 concentrations would be a useful development. Indeed, as would combining both direct CO_2 effects on tree physiology with climatic change scenarios from GCMs. In addition, investigation of the impact of changes in carbon sequestration on the physical climate system could be achieved by coupling an ESM to an atmospheric model (e.g., SiB Table 2.2) (Hunt *et al.*, 1996).

Furthermore, by determining carbon use efficiency (CUE), the ratio of net production to production plus autotrophic respiration (Ryan *et al.* 1997), it may be possible for researchers to quantify the proportion of change in carbon sequestration due to autotrophic respiration alone.

A criticism of the model predictions presented in this chapter could be that no attempt was made to accommodate changes in land cover. Although the biological processes of boreal tree species are sensitive to small changes in climate (e.g., increased spring temperature causes earlier leaf emergence in deciduous boreal forest, causing more solar radiation to be absorbed, increasing photosynthesis and carbon sequestration (Chen *et al.* 1999; Hasenauer *et al.* 1999), generally, in terms of stand dynamics, the species are particularly resilient to small changes in temperature (Street and Öpik, 1970; Farrar 1995; Oliver and Larson 1996). Indeed, they are adapted to experiencing considerable annual temperature ranges in excess of 70 °C (Figure 3.6). This is not to suggest that the boundaries of the contemporary boreal forests will remain static. The northern boundary of the forest is delineated by temperature, whilst the southern boundary is determined by moisture stress, fire frequency and ecological competition with temperate deciduous forest (§3.1.1). Therefore, migration to higher latitudes, occupied currently by tundra, is probable (Smith *et al.* 1992) as warming may lead to a lengthening of the approximately 150-day growing season (Figure 4.3) by about 6 days (Keeling *et al.* 1996a; Myneni *et al.* 1997). However, the total area occupied by the boreal forests may remain relatively constant.

Sulzman *et al.* (1995) discussed the utility and limitations of using climate model outputs for exploring ecological sensitivity to climate change. In particular they emphasised the issue of physical inconsistencies arising in modified climates generated from the outputs of climate models. The strong possibility of such inconsistencies is acknowledged, however, checks used within Vegetation/Ecosystem Modelling and Analysis Project (VEMAP) (http://www.cgd.ucar.edu/vemap/) were applied to the data used for these modelling experiments (§8.2.2.2) and were considered sufficient, given the relatively short time frame of 106 years. Equally, the appropriateness of using global climate change scenarios has been discussed (§8.2.1.3) and given other assumptions within the methodology, although the absolute results presented in this chapter must be interpreted with caution, it is the relative trends in the data that demand attention.

8.6 Summary of Chapter Findings

The four objectives of this chapter (§8.1) have been met. In addition, the following three conclusions can be drawn from the research in this chapter:

1. Boreal forests may continue to provide a substantial 'brake' on the rate of increase in atmospheric CO_2 until well into the twenty second century, provided anthropogenic emissions of CO_2 are reduced dramatically to within the limits shown within Figure 8.2

2. However, if the unmitigated emissions scenario is followed, carbon sequestration of the boreal forests increases to a maximum by 2050 but thereafter collapse is likely, resulting in a disappearance of the carbon sink by approximately 2080.
3. There is still a considerable amount of work to be done in order to estimate accurately future carbon sequestration of the boreal forest. Indeed, because the contemporary boreal forests are still evolving since the last glaciation on a time scale of millennia (Davis 1969), whether the results shown in this chapter may just be shorter-term disequilibria on the scale of decades and centuries that must be superimposed on these longer-term changes, remains to be seen.
4. Finally, although the relative trends in the model estimates demand attention, it must be acknowledged that the absolute results presented here should be interpreted with caution as FOREST-BGC has been employed beyond the confines of the limited data range used to test the accuracy of model estimates within Chapter 4.

Chapter 9

Conclusions

This research has realised its aim of driving FOREST-BGC with remotely sensed data in order to investigate the impact of future climate on the carbon budget of the boreal forest. In this final chapter the findings of this thesis are summarised. Possibilities for future research, building upon the findings and limitations of this investigation are suggested before outlining the impetus of this research within the context of regional to global scale environmental modelling.

9.1 Findings

The pilot study was instrumental in realising the potential of driving FOREST-BGC with remotely sensed data. The model was 'initialised' and 'optimised' with a range of data from the BORIS as well as species-specific data from unpublished site observations and detailed literature searches. Comparisons between model simulations and ground estimates of NPP were extremely encouraging, especially given the general nature of FOREST-BGC with regard to stand morphology (§2.4). Running and Coughlan's (1988) observations that climate and LAI alone can represent much of the productivity of ecosystems were confirmed by testing the sensitivity of FOREST-BGC to its inputs. Realisation of the first objective of this thesis (by producing an accurate map of NPP for 20 km^2 of boreal forest) identified the need to increase the accuracy of spatial estimates of LAI. Consequently, three avenues were investigated to maximise the accuracy with which remotely sensed data could be used to estimate boreal forest LAI.

9.1.1 The adoption of areal sampling units

The 'challenge' of spatial dependence (Curran and Atkinson 1999, p.17) is that of choosing a spatial dimension best suited to a specific application. Chapter 5 of this thesis presented one such example, resulting in a new technique of landscape partitioning for use within ecosystem simulation modelling.

Results confirmed the potential of per-ASU aggregation for increasing the accuracy of LAI estimation at regional scales in contrast to traditional stand polygons or '*arbitrary pixels*' (Fisher 1997, p. 680). The sampling units captured spatial variation of the landscape, while high spatial frequency features, (some associated with noise in the data), were removed, hence, more representative estimates of LAI were attained. Excluding the edge pixels of each ASU from the aggregation procedure attained further increases in estimation accuracy per ASU (relative to per-pixel). Such landscape partitioning may also facilitate model implementation as fewer model runs are required and each ASU can have a lower variability than the threshold sensitivity of the ESM employed.

9.1.2 Methods of spatial estimation

Theoretical differences among the methods of spatial estimation (aspatial regression, co-kriging and conditional simulation) may have less to do with their relative frequency in the research literature than practical considerations. Indeed, the dominance of aspatial regression in the remote sensing literature may be explained by its simplicity and the wide availability of software for implementation. However, these practical advantages can be outweighed by the need for spatial estimation methods that exploit fully the information content of remotely sensed (secondary) data. Other advantages of geostatistical methods are the:

- inclusion of measurement error for the secondary data;
- consideration of measurement location and sample arrangement and
- exploitation (instead of the neglect) of spatial autocorrelation.

Indeed, the variogram is clearly a useful tool, allowing the characterisation of the spatial variation of variables (Atkinson and Martin 1999). Estimation accuracy certainly has the potential to be increased by using spatial information in addition to the correlation information. However, as shown by the example within Chapter 6, the quality of results is dependent on the adequacy of the variogram models, stationarity assumptions and the strength of the relationship between primary and secondary variables.

Although geostatistical methods have been cited as reducing the number of samples required to achieve a required level of accuracy (e.g., Webster and Burgess 1984; Dungan *et al.* 1994), they do need robust estimation of spatial covariance, which in turn require, at the very minimum, 100 sample measurements of the primary variable (Curran and Williamson 1987; Webster and Oliver 1990; Cusack *et al.* 1999; Dungan 2000). For this investigation, because of the lack of a robust estimation of spatial covariance, the aspatial regression approach (the next best option, §6.1.4) was adopted.

Ultimately, the best choice of mapping approach is dependent on the purpose for which the map is intended and must be governed by both theoretical and practical considerations (Dungan *et al.* 1994; Brunsdon *et al.* 1999).

9.1.3 The value of AVHRR MIR (3.0–5.0 μm)

Vegetation indices provide a simple approach to the analysis of remotely sensed data. Interpretation of these indices, however, requires understanding of their nature, properties and characteristics. Recent advances in index design and evaluation, together with the advent of new space sensors, have stimulated the development of optimal vegetation indices (Govaerts *et al.* 1999).

Chapter 7 established that MIR radiation contains valuable information for estimating boreal forest LAI at regional scales and with an increased understanding of the interaction between MIR radiation and forest canopies, reflected MIR should be adopted more widely for ecological applications of remote sensing at and beyond regional scales. In particular, the VI3 (incorporating reflected MIR) was identified as being more strongly related to boreal forest LAI than the more widely used NDVI. Indeed, the NDVI may be considered a sub-optimal index for the estimation of boreal forest LAI.

Realisation of the second objective of this research, to maximise the accuracy with which spatial estimates of LAI could be attained from remotely sensed data, was a pre-requisite of the final phase of this research.

9.1.4 Modelling the impact of future climate change

To date, the majority of ESMs have 'only been used as research tools' (Coops 1999, p. 1149), although their ultimate aim was to provide prognostic capabilities (Hibbard and Sahagian 1997). Therefore, the third objective of this research was to investigate the impact of future climate on the carbon budget of the boreal forest. This was achieved in Chapter 8 by driving the

'automated' FOREST-BGC with climate change predictions and the spatial estimates of LAI that were a result of the second research objective.

Results suggested that boreal forests would continue to provide a substantial 'brake' on the rate of increase in atmospheric CO_2, provided anthropogenic emissions reduce dramatically. However, if emissions follow the unmitigated scenario, carbon sequestration of the boreal forests would increase to a maximum by 2050 but thereafter collapse, resulting in a disappearance of the carbon sink by approximately 2080.

9.2 Limitations as Drivers for Future Research

The research within this thesis has highlighted several potential areas for future investigation, Data requirements and advances in modelling are central themes.

9.2.1 Data requirements

Several suggestions for further increases in the accuracy of spatial LAI estimates have already been presented within this thesis (§5.6; §6.3 and §7.7). Rather than repeat these suggestions here, brief consideration is given to the advantages offered by (i) optimisation of ground measurement sample size and design and (ii) future satellite sensors for LAI estimation.

In particular, Chapter 6 demonstrated the need for large quantities of independent ground data, for deriving relationships and assessing the accuracy of results. Indeed, regardless of the spatial estimation method used, if researchers require accurate spatial estimates, increasing sample size will be an important factor (Curran and Atkinson 1998). Sample design is also a critical consideration if bias in the primary variable measurements is to be avoided (Atkinson and Martin 1999) but the cost of obtaining a spatially random and plentiful primary variable data may be excessive (Curran and Atkinson 1998).

Future monitoring and accuracy assessment of spatial estimates of LAI for large areas will benefit from co-operation between researchers and national agencies. One very recently established existing example is the IGBP Terrestrial Transects Project (http://gcte.org/LEMA-IGBP/LEMA-IGBP.html), comprising a set of study sites arranged along an underlying climatic gradient. Currently 13 transects exist globally, each approximately 1000 km long and sufficiently wide to encompass the dimensions of remotely sensed images. The establishment of data archiving centres is crucial for international distribution and long-term availability of such data. A centralised, permanently funded data centre, such as the Oak Ridge Distributed Active Archive Centre (DAAC) ensures continuity, consistency and data availability.

Secondly, optimisation of remotely sensed data, acquired by a number of sensors operating currently (e.g., NOAA AVHRR, ERS ATSR, Terra MODIS) and in the future (Envisat AATSR and MERIS) each of which have considerable potential for the estimation and mapping of biophysical variables, such as LAI, has important implications for regional to global scale ecological modelling (Cohen and Justice 1999, Verstraete and Pinty 1999). In particular, the Global Terrestrial Observing system (GTOS)-LAI project (http://www.fao.org/GTOS/), which aims to distribute the Terra LAI products every 8 days to regional networks for evaluation and accuracy assessment, is one of the most exciting prospects for future global monitoring of the terrestrial biosphere (Justice *et al.* 1998).

9.2.1.1 Climate data

Uncertainties still surround the generation of future climate predictions. Sulzman *et al.* (1995) discussed the utility and limitations of using climate model experiment outputs for exploring ecological sensitivity to climate change. They emphasised the issue of physical inconsistencies arising in modified climates generated from the outputs of climate models (§8.2.1.3). Detailed impact assessments (such as the final research chapter of this thesis) require accurate regional-scale information. The provision of such information as well as predictions not just for mean changes but changes in the variability and extremes of climate (both temporal and spatial) would add a further dimension to such impact assessments and continues to present researchers with considerable challenges.

9.2.1.2 Data for accuracy assessment

When driving an ESM with remotely sensed data it is necessary to determine the accuracy of both the remotely sensed estimates of the model driving variables (§9.2.1.1) and model estimates of ecosystem processes (§4.3.2.1). However, ecological modelling is still criticised for its lack of accuracy assessment (Running 1994; Lucas and Curran 1999; Running *et al.* 1999). Running (1994) contested that it is impossible, practically, to determine the accuracy of models of systems as complex as an ecosystem. However, it is possible to determine the accuracy of certain model outputs as a measure of the model's function (e.g., Fan *et al.* 1998) for example, the use of tree cores to infer annual biomass increment (§3.2.2.1). Another approach to assess accuracy is by model inter-comparisons (§2.2.1) as discrepancies in results draw attention to problem areas, data inadequacies or weak process understanding. Such measures of 'quality control' will remain an essential focus of ESM impact assessments for the foreseeable future if ecosystem modelling is to gain credibility as a research and prognostic tool.

9.2.2 Developments in ecosystem simulation modelling

Recent detailed physiological and micro-meteorological studies of forest ecosystems have led to new insights that simplify greatly the prediction of NPP (e.g., Coops 1999; Gobron *et al.* 1999). One such example of a model of minimum process complexity has been used to generate the MODIS global NPP estimates (§2.2.1). However, models of higher process detail (e.g., FOREST-BGC) are essential for assessing the accuracy and interpreting such estimates but cannot be run globally because of a lack of data and computing limitations.

A criticism of the impact assessment of future climate on the boreal forest could be that no attempt was made to accommodate changes in land cover (§8.5.4). Modelling investigations of the northward migration of the boreal forest boundaries would be an exciting development in ecosystem modelling, requiring the coupling of ESMs (such as FOREST-BGC) with dynamic biogeography models that account for succession, species development and migration processes. In addition, coupling the models to an atmospheric model (e.g., SiB Table 2.2) would enable integrated, interactive investigation of the impact of such changes on atmospheric CO_2 (i.e. a 'full system study' (Moore 1999, p.3)).

9.3 Thesis Findings in Context

Accurate monitoring of regional to global scale changes in the terrestrial biosphere has become acutely important as the scope of human impacts on biological systems and atmospheric chemistry increases (Running *et al.* 1999). An example of this is the Kyoto Protocol of 1997, signalling some of the dramatic socio-economic and political decisions that may lie ahead concerning CO_2 emissions and global carbon cycle impacts (Grubb *et al.* 1999). These decisions will be heavily reliant on accurate measurements of current and realistic estimates of future regional to global biospheric changes (Schimel 1998). An array of national and international programmes have inaugurated satellite sensor observations, critical field measurements of carbon and water fluxes and model development to monitor the biosphere in an attempt to increase understanding of the processes involved. Indeed, monitoring and accuracy assessment exercises at regional to global scales cannot be undertaken without international co-operation that transcends national agencies. As an example, Figure 9.1 depicts the modelling and data collection initiatives encountered during the completion of this research, illustrative of the potential synergy for terrestrial ecosystem research at different spatial and temporal scales. More comprehensive co-ordination of such data and modelling initiatives will undoubtedly have direct relevance to the political decision making of global change (Figure 9.2).

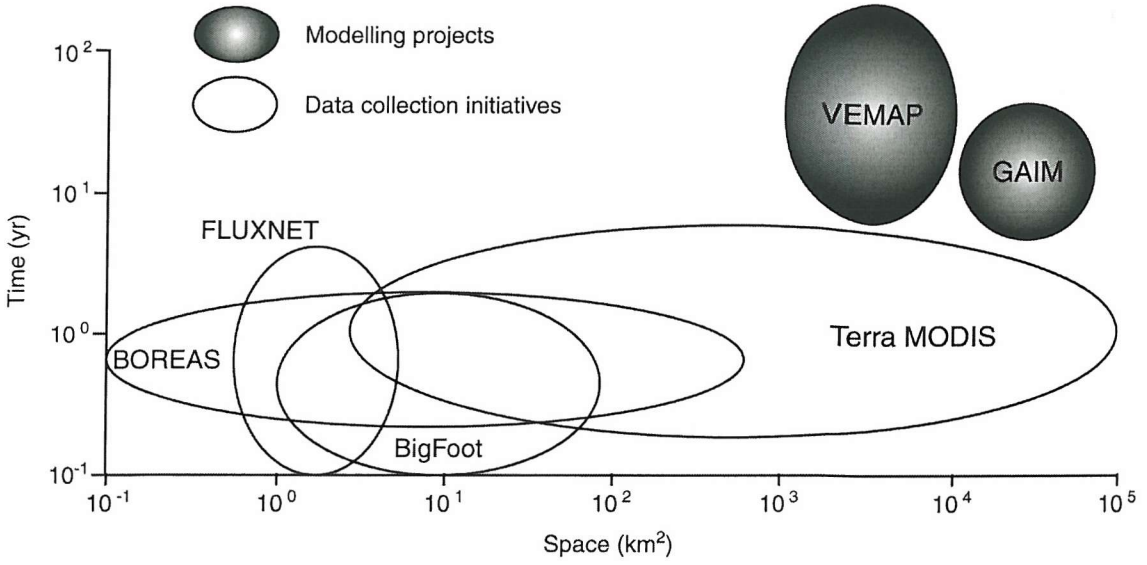

BOREAS = BOReal Ecosystem-Atmosphere Study; FLUXNET = global network of eddy covariance flux towers; BigFoot = a study to establish scaling principles for sampling vegetation over large areas; Terra MODIS = Moderate Resolution Imaging Spectroradiometer on the Terra satellite; VEMAP = Vegetation/Ecosystem Modelling and Analysis Project; GAIM = IGBP initiative for Global Analysis Integration and Modelling.

Figure 9.1 Potential synergism of international projects for accuracy assessment of terrestrial ecosystem variables at different spatial and temporal scales (adapted from Running *et al.* 1999).

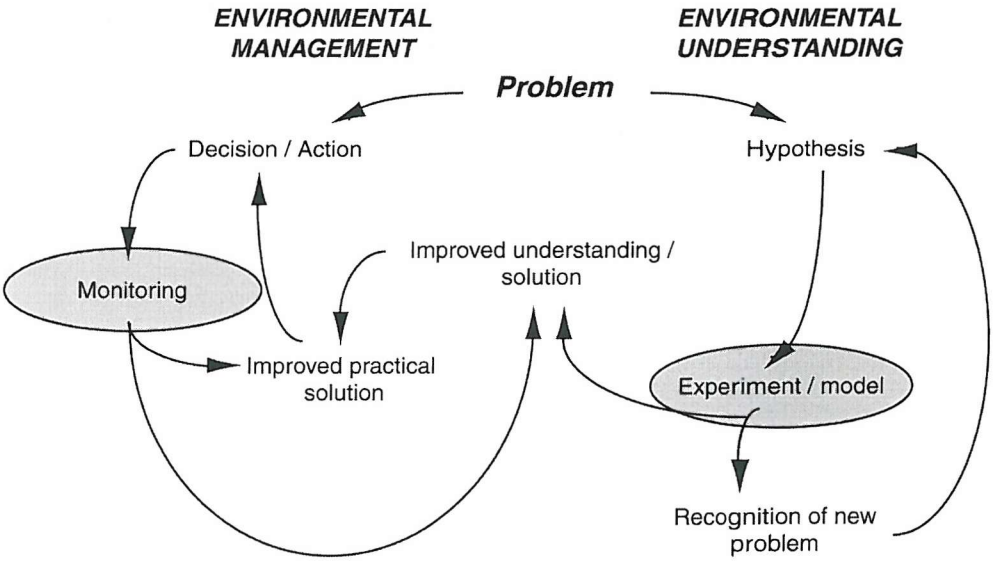

Figure 9.2 The important rôles of modelling and monitoring in the interactive relationship between environmental understanding and environmental management (adapted from Landsberg and Gower 1997).

9.4 Conclusion

Uncertainties still exist surrounding the nature and magnitude of various feedbacks and the total response of the boreal forest ecosystem to the effects of climate change (Coops 1999). In particular, progress is hampered by uncertainty about the effects of climate change that must be understood in the context of natural variability, as well as changes induced by human activities. In part this has been due to the sheer complexity of the issue and the state of the science in impact assessment that is less well developed than in climate change modelling (Parry *et al.* 1999). However, regional scale investigations such as that within this thesis are essential to increase (i) the accuracy of estimates and (ii) understanding of biosphere-atmosphere interaction.

Indeed, driving FOREST-BGC with accurate spatial estimates of LAI derived from remotely sensed data is a powerful tool with which to gain a quantitative understanding of current and future biogeochemical cycling through the boreal forest ecosystem. Such integrated regional studies, by enabling a connection of the global with the local while avoiding confronting directly internal national issues and associated political questions and motivations, would provide essential predictive tools to facilitate policy and management decisions in a changing environment.

Appendix A

The following flow diagram outlines the procedure to split the full radiation in MIR wavelengths into its reflected and emitted components (definitions overleaf).

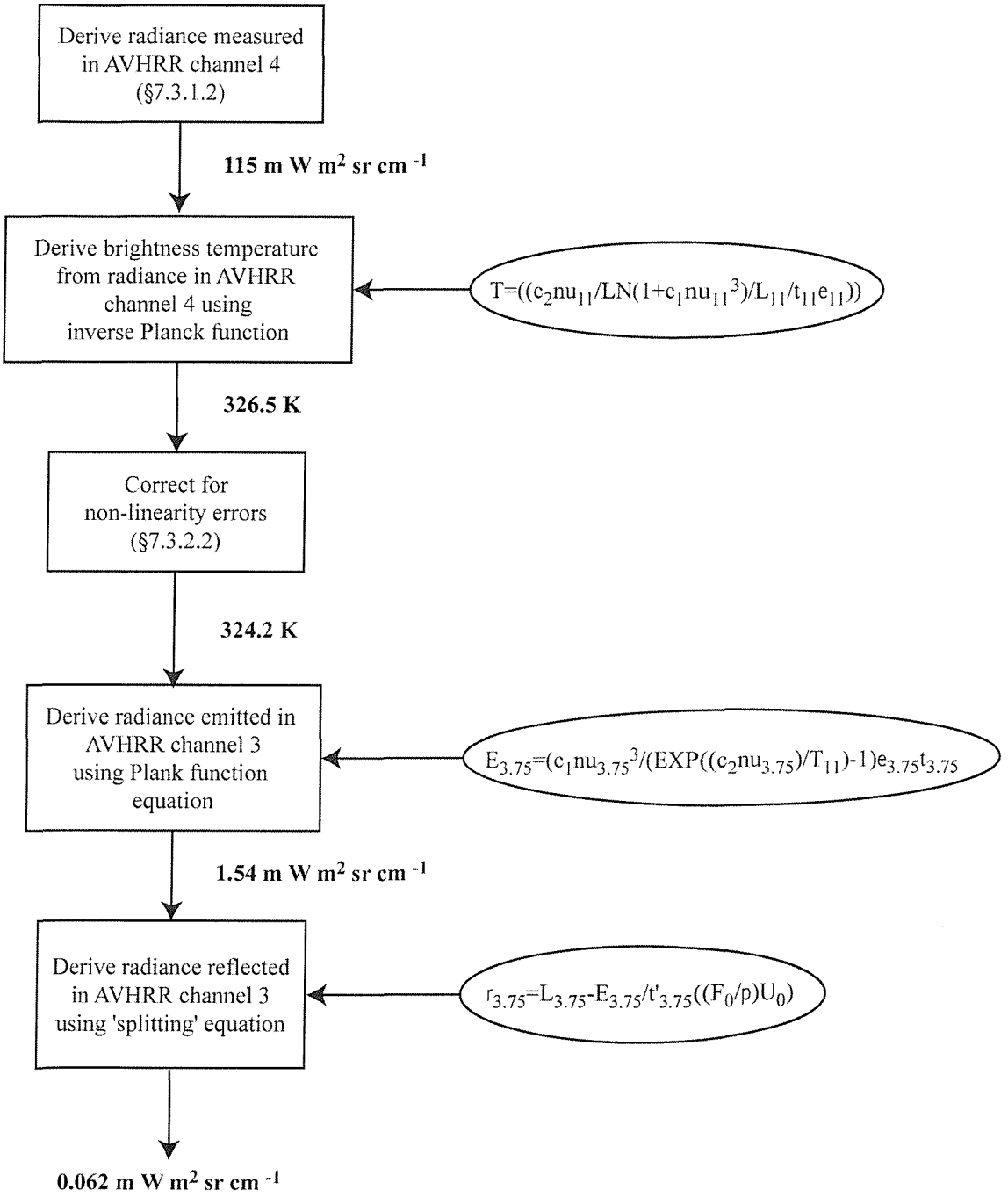

Figure A1 Splitting process flow diagram (adapted from Boyd 1996).

For the purpose of this study, the solar flux in channel 3 (F_0/π) was assumed to be 5.26 mW m^2 sr cm^{-1}; the cosine of the solar zenith angle (U_0) was computed from the orbital characteristics appended to the image (for this example 0.866 was used); the one-way atmospheric transmission (t) in channels 3 and 4 as being 0.93 and 0.92 respectively; the two-way atmospheric transmission (t') in channel 3 to be 0.92; the emissivity (ε) in channels 3 and 4 to be 1.0, the full radiation in channel 3 ($L_{3.75}$) calculated from Kidwell (1991) (for this example 1.8 was used) and the channel frequency (nu) to be 1/wavelength) (i.e., channel 3 = 2667 cm^{-1} and channel 4 = 909.18 cm^{-1}).

Appendix B

1. Source code for 'PROCESS':

```
#!/usr/bin/perl

# process
# version very early!
# written tew and djb 26-8-99

# 13-10-99 added command line argument
#          re-named command process
#          looped through all available files


$val = pack("l",0x41424344);

if ($val eq "ABCD") {
      # a big-endian machine - no need to swap
      $swap = 0;
} elsif ($val eq "DCBA") {
        # a little-endian machine - need to swap bytes
      $swap = 1;
} else {
      # bizarre doesn't believe in ascii codes
      print "This machine doesn't understand ascii!";
      exit;
};

# number of variables (per year) recorded
$NumVars = 1;

if (@ARGV != 1) {
          print "\n";
          print "Usage: process <rootname> \n";
          print "\n";
} else {

      # process rootname - strip out junk
      $rootname = @ARGV[0];
        $rootname =~ s/\s.*//;

      $counter = 1;
      # for each file read in

      $filename = $rootname .  "_" .$counter . ".annout";

      if (-e $filename) {
            while (-e $filename) {
                  #read in data from file 4 bytes at a time
                  #again I KNOW this a priori - how to get this info
on the fly?
                  print "Reading file: $filename \n\n";

                  open(BINFILE,$filename);
```

```
                    $readcount = read(BINFILE, $buf, 4);
                    $varcount  = 0;

                          while ($readcount == 4) {
                          if ($swap) {
                                $buf=reverse($buf);
                          }
                          $vars[$varcount] = unpack('f',$buf);
                          $readcount = read(BINFILE, $buf, 4);
                          $varcount++;
                          };
                    close(BINFILE);

                    # use first loop to get num years
                    if ($counter==1) {
                                $NumYrs    = int($varcount / $NumVars);
                                if  ($NumYrs != $varcount / $NumVars) {
                                print "Bad file length\n";
                                exit;
                          };
                    # check to see if this rootname has already been
used
                    # don't want to overwrite files!!

                          $outname = $rootname . ".yr1";
                          if (-e $outname) {
                                #quit file exists
                                print "Processed files already exist for
\"$rootname\" - exiting\n\n";
                                exit;
                          };

                    };

                          if  ($NumYrs != $varcount / $NumVars) {
                                print "Bad file length - $filename
\n";
                                exit;
                          };

                    # now open output files and send off the data...

                    $count = 0;
                    while ($count < $NumYrs) {
                          $outname = $rootname . ".yr" . ($count+1);
                                open(OUT,">>" .  $outname) || die
"cannot open \"$outname\" file";
                                $index=$count * $NumVars;
                                print OUT "[",$count+1,"] ";
                                $loop=0;
                                while ($loop < $NumVars) {
                                      print OUT "(",$loop+1,")
",@vars[$index+$loop], " ";
                                      print OUT @vars[$index+$loop],
" ";
                                      $loop++;
                                };
                                print OUT "\n";
                          close(OUT);
                          $count++;
```

```
                    };

                print "read $NumVars variables for $NumYrs years\n";
                $counter++;
                $filename = $rootname .  "_" .$counter . ".annout";

        };
    } else {
        print "$filename doesn't exist\n";

        };
    };
```

2. Source code for 'RUN CODE'

```
#!/usr/bin/perl

# runcode <filename>
# version very early!
# written tew and djb 24-8-99
#
# builds initialisation files for pointbgc code and then runs code.
# initialisation files  based on a template file that is assumed to
# be in "examples/infiles" along with the "grid.asc" file that
# supplies updated values for *.ini files

# define base directories to work from
$base_dir = "/usr/local/perws/toby/biome/pointbgc_v4.1/examples/";
$in_dir = $base_dir . "inifiles/";
$out_dir = $base_dir . "outputs/350/";
$bin_dir = $base_dir;
substr($bin_dir,-9,9)="bin/";


if (@ARGV){

    # check correct number of parameters
      if (@ARGV > 1) {
        print "\n";
        print "Too many command line variables\n";
        print "\n";
        print "Usage: runcode <filename> \n";
        print "\n";
        exit;
      };

    # read template file into variable tlines

    open(TEMPLATE,$in_dir . 'template.ini') || die "Couldn\'t open
template file";

    $counter = 0;

    while ($tlines[$counter] = <TEMPLATE>) {

    # check for lat
        if ( index($tlines[$counter],'latitude',0) > 0) {
```

```
            $line_lat = $counter;
        # check for leaf carbon
            } elsif ( index($tlines[$counter],'leaf carbon',0) > 0) {
               $line_lai = $counter;
        # check for elevation
            } elsif ( index($tlines[$counter],'elevation',0) > 0) {
               $line_ele = $counter;
        # check for output
            } elsif ( index($tlines[$counter],'output files',0) > 0) {
               $line_out = $counter;
           };

        # increment counter and around we go again
           $counter++;
        };

        close(TEMPLATE);

        #check that necessary lines have been found

        die "Did not find \"latitude\" in template file" if ($line_lat
== undef);
        die "Did not find \"leaf carbon\" in template file" if
($line_lai == undef);
        die "Did not find \"elevation\" in template file" if ($line_ele
== undef);
        die "Did not find \"output files\" in template file" if
($line_out == undef);


        # template file OK now read "control file"

        open(CNTRL, $in_dir . 'grid.asc') || die "Couldn\'t open
\"grid_polys.asc\" ";

        #we start at line 1 on cntrl file

        $counter = 1;

        #read line
        while ($line = <CNTRL>) {

        #process line to get values
              @vars = split(/\s/,$line);
              $lat = @vars[0];
              $lai = @vars[1];
              $ele = @vars[2];

              #process values into fixed length strings

              $lat_string = sprintf("%-10.3f",$lat);
              $lai_string = sprintf("%-10.3f",$lai);
                    $ele_string = sprintf("%-10.3f",$ele);

              # process the ouptut file string from the calling
parameter
              $out_string = @ARGV[0];
              #strip of the junk from end of line
                  chop ($_out_string);
                  $out_string =~ s/\s.*//;
              #now add the counter to filename
```

```
            #$out_string = $out_string . "_" . $counter;
           #use same base for initialisation file
           $ini_string = $out_string . "\.ini";
            $out_string = $out_dir . $out_string . "_" . $counter;

           #now create ini file from template replacing values as
necessary

           # update latitude value
                substr($tlines[$line_lat],0,10) = $lat_string;

           # update leaf carbon value
           substr($tlines[$line_lai],0,10) = $lai_string;

           # update elevation value
           substr($tlines[$line_ele],0,10) = $ele_string;

           # update output value - including comment for completeness
              # do this line by wholesale replacement rather than
substitution
           $tlines[$line_out] = $out_string . "    (text) prefix for
output files\n";

           # done all substitutions now output

           # create ini file from template replacing values as
necessary

              open(INI,">" . $in_dir . $ini_string) || die "cannot
create \"$ini_string\" file" ;

           $line_counter = 0;
           while ($tlines[$line_counter]) {
            print INI $tlines[$line_counter];
            $line_counter++;
           };

              #close initialisation file
           close(INI);

           # build up the command line string to run the model for
current point
              $run_string = $bin_dir . "pointbgc " . $in_dir .
$ini_string ;
              # and run
           system($run_string);

           #increment counter and go around again
           $counter++;
     };

     close(CNTRL);
} else {
#no parameters passed
  print "\n";
  print "Usage: runcode <filename> \n";
  print "\n";
};
```

Bibliographic references

Aber, J.D. and Federer, C.A., 1992, A generalised, lumped-parameter model of photosynthesis, evapotranspiration and net primary production in temperate and boreal forest ecosystems. *Ocecologia,* **92**: 463–464.

Aber, J.D., Driscoll, C., Federer, C.A., Lathrop, R., Lovett, G., Melillo, J.M., Steudler, P. and Vogelmann, J., 1993, A system for the regional analysis of the effects of physical and chemical climate change on biogeochemical cycles in north-eastern (U.S.) forests. *Ecological Modelling,* **67**: 37–47.

Agbu, P.A., 1993, *Pathfinder AVHRR Land Data Set, Documentation, Product Description and User's Guide.* NASA Goddard Distribution Active Archive Centre (DAAC) Earth Observing System Data Information System (EOSDIS), Washington DC.

Ahern, F., Erdle, T., MacLean, D.A. and Kneppeck, I.D., 1991, A quantitative relationship between Landsat TM spectral response and forest growth rates. *International Journal of Remote Sensing*, **12**: 387–400.

Anderson, M.C., 1964, Studies of the woodland light climate 1: The photographic computation of light condition. *Journal of Ecology*, **52**: 27–41.

Anderson, M.C., 1971, Radiation and crop structure. In Sestak, Z., Catsky, J. and Jarvis, P.G. (eds.), *Plant Photosynthetic Production Manual of Methods.* Junk, Hague: 77–90.

Anselin, L. and Griffith, D.A., 1988, Do spatial effects really matter in regression analysis? *Papers of the Regional Science Association*, **65**: 11–34.

Aplin, P., 1999, *Fine Spatial Resolution Satellite Sensor Imagery for Per-Field Land Cover Classification.* Unpublished Ph.D. Thesis, University of Southampton, Southampton.

Aplin, P., Atkinson, P.M. and Curran, P.J., 1997, Using the spectral properties of fine spatial resolution satellite sensor imagery for national land cover and land use mapping. *Proceedings of the Seventh International Symposium on Physical Measurements and Signatures in Remote Sensing*, Balkema, Rotterdam: 661–668,

Aplin, P., Atkinson, P.M. and Curran, P.J., 1999, Fine spatial resolution satellite sensor imagery for land cover mapping in the UK. *Remote Sensing of Environment*, **68**: 206–216.

Apps, M.J., Kurz, W.A., Luxmoore, R.J., Nilsson, L.O., Sedjo, R.A., Schmidt, R., Simpson, L.G. and Vinson, T.S., 1993, Boreal forests and tundra. *Water, Air and Soil Pollution*, **70**: 39–53.

Apps, M.J. and Price, D.T. (eds.), 1996, *Forest Ecosystems, Forest Management and the Global Carbon Cycle.* NATO ASI Series. I: Global Environmental Change. Edmonton, Canada, **40**: 454–455.

Asrar, G., Fuchs, M., Kanemasu, E.T. and Hatfield, J.L., 1984, Estimating absorbed photosynthetic radiation and leaf area index from spectral reflectance in wheat. *Agronomics Journal*, **76**: 300–306.

Asrar, G., Kanemasu, E., Jackson, R. and Pinter, P., 1985, Estimation of total aboveground phytomass production using remotely sensed data. *Remote Sensing of Environment*, **41**: 45–60.

Asrar, G., Tilford, S.G. and Butler, D.M., 1992, Mission to Planet Earth: Earth Observing System. *Palaeogeography, Palaeoclimatology, Palaeoecology,* **98**: 3–8.

Atkinson, P.M., 1991, Optimal ground-based sampling for remote sensing investigations: Estimating the regional mean. *International Journal of Remote Sensing*, **12**: 559–567.

Atkinson, P.M., 1993, The effect of spatial resolution on the experimental variogram of airborne MSS imagery. *International Journal of Remote Sensing*, **14**: 1005–1001

Atkinson, P.M., 1999, Geographical information science: Geostatistics and uncertainty. *Progress in Physical Geography*, **23**: 134–142.

Atkinson, P.M., Curran, P.J. and Webster, R., 1990, Sampling remotely sensed imagery for storage, retrieval and reconstruction. *Professional Geographer*, **42**: 345–352.

Atkinson, P.M., Curran, P.J. and Webster, R., 1992, Co-kriging with ground-based radiometry. *Remote Sensing of Environment*, **41**: 45–60.

Atkinson, P.M., Webster, R. and Curran, P.J., 1994, Cokriging with airborne MSS imagery. *Remote Sensing of Environment*, **50**: 335–345.

Atkinson, P.M. and Curran, P.J., 1995, Defining an optimal size of support for remote sensing investigations. *IEEE Transactions on Geoscience and Remote Sensing*, **33**: 768–776.

Atkinson, P.M. and Curran, P.J., 1997, Choosing an appropriate spatial resolution for remote sensing investigations. *Photogrammetric Engineering and Remote Sensing*, **63**: 1345–1351.

Atkinson, P.M. and Tatnall, A.R.L., 1997, Neural networks in remote sensing. *International Journal of remote Sensing*, **18**: 699–709.

Atkinson, P.M. and Emery, D.R., 1999, Exploring the relation between spatial structure and wavelength: Implications for sampling reflectance in the field. *International Journal of Remote Sensing*, **20**: 2663–2678.

Atkinson, P.M. and Martin, D.J., 1999, Investigating the effect of support size on population surface models. *Geographical and Environmental Modelling*, **3**: 101–119.

Avery, T.E. and Berlin, G.L., 1985, *Fundamentals of Remote Sensing and Airphoto Interpretation.* Macmillan, New York.

Avissar, R. and Verstraete, M., 1990, The representation of continual surface processes in atmospheric models. *Reviews of Geophysics*, **28**: 35–52.

Badhwar, G.D., Macdonald, R.B., Hall, F.G. and Carnes, J.G., 1986, Spectral characteristics of biophysical characteristics in a boreal forest: Relationship between Thematic Mapper band reflectance and leaf area index for aspen. *IEEE Transactions on Geoscience and Remote Sensing*, **24**: 322–326.

Bailey, P., 1997, *Exploring Remotely Sensed Shadow in Amazonian Regrowth Forests.* Unpublished Ph.D. Thesis, University of Southampton, Southampton.

Baldocchi, D.D., Vogel, C.A. and Hall, B., 1996, Seasonal variation of carbon dioxide exchange rates above and below a boreal jack pine forest. *Agricultural and Forest Meteorology*, **83**: 147–170.

Band, L.E., Peterson, D.L., Running, S.W., Coughlan, J., Lammers, R., Dungan, J. and Nemani, R., 1991, Forest ecosystem processes at the watershed scale: Basis for distributed simulation. *Ecological Modelling,* **56**: 171–196.

Band, L.E., Patterson, P., Nemani, R.R. and Running, S.W., 1993, Forest ecosystem processes at the watershed scale: Incorporating hillslope hydrology. *Agricultural and Forest Meteorology,* **63**: 93–126.

Banninger, C., 1991, Phenological changes in the red edge shift of Norway spruce needles and their relationship to needle chlorophyll content. *Proceedings of the 5th International Colloquium - Physical Measurements and Signatures in Remote Sensing*. ESA, Noordwijk: 155–158.

Banwell, C.N., 1983, *Fundamentals of Molecular Spectroscopy*. McGraw-Hill, London.

Baret, F. and Guyot, G., 1991, Potentials and limits of vegetation indices for LAI and APAR assessment. *Remote Sensing of Environment*, **35**: 161–173.

Baret, F., Jacquemoud, S., Guyot, G. and Leprieur, C., 1992, Modelled analysis of the biophysical nature of spectral shifts and comparison with information content of broad bands. *Remote Sensing of Environment*, **41**: 133–142.

Barrett, E.C. and Curtis, L.F., 1999, *Introduction to Environmental Remote Sensing* (fourth edition). Stanley Thornes, Cheltenham.

Bastin, G., Lorent, B., Duque C. and Gevers, M., 1984, Optimal estimation of the average areal rainfall and optimal selection of rain gauge locations. *Water Resources Research*, **20**: 463–470.

Bazzaz, F.A., Basssow, S.L., Berntson, G.M. and Thomas, S.C., 1996, Elevated CO_2 and terrestrial vegetation: Implications for and beyond the global carbon budget. In Walker, B. and Steffen, W. (eds.), *Global Change and Terrestrial Ecosystems*. Cambridge University Press, Cambridge: 43–76.

Becker, P., Erhart, D.W. and Smith, A.P., 1989, Analysis of forest light environments.1. Computerised estimation of solar-radiation from hemispherical canopy photographs. *Agricultural and Forest Meteorology*, **44**: 217–232.

Beerling, D.J., 1999, Long-term responses of boreal vegetation to global change: an experimental and modelling investigation. *Global Change Biology*, **5**: 55–74.

Belward, A.S., 1992, Spatial attributes of AVHRR for environmental monitoring. *International Journal of Remote Sensing*, **13**: 193–208.

Bender, M.E., Taylor, E., Tans, P., Francey, R. and Lowe, D., 1996, Variability in the N_2/O_2 ratio of southern hemisphere air, 1991-1994: Implications for the carbon cycle. *Global Biogeochemical Cycles*, **10**: 9–21.

Bian, L. and Butler, R., 1999, Comparing effects of aggregation methods on statistical and spatial properties of simulated spatial data. *Photogrammetric Engineering and Remote Sensing*, **65**: 73–84.

Biging, G.S., Congalton, R.G. and Murphy, E.C., 1992, A comparison of photo-interpretation and ground measurements of forest structure. *Proceedings, ASPRS Annual Meeting*, ASPRS, Bethesda, MD, **3**: 6–15.

Billings, W.D. and Mooney, H.A., 1968, The ecology of arctic and alpine plants. *Biological Review*, **48**: 481–529.

Binkley, D. and Arthur, M., 1993, How to count dead trees. *Bulletin of the Ecological Society of America*, **74**: 15–16.

Blackburn, G.A. and Milton, E.J., 1997, An ecological survey of deciduous woodlands using airborne remote sensing and geographical information systems (GIS). *International Journal of Remote Sensing*, **18**: 1919–1935.

Blackman, F.F., 1905, Optima and limiting factors. *Annals of Botany*, **14**: 281–295.

Blakemore, M., 1984, Generalisation and error in spatial databases, *Cartographica*. **21**:131–139.

Bliss, L.C. and Matveyeva, N.V., 1992, Flora of Alaska and neighbouring territories. In Chapin, F.S., Jefferies, R.L., Reynolds, J.F., Shaver, G.R., Svboda, J. and Chu, E.W. (eds.), *Arctic Ecosystems in a Changing Climate: an Eco-physiological Perspective*. Academic Press, New York: 59–89.

Bolle, H.J., Andre, J.C. and Arrue, J.L., 1993, EFEDA: European field experiment in a desertification threatened area. *Annals of the Geophysical Union*, **2**: 173–189.

Bonan, G.B., 1992, Physiological controls of the carbon balance of boreal forest ecosystems. *Canadian Journal of Forest Research*, **23**: 1453–1471.

Bonan, G.B., 1993, Importance of LAI and forest type when estimating photosynthesis in boreal forests. *Remote Sensing of Environment*, **43**: 303–314.

Bonan, G.B., 1995, Land-atmosphere interactions for climate system models: Coupling biophysical, biogeochemical and ecosystem dynamical processes. *Remote Sensing of Environment*, **51**: 57–73.

Bonan, G.B., Pollard, D. and Thompson, S.L., 1992, Effects of boreal forest vegetation on climate. *Nature*, **359**: 716–718.

Bonan, G.B., Chapin, F.S. and Thompson, S.L., 1995, Boreal forest and tundra ecosystems as components of the climate system. *Climatic Change*, **29**: 145–167.

Bonham-Carter, G.F., 1988, Numerical procedures and computer program for fitting an inverted Gaussian model to vegetation reflectance data. *Computers and Geosciences*, **11**: 339–356.

Bonhomme, R. and Chartier, P., 1972, The interpretation and automatic measurement of hemispherical photographs to obtain sunlit foliage area and gap frequency. *Journal of Agricultural Research*, **22**: 53–61.

Boochs, F., Kupfer, G., Dockter, K. and Ühbauch, W., 1990, Shape of the red edge as vitality indicator for plants. *International Journal of Remote Sensing*, **11**: 1741–1753.

BOREAS Science Team, 1993, *Boreal Ecosystem-Atmosphere Study, Experiment Plan.* Version 1, NASA/GSFC.

BOREAS Science Team, 1996, *Boreal Ecosystem-Atmosphere Study, 1996 Experiment Plan.* Version 2, NASA/GSFC.

Borrough, P., 1987, Multiple sources of spatial variation and how to deal with them. *AUTO-CARTO*, **8**: 145–154.

Bossel, H., 1991, Modelling forest dynamics: Moving from description to explanation. *Forest Ecology and Management,* **42**: 129–142.

Boyd, D.S., 1996, *Estimating the Biophysical Properties of Tropical Forests: The Rôle of Middle Infrared Radiation (1.5-5.0 μm).* Unpublished Ph.D. Thesis, University of Southampton, Southampton.

Boyd, D.S., Foody, G.M., Curran, P.J., Lucas, R.M, and Honzák, M., 1996, An assessment of radiance in Landsat TM middle and thermal infrared wavebands for the detection of tropical forest regeneration. *International Journal of Remote Sensing,* **17**: 249–261.

Boyd, D.S. and Ripple, W.J., 1997, Potential vegetation indices for determining global forest cover. *International Journal of Remote Sensing*, **18**: 1395–1410.

Boyd, D.S. and Curran, P.J., 1998, Using remote sensing to reduce uncertainties in the global carbon budget: The potential of radiation acquired in middle infrared wavelengths. *Remote Sensing Reviews*, **16**: 293–327.

Boyd, D.S., Foody, G.M. and Curran, P.J., 1999, The relationship between the biomass of Cameroonian tropical forests and radiation reflected in middle infrared wavelengths (3.0 – 5.0 μm). *International Journal of Remote Sensing*, **20**: 912–920.

Boyd, D.S., Wicks, T.E. and Curran, P.J., 2000, Use of middle infrared radiation to estimate the leaf area index of a boreal forest. *Tree Physiology*, (In press).

Brass, J.A., Ambrosia, V.G. and Higgins, R., 1996. AIRDAS development of a unique four channel scanner for disaster assessment and management. *Proceedings of the 2nd International Airborne Remote Sensing Conference*. Environmental Research Institute of Michigan, Ann Arbor, Michigan: 781–787.

Brest, C. and Rossow, W.R., 1992, Radiometric calibration and monitoring of NOAA AVHRR data for ISCCP. *International Journal of Remote Sensing,* **13**: 235–273.

Briggs, D.J., Ashmore, M., Bell, M. and McClatchey, J., 1999, Effects of traffic management on air pollution and human exposure: The NAPS project. *Epedimiology*, **10**: 375–379.

Briggs, D.J., Collins, S., Elliot, P., Fischer, P., Kingham, S., Lebret, E., Pryl, K., Van Trruwijk, H., Smallbone, K. and Van Der Veen, A., 1997, Mapping urban air pollution using GIS: A regression-based approach. *International Journal of Geographical Information Science*, **11**: 699–718.

Briggs, S.A., 1991, *The Relevance of Future Earth Observation System Options to Terrestrial Science.* Unpublished notes from the Remote Sensing Development Unit, NERC, Monks Wood.

Brown, D.G., Duh, J.D. and Drzyzga, S.A., 2000, Estimating error in an analysis of forest fragmentation change using North American Landscape Characterization (NALC) data. *Remote Sensing of Environment*, **71**: 106–117.

Brown, J.W., Brown, O.B. and Evans, R.H., 1985, Calibration of Advanced Very High Resolution Radiometer infrared observations. *Journal of Geophysical Research*, **90**: 11667–11677.

Brown, J.W., Brown, O.B. and Evans, R.H., 1993, Calibration of Advanced Very High Resolution Radiometer infrared channels: a new approach. *Journal of Geophysical Research*, **98**: 18257–18268.

Brown, R.J.E. and Péwé, T.L., 1973, Distribution of permafrost in North America and its relationship to the environment: A review, 1963–1973. *Permafrost, the North American Contribution to the Second International Conference*, Siberia, USSR. National Academy of Sciences, Washington D.C.: 71–100.

Brown, S., Hall, C.A., Knabe, W., Raich, J., Trexler, M.C. and Woomer, P., 1993, Tropical forests: Their past, present and potential future role in the terrestrial carbon budget. *Water, Air and Soil Pollution*, **70**: 71–94.

Brumbley, C. and Chang, C.I., 1999, An unsupervised vector quantization-based target subspace projection approach to mixed pixel detection and classification in unknown background for remotely sensed imagery. *Pattern Recognition*, **32**: 1161–1174.

Brunsdon, C., Aitkin, M., Fotheringham, S. and Charlton, M., 1999, A comparison of random coefficient modelling and geographically weighted regression for spatially non-stationary regression problems. *Geographical and Environmental Modelling*, **3**: 47–62.

Brunsdon, C., Fotheringham, A. and Charlton, M., 1996, Geographically weighted regression: A method for exploring spatial nonstationarity. *Geographical Analysis*, **28**: 281–289.

Brutsaert, W., 1988, *Evaporation into the Atmosphere.* Reidel, Dordrecht.

Burke, I.C., Schimel, D.S., Yonker, C.M., Parton, W.J., Joyce, L.A. and Lauenroth, W.K., 1990, Regional modelling of grassland biochemistry using GIS. *Landscape Ecology*, **4**: 45–54.

Burke, R.A., Zepp, R.G., Tarr, M.A., Miller, W.L. and Stocks, B.J., 1997, Effect of fire on soil-atmosphere exchange of methane and carbon dioxide in Canadian boreal forest sites. *Journal of Geophysical Research*, **102**: 29289–29300.

Calow, P., (ed.), 1998, *The Encyclopaedia of Ecology and Environmental Management.* Blackwell, Oxford.

Campbell, J.B. and Browder, J.O., 1995, Field data collection for remote sensing analysis, SPOT data, Rondonia, Brazil. *International Journal of Remote Sensing*, **16**: 333–350.

Canadian Forest Service, 1999, *The State of Canada's Forests.* Natural Resources Canada, Ottawa.

Carter, G.A., Cibula, W.G. and Miller, R.L., 1996, Narrow-band reflectance imagery compared with thermal imagery for early detection of plant stress. *Journal of Plant Physiology*, **148**: 515–522.

Carver, S.J. and C.F. Brunsdon, 1994, Vector to raster conversion error and feature complexity: an empirical study using simulated data. *International Journal of Geographical Information Systems*, **8**: 261–270.

Catlow, D.R., Parsell, R.J. and Wyatt, B.K., 1984, The integrated use of digital cartographic data and remotely sensed imagery. *Earth Orientation Applications in Space Technology*, **4**: 255–260.

Ceulemans, R. and Mousseau, M., 1994, Effects of elevated atmospheric CO_2 on woody plants. *New Phytologist*, **127**: 425–446.

Chang, S.H. and Collins, W., 1983, Confirmation of the airborne biogeophysical mineral exploration technique using laboratory methods. *Economic Geology and the Bulletin of the Society of Economic Geologists*, **78**: 723–736.

Chappelle, E.W., Moon, S.K. and McMurtrey, J.E., 1992, Ratio analysis of reflectance spectra (RARS): An algorithm for the remote estimation of the concentrations of chlorophyll a, chlorophyll b and carotenoids in soybean leaves. *Remote Sensing of Environment*, **39**: 239–247.

Chase, T.N., Pielk, R.A., Kittel, T.G.F, Nemani, R. and Running, S.W., 1996, Sensitivity of a general-circulation model to global changes in leaf area index. *Journal of Geophysical Research*, **101**: 7393–7408.

Chazdon, R.L. and Field, C.B., 1987, Photographic estimation of photosynthetically active radiation: Evaluation of a computerised technique. *Oecologia*, **73**: 525–532.

Che, N. and Price, J.C., 1992, Survey of radiometric calibration results and methods for visible and near-infrared channels of NOAA-7, -9 and -11 AVHRRs. *Remote Sensing of Environment*, **41**: 19–27.

Chen, J.M., 1996a, Optically-based methods for measuring seasonal variation of leaf area index in boreal conifer stands. *Agricultural Forest Meteorology*, **80**: 135–163.

Chen, J.M., 1996b, Evaluation of vegetation indices and a modified simple ratio for boreal applications. *Canadian Journal of Remote Sensing*, **22**: 229–241.

Chen, J.M., 1999, Spatial scaling of a remotely sensed surface parameter by contexture. *Remote Sensing of Environment*, **69:** 30–42.

Chen, J.M., Black, T.A. and Adams, R.S., 1991, Evaluation of hemispherical photography for determining plant area index and geometry of a forest stand. *Agricultural and Forest Meteorology*, **56**: 129–143.

Chen, J.M. and Black, T.A., 1992a, Defining leaf area index for non-flat leaves. *Plant Cell and Environment*, **15**: 421–429.

Chen, J.M. and Black, T.A., 1992b, Foliage area and architecture of plant canopies from sunfleck size distributions. *Agricultural and Forest Meteorology*, **60**: 249–266.

Chen, J.M. and Cihlar, J., 1995a, Plant canopy gap size analysis theory for improving optical measurements of leaf area index of plant canopies. *Applied Optics*, **34**: 6211–6222.

Chen, J.M. and Cihlar, J., 1995b, Quantifying the effect of canopy architecture on optical measurements of leaf area index using two gap size analysis methods. *IEEE Transactions on Geosciences and Remote Sensing*, **33**: 777–787.

Chen, J.M. and Cihlar, J., 1996, Retrieving leaf area index of boreal conifer forests using Landsat TM images. *Remote Sensing of Environment*, **55**: 153–162.

Chen, J.M. and Cihlar, J., 1997, A hotspot function in a simple bi-directional reflectance model for satellite applications. *Journal of Geophysical Research*, **102**: 25907–25913.

Chen, J.M., Rich, P.M., Gower, S.T., Norman, J.M. and Plummer, S., 1997, Leaf area index of boreal forests: Theory, techniques, and measurements. *Journal of Geophysical Research*, **102**: 29429–29444.

Chen, W.J., Black, T.A., Yang, P.C., Barr, A.G., Neumann, H.H., Nesic, Z., Blanken, P.D., Novak, M.D., Eley, J., Ketler, R.J. and Cuenca, R., 1999, Effects of climatic variability on the annual carbon sequestration by a boreal aspen forest. *Global Change Biology*, **5**: 41–53.

Chrisman, N.R., 1987, The accuracy of map overlays: A reassessment. *Landscape and Urban Planning*, **14**: 427–439.

Christakos, G., 1992, *Random Field Modelling in Earth Sciences*. Academic Press, New York.

Christakos, G. and Panagopoulos, C., 1992, Space transformation methods in the representation of geophysical random fields. *IEEE Transactions on Geoscience and Remote Sensing*, **30**: 55–70.

Ciais, P., Tans, P.P., White, J.W., Trolier, M., Francey, R.J., Berry, J.A. and Randall, D.R., 1995, Partitioning of ocean and land uptake of CO_2 as inferred by δ13C measurements from NOAA Climate Monitoring and Diagnostics Laboratory Global Air Sampling Network. *Journal of Geophysical Research*, **100**: 5051–5070.

Cienciala, E. and Lindroth, A., 1995, Gas-exchange and sap flow measurements of *Salix viminalis* trees in short-rotation forest. II. Diurnal and seasonal variations of stomatal response and water use efficiency. *Trees, Structure and Function*, **9**: 295–301.

Cienciala, E., Running, S.W., Lindroth, A., Grelle, A. and Ryan, M.G., 1998, Analysis of carbon and water fluxes from the NOPEX boreal forest: Comparison of measurements with FOREST-BGC simulations. *Journal of Hydrology*, **213**: 62–78.

Cihlar, J. and Teillet, P.M., 1995, Forward piecewise linear model for quasi-real time processing of AVHRR data. *Canadian Journal of Remote Sensing*, **21**: 22–27.

Cihlar, J., Chen, J. and Li, Z., 1998, Seasonal AVHRR multichannel data sets and products for studies of surface-atmosphere interactions. *Journal of Geophysical Research*, **102**: 29625–29640.

Clevers, J.G., Büker, C., van Leeuwen, H.J. and Bouman, B.A., 1994, A framework for monitoring crop growth by combining directional and spectral remote sensing information. *Remote Sensing of Environment*, **50**: 161–170.

Cloutis, E.A., Connery, D.R., Major, D.J. and Dover, F.J., 1996, Airborne multi-spectral monitoring of agricultural crop status: Effect of time of year, crop type and crop condition parameter. *International Journal of Remote Sensing*, **17**: 2579–2601.

Cochran, W.G., 1977, *Sampling Techniques*. Wiley, New York.

Cohen, W.B. and Justice, C.O., 1999, Validating MODIS Terrestrial Ecology products: Linking *in situ* and satellite measurements. *Remote Sensing of Environment*, **70**: 1–3.

Collinson, A.S., 1988, *Introduction to World Vegetation* (second edition). Unwin, London.

Colwell, J.E., 1974, Grass canopy bidirectional spectral reflectance. *Proceedings of the 9th International Symposium on Remote Sensing of Environment*. University of Michigan, Ann Arbor: 1061–1085.

Congalton, R.G., 1997, Exploring and evaluating the consequences of vector-to-raster and raster-to-vector conversion. *Photogrammetric Engineering and Remote Sensing*, **59**: 641–644.

Congalton, R.G., Balogh, M., Bell, C., Green, K., Milliken, J.A. and Ottman, R., 1998, Mapping and monitoring agricultural crops and other land cover in the Lower Colorado River Basin. *Photogrammetric Engineering and Remote Sensing*, **64**: 1107–1113.

Coops, N., 1999, Improvement in predicting stand growth of *Pinus radiata* across landscapes using NOAA AVHRR and Landsat MSS imagery combined with a forest growth process model (3-PGS). *Photogrammetric Engineering and Remote Sensing*, **65**: 1149–1156.

Coops, N.C., Waring, R.H. and Landsberg, J.J., 1998, Assessing forest productivity in Australia and New Zealand using a physiologically-based model driven with averaged monthly weather data and satellite derived estimates of canopy photosynthetic capacity. *Forest Ecology and Management*, **104**: 113–127.

Coughlan, J.C. and Running, S.W., 1994, BOREAS Model Inter-comparisons Plan. (http://boreas.gsfc.nasa.gov/).

Cracknell, A.P., 1997, *AVHRR: The Advanced Very High Resolution Radiometer*. Taylor and Francis, London.

Cracknell, A.P., 1999, Twenty years of publication of the *International Journal of Remote Sensing*. *International Journal of Remote Sensing* **20**: 3469–3484.

Craig, R.G. and Labovitz, M.L., 1980, Sources of variation in Landsat autocorrelation. *Proceedings of the 14th International Symposium on Remote Sensing of Environment*. ISRSE, Costa Rica: 1755–1767.

Craig, S.G. and Holmén, K.J., 1995, Uncertainties in future CO_2 projections. *Global Biogeochemical Cycles*, **9**: 139–152.

Cressie, N., 1990, The origins of kriging. *Mathematical Geology*, **22**: 239–252.

Cropper, W.P. and Gholz, H.L., 1991, *Simulation of the Carbon Dynamics of a Florida Slash Pine Plantation*. Department of Forestry, University of Florida, Florida.

Csillag, F., 1997, Quadtrees: Hierarchical multi-resolution data structures for analysis of digital images. In Quattrochi, D.A. and Goodchild, M.F. (eds.), *Scale in Remote Sensing and GIS*. CRC Press, Boca Raton: 247–271.

Csillag, F., Davidson, A., Mitchell, S., Wylie, B., Wedin, D., Peat, H. and Kertész, M., 1996, Subpixel spatiotemporal pattern analysis of remote sensing observations for predicting grassland ecological and biophysical parameters. *IEEE Transactions on Geoscience and Remote Sensing*, **34**: 2377–2379.

Culotta, E., 1995, Will plants benefit from high CO_2? *Science*, **268**: 654–656.

Curran, P.J., 1980, Multispectral remote sensing of vegetation amount. *Progress in Physical Geography*, **4**: 315–341.

Curran, P.J., 1985, *Principles of Remote Sensing*. Longman, Harlow.

Curran, P.J., 1987, Remote sensing methodologies and geography. *International Journal of Remote Sensing*, **8**: 1255–1275.

Curran, P.J., 1988, The semi-variogram in remote sensing: An introduction. *Remote Sensing of Environment*, **3**: 493–507.

Curran, P.J., 1989, Remote sensing of foliar chemistry. *Remote Sensing of Environment*, **30**: 271–278.

Curran, P.J., 1991, *Remote Sensing of Leaf Area Index*. Unpublished notes, Department of Geography, University of Wales Swansea, Swansea.

Curran, P.J., 1993a, *Coupling Remotely Sensed Data to Ecosystem Simulation Models: BOREAS Research Proposal*. NERC, Swindon.

Curran, P.J., 1993b, Earth observation comes of age. *GIS Europe*, **2**: 27–31.

Curran, P.J., 1994a, Attempts to drive ecosystem simulation models at local to regional scales. In Foody, G.M. and Curran, P.J. (eds.), *Environmental Remote Sensing from Regional to Global Scales*. Wiley, Chichester: 149–166.

Curran, P.J., 1994b, Imaging spectrometry. *Progress in Physical Geography*, **18**: 247–266.

Curran, P.J. and Atkinson, P.M., 1998, Geostatistics and remote sensing. *Progress in Physical Geography*, **22**: 61–78.

Curran, P.J. and Williamson, D.H., 1986, Sample size for ground and remotely sensed data. *Remote Sensing of Environment*, **20**: 31–41 .

Curran, P.J. and Williamson, D.H., 1987, Airborne MSS data to estimate GLAI. *International Journal of Remote Sensing*, **8**: 57–74.

Curran, P.J. and Dungan, J.L., 1989, Estimation of signal to noise: A new procedure applied to AVIRIS data. *IEEE Transactions on Geoscience and Remote Sensing*, **27**: 620–628.

Curran, P.J, Dungan, J.L. and Gholz, H.L., 1990, Exploring the relationship between reflectance red edge and chlorophyll content in slash pine. *Tree Physiology*, **7**: 33–48.

Curran, P.J., Dungan, J.L., Macler, B.A. and Plummer, S.E., 1991, The effect of red leaf pigment on the relationship between red edge and chlorophyll concentration. *Remote Sensing of Environment*, **35**: 69–76.

Curran, P.J, Dungan, J.L. and Gholz, H.L., 1992, Seasonal LAI in slash pine estimated with Landsat TM. *Remote Sensing of Environment,* **39**: 3–13.

Curran, P.J. and Plummer, S.E., 1992, Remote sensing of forest productivity. *NERC News,* Swindon, **20**: 22–23.

Curran, P.J. and Foody, G.M., 1994, Environmental issues at regional to global scales. In Foody, G.M. and Curran, P.J. (eds.), *Environmental Remote Sensing from Regional to Global Scales.* Wiley, Chichester: 1–7.

Curran, P.J., Windham, W.R. and Gholz, H.L., 1995, Exploring the relationship between reflectance red edge and chlorophyll concentration in slash pine leaves. *Tree Physiology*, **15**: 203–206.

Curran, P.J. and Kupiec, J.A., 1995, Imaging spectrometry: A new tool for ecology. In Danson, F.M. and Plummer, S.E. (eds.), *Advances in Environmental Remote Sensing.* Wiley, Chichester: 71–88.

Curran, P.J., Foody, G.M., Lucas, R.M., Honzák, M. and Grace, J., 1997, The carbon balance of tropical forests: From the local to the regional scale. In van Gardingen, P.R., Foody, G.M. and Curran, P.J., (eds.), *Scaling-up: From Cell to Landscape*. Cambridge University Press, Cambridge: 201–227.

Curran, P.J. and Atkinson, P.M., 1998, Geostatistics and remote sensing. *Progress in Physical Geography*, **22**: 61–78.

Curran, P.J. and Atkinson, P.M., 1999, Issues of scale and optimal pixel size. In Stein A., van der Meer, F.D. and and Gorte, B. (eds.), *Spatial Statistics in Remote Sensing*. Kluwer, Dordrecht: 115–133.

Cusack, G.A., Hutchinson, M.F. and Kalma, J.D., 1999, Calibrating airborne vegetation data for hydrological applications under dry conditions. *International Journal of Remote Sensing*, **20**: 2221–2233.

Cushnie, J.L., 1987, The interactive effect of spatial resolution and degree of internal variability within land-cover types on classification accuracies. *International Journal of Remote Sensing*, **8**: 15–29.

Cutler, M.E., 1998, *Assessing Variation in the Relationships Between Remotely sensed Data and Canopy Chlorophyll Composition*. Unpublished Ph.D. Thesis, University of Southampton, Southampton.

Daly, C., Neilson, R.P. and Phillips, D.L., 1994, A statistical-topographic model for mapping climatological precipitation over mountainous terrain. *Journal of Applied Meteorology*, **33**: 140–158.

Dang, Q.L., Margolis, H.A., Sy M., Coyea, M.R., Collatz, G.L and Walthall, C.L., 1997, Profiles of PAR, nitrogen and photosynthetic capacity in boreal forest: Implications from scaling from leaf to canopy. *Journal of Geophysical Research*, **102**: 28845–28859.

Danson, F.M., 1995a, Comparison of high spectral resolution indices for estimating forest LAI. *RSS'95, Remote Sensing in Action,* Remote Sensing Society, Nottingham: 450–465.

Danson, F.M., 1995b, Development in the remote sensing of forest canopy structure. In Danson, F.M. and Plummer, S.E. (eds.), *Advances in Environmental Remote Sensing.* Wiley, Chichester: 53–69.

Danson, F.M., Curran, P.J. and Plummer, S.E., 1992, Remotely-sensed inputs to a forest ecosystem model. *Proceedings of the 6th Australasian Conference,* New Zealand Remote Sensing Society, Wellington: 130–139.

Danson, F.M. and Curran, P.J., 1993, Factors affecting the remotely sensed response of coniferous forest plantations. *Remote Sensing of Environment.* **43**: 55–65.

Danson, F.M. and Plummer, S.E. (eds.), 1995a, *Advances in Environmental Remote Sensing*. Wiley, Chichester.

Danson, F.M. and Plummer, S.E., 1995b, Red-edge response to forest leaf area index. *International Journal of Remote Sensing*, **16**: 183–188.

Davis, F.W., Quattrochi, D.A., Ridd, M.K., Lam, N.S.N., Walsh, S.J., Michaelsen, J.C., Franklin, J., Stow, D.A., Johannsen, C.J. and Johnston, C.A., 1991, Environmental analysis using integrated GIS and remotely sensed data: some research needs and priorities. *Photogrammetric Engineering and Remote Sensing*, **57**: 689–697.

Davis, M.B., 1969, Climatic changes in southern Connecticut recorded by deposition at Rogers Lake, *Ecology*, **50**: 409–422.

Dawson, T.P., Curran, P.J. and Plummer, S.E., 1995, Modelling the spectral response of coniferous leaf structures for the estimation of biochemical concentrations. *RSS'95, Remote Sensing in Action,* Remote Sensing Society, Nottingham: 587–594.

Dawson, T.P. and Wicks, T.E., 1998, The carbon cycle in forest ecosystems: Solar radiation and photosynthesis. *RSS '98: Developing International Connections*. Remote Sensing Society, Nottingham: 160–166.

Dawson, T.P., North, P.R.J., Plummer, S.E. and Curran, P.J., 1999a, Estimating photosynthetic activity in vegetation from NDVI: A reanalysis. *RSS '99: Earth Observation, From Data to Information*. Remote Sensing Society, Nottingham: 265–272.

Dawson, T.P., Curran, P.J., North, P.R. and Plummer, S.E., 1999b, The propagation of foliar biochemical absorption features in forest canopy reflectance: A theoretical analysis. *Remote Sensing of Environment*, **67**: 147–159.

Dawson, T.P., North, P.R.J., Plummer, S.E. and Curran, P.J., 2000, Remote sensing estimates of forest carbon sequestration. *Journal of Geophysical Research*, (submitted).

Deering, D.W., 1978, *Rangeland Reflectance Characteristics Measured by Aircraft and Spacecraft Sensors*. Unpublished Ph.D. Thesis, Texas University, Texas.

Deering, D.W., Middleton, E.M. and Fit, T.F., 1994, Reflectance anisotropy for a spruce-hemlock forest canopy. *Remote Sensing of Environment*, **47**: 242–260.

Deering, D.W. and Kozoderov, V.V. (eds.), 1995, KUREX Special Issue. *Remote Sensing Reviews*, **11**: 289–310.

Defries, R., Hansen, M., Steininger, M., Dubayah, R., Sohlberg, R. and Townshend, J., 1997, Subpixel forest cover in central Africa from multisensor, multitemporal data. *Remote Sensing of Environment*, **60**: 228–246.

Demetriades-Shah, T.H., Steven, M.D. and Clark, J.A., 1990, High resolution derivative spectra in remote sensing. *Remote Sensing of Environment*, **33**: 55–64.

Denning, A.S., Fung, I.Y. and Randall, D., 1995, Latitudinal gradient of atmospheric CO_2 due to seasonal exchange with land biota. *Nature*, **376**: 240–243.

DETR (Department of the Environment Transport and the Regions), 1999, *LINK Climate Impacts, Newsletter of the U.K. DETR Climate Impacts LINK Project*. Climate Research Unit, Norwich.

DETR (Department of the Environment Transport and the Regions), 1997, *Climate Change and its Impacts: A Global Perspective*. The Meteorological Office, Bracknell.

Detwiler, R.P. and Hall, C.A.S., 1988, Tropical forests and the global carbon cycle. *Science*, **239**: 42–47.

Deutsch, C., 1989, DECLUS: A FORTRAN program for determining optimal spatial declustering weights. *Computers and Geosciences*, **145**: 325–332.

Dewar, R.C. and Cannell, M.G., 1992, Carbon sequestration in the trees, products and soils of forest plantations: An analysis using UK examples. *Tree Physiology*, **11**: 49–71.

Di, L. and Rundquist, D.C., 1994, A one-step algorithm for correction and calibration of AVHRR level 1b data. *Photogrammetric Engineering and Remote Sensing*, **60**: 55–65.

Dick, R.C. and Jordan, G.A., 1990, GIS activity in Canadian forestry. *Forest Management and Geographic Information Systems*, **1**: 144–176.

Dickenson, R.E., 1984, Modelling evapotranspiration for three-dimensional global climate models. *Geophysical Monographs, American Geophysical Union*, **29**: 58–72.

Dilworth, J.R. and Bell, J.F., 1979, *Variable Probability Sampling -Variable Plots and Three-P*. OSU Press, Oregon.

Dingman, S.L., Seely-Reynolds, D.M. and Reynolds, R.C., 1988, Application of kriging to estimating mean annual precipitation in a region of orographic influence. *Water Resources Bulletin*, **24**: 329–339.

Dirks, B.O., Hensen, A. and Goudriaan, J., 2000, Effect of drainage on CO_2 exchange patterns in an intensively managed peat pasture. *Climate Research*, **14**: 57–63.

Dixon, R.K., Winjum, J.K. and Schroeder, P.E., 1993, Conservation and sequestration of carbon. *Global Environmental Change*, **15**: 159–173.

Dixon, R.K., Brown, S., Houghton, R.A., Soloman, A.M., Trexler, M.C. and Wisniewski, J., 1994, Carbon pools and flux of global forest ecosystems. *Science,* **263**: 185–90.

Dixon, R.K. and Wisniewski, J., 1995, Global forest systems: An uncertain response to atmospheric pollutants and climate change. *Water, Air and Soil Pollution,* **85**: 101–110.

Dixon, R.K., Perry, J.A., Vanderklein, E.L. and Hiol, F.H., 1996, Vulnerability of forest resources to global climate change. *Climate Research,* **6**: 127–133.

Donoghue, D.N.M, 1999, Remote sensing. *Progress in Physical Geography*, **23**: 271–281.

Drake, B.G., Gonzàlez-Meler, M.A. and Long, S.P., 1997, More efficient plants: A consequence of rising atmospheric CO_2? *Annual Review of Plant Physiology and Plant Molecular Biology*, **48**: 609–639.

Dungan, J.L., 2000, Predicting vegetation amount using ground and remotely sensed data: Geostatistical alternatives. *Environmental and Ecological Statistics*. (submitted).

Dungan, J.L., 1998, Spatial prediction of vegetation quantities using ground and image data. *International Journal of Remote Sensing*, **19**: 267–285.

Dungan, J.L., Peterson, D.L. and Curran, P.J., 1994, Alternative approaches for mapping vegetation quantities using ground and image data. In Michener, W.K., Brunt, J.W. and Stafford, S.G. (eds.), *Environmental Information Management and Analysis: Ecosystem to Global Scales.* Taylor and Francis, London: 237–261.

Dungan, J.L. and Keller, R.M., 1991, Review of an advanced software tool for ecosystem simulation modelling (Abstract). *Bulletin of the Ecological Society of America*, **72**: 104.

Dunn, R., Harrison, A.R. and White, J.C., 1990, Positional accuracy and measurement error in digital databases of land use: An empirical study. *International Journal of Geographical Information Systems*, **4**: 385–398.

Ebdon, D., 1985, *Statistics in Geography* (second edition). Blackwell, Oxford.

Edwards, G. and Lowell, K.E., 1996, Modelling uncertainty in photointerpreted boundaries. *Photogrammetric Engineering and Remote Sensing*, **62**: 377–391.

Ehlers, M., Edwards, G. and Bedard, Y., 1989, Integration of remote sensing with Geographic Information Systems: A necessary evolution. *Photogrammetric Engineering and Remote Sensing*, **55**: 1619–1627.

Ehlers, M., 1990, Remote sensing and geographic information systems: towards integrated spatial information processing. *IEEE Transactions in Geosciences and Remote Sensing*, **28**: 763–766.

Ehlers, M., Greenlee, D., Smith, T. and Star, J., 1991, Integration of remote sensing and GIS: Data and access. *Photogrammetric Engineering and Remote Sensing*, **57**: 669–675.

Ehrlich, D., Estes, J.E. and Singh, A., 1994, Applications of NOAA AVHRR I km data for environmental monitoring. *International Journal of Remote Sensing*, **15**: 145–161.

Environment Canada, 1997, *L'Étude Pan-Canadienne: Sur les Impacts et l'Adaptation à la Variabilité et au Changement Climatique, Points Saillants pour les Canadiens.* Environment Canada, Quebec.

EOSC, 1985, *User's Guide for Landsat Thematic Mapper Computer Compatible Tapes*. Earth Observation Satellite Company, Lanham, M.D.

Fan, S.M., Gloor, M. and Mahlman, J., 1998, A large terrestrial carbon sink in North America implied by atmospheric and oceanic CO_2 data and models. *Science*, **282**: 442–446.

Farrar, J.L., 1995, *Trees in Canada*. Fitzhenry and Whiteside, Ottawa.

Fassnacht, K.S., Gower, S.T., Norman, J.M. and McMurtrie, R.E., 1994, A comparison of optical and direct methods for estimating foliage surface area index in forests. *Argricultural and Forest Meteorology*, **71**: 183–207.

Faust, N.L., Anderson, W.H. and Starr, J.L., 1991, Geographic information systems and remote sensing future computing environment. *Photogrammetric Engineering and Remote Sensing*, **57**: 655–668.

Fazakas, Z. and Nilsson, M., 1996, Volume and forest cover estimation over southern Sweeden using AVHRR data calibrated with TM data. *International Journal of Remote Sensing*, **17**: 1701–1709.

Filella, I. and Peñuelas, J., 1994, The red edge position and shape as indicators of plant chlorophyll content, biomass and hydric status. *International Journal of Remote Sensing*, **15**: 1459–1470.

Fisher, P., 1997, The pixel: A snare and a delusion. *International Journal of Remote Sens*ing, **18**: 679–685.

Flavelle, P., 1992, A quantitative measure of model validation and its potential use for regulatory purposes. *Advances in Water Research*, **15**: 5–13.

Florinsky, I.V., Kulagina, T.B., and Meshalkina, J.L., 1994, Influence of topography on landscape radiation temperature distribution. *International Journal of Remote Sensing*, **15**: 3147–3153.

Foody, G.M., 1997, Fully fuzzy supervised classification of land cover from remotely sensed imagery with an artificial neural network. *Neural Computing and Applications*, **5**: 238–247.

Foody, G.M., Palubinskas, G., Lucas, R.M., Curran, P.J. and Honzák, M., 1996a, Identifying terrestrial carbon sinks: Classification of successional stages in regenerating tropical forest from Landsat TM data. *Remote Sensing of Environment,* **55**: 205–216.

Foody, G.M. and Curran, P.J. (eds.), 1994a, *Environmental Remote Sensing from Regional to Global Scales*. Wiley, Chichester.

Foody, G.M. and Curran, P.J., 1994b, Scale and environmental remote sensing. In Foody, G.M. and Curran, P.J. (eds.), *Environmental Remote Sensing from Regional to Global Scales*. Wiley, Chichester: 223–232.

Foody, G.M. and Curran, P.J., 1994c, Estimation of tropical forest extent and regenerative stage using remotely sensed data. *Journal of Biogeography*, **21**: 223–244.

Foody, G.M., Boyd, D.S. and Curran, P.J., 1996, Relations between tropical forest biophysical properties and data acquired in AVHRR channels 1–5. *International Journal of Remote Sensing,* **17**: 1341–1355.

Fotheringham, S., 1999, Local Modelling. *Geographical and Environmental Modelling*, **3**: 5–8.

Fotheringham, A.S. and Wong, D.W.S., 1991, The modifiable areal unit problem in mulitvariate statistical analysis. *Environment and Planning A*, **23**: 1025–1034.

Fournier, R.A., Rich, P.M. and Landry, R., 1997, Hierarchical characterisation of canopy architecture for boreal forest. *Journal of Geophysical Research*, **102**: 29445–29454.

França, H. and Setzer, A.W., 1998, AVHRR temporal analysis of a savanna site in Brazil. *International Journal of Remote Sensing*, **19**: 3127–3140.

Franklin, S.E., Lavigne, M.B., Deuling, M.J., Wulder, M.A. and Hunt, E.R. (Jr.), 1997a, Estimation of forest leaf area index using remote sensing and GIS data for modelling net primary production. *International Journal of Remote Sensing*, **18**: 3459–3471.

Franklin, S.E., Lavigne, M.B., Deuling, M.J., Wülder, M.A. and Hunt E.R. (Jr.), 1997b, Landsat TM derived forest cover-types for modelling net primary production. *Canadian Journal of Remote Sensing*, **23**: 243–251.

Fransson, J.E. and Israelsson, H., 1999, Estimation of stem volume in boreal forests using ERS-1 C- and JERS-1 L-band SAR data.

Friedel, J., 1992, *System Description of the Geocoded Image Correction System*. Report GC-MA-50-3915. MacDonald Detwiller, Richmond, B.C.

Friedl, M.A., Michaelsen, J., Davis, F.W., Walker, H. and Schimel, D.S., 1994, Estimating grassland biomass and leaf area index using ground and satellite data. *International Journal of Remote Sensing*, **15**: 1401–1420.

Friend, A.D., Shugart, H.H. and Running, S.W., 1993, A physiology-based gap model of forest dynamics. *Ecology*, **74**: 792–797.

Friend, A.D., Stevens, A.K., Knox, R.G., Cannell, M.G.R., 1997, A process-based, terrestrial biosphere model of ecosystem dynamics (Hybrid v3.0). *Ecological Modelling*, **93**: 249–287.

Fritts, H.C., 1976, *Tree Rings and Climate*. Academic Press, New York.

Fung, I.Y., Tucker, C.J. and Prentice, K.C., 1987, Application of Advanced Very High Resolution Radiometer vegetation index to study atmosphere-biosphere exchange of CO_2. *Journal of Geophysical Research*, **92**: 2999–3015.

Gastellu-Etchegorry, J.P., Estreguil, C., Mougin, E. and Laumonier, Y., 1993, A GIS based methodology for small scale monitoring of tropical forests – a case study in Sumatra. *International Journal of Remote Sensing*, **14**: 2349–2368.

Gastellu-Etchegorry, J.P., Zagolski, F., Mougin, E., Marty, G. and Giordano, G., 1995, An assessment of canopy chemistry with AVIRIS: A case study in the Landes Forest, south-west France. *International Journal of Remote Sensing*, **16**: 487–501.

Gates, D., Keegan, J.J., Schleter, J.C. and Weidner, V.R., 1965, Spectral properties of plants. *Applied Optics*, **4**: 11–20.

Gausman, H.W., 1985, *Plant Leaf Optical Parameters in Visible and Near-infrared Light*. Texas Technical Press, Lubbock.

Gauthier, R.P. and Neville, R.A., 1985, Narrow-band multi-spectral imagery of the vegetation red reflectance edge for use in geobotanical remote sensing. *Proceedings, International Colloquium on Spectral Signatures of Objects in Remote Sensing*. ESA, Noordwijk, SP-247: 233–236.

Gemmell, F. and Varjo, J., 1999, Utility of reflectance model inversion versus two spectral indices for estimating biophysical characteristics in a boreal forest test site. *Remote Sensing of Environment*, **68**: 95–111.

Gershon, N.D. and Miller, C.G., 1993, Dealing with the data deluge. *IEEE Spectrum*, **30**: 28–32.

Gervin, J.C., Kerber, A.G., Witt, R.G., Lu, Y.C. and Sekhon, R., 1985, Comparison of level 1 land cover classification accuracy for MSS and AVHRR data. *International Journal of Remote Sensing*, **6**: 47–57.

Gholz, H.L., Vogel, S.A., Cropper, W.P., McKelvey, K., Ewel, K.C., Tesky, R.O. and Curran, P.J., 1991, Dynamics of canopy structure and light interception in *Pinus elliottii* stands, north Florida. *Ecological Monographs*, **6**: 35–51.

Gholz, H.L., Nakane, K. and Shimoda, H. (eds.), 1996, *The use of Remote Sensing in the Modelling of Forest Productivity*. Kluwer, Dordrecht.

Gilabert, M.A., Gandía, S. and Meliá, J., 1996, Analysis of spectral-biophysical relationships for a corn canopy. *Remote Sensing of Environment*, **55**: 11–20.

Gilbert, N., 1989, *Biometrical Interpretation*. Oxford University Press, Oxford.

Gitelson, A.A., Merzlyak, M.N. and Lichtenthaler, H.K., 1996, Detection of red edge position and chlorophyll content by reflectance measurements near 700 nm. *Journal of Plant Physiology*, **148**: 501–508.

Gobron, N., Pinty, B. Verstraete, M. and Govaerts, Y., 1999, The MERIS Global Vegetation Index (MGVI): description and preliminary application. *International Journal of Remote Sensing*, **20**: 1917–1927.

Goel, N.S., 1989, Inversion of canopy reflectance models for estimation of biophysical parameters from reflectance data. In Asrar, G. (ed.), *Theory and Applications of Optical Remote Sensing*. Wiley, New York: 205–251.

Goel, N.S. and Thompson, R.L., 1984, Inversion of canopy reflectance models for estimating agronomic variables. V. estimation of leaf area index and average leaf angle using measured canopy reflectances. *Remote Sensing of Environment*, **16**: 69–85.

Goel, N.S. and Norman, J.M., 1992, Biospheric models, measurements and remote sensing of vegetation. *ISPRS Journal of Photogrammetry and Remote Sensing*, **47**: 163–188.

Goetz, S.J. and Prince, S.D., 1996, Remote sensing of net primary production in boreal forest stands. *Agricultural and Forest Meteorology*, **78**: 149–179.

Goetz, S.J., Prince, S.D., Goward, S.N., Thawley, M.M., Small, J. and Johnston, A., 1999, Mapping net primary production and related biophysical variables with remote sensing: Application to the BOREAS region. *Journal of Geophysical Research*, **104**: 27719–27734.

Gong, P., Pu, R. and Miller, J.R., 1995, Coniferous forest leaf area index estimation along the Oregon transect using CASI data. *Photogrammetric Engineering and Remote Sensing*, **61**: 1107–1117.

Goodchild, M.F., 1977, Statistical aspects of the polygon overlay problem. In Dutton, G. (ed.), *Harvard Papers on Geographical Information Systems*. Addison Wesley, Massachusetts: 1–22.

Goovaerts, P., 1998, Ordinary cokriging revisited. *Mathematical Geology*, **30**: 21–42.

Goovaerts, P., 1999a, Geostatistics in soil science: State-of-the-art perspectives. *Geoderma*, **89**: 1–45.

Goovaerts, P., 1999b, Using elevation to aid the geostatistical mapping of rainfall erosivity. *Catena*, **34**: 227–242.

Goovaerts, P. and Journel, A.G., 1995, Integrating soil map information in modelling the spatial variation of continuous soil properties. *European Journal of Soil Science*, **46**: 397–414.

Gorham, E., 1991, Northern peatlands: Role in the carbon cycle and probable responses to climatic warming. *Ecological Applications*, **1**: 182–195.

Gorte, B., 1999, Description of the data used in this book. In Stein, A., van der Meer, F. and Gorte, B. (eds.), *Spatial Statistics for Remote Sensing*. Kluwer, Dordrecht: 3–7.

Goulden, M.L., Wofsy, S.C., Harden, J.W., Trumbore, S.E., Crill, P.M., Gower, S.T. and Fries, T., 1998, Sensitivity of boreal forest carbon balance to soil thaw. *Science*, **279**: 214–217.

Govaerts, Y.M., Verstraete, M.M., Pinty, B. and Gobron, N., 1999, Designing optimal spectral indices: a feasibility and proof concept study. *International Journal of Remote Sensing*, **20**: 1853–1875.

Goward, S.N., Cruickshanks, G.D. and Hope, A.S., 1985, Observed relation between thermal emission and reflected spectral radiance of a complex vegetation landscape. *Remote Sensing of Environment*, **18**: 137–146.

Goward, S.N., Tucker, C.J. and Dye, D.G., 1987, North American vegetation patterns observed with NOAA-7 AVHR. *Vegetatio*, **64**: 3–14.

Goward, S.N., Markham, B., Dye, D.G., Dulaney, W. and Yang, J., 1991, Normalised difference vegetation index measurements from the AVHRR. *Remote Sensing of Environment*, **35**: 257–277. Goward, S.N., Waring, R.H., Dye, D.G. and Yang, J., 1994, Ecological remote sensing at OTTER: Satellite macro-scale observations. *Ecological Applications*, **4**: 322–343.

Gower, S.T. and Norman,. J.M., 1991, Rapid estimation of leaf area index in forests using the LI-COR LAI-2000. *Ecology*, **72**: 1896–1900.

Gower, S.T., Vogt, K.A. and Grier, C.C., 1992, Carbon dynamics of Rocky Mountain Douglas fir: influence of water and nutrient availability. *Ecological Monographs*: **62**: 43–65.

Gower, S.T., Vogel, J.G., Norman, J.M., Kucharik, C.J., Steele, S.J. and Stow, T.K., 1997, Carbon distribution and aboveground net-primary production of BOREAS tower flux forest. *Journal of Geophysical Research*, **102**: 29029–29042.

Gower, S.T., Kucharik, C.J. and Norman, J.M., 1999, Direct and indirect estimation of leaf area index, fapar and net primary production of terrestrial ecosystems. *Remote Sensing of Environment*, **70**: 29–51.

Grace, J., van Gardingen, P.R. and Luan, J., 1997, Tackling large-scale problems of scaling-up. In van Gardingen, P.R., Foody, G.M. and Curran, P.J. (eds.), *Scaling-up: From Cell to Landscape*. Cambridge University Press, Cambridge: 7–16.

Grace, J. and Rayment, M., 2000, Respiration in the balance. *Nature*, **404**: 819–820.

Grainger, A., 1993, Rates of deforestation in the humid tropics: Estimates and measurements. *The Geographical Journal*, **159**: 33–44.

Green, N.P.O., Stout, G.W. and Taylor, D.J., 1990, *Biological Science 1 and 2* (second edition). Cambridge University Press, Cambridge.

Green, R.M., Lucas, N.S., Curran, P.J and Foody, G.M., 1997, Coupling remotely sensed data to an ecosystem simulation model: An example involving a coniferous plantation in upland Wales. *Global Ecology and Biogeography Letters*, **5**: 192–205.

Grier, C.C., 1988, Foliage loss due to snow, wind and winter drying damage: its effects on leaf biomass of some western conifer forests. *Canadian Journal of Forest Research*, **18**: 1097–1102.

Grissino-Mayer, H.D., 1997, Computer assisted, independent observer verification of tree-ring measurements. *Tree-Ring Bulletin*, **54**: 29–41.

Grubb, M., Brack, D. and Vrolijk, C., 1999, The Kyoto Protocol: A Guide and Assessment. Royal Institute of International Affairs and Cambridge Univesrity Press, Cambridge.

Gu, L.H., Shugart, H.H., Fuentes, J.D., Black, T.A., Shewchuk, S.R., 1999, Micrometeorology, biophysical exchanges and NEE decomposition in a two-storey boreal forest: Development and test of an integrated model. *Agricultural and Forest Meteorology*, **94**: 123–148.

Guoquan, D. and Zhengzhi, L., 1992, The apparent emissivity of vegetation canopies. *International Journal of Remote Sensing*, **14**:183–188.

Gutman, G., Ignatov, A. and Olson, S., 1996, Global land monitoring using AVHRR time series. *Advances in Space Research*, **17**: 51–54.

Guyot, G., Guyon, D. and Riom, J., 1989, Factors affecting the spectral response of forest canopies: A review. *Geocarto International*, **3**: 3–18.

Guyot, G., Baret, F. and Jacquemoud, S., 1992, Imaging spectroscopy for vegetation studies. In Toselli, F. and Bodechtel, J. (eds.), *Imaging Spectroscopy: Fundamentals and Prospective Applications*. Kluwer, Dordrecht: 51–61.

Haining, R.P., 1990, *Spatial Data Analysis in the Social and Environmental Sciences*. Cambridge University Press, Cambridge.

Hall, F.G., Sellers, P.J. and Apps, M.J., 1993, BOREAS: BOReal Ecosystem-Atmosphere Study, *IEEE, Geoscience Remote Sensing Society Newsletter.* (March): 9–17.

Hall, F.G., Shimabukuro, Y.E. and Huemmrich, K.F., 1995a, Remote sensing of forest biophysical structure in boreal stands of *Picea mariana* using mixture decomposition and geometric reflectance models. *Ecological Applications*, **5**: 993–1013.

Hall, F.G., Townshend, J.R.G. and Engman, E.T., 1995b, Status of remote sensing algorithms for estimation of land surface state parameters. *Remote Sensing of Environment*, **51**: 138–156.

Hall, J.F., 1995, Forest health monitoring in Canada: How healthy is the boreal forest? *Water, Air and Soil Pollution*, **82**: 77–85.

Halliwell, D.H. and Apps, M.J., 1997a, *BOReal Ecosystem-Atmosphere Study (BOREAS) Biometry and Auxiliary Sites: Locations and Descriptions*. Canadian Forest Service, Alberta.

Halliwell, D.H. and Apps, M.J., 1997b, *BOReal Ecosystem-Atmosphere Study (BOREAS) Biometry and Auxiliary Sites: Overstory and Understory Data*. Canadian Forest Service, Alberta.

Halliwell, D.H. and Apps, M.J., 1997c, *BOReal Ecosystem-Atmosphere Study (BOREAS) Biometry and Auxiliary Sites: Soils and Detritus Data*. Canadian Forest Service, Alberta.

Halliwell, D.H., Apps, M.J. and Price, D.T., 1995, A survey of the forest site characteristics in a transect through the central Canadian boreal forest. *Water, Air and Soil Pollution,* **82**: 257–270.

Häme, T., Salli, I., Andersson, K. and Lohi, A., 1997, A new methodology for the estimation of biomass and conifer dominated boreal forest using NOAA AVHRR data. *International Journal of Remote Sensing*, **18**: 3211–3243.

Hanselman, D.C. and Littlefield, B., 1998, *Mastering Matlab 5: A Comprehensive Tutorial and Reference*. Prentice Hall, New Jersey.

Harding, R.G., Taylor, C.M. and Finch, J.W., 1996, Areal average surface fluxes from mesoscale meteorological models: The application of remote sensing. In Stewart, J.B., Engman, E.T., Feddes, R.A. and Kerr, Y. (eds.), *Scaling Up in Hydrology Using Remote Sensing*. Wiley, Chichester: 59–76.

Hare, F.K. and Hay, J.E., 1971, Climate of Canada and Alaska. In Bryson, R.A. and Hare, F.K. (eds.), *World Survey of Climatology, The Climates of North America, Volume 11*. Elsevier, Amsterdam: 49–192.

Hasenauer, H., Nemani, R.R., Schadauer, K. and Running, S.W., 1999, Forest growth response to changing climate between 1961 and 1990 in Austria. *Forest Ecology and Management*, **22**: 209–219.

Hastings, D.A. and Emery, W.J., 1992, The Advanced Very High Resolution Radiometer (AVHRR), a brief reference guide. *Photogrammetric Engineering and Remote Sensing*, **58**: 1183–1188.

Hay, G.J., Niemann, K.O. and Goodenough, D.G., 1997, Spatial thresholds, image-objects and upscaling: A multi-scale evaluation. *Remote Sensing of Environment*, **62**: 1–19.

Hayes, L., 1985, The current use of TRIOS-N series of meteorological satellites for land-cover studies. *International Journal of Remote Sensing*, **6**: 34–45.

Hedger, R.D., Atkinson, P.M., Malthus, T.J. and George, D.G., 1996, Planning optimal sdampling strategies for estimating the regional mean water quality in lakes. *RSS96: Remote Sensing Science and Industry*. Remote Sensing Society, Nottingham: 221–228.

Henderson-Sellers, A., 1991, Developing an interactive biosphere for global climate models. *Vegetatio*, **91**: 149–166.

Henderson-Sellers, A., Wilson, M.F. and Thomas, G., 1985, The effect of spatial resolution on archives of land cover type. *Climatic Change*, **7**: 391–402.

Hendrick, R.L. and Pregitzer, K.S., 1993, The dynamics of fine root length, biomass and nitrogen content in two northern hardwood ecosystems. *Canadian Journal of Forest Research*, **23**: 2507– 2520.

Huete, A.R., 1988, A soil-adjusted vegetation index (SAVI). *Remote Sensing of Environment*, **25**: 295–309.

Huete, A.R., Justice, C. and Liu, H., 1994, Development of soil and vegetation indices for MODIS-EOS. *Remote Sensing of Environment*, **49**: 224–234.

Heric, M., Lucas, C. and Devine, C., 1996, The open skies treaty: qualitative utility evaluations of aircraft reconnaissance and commercial satellite imagery. *Photogrammetric Engineering and Remote Sensing*, **62**: 279–284.

Hibbard, K. and Sahagian, D. (eds.), 1997, GAIM 1993-1997. The First Five Years: Setting the Stage for Synthesis. IGBP-GAIM Report Series, Report 7, IGBP, Stockholm.
(URL http://gaim.unh.edu/93-97/NPP.html).

Hill, J.L., 1995, *The Effect of Forest Spatial Geometry on Tree Species Diversity in Tropical Forest Patches*. Unpublished Ph.D. thesis, University of Wales, Swansea.

Hinkley, T.M. and Ceulemans, R., 1989, Current focuses in woody plant water relations and drought resistance. *Annals of Science in Forestry*, **46**: 317–324.

Hinton, J.C., 1996, GIS and remote sensing integration for environmental applications. *International Journal of Geographical Information Systems*, **10**: 877–890.

Hobbs, R.J. and Mooney, H.A. (eds.), 1990, *Remote Sensing and Biosphere Functioning*. Springer-Verlag, New York.

Hoffer, R.M., 1978, Biological and physical considerations in applying computer-aided analysis to remote sensor data. In Swain, P.H. and Davis, S.M. (eds.), *Remote Sensing: The Quantitative Approach*. McGraw-Hill, New York: 43–56.

Holben, B.N., 1986, Characteristics of maximum value composite images for temporal AVHRR data. *International Journal of Remote Sensing*, **7**: 1417–1437.

Holben, B.N., Tucker, C.J. and Fan, C.J., 1980, Spectral assessment of soybean leaf area and leaf biomass. *Photogrammetric Engineering and Remote Sensing*, **46**: 651–656 .

Holmgren, P. and Thuresson, T., 1998, Satellite remote sensing for forestry planning: A review. *Scandinavian Journal of Forest Research*, 13: 90–110.

Horler, D.N.H, Barber, J. and Barringer, A.R., 1980, Effects of heavy metals on the absorptance and reflectance spectra of plants. *International Journal of Remote Sensing*, **1**: 121–136.

Horler, D.N.H., Dockray, M. and Barber, J., 1983, The red edge of plant leaf reflectance. *International Journal of Remote Sensing*, **4**: 273–288.

Horler, D.N.H. and Ahern, F.J., 1986, Forestry information content of Thematic Mapper data. *International Journal of Remote Sensing*, **7**: 405–428.

Houghton, R.A., 1995, Changes in the storage of terrestrial carbon since 1850. In Lal, R., Kimble, J., Levine, E. and Stewart, B.A., (eds.), Soils and Global Change. Lewis Publishers, Boca Raton: 45–64.

Houghton, R.A., 1999, The annual net flux of carbon to the atmosphere from changes in land use 1850-1990. *Tellus B*, **51**: 298–313.

Houghton, R.A., Callander, B.A. and Varney, S.K. (eds.), 1996, *Climate Change 1995 - The Supplementary Report to the IPCC Scientific Assessment.* IPCC, Cambridge University Press, Cambridge.

Houghton, R.A., Davidson, E.A. and Woodwell, G.M., 1998, Missing sinks, feedbacks and understanding the role of terrestrial ecosystems in the global carbon balance. *Global Biogeochemical Cycles*, **12**: 25–34.

Houghton, R.A., Skole, D.L., Nobre, C.A., Hackler, J.L., Lawrence, K.T. and Chomentowski, W.H., 2000, Annual fluxes of carbon from deforestation and regrowth in the Brazilian Amazon. *Nature*, **403**: 301–304.

Hulme, M., Barrow, E.M., Arnell, N.W., Harrison, P., Johns, T.C. and Downing, T.E., 1999a, Relative impacts of human-induced climate change and natural variability. *Nature*, **397**: 688–691.

Hulme, M., Mitchell, J., Ingram, W., Lowe, J., Johns, T., New, M. and Viner, D., 1999b, Climate change scenarios for global impact studies. *Global Environmental Change*, **9** (Supplementary Issue): 3–20.

Hunt, E.R. (Jr.), Martin, F.C. and Running, S.W., 1991, Simulating the effects of climatic variation on stem carbon accumulation of a *Ponderosa* pine stand: Comparison with annual growth increment data. *Tree Physiology*, **9**: 161–171.

Hunt, E.R. (Jr.) and Running, S.W., 1992, Simulated dry matter yields for aspen and spruce stands in the North American boreal forest. *Canadian Journal of Remote Sensing*, **18**: 126–133.

Hunt, E.R. (Jr.), Piper, S.C., Nemani, R., Keeling, C.D., Otto, R.D. and Running, S.W., 1996, Global net carbon exchange and intra-annual atmospheric CO2 concentrations predicted by an ecosystem process model and three-dimensional atmospheric transport model. *Global Biogeochemical Cycles*, **10**: 431–456.

Idso, K.E. and Idso, S.B., 1994, Plant responses to atmospheric CO_2 enrichment in the face of environmental constraints: A review of the past 10 years' research. *Agricultural and Forest Meteorology*, **69**: 153–203.

IGBP, 1990, The International Geosphere-Biosphere Programme: A study of global change: The initial core projects, *Global Terrestrial Net Primary Productivity*. IGBP, Stockholm, **19**: 6–8.

IGBP Terrestrial Carbon Working Group, 1998, The terrestrial carbon cycle: Implications for the Kyoto protocol. *Science*, **280**: 1393–1394.

IGPO (International GEWEX Project Office), 1992, Scientific plan for the GEWEX Continental-Scale International Project (GCIP). No. 461, IGPO, Washington DC.

Ikeda, H., Okamoto, K. and Fukihara, M., 1999, Estimation of aboveground grassland phytomass with a growth model using Landsat TM and climate data. *International Journal of Remote Sensing*, **20**: 2283–2294.

IPCC (Intergovernmental Panel on Climate Change), Houghton, J.T., Filho, L.G.M., Callander, B.A., Harris, N., Kattenberg, A. and Maskell, K., (eds.), 1996, *Climate Change 1995. The Science of Climate Change*. Cambridge University Press, Cambridge.

Isaaks, E.H. and Srivastava, R.M., 1988, Spatial continuity measures for probabilistic and deterministic geostatistics. *Mathematical Geology*, **20**: 313–341.

Ishida, T. and Ando, H., 1999, Use of disjunctive cokriging to estimate soil organic matter from Landsat Thematic Mapper images. *International Journal of Remote Sensing*, **20**: 1549–1565.

Janssen, L.L.F. and Molenaar, M., 1995, Terrain objects, their dynamics and their monitoring by the integration of GIS and remote sensing. *IEEE Transactions on Geoscience and Remote Sensing*, **33**: 749–758.

Jarvis, P.G., 1994, Scaling processes and problems. *Plant, Cell and Environment,* **18**: 1079–1089.

Jarvis, P.G., 1995a, The role of temperate trees and forests in CO_2 fixation. *Vegetatio,* **121**: 157–174.

Jarvis, P.G., 1995b, Scaling: Processes and problems. *Plant, Cell and Environment*, **18**: 1079–1089.

Jarvis, P.G. and Leverenz, J.W., 1984, Productivity of temperate deciduous and evergreen forests. In Calow, P. (ed.), *Encyclopedia of Plant Physiology*. Springer-Verlag, Berlin: 233–280.

Jarvis, P.G. and Moncrieff, J.B., 1992, Atmosphere-biosphere exchange of CO_2. In Mather, P.M. (ed.), *TERRA-1: Understanding the Terrestrial Environment*. Taylor and Francis, London: 85–99.

Jasinski, M., 1996, Estimation of sub-pixel vegetation density of natural regions using satellite multi-spectral imagery. *IEEE Transactions on Geoscience and Remote Sensing*, **34**: 804–813.

Jensen, J.R., 1983, Biophysical remote sensing. *Annals of the Association of American Geographers*, **73**: 111–132.

Johns, T.C., Carnell, R.E., Crossley, J.F., Gregory, J.M., Mitchell, J.F.B., Senior, C.A., Tett, S.F.B. and Wood, R.A., 1997, The second Hadley Centre coupled ocean-atmosphere GCM: model description, spin-up and validation. *Climate Dynamics*, **13**: 103–134.

Johnson, L.F., Hlavka, C.A. and Peterson, D.L., 1994, Multivariate analysis of AVIRIS data for canopy biochemical estimation along the Oregon transect. *Remote Sensing of Environment,* **47**: 216–230.

Johnston, R.J., 1980, *Multivariate Statistical Analysis in Geography: A Primer on the General Linear Model.* Longman, London.

Jordan, C.F., 1969, Derivation of leaf area index from quality of light on the forest floor. *Ecology*, **50**: 663–666.

Journel, A.G., 1996a, Geostatistics. *Mathematical Geology*, **28**: 827.

Journel, A.G., 1996b, Modelling uncertainty and spatial dependence: Stochastic imaging. *International Journal of Geographical Information Science*, **10**: 517–522.

Journel, A.G. and Huijbregts, C.J., 1978, *Mining Geostatistics*. Academic Press, London.

Journel, A.G. and Alabert, F., 1989, Non-Gaussian data expansion in the Earth sciences. *Terra Nova*, **1**: 123–134.

Jozsa, L., 1988, *Increment Core Sampling Techniques for High Quality Cores*. Forintek, Vancouver.

Jupp, D.L.B., Strahler, A.H. and Woodcock, C.E., 1988, Autocorrelation and regularisation in digital images: I. Basic theory. *IEEE Transactions on Geoscience and Remote Sensing*, **26**: 463–473.

Jupp, D.L.B., Strahler, A.H. and Woodcock, C.E., 1989, Autocorrelation and regularisation in digital images: II. Simple image models. *IEEE Transactions on Geoscience and Remote Sensing*, **27**: 247–258.

Justice, C.O., Vermote, E., Townshend, J.R.G., Defries, R., Roy, D.P., Hall, D.K., Salomonson, V.V., Privette, J.L., Riggs, G., Strahler, A., Lucht, W., Myneni, R.B., Knyazikhin, Y., Running, S.W., Nemani, R.R., Wan, Z.M., Huete, A.R., van Leeuwen, W., Wolfe, R.E., Giglio, L., Muller, J.P., Lewis, P., Barnsley, M.J., 1998, The Moderate Resolution Imaging Spectroradiometer (MODIS): Land remote sensing for global change research. *IEEE Transactions on Geoscience and Remote Sensing*, **36**: 1228–1249.

Kabat, P., 1999, The role of biospheric feedbacks in the hydrological cycle. In Steffan, W., (ed.), *IGBP Global Change Newsletter 39*. IGBP, Stockholm.

Kaufman, L. and Tanré, D., 1992, Atmospherically resistant vegetation index (ARVI) for EOS-MODIS. *IEEE Transactions on Geoscience and Remote Sensing*, **30**: 261–270.

Kaufman, L. and Holben, B.J., 1993, Calibration of AVHRR visible and near-IR bands by atmospheric scattering, ocean glint and desert reflection. *International Journal of Remote Sensing*, **14**: 21–52.

Kaufman, Y.J. and Remer, L.A., 1994, Detection of forests using mid-IR reflectance: An application for aerosol studies. *IEEE Transactions on Geoscience and Remote Sensing*, **32**: 672–683.

Kaufman, L. and Tanré, D., 1996, Strategy for direct and indirect methods for correcting the aerosol effect on remote sensing: From AVHRR to EOS-MODIS. *Remote Sensing of Environment*, **55**: 65–79.

Kasischke, E.S and Christensen, N.L. (Jr.), 1990, Connecting forest ecosystem and microwave backscatter models. *International Journal of Remote Sensing*, **11**: 1277–1298.

Keane, R.E., Morgan, P. and Running, S.W., 1996a, FIRE-BGC: A mechanistic ecological process model for simulating fire succession on coniferous forest landscapes of the northern Rocky mountains. *USDA Forest Service Intermountain Research Station Research Paper*, **484**: 1–23.

Keane, R.E., Morgan, P. and Running, S.W., 1996b, Simulating effects of fire on northern Rocky mountain landscapes with the ecological process model FIRE-BGC. *Tree Physiology*, **16**: 319–331.

Keeling, C.D. and Shertz, S.R., 1992, Seasonal and inter-annual variations in atmospheric oxygen and implications for the global carbon cycle. *Nature*, **358**: 723–727.

Keeling, C.D., Chin, J.F. and Whorf, T.P., 1996a, Increased activity of northern vegetation inferred from atmospheric CO_2 measurements. *Nature*, **382**: 146–149.

Keeling, C.D., Piper, S.C. and Heimann, M., 1996b, Global hemispheric CO_2 sinks deduced from changes in atmospheric O_2 concentration. *Nature*, **381**: 218–221.

Keller, R.M., 1995, Building the Scientific Modelling Assistant: An interactive environment for specialised software design. *American Association for Artificial Intelligence Workshop on Automating Software Design*, AAAI Press, Anaheim: 71–80.

Keller, R.M. and Dungan, J.L., 1999, Meta-modelling: A knowledge-based approach to facilitating process model construction and reuse. *Ecological Modelling*, **119**: 89–116.

Kershaw, K.A. and Rousse, W.R., 1971, Studies on lichen dominated systems. *Canadian Journal of Botany*, **49**: 1401–1410.

Kidwell, K.B., 1991, *NOAA Polar Orbiter Data TIROS-N, NOAA-6, NOAA-7, NOAA-8, NOAA-9, NOAA-10, NOAA-11 and NOAA-12. Users Guide.* NASA: Washington D.C.

Kimball, J.S., Thornton, P.E., White, M.A. and Running, S.W., 1997, Simulating forest productivity and surface-atmosphere carbon exchange in the BOREAS study region. *Tree Physiology*, **17**: 589–599.

Kimes, D.S. and Sellers P.J., 1986, Inferring hemispherical reflectance of the Earth's surface for global energy budgets from remotely sensed NADIR or directional radiance values. *Remote Sensing of Environment*, **18**: 205–224.

King, G.A. and Neilson, R.P., 1992, The transient response of vegetation to climate change: A potential source of CO_2 to the atmosphere. *Water, Air and Soil Pollution*, **64**: 365–383.

Klinger, L.F., Taylor, J.A. and Franzen, L.G., 1996, The potential role of peatland dynamics in ice-age initiation. *Quaternary Research*, **45**: 89–92.

Kondratyev, K.Y., 1996, Greenhouse warming versus aerosol cooling in the context of global climate change. *Energy Conservation and Management*, **37**: 763–768.

Koomanoff, F.A., Ye, D.Z., Zhao, J.P., Rimes, M.R., Wang, W.C. and Tao, S.Y., 1988, The US Department of Energy and the Peoples Republic of China joint research on the greenhouse effect. *Bulletin of the American Meteorological Society*, **69**: 1301–1308.

Korol, R.L., Running, S.W., Milner, K.S. and Hunt, E.R. (Jr.), 1991, Testing a mechanistic carbon balance model against observed tree growth. *Canadian Journal of Forest Research,* **21**: 1098–1105.

Korol, R.L., Milner, K.S. and Running, S.W., 1995, Incorporating inter-tree competition into an ecosystem model. *Canadian Journal of Forest Research,* **25**: 413–424.

Kremer, R.G., 1991, Simulating forest response to air pollution: Integrating physiological responses to sulphur dioxide with climate dependant growth processes. *Ecological Modelling,* **54**: 111–126.

Kruse, F.A., 1992, The analysis of scientific data from NASA airborne systems. *Scientific Computing and Automation,* **56**: 83–92.

Kruse, F.A., 1999, Visible-Infrared sensors and case studies. In Rencz, A.N. (ed.), *Remote Sensing for the Earth Sciences: Manual of Remote Sensing, Volume 3* (third edition). Wiley, New York: 567–611.

Kull, O. and Jarvis, P.G., 1995, The rôle of nitrogen in a simple scheme to scale up photosynthesis from leaf to canopy. *Plant, Cell and Environment,* **18**: 1174–1182.

Kunz, R.P., Schulze, R.E. and Scholes, R.J., 1995, An approach to modelling spatial changes of plant carbon-nitrogen ratios in southern Africa in relation to anticipated global climate change. *Journal of Biogeography,* **22**: 401–408.

Kupiec, J.A., 1994, *The Remote Sensing of Foliar Chemistry.* Unpublished Ph.D. Thesis, University of Wales, Swansea.

Kupiec, J.A. and Curran, P.J., 1994, *Remote sensing of foliar chemistry: Moving from the leaf to the canopy.* NASA Accelerated Canopy Chemistry Programme 1993–1995, Report IV, Department of Geography, University of Wales Swansea, Swansea.

Kurz, W.A. and Apps, M.J., 1994, The carbon budget of Canadian forests: A sensitivity analysis of changes in disturbance regimes, growth-rates and decomposition rates. *Environmental Pollution,* **83**: 55–61.

Kyriakidis, P.C. and Journel, A.G., 1999, Geostatistical space-time models: A review. *Mathematical Geology,* **31**: 651–684.

Lal, R., Kimble, J., Levine, E. and Whitman, C., 1995, World soils and greenhouse effects: An overview. In Lal, R., Kimble, J., Levine, E. and Stewart, B.A., (eds.), *Soils and Global Change,* Lewis Publishers, Boca Raton: 1–8.

Lambert, N.J., Ardo, J., Rock, B.N. and Vogelmann, J.E., 1995, Spatial characterisation and regression-based classification of forest change in Norway spruce stands in the Czech Republic using Landsat TM data. *International Journal of Remote Sensing,* **16**: 1261–1287.

Lambin, E.F. and Ehrlich, D., 1996, The surface temperature-vegetation index space for land cover and land cover change analysis. *International Journal of Remote Sensing,* **17**: 463–487.

Landgreb, D.A. and Malaret, E., 1986, Noise in remote sensing systems, the effect on classification error. *IEEE Transactions on Geoscience and Remote Sensing,* **24**: 294–298.

Landsberg, J.J. and Gower, S.T., 1997, *Applications of Physiological Ecology to Forest Management*. Academic Press, San Diego.

Landsberg, J.J., Kaufmann, M.R., Binkley, D., Isebrands, J. and Jarvis, P.G., 1991, Evaluating progress towards closed forest models based on fluxes of carbon, water and nutrients. *Tree Physiology*, **9**: 1–15.

Lang, A.R.G., 1987, Simplified estimate of leaf area index from transmittance of the Sun's beam. *Agricultural and Forest Meteorology*, **41**: 179–186.

Lang, M.K., Donohoe, G.W., Zaidi, S.H. and Brueck, S.R.J., 1994, Real-time image processing techniques for non-contact temperature measurement. *Optical Engineering*, **33**: 3465–3471.

Laporte, N., Justice, C. and Kendall, J., 1995, Mapping the dense humid forest of Cameroon and Zaire using AVHRR satellite data. *International Journal of Remote Sensing*, **16**: 1127–1145.

Larsen, J.A., 1980, *The Boreal Ecosystem*, Academic Press, New York.

Lathrop, R.G., Aber, J.D., Bognar, J.A., Ollinger, S.V., Casset, S. and Ellis, J.M., 1994, GIS development to support regional simulation modelling of north-eastern USA forest ecosystems. In Michener, W.K., Brunt, J.W. and Stafford, S.G. (eds.), *Environmental Information Management and Analysis*. Taylor and Francis, London: 431–451.

Lathrop, R.G., Aber, J.D. and Bognar, J.A., 1995, Spatial variability of digital soil maps and its impact on regional ecosystem modelling. *Ecological Modelling*, **82**: 1–10.

Lavigne, M., Luther, J., Franklin, S. and Hunt, E.R. (Jr.), 1996, Comparing branch biomass prediction equations for *Abies balsamea*. *Canadian Journal of Forest Research*, **26**: 611–616.

Lawlor, D.W., 1993, *Photosynthesis: Molecular, Physiological and Environmental Processes* (second edition). Longman, Harlow.

Lebel, T., Bastin, G., Obled C. and Creutin, J.D., 1987, On the accuracy of areal rainfall estimation: A case study. *Water Resources Research*, **23**: 2123–2134.

Lee, H.S. and Jarvis, P.G., 1995, Trees differ from crops and each other in their responses to increases in CO_2 concentration. *Journal of Biogeography*, **22**: 323–330.

Leenaers, H., Okx, J. and Borrough, P., 1990, Comparison of spatial prediction methods for mapping floodplain soil pollution. *Catena*, **17**: 535–550.

Lieth, H., 1975, Modelling the primary production of the world. In Lieth, H. and Whittaker, R.H. (eds.), *Primary Productivity of the Biosphere*. Springer-Verlag, New York: 237–263.

Lieth, H. and Whittaker, R.H., 1975, *Primary Productivity of the Biosphere*. Springer-Verlag, New York.

Lillesand, T.M. and Kiefer, R.W., 1999, *Remote Sensing and Image Interpretation* (fourth edition). Wiley, New York.

Linder, S., Benson, M.L., Meyers, B.J., and raison, R.J., 1987, canopy dynamics and growth of *Pinus radiata*. 1. Effects of irrigation and fertilisation during a drought. *Canadian Journal of Forest Research*, **17**: 1157– 1165.

Lindroth, A., Grelle, A. and Moren, A.S., 1998, Long-term measurements of boreal forest carbon balance reveal large temperature sensitivity. *Global Change Biology*, **3**: 443–450.

Loveland, T.R. and Belward, A.S., 1997, The IGBP-DIS global 1 km land cover data set, DISCover: First results. *International Journal of Remote Sensing*, **18**: 3289–3295.

Lucas, N.S., 1995, *Coupling Remotely Sensed Data to a Forest Ecosystem Simulation Model.* Unpublished Ph.D. Thesis, University of Wales Swansea, Swansea.

Lucas, N.S., Curran, P.J. and Plummer, S., 1995, Using the red edge inflection point to drive an ecosystem simulation model for calculating the stem carbon production of an upland coniferous forest plantation. *RSS'95, Remote Sensing in Action,* Remote Sensing Society, Nottingham: 1020–1027.

Lucas, N.S. and Curran, P.J., 1999, Forest ecosystem simulation modelling: The rôle of remote sensing. *Progress in Physical Geography*, **23**: 391–423.

Lucas N.S., Curran, P.J., Plummer, S.E. and Danson, F.M., 2000, Estimating the stem carbon production of a coniferous forest using an ecosystem simulation model driven by the remotely sensed red edge. *International Journal of Remote Sensing*, **21**: 619–632.

Luvall, J.C., Lieberman, D., Lieberman, M., Hartshorn, G.S. and Peralta, R., 1990, Estimation of tropical forest canopy temperature, thermal response number, and evapotranspiration using an aircraft-based thermal sensor. *Photogrammetric Engineering and Remote Sensing*, **56**: 1393–1401.

Luxmoore, R.J., Wullschleger, S.D. and Hanson, P.J., 1993, Forest responses to CO_2 enrichment and climate warming. *Water, Air and Soil Pollution*, **70**: 309–323.

Lymburner, L., Beggs, P.J. and Jacobson, C.R., 2000, Estimation of canopy-average surface-specific leaf area using Landsat TM data. *Photogrammetric Engineering and Remote Sensing*, **66**: 183–191.

McClain, E.P., Pichel, W.G. and Walton, C.C., 1985, Comparative performance of AVHRR-based multi-channel sea surface temperatures. *Journal of Geophysical Research*, **90**: 11587–11601.

McClean, C., Cherrill, A. and Fuller, R., 1995, The integration of three land classifications within a decision support system for land use planning. In Fisher, P. (ed.), *Innovations in GIS 2*. Taylor and Francis, London: 137–149.

McDonald, A.J., Gemmell, F.M. and Lewis, P.E., 1998, Investigation of the utility of spectral vegetation indices for determining information on coniferous forests. *Remote Sensing of Environment*, **66**: 250–272.

McMichael, C.E., Hope, A.S., Stow, D.A, Flemming, J.B., Vourlitis, G. and Oechel, W., 1999, Estimating CO_2 exchange at two sites in Arctic tundra ecosystems during the growing season using a spectral vegetation index. *International Journal of Remote Sensing*, **20**:683 – 698.

Magellan, 1999, *Magellan GPS 300 User Manual.* Ashtec, San Dimas.

Malingreau, J.P. and Belward, A.S., 1992, Scale considerations in vegetation monitoring using AVHRR data. *International Journal of Remote Sensing*, **13**: 2289–2307.

Malingreau, J.P. and Belward, A.S., 1994, Recent analysis in the European Community for the creation and analysis of global AVHRR data sets. *International Journal of Remote Sensing*, **15**: 3397–3416.

Malthus, T.M., Andrieu, B., Danson, F.M., Jaggard, K.W. and Steven, M.D., 1993, Candidate high spectral resolution infrared indices for crop cover. *Remote Sensing of Environment*, **46**: 204–212.

Mantovani, A.C.D.M. and Setzer, A.W., 1997, Deforestation detection in the Amazon. *International Journal of Remote Sensing*, **18**: 319–333.

Marceau, D.J., Howarth, P.J. and Gratton, D.J., 1994, Remote sensing and the measurement of geographical entities in a forests environment. 1. The scale and spatial aggregation problem. *Remote Sensing of Environment*, **49**: 93–104.

Marshall, J.D. and Waring R.H., 1986, Comparisons of methods of estimating leaf area index in old growth Douglas fir. *Ecology*, **67**: 975–979.

Martin, M.E., Newman, S.D., Aber, J.D. and Congalton, R.G., 1988, Determining forest species composition using high spectral resolution remote sensing data. *Remote Sensing of Environment*, **65**: 249–254.

Matarira, C.H. and Mwamuka, F.C., 1996, Vulnerability of Zimbabwe forests to global climate change. *Climate Research,* **6**: 135–136.

Mather, P.M., 1992, Remote sensing and geographical information systems. In Mather, P.M. (ed.), *TERRA-1: Understanding the Terrestrial Environment*. Taylor and Francis, London: 211–219.

Mather, P.M., 1999, *Computer Processing of Remotely-Sensed Images: An Introduction* (second edition). Wiley, Chichester.

Matson, P.A., Johnson, L., Billow, C., Miller, J. and Pu, R., 1994, Seasonal patterns and remote spectral estimation of canopy chemistry across the Oregon transect. *Ecological Applications*, **4**: 280–298.

Matthews, J.A., 1981, *Quantitative and Statistical Approaches to Geography: A Practical Manual.* Pergamon Press, Oxford.

Mattikali, N.M., Devereux, B.J. and Richards, K.S., 1995, Integration of remotely sensed satellite images with a geographical information system. *Computers and Geosciences*, **21**: 947–956.

Mauser, W. and Bach, H., 1994, Imaging spectroscopy in hydrology and agriculture- determination of model parameters. In Hill, J. and Mégier, J. (eds.), *Imaging Spectrometry: A Tool for Environmental Observations*. Kluwer, Dordrecht: 261–283.

Mayer, D.G., Stuart, M.A. and Swain, A.J., 1994, Regression of real-world data on model output: An appropriate overall test of validity. *Agricultural Systems*, **45**: 93–104.

Melillo J.M., Prentice, I.C., Farquhar, G.D., Schulze, E.D. and Sala, O.E., 1996, Terrestrial biotic responses to environmental change and feedbacks to climate. In Houghton, J.T., Filho, L.G.M., Challander, B.A., Harris, N., Kattenberg, A. and Maskell, K., (eds.), Climate Change 1995. Cambridge University Press, Cambridge: 445–482.

Merrill, E., Bramblebrodahi, M., Marrs, R. and Boyce, M., 1993, Estimation of green herbaceous phytomass from Landsat MSS data in Yellowstone National Park. *Journal of Range Management*, **46**: 151–157.

Merzlyak, M.N. and Gitelson, A., 1996, Signature analysis of leaf reflectance spectra: Algorithm development for remote sensing of chlorophyll. *Journal of Plant Physiology*, **148**: 494–500.

Michaud, J. and Sorooshain, S., 1994, Comparison of simple versus complex distributed runoff models on a midsized semiarid watershed. *Water Resources Research*, **30**: 593–605.

Middleton, E.M., Sullivan, J.H., Bovard, B.D., Deluca, A.J., Chan, S.S. and Cannon, T.A., 1997a, Seasonal variability in foliar characteristics and physiology for boreal forest species at the five Saskatchewan tower sites during the 1994 Boreal Ecosystem-Atmosphere Study. *Journal of Geophysical Research*, **102**: 28831–28844.

Middleton, E.M., Chan, S.S., Rusin, R.J. and Mitchell, S.K., 1997b, Optical properties of black spruce and jack pine needles at BOREAS sites in Sakatchewan, Canada. *Canadian Journal of Remote Sensing*, **23**: 108–119.

Miller, J.R., Hare, W. and Wu, J., 1990, Quantitative characterisation of the vegetation red edge reflectance, 1. An inverted-Gaussian reflectance model. *International Journal of Remote Sensing*, **11**: 1755–1773.

Milner, K., Running, S.W. and Coble, D.W., 1996, A biophysical soil-site model for estimating potential productivity of forested landscape. *Canadian Journal of Forest Research*, **26**: 1174–1186.

Milton, E.J., 1980, A portable multi-band radiometer for ground data collection in remote sensing. *International Journal of Remote Sensing*, **1**: 153–165.

Mitchell, J.F.B., 1983, The seasonal response of a general circulation model to changes in CO_2 and sea temperature. *Quarterly Journal of the Royal Meteorological Society*, **109**: 13–152.

Mitchell, P.L., 1997, Misuse of regression for empirical validation of models. *Agricultural Systems*, **54**: 313–326.

Mitchell, P.L. and Sheehy, J.E., 1997, Comparison of predictions and observations to assess model performance: A method of empirical validation. In Kropff, M.J., Teng, P.S., Aggarwal, P.K., Bouma, J., Bouman, B.A.M., Jones, J.W. and van Laar, H.H. (eds.), *Applications of System Approaches at the Field Level*. Kluwer, Dordrecht: 437–451.

Monte, L., Hakanson, L., Bergström, U., Brittain, J. and Heling, R., 1996, Uncertainty analysis and validation of environmental models: The empirically based uncertainty analysis. *Ecological Modelling*, **91**: 139–152.

Monteith, J.L., 1965, Evaporation and environment. In Fogg, G.E. (ed.), *The State and Movement of Water in Living Organisms*. Society for Experimental Biology Symposium, XIX, Cambridge University Press, Cambridge: 205–233.

Mooney, H.A. and Hobbs, R.J., 1989, Introduction. In Hobbs, R.J. and Mooney, H.A. (eds.), *Remote Sensing of Biosphere Functioning*, Springer-Verlag, New York: 1–4.

Mooney, H.A., Drake, B.G., Luxmoore, R.J., Ochel, W.C. and Pitelka, L.F., 1991, Predicting ecosystem responses to elevated CO_2 concentrations. *Bioscience,* **41**: 96–104.

Moore, B., 1999, International Geosphere-Biosphere Programme: A study of global change, some reflections. In Steffen, W. (ed.), *IGBP Global Change Newsletter*, **40**: 1–3.

Moore, R.D. and J.C. Thompson, 1996, Are water table variations in a shallow forest soil consistent with the TOPMODEL concept? *Water Resources Research*, **32**: 663–669.

Murray, M.B., Leith, I.D. and Jarvis, P.G., 1996, The effect of long term CO_2 enrichment on the growth, biomass partitioning and mineral nutrition of *Sitka* spruce. *Trees,* **10**: 393–402.

Murtha, P.A., 1977, *A Guide to Air Photo Interpretation of Forest Damage in Canada.* Canadian Forestry Service, Ottawa.

Murtha, P.A., 1983, Some air-photo scale effects on Douglas fir damage type interpretation. *Photogrammetric Engineering and Remote Sensing*, **49**: 327–335.

Myers, D.E., 1983, Estimation of linear combinations and cokriging. *Mathematical Geology*, **15**: 633–637.

Myneni, R.B., Hall, F.G., Sellers, P.J. and Marshak, A.L., 1995, The interpretation of spectral vegetation indices. *IEEE Transactions on Geoscience and Remote Sensing*, **33**: 481–486.

Myneni, R.B., Keeling, C.D., Tucker, C.J., Asrar, G. and Nemani, R.R., 1997, Increased plant growth in northern high latitudes from 1981 to 1991. *Nature*, **386**: 698–702.

Nash, M., Toorman, A. and Wierenga, P., 1992, Estimation of vegetation curves in an arid rangeland based on soil moisture using co-kriging. *Soil Science*, **154**: 25–36.

Nel, E.M. and Wessman, C.A., 1995, Canopy transmittance models for estimating leaf area index. *Canadian Journal of Forest Research*, **21**: 356–368.

Nemani, R.R. and Running, S.W., 1989a, Testing a theoretical climate soil leaf area hydrologic equilibrium of forests using satellite data and ecosystem simulation. *Agricultural and Forest Meteorology,* **44**, 245–260.

Nemani, R.R. and Running, S.W., 1989b, Estimation of regional surface evapotranspiration from NDVI and thermal IR AVHRR data. *Journal of Applied Meteorology*, **28**: 276–284.

Nemani, R.R, Running, S.W., Band, L.E. and Peterson, D.L., 1992, Regional hydro-ecological simulation system: An illustration of the integration of ecosystem models in a GIS. In Goodchild, M., Parks, B. and Skywert, L. (eds.), *Environmental Modelling with GIS.* Oxford University Press, Oxford: 296–304.

Nemani, R.R., Pierce, L. and Running, S.W., 1993a, Forest ecosystem processes at the watershed scale: Sensitivity to remotely sensed leaf area index estimates. *International Journal of Remote Sensing,* **14**: 2519–2534.

Nemani, R.R., Pierce, L., Running, S.W. and Goward, S., 1993b, Developing satellite-derived estimates of surface moisture status. *Journal of Applied Meteorology*, **32**: 548–557.

Nerry, F., Petitcolin, F. and Stoll, M.P., 1998, Bidirectional reflectivity in AVHRR channel 3: Application to a region in northern Africa. *Remote Sensing of Environment*, **66**: 298–316.

New, M., Hulme, M. and Jones, P.D., 1999, Representing twentieth century space-time climate variability. Part 1: Development of a 1961-1990 mean monthly terrestrial climatology. *Journal of Climate*, **12**: 829–856.

Nichol, J.E., 1995, Monitoring tropical rain forest microclimate. *Photogrammetric Engineering and Remote Sensing*, **61**: 1159–1165.

Nicholls, N., Gruza, G.V., Jouzel, J., Karl, T.R., Ogallo, L.A. and Parker, D.E., 1996, Observed climate variability and change. In Houghton, J.T., Filho, L.G.M., Challander, B.A., Harris, N., Kattenberg, A. and Maskell, K., (eds.), Climate Change 1995. Cambridge University Press, Cambridge: 133-192.Oliver, C.D. and Larson, B.C., 1996, *Forest Stand Dynamics*. Wiley, New York.

Nilson, A., Kiviste, A., Korjus, H., Mihkelson, S., Etverk, I. and Oja, T., 1999, Impact of recent and future climate change on Estonian forestry and adaptation tools. *Climate Research*, **12**: 205–214.

Nobel, P.S., 1991, *Physiochemical and Environmental Plant Physiology*. Academic Press, New York.

North, P.R.J., 1996, Three-dimensional forest light interaction model using a Monte Carlo method. *IEEE Transactions on Geoscience and Remote Sensing*, **34**: 946–56.

Norman, J.M., Welles, J.M. and Walter, E.A., 1985, Contrasts among bidirectional reflectance of leaves, canopies and soils. *IEEE Transactions on Geosciences and Remote Sensing*, **23**: 695–704.

Norman, J.M. and Campbell, G.S., 1989, Canopy structure. In Pearcy, R.W., Ehleringer, J., Mooney, H.A. and Rundel P.W. (eds.), *Plant Physiological Ecology: Field Methods and Instrumentation*. Chapman and Hall, New York: 301–326.

O'Riordan, T., (ed.), 2000, *Environmental Science for Environmental Management* (second edition). Prentice Hall, Harlow.

Oliver, C.D. and Larson, B., 1996, *Forest Stand Dynamics* (second edition). Wiley, New York.

Openshaw, S., 1984, *Modifiable Areal Unit Problem*. CATMOG No. 38, GeoAbstracts, Norwich.

Osborne, B.G. and Fearn, T., 1986, *Near Infrared Spectroscopy in Food Analysis*. Longman, London.

Olioso, A., 1995, Simulating the relationship between thermal emissivity and the normalised difference vegetation index. *International Journal of Remote Sensing*, **16**: 3211–3216.

Oliver, C.D. and Larson, B., 1996, *Forest Stand Dynamics* (second edition). Wiley, New York.

Parry, M., Arnell, N.W., Hulme, M., Nicholls, R. and Livermore, M., 1998, No room for complacency over climate. *Nature*, **396**: 509.

Parry, M., Arnell, N.W., Hulme, M., Martens, P., Nicholls, R. and White, A., 1999, The global impact of climate change: A new assessment. *Global Environmental Change*, **9** (Supplementary Issue): 1–2.

Parton, W.J., Scurlock, J.M.O., Ojima, D.S., Gilmanov, T.G., Scholes, R.J., Schimel, D.S., Kirchner, T., Menaut, J-C., Seastedt, T., Moya, G.E., Kamnalrut, A. and Kinyamario, J.I., 1993, Observations and modelling of biomass and soil organic matter dynamics for the grassland biome world-wide. *Global Biogeochemical Cycles*, **7**: 785–809.

Parton, W.J., Schimel, D.S., Cole, C.V. and Ojima, D.S., 1987, Analysis of factors controlling soil organic matter levels in Great Plains' grasslands. *Soil Science Society of America Journal,* **51**: 1173–1179.

Paruelo, J.M. and Sala, O.E., 1995, Water losses in the Patagonian steppe: A modelling approach. *Ecology*, **76**: 510–520.

Pastor, J. and Post, W.M., 1988, Response of northern forests to CO_2-induced climate change. *Nature,* **334**: 55–58.

Pate-Cornell, E., 1996, Uncertainties in global climate change estimates: An editorial essay. *Climatic Change,* **33**: 145–149.

Pebesma, E.J., 1997, *Gstat User Manual.* University of Amsterdam, Amsterdam.

Pebesma, E.J. and Wesseling, C.G., 1998, Gstat: a program for geostatistical modelling, prediction and simulation. *Computers and Geosciences*, **24**: 17–31.

Peddle, D., Hall, F.G. and LeDrew, E.F., 1996, Remote Sensing of boreal forest biophysical variables using spectral mixture analysis and a canopy reflectance model. *Proceedings of the 18th Canadian Symposium on Remote Sensing: Vancouver.* Canadian Aeronautics and Space Institute, Ottawa: 418–421.

Peddle, D.R., Hall, F.G., Ledrew, E.F. and Knapp, D.E., 1997, Classification of forest land cover in BOREAS. II: Comparison of results from a sub-pixel scale physical modelling approach and a training based method. *Canadian Journal of Remote Sensing*, **23**: 131–142.

Peddle, D.R., Hall, F.G. and LeDrew, E.F., 1999, Spectral mixture analysis and geometric-optical reflectance modelling of boreal forest biophysical structure. *Remote Sensing of Environment,* **67**: 288–297.

Pedley, M.I. and Curran, P.J., 1991, Per-field classification: An example using SPOT HRV imagery. *International Journal of Remote Sens*ing, **12**: 2181–2192.

Peñuelas, J., Filella, I., Biel, C., Serrano, L. and Save, R., 1993, The reflectance at the 950–970 nm region as an indicator of plant water status. *International Journal of Remote Sensing*, **14**: 1887–1905.

Pereira, J.M.C., 1999, A comparative evaluation of NOAA AVHRR vegetation indexes for burned surface detection and mapping. *IEEE Transactions on Geoscience and Remote Sensing*, **37**: 217–226.

Perruchoud, D.O. and Fischlin, A., 1995, The response of the carbon cycle in undisturbed forest ecosystems to climate change: A review of plant soil models. *Journal of Biogeography*, **22**: 759–774.

Perry, C.R. (Jr.) and Lautenschlager, L.F., 1984, Functional equivalence of spectral vegetation indices. *Remote Sensing of Environment*, **14**: 169–182.

Peterson, D.L., Spanner, M.A., Running, S.W. and Teuber, K.B., 1987, Relationships of Thematic Mapper Simulator data to leaf area index of temperate coniferous forests. *Remote Sensing of Environment*, **22**: 323–341.

Peterson, D.L. and Running, S.W., 1989, Applications in forest science and management. In Asrar, G. (ed.), *Theory and Applications of Optical Remote Sensing*. Wiley, New York: 429–473.

Peterson, D.L. and Waring, R.H., 1994, Overview of the Oregon transect ecosystem research project. *Ecological Applications*, **4**: 211–225.

Petrou, M. and Foschi, P.G., 1999, Confidence in linear spectral unmixing of single pixels. *IEEE Transactions on Geoscience and Remote Sensing*, **37**: 624–626.

Philpot, W., Duggin, M., Raba, R. and Tsai, F., 1996, Analysis of reflectance and fluorescence spectra for atypical features: Fluorescence in the yellow-green. *Journal of Plant Physiology*, **148**: 567–573.

Phipps, R.L., 1985, *Collecting, Preparing, Cross-Dating and Measuring Tree Increment Cores*. USGS, Reston.

Pierce, L.L. and Running, S.W., 1988, Rapid estimation of coniferous forest canopy leaf area index using a portable integration radiometer. *Ecology*, **69**: 1762–1767.

Pierce, LL., Running, S.W. and Walker, J., 1994, Regional scale relationships of leaf area index to specific leaf area and leaf nitrogen content. *Ecological Applications*, **4**: 313–321.

Pierce, L.L. and Running, S.W., 1995, The effects of aggregating sub-grid land surface variation on large-scale estimates of net primary production. *Landscape Ecology*, **10**: 239–253.

Pinar, A. and Curran, P.J., 1996, Grass chlorophyll and the reflectance red edge. *International Journal of Remote Sensing*, **17**: 351–357.

Pinty, B. and Verstraete, M.M., 1992, GEMI: A non-linear index to monitor global vegetation from satellites. *Vegetatio*, **101**: 15–20.

Pinty, B., Leprieur, C. and Verstraete, M.M., 1993, Towards a quantitative interpretation of vegetation indices. Part 1: Biophysical canopy properties and classical indices. *Remote Sensing Reviews*, **7**: 127–150.

Plummer, S.E., Danson, F.E., Curran, P.J., Foody, G.M., Green, R.M., Kupiec, J.A., Lucas, N.S., McCulloch, M.B. and Smith, G.M., 1993, Driving an ecosystem model with remotely sensed data. *25th International Symposium, Remote Sensing and Global Environmental Change*. University of Michigan, Ann Arbor: 374–384.

Plummer, S.E., Danson, F.M. and Wilson, A.K., 1995, Advances in remote sensing technology. In Danson, F.M. and Plummer, S.E. (eds.), *Advances in Environmental Remote Sensing*. Wiley, Chichester: 1–7.

Plummer, S.E., Lucas, N.S. and Curran, P.J., 1997, *Report of the BOREAS Intensive Field Campaign 1994.* Remote Sensing Applications Development Unit Report No. 97/5. British National Space Centre, London.

Poole, M.A. and O'Farrell, P.N., 1971, The assumptions of the linear regression model. *Transactions of the Institute of British Geographers*, **52**: 145–158.

Post, W.M., 1990, *Report of a Workshop on Climate Feedbacks and the Role of Peatland, Tundra and Boreal Ecosystems in the Global Carbon Cycle.* Oak Ridge National Laboratory, Tennessee.

Prentice, K.C. and Fung, I.Y., 1990, The sensitivity of terrestrial carbon storage to climate change. *Nature,* **346**: 48–51.

Price, J.C., 1983, Estimating surface temperature from satellite thermal infrared data: A simple formulation of the atmospheric effect. *Remote Sensing of Environment*, **13**: 353–361.

Price, J.C., 1984, Land surface temperature measurements from the split window channels of the NOAA-7 AVHRR. *Journal of Geophysical Research*, **89**: 7231–7237.

Price, J.C., 1989, Quantitative aspects of remote sensing in the thermal infrared. In Asrar, G. (ed.), *Theory and Applications of Optical Remote Sensing*. Wiley, New York: 578–603.

Price, D.T. and Apps, M.J., 1996, Boreal forest responses to climate-change scenarios along an ecoclimatic transect in central Canada. *Climatic Change,* **34**: 179–190.

Price, D.T., Apps, M.J., Kurz, W.A., Prentice, I.C. and Sykes, M.T., 1993, Simulating the carbon budget of the Canadian boreal forest using an integrated suite of process-based models. In Chang, C.H. (ed.), *Forest Growth Models and their Uses. Proceedings of the International Workshop on Natural Resources, Canada.* Canadian Forest Service, Quebec: 251–264.

Prince, S.D., Bessemoulin, P., Brouwer, J., 1994, Geographical, biological and remote sensing aspects of the Hydrological Atmospheric Pilot Experiment in the Sahel (HAPEX-Sahel). *Remote Sensing of Environment,* **51**: 38–47.

Privette, J.L., Myneni, R.B. and Emery, W.J., 1996, Optical sampling conditions for estimating grassland parameters via reflectance model inversions. *IEEE Transactions on Geoscience and Remote Sensing*, **34**: 272–383.

Qi, J., Chehbouni, A., Huete, A.R., Kerr, Y.H. and Sorooshian, S., 1994, A modified soil adjusted vegetation index. *Remote Sensing of Environment*, **48**: 119–126.

Ranson, K.J., Caugherty, C.S.T., Biehl, L.L. and Bauer, M.E., 1986, Sun angle, view angle and background effects on spectral response of simulated balsam fir canopies. *Photogrammetric Engineering and Remote Sensing*, **52**: 649–658.

Ranson, K.J., Sun, G., Lang, R.H., Chauhan, N.S., Cacciola, R.J. and Kilic, O., 1997, Mapping of boreal forest biomass from spaceborne synthetic aperture radar. *Journal of Geophysical Research*, **102**: 29599–29610.

Rao, C.R.N., 1995, Calibration formulae for the visible and near-infrared channels of the Advanced Very High Resolution Radiometer on board the NOAA-7, -9 and -11 spacecraft, an update.

Report to NOAA/NESDIS Satellite Research Laboratory. US Department of Commerce, Washington DC.

Rao, C.R.N., Holmes, S.J., Anderson, R.K., Winston, J.S. and Lehr, P.E., 1990, *Weather Satellites: Systems, Data and Environmental Applications*. American Meteorological Society, Boston.

Rao, C.R.N., Chen, J., Zhang, N., Sullivan, J.T., Walton, C.C. and Weinreb, M.P., 1996, Calibration of meteorological satellite sensors. *Advances in Space Research*, **17**: 11–20.

Rasmussen, M.S., 1998a, Developing simple, operational, consistent NDVI-vegetation models by applying environmental and climatic information. Part II: Crop yield assessment. *International Journal of Remote Sensing*, **19**: 119–139.

Rasmussen, M.S., 1998b, Developing simple, operational, consistent NDVI-vegetation models by applying environmental and climatic information. Part I: Assessment of net primary production. *International Journal of Remote Sensing*, **19**: 97–117.

Rast, M., Bézy, J.L. and Bruzzi, S., 1999, The ESA Medium Resolution Imaging Spectrometer MERIS: A review of the instrument and its mission. *International Journal of Remote Sensing*, **20**: 1691–1702.

Rastetter, E.B., 1996, Validating models of ecosystem response to global change. *Bioscience*, **46**: 190–198.

Rayment, M.B. and Jarvis, P.G., 1997, An improved open chamber system for measuring soil CO_2 effluxes in the field. *Journal of Geophysical Research*, **102**: 28779–28784.

Reckhow, K.H., Clements, J.T. and Dodds, R.C., 1990, Statistical evaluation of mechanistic water-quality models. *Journal of Environmental Engineering*, **116**: 250–268.

Reich, P.B., Turner, D. and Bolstad, P., 1999, An approach to spatially distributed modelling of net primary production at the landscape scale and its application in validating EOS NPP products. *Remote Sensing of Environment*, **70**: 69–81.

Rencz, A.N. (ed.), 1999, *Remote Sensing for the Earth Sciences: Manual of Remote Sensing, Volume 3* (third edition). Wiley, New York.

Rhind, D.W. and Green, N.P.A., 1988, Design of a Geographical Information System for a heterogeneous scientific community. *Proceedings of the GIS Conference,* British Geological Survey, Nottingham. Volume 2: Selected Papers. NERC, Swindon: 39–57.

Rich, P.M., 1990, Characterising plant canopies with hemispherical photographs. *Remote Sensing Reviews*, **5**: 13–29.

Rich, P.M., Clark, D.A., Clark, D.B. and Oberbauer, S.F., 1993, Long-term study of solar radiation regimes in a tropical wet forest using quantum sensors and hemispherical photography. *Agricultural and Forest Meteorology*, **65**:107–127.

Richards, J.A., 1993, *Remote Sensing Digital Image Analysis: An Introduction* (second edition). Springer-Verlag, Berlin.

Riedo, M., Gyalistras, D. and Fischlin, A., 1999, Using an ecosystem model linked to GCM-derived local weather scenarios to analyse effects of climate change and elevated CO_2 on dry matter

production and partitioning and water use in temperate managed grasslands. *Global Change Biology*, **5**: 213–223.

Roberts, D.A., Green, R.O. and Adams, J.B., 1997, Temporal and spatial patterns in vegetation and atmospheric properties from AVIRIS. *Remote Sensing of Environment*, **62**: 223–240.

Robertson, B., Erickson, A., Friedel, J., Guindon, B., Fisher, T., Brown, R., Teillet, P., D'iorio, M., Cihlar, J. and Sancz, A., 1992, GEOCOMP, a NOAA AVHRR geocoding and compositing system. *Proceedings of the International Society of Photogrammetry and Remote Sensing Conference*. ISPRS, Washington DC: 223–228.

Rock, B.N., Hoshizaki, T. and Miller, J.R., 1988, Comparison of *in situ* and airborne spectral measurements of blue shift associated with forest decline. *Remote Sensing of Environment,* **24**: 109–127.

Rock, B.N., Williams, D.L., Moss, D.M., Lauten, G.N. and Kim, M., 1994, High-spectral resolution field and laboratory optical reflectance measurements of red spruce and eastern Hemlock needles and branches. *Remote Sensing of Environment*, **47**: 176–189.

Roger, J.C. and Vermote, E.F., 1998, A method to retrieve the reflectivity signature at 3.75 μm from AVHRR data. *Remote Sensing of Environment,* **64**: 103–114.

Rossi, R.E., 2000, How the support effect affects summary statistics. *Geostatistics* (submitted)

Rossi, R.E., Dungan, J. and Beck, L., 1994, Kriging in the shadows: Geostatistical interpolation for remote sensing. *Remote Sensing of Environment*, **49**: 32–40.

Roughgarden, J., Running, S.W. and Matson, P.A., 1991, What does remote sensing do for ecology? *Ecology*, **72**: 1918–1922.

Rouse, J.W., Haas, R.H., Shell, J.A and Deering, D.W., 1973, Monitoring vegetation systems in the Great Plains with ERTS-1. *Earth Resources Technology Satellite Symposia*, **1**: 309–317.

Running, S.W., 1984, Documentation and preliminary validation of H_2OTRANS and DAYTRANS, two models for predicting transpiration and water stress in western coniferous forests. *USDA Forest Service Rocky Mountain Forest and Range Experiment Station Research Paper*, **252**: 1–45.

Running, S.W., 1990, Estimating terrestrial primary productivity by combining remote sensing and ecosystem simulation. In Hobbs, R.J. and Mooney, H.A. (eds.), *Remote Sensing of Biosphere Functioning*. Springer-Verlag, New York: 65–86.

Running, S.W., 1994, Testing FOREST-BGC ecosystem process simulations across a climatic gradient in Oregon. *Ecological Applications,* **4**: 238–247.

Running, S.W., Peterson, D.L., Spanner, M.A. and Teuber, K.B., 1986, Remote sensing of coniferous leaf area. *Ecology,* **67**: 273–276.

Running, S.W, Nemani, R.R. and Hungerford, R.D., 1987, Extrapolation of synoptic meteorological data in mountainous terrain and its use for simulating forest evapotranspiration and photosynthesis. *Canadian Journal of Forest Research*, **17**: 472–483.

Running, S.W. and Coughlan, J.C., 1988, A general model of forest ecosystem processes for regional applications; I. Hydrologic balance, canopy gas exchange and primary production processes. *Ecological Modelling,* **42**: 125–154.

Running, S.W. and Nemani, R.R., 1988, Relating seasonal patterns of the AVHRR vegetation index to simulated photosynthesis and transpiration of forests in different climates. *Remote Sensing of Environment*, **24**: 347–367.

Running, S.W., Nemani, R.R., Peterson, D.L., Band, L.E., Potts, D.F., Pierce, L.L., and Spanner, M.A., 1989, Mapping regional forest evapotranspiration and photosynthesis by coupling satellite data with ecosystem simulation. *Ecology,* **70**: 1090–1101.

Running, S.W. and Nemani, R.R., 1991, Regional hydrologic and carbon balance responses of forests resulting from potential climate change. *Climatic Change*, **19**: 349–368.

Running, S.W. and Gower, S.T., 1991, FOREST-BGC, a general model of forest ecosystem processes for regional applications. II. Dynamic carbon allocation and nitrogen budgets. *Tree Physiology,* **9**: 147–160.

Running, S.W. and Hunt, E.R. (Jr.), 1993, Generalisation of a forest ecosystem process model for other biomes, BIOME-BGC and an application for global scale models. In Ehleringer, J.R. and Field, C.B. (eds.), *Scaling Physiological Processes: Leaf to Globe*, Academic Press, San Diego: 156–169.

Running, S.W, Loveland, T.R., Pierce, L.L., Nemani, R.R., and Hunt, E.R. (Jr.), 1995, A remote sensing based vegetation classification logic for global land cover analysis. *Remote Sensing of Environment*, **51**: 39–48.

Running, S.W., Baldocchi, D.D., Turner, D.P., Gower, S.T., Bakwin, P.S. and Hibbard, K.A., 1999, A global terrestrial monitoring network integrating tower fluxes, flask sampling, ecosystem modelling and EOS satellite data. *Remote Sensing of Environment*, **70**: 108–127.

Ryan, M.G., 1991, A simple method for estimating gross carbon budgets for vegetation in forest ecosystems. *Tree Physiology*, **9**: 255–266.

Ryan, M.G., Lavigne, M.B. and Gower, S.T., 1997, Annual carbon cost of autotrophic respiration in boreal forestecosystems in relation to species and climate. *Journal of Geophysical Research*, **102**: 28871–28884.

Ryherd, S. and Woodcock, C., 1996, Combining spectral and texture data in the segmentation of remotely sensed images. *Photogrammetric Engineering and Remote Sensing*, **62**: 181–192.

Sader, S.A., Waide, R.B., Lawrence, W.T. and Joyce, A.T., 1989, Tropical forest biomass and successional age class relationships to a vegetation index derived from Landsat TM data. *Remote Sensing of Environment*, **28**: 143–156.

Sader, S.A., Douglas, A. and Liou, W.S., 1995, Accuracy of Landsat TM and GIS rule-based methods for forest wetland classification in Maine. *Remote Sensing of Environment*, **53**: 133–144.

Sahagian, D. (ed.), 1997, *Research GAIM: The Newsletter of the Global Analysis, Interpretation and Modelling Task Force*, **1**. IGBP, Stockholm.
(URL http://gaim.unh.edu/News/Winter97/).

Salisbury, F.B. and Ross, C.W., 1992, *Plant Physiology* (fourth edition). Wadsworth, California.

Salisbury, J.W., Milton, N.M. and Walsh, P., 1987, Significance of non-isotropic scattering from vegetation for geobotanical remote sensing. *International Journal of Remote Sensing*, **8**: 997–1009.

Sampson, R.N., Apps, M.J., Brown, S., Cole, C.V., Downing, J., Heath, L.S., Ojima, D.S., Smith, T.M., Solomon, A.M. and Wisniewski, J., 1993, Workshop summary statement, terrestrial biospheric carbon fluxes: Quantification of sinks and sources of CO_2. *Water, Air and Soil Pollution*, **70**: 3–15.

Santantonio, D., Hermann, R.K. and Overton, W.S., 1977, Root biomass studies in forest ecosystems. *Pedobiologia*, **17**: 1–31.

Santantonio, D., 1988, Correction. *Canadian Journal of Forest Research*, **18**: 651–657.

Sasamal, S.K., 1999, Sea surface temperature of North Indian Ocean during April 1998. *International Journal of Remote Sensing*, **20**: 2485–2490.

Schanda, E., 1986, *Physical Fundamentals of Remote Sensing*. Springer-Verlag, New York.

Schellnhuber, H.J., 1999, 'Earth system' analysis and the second Copernican revolution. *Nature*, **402**: c19–c22.

Schenoi, S.C., 1999, On the suitability of global algorithms for the retrieval of SST from the North Indian Ocean using NOAA AVHRR data. *International Journal of Remote Sensing*, **20**: 11–29.

Schimel, D.S., 1998, The carbon equation. *Nature*, **393**: 208–209.

Schimel, D.S., Wessman, C.A., Parton, W., Curtiss, B., Knapp, A. and Seastedt, T., 1990, Modelling of terrestrial ecosystems with remotely sensed inputs. *Proceedings, International Geosciences and Remote Sensing Symposium*, **1**: 557.

Schimel, D., 1994, Radiative forcing of climate change and an evaluation of the IPCC IS92 emission scenarios. In Houghton, J.T. (ed.), *Climate Change in 1994*. Cambridge University Press, Cambridge: 39–71.

Schimel, D., Alves, D., Enting, I., Heimann, M., Joos, F., Raynaud, D. and Wigley, T., 1996, Radiative forcing of climate. In Houghton, J.T., Filho, L.G.M., Challander, B.A., Harris, N., Kattenberg, A. and Maskell, K., (eds.), Climate Change 1995. Cambridge University Press, Cambridge: 65–132.

Schmugge, D.A., 1991, *Land Surface Evaporation: Measurement and Parameterisation*. Springer-Verlag, New York.

Schmugge, D.A. and Jackson, T.J., 1996, Soil moisture variability. In Stewart, J.B., Engman, E.T., Feddes, R.A. and Kerr, Y. (eds.), *Scaling up in Hydrology Using Remote Sensing*. Wiley, Chichester: 183–192.

Schowalter, T.D., Hargrove, W.W. and Crossley, D.A., 1986, Herbivory in forest ecosystems. *Annual Review of Entomology*, **31**: 177–196.

Schowengerdt, R.A., 1996, On the estimation of spatial-spectral mixing with classifier likelihood functions. *Pattern Recognition Letters*, **17**: 1379–1387.

Schulze, E.D., Kelliher, F.M., Körner, C., Lloyd, J. and Leuning, R., 1994, Relationships among maximum stomatal conductance, carbon assimilation rate, and plant nitrogen nutrition: A global ecology scaling exercise. *Annual Review of Ecology and Systematics*, **25**: 629–660.

Sedjo, R.A., 1993, The carbon cycle and global forest ecosystems. *Water, Air and Soil Pollution*, **70**: 295–307.

Seguin, B., Assad, E., Freteaud, J.P., Imbernon, J., Kerr, Y.H. and Lagouarde, J.P., 1989, Use of meteorological satellite for water balance monitoring in Sahelian regions. *International Journal of Remote Sensing*, **10**: 1001–1017.

Sellers, P.J., 1985, Canopy reflectance, photosynthesis and transpiration. *International Journal of Remote Sensing*, **6**: 1335–1372.

Sellers, P.J., 1987, Canopy reflectance, photosynthesis and transpiration II: The rôle of biophysics in the linearity of their interdependence. *Remote Sensing of Environment*, **21**: 143–183.

Sellers, P.J., Mintz, Y., Sud, Y.C., and Dalcher, A., 1986, A simple biosphere model (SiB) for use with general circulation models. *Journal of Atmospheric Sciences*, **43**: 505–531.

Sellers, P.J., Hall, F.G., Asrar, G., Strebel, D.E. and Murphy, R.E, 1988, The first ISLSCP field experiment (FIFE). *Bulletin of the American Meteorological Society*, **69**: 22–27.

Sellers, P.J., Hall, F.G., Margolis, H., Cihlar, J., and Ryan, M.G., 1991, Charting the boreal forest's role in global change. *EOS Transactions of the American Geophysical Union*, **72**: 33–35.

Sellers, P.J. and Hall, F.G. (eds.), 1992, FIFE Special Issue. *Journal of Geophysical Research*, **97**: 18343–19109.

Sellers, P.J., Berry, J.A., Collatz, G.J., Field, C.B. and Hall, F.G., 1992, Canopy reflectance, photosynthesis and transpiration. III: A reanalysis using improved leaf modles and a new canopy integration scheme. *Remote Sensing of Environment*, **42**: 187–216.

Sellers, P.J., Nobre, C.A., Fitzjarrald, D.J, Try, P.D. and Lucid, D.T., 1993, LAMBADA-BATERISTA: *A Preliminary Science Plan for a Large Scale Biosphere-Atmosphere Field Experiment in the Amazon Basin*. ISLSCP, IGPO, Washington DC.

Sellers, P.J., Tucker, C.J., Collata, G.J., Los, S.O., Justice, C.O., Dazlich, D.A. and Randall, D.A., 1994, A global one degree by one degree NDVI data set for climate studies. 2. The generation of global fields of terrestrial biophysical parameters from the NDVI. *International Journal of Remote Sensing*, **15**: 3519–3545.

Sellers, P.J., Meeson, B.W., Hall, F.G., Asrar, G., Murphy, R.E., Schiffer, R.A., Bretherton, F.P., Dickenson, R.E., Ellingson, R.G., Field, C.B., Huemmrich, K.F., Justice, C.O., Melack, J.M., Roulet, N.T., Schimel, D.S. and Try, P.D., 1995a, Remote sensing of the land surface for

studies of global change: Models-algorithms-experiments. *Remote Sensing of Environment,* **51**: 3–26.

Sellers, P.J., Hall, F.G., Margolis, H., Kelly, B., Baldocchi, D., den Hartog, G., Cihlar, J., Ryan, M.G., Goodison, B., Crill, P., Ranson, K.J., Lettenmaier, D. and Wickland, D.E., 1995b, The Boreal Ecosystem-Atmosphere Study (BOREAS): An overview and early results from the 1994 field year. *Bulletin of the American Meteorological Society,* **76**: 1549–1577.

Sellers, P.J., Randall, D.A., Collatz, G.J., Berry, J., Field, C., Dazlich, D.A. and Zhang, C., 1996a, A revised land-surface parametrisation (SiB2) for atmospheric GCMs. Part 1: Model formulation. *Journal of Climate*, **9**: 738–763.

Sellers, P.J., Hall, F.G., Baldocchi, D., Black, A., Goodison, B., Berry, J. and Ryan, M.G., 1996b, Comparison of radiative and physiological effects of doubled atmospheric CO_2 on continental climate. *Science*, **271**: 1402–1406.

Sellers, P.J., Hall, F.G., Kelly, R.D., Black, A., Baldocchi, D., Berry, J., Ryan, M.G., Ranson, K.J., Crill, P.M., Lettenmaier, D., Margolis, H., Cihlar, J., Newcomer, J., Fitzjarrald, D., Jarvis, P.G., Gower, S.T., Halliwell, D., Williams, D., Goodison, B., Wickland, D.E. and Guertin, F.E., 1997, BOREAS in 1997: Experiment overview, scientific results and future directions. *Journal of Geophysical Research,* **102**: 28731–28769.

Senftle, J., 1997, ECS successfully demonstrates launch ready capabilities. *The Earth Observer*, **22**. NASA, Maryland.

Shapiro, M. and Waupotitsch, O., 1993, *GRASS 4.1 Reference Manual.* U.S. Army Construction Engineering Research Laboratory, Illinois.

Shaw, G. and Wheeler, D., 1985, *Statistical Techniques in Geographical Analysis.* Wiley, New York.

Shimabukuro, Y.E., Holben, B.J. and Tucker, C.J., 1994, Fraction images derived from NOAA AVHRR data for studying the deforestation in the Brazilian Amazon. *International Journal of Remote Sensing*, **15**: 517–520.

Shugart, H.H. and Urban, D.L., 1989, Factors affecting the relative abundance of forest tree species. In Grubb, P.J. and Whittaker, J.B. (eds.), *Toward a More Exact Ecology.* Blackwell, Oxford: 249–273.

Siddiqui, K.M., Mohammad, I. And Ayaz, M., 1999, Forest ecosystem climate change impact assessment and adaptation strategies for Pakistan. *Climate Research*, **12**: 195–203.

Siegenthaler, H. and Sarmiento, J.L., 1993, Atmospheric carbon dioxide and the ocean. *Nature*, **365**: 119–125.

Sigrist, P., Coppin, P. and Hermy, M., 1999, Impact of forest canopy on quality and accuracy of GPS measurements. *International Journal of Remote Sensing*, **20**: 3595–3610.

Singh, T., 1982, *Biomass Equations for Ten Major Tree Species of the Prairie Provinces*, Information Report NOR-X-242, Canadian Forest Service, Edmonton.

Slaughter, C.W., Glotov, V.Y., Viereck, L.A. and Mikhailov, V.M., 1995, Boreal forest catchments: Research sites for global change at high latitudes. *Water, Air and Soil Pollution*, **82**: 351–361.

Smith, G.M., 1994, *Towards the Remote Sensing of Foliar Chemistry.* Unpublished Ph.D. Thesis, University of Wales Swansea, Swansea.

Smith, G.M., Fuller, R.M., Amable, G., Costa, C. and Devereux, B.J., 1997, CLEVER-Mapping: An implementation of a per-parcel classification procedure within an integrated GIS environment. *RSS'97: Observations and Interactions.* Remote Sensing Society, Nottingham: 21–26.

Smith, G.M., Fuller, R.M., Costa, C. and Devereux, B.J., 1998, An integrated vector/raster system for land cover mapping. *IEE Colloquium Digest – Integrated Systems for Commercial Remote Sensing Applications.* The Institute of Electrical Engineers, London: 1–6.

Smith, G.M. and Curran, P.J., 1999, Methods for estimating image signal-to-noise ratio (SNR). In Atkinson, P.M. and Tate, N.J. (eds.), *Advances in Remote Sensing and GIS Analysis.* Wiley, Chichester: 61–74.

Smith, G.M. and Milton, E.J., 1999, The use of the empirical line method to calibrate remotely sensed data to reflectance. *International Journal of Remote Sensing*, **20**: 2653–2662.

Smith, T.M., Leemans, R. and Shugart, H.H., 1992, Sensitivity of terrestrial carbon storage to CO_2 induced climate change: Comparison of four scenarios based on general circulation models. *Climatic Change,* **21**: 367–384.

Smith, T.M. and Shugart, H.H., 1993, The transient response of terrestrial carbon storage to a perturbed climate. *Nature,* **361**: 523–526.

Smith, T.M., Cramer, W.P., Dixon, R.K., Leemans, R., Neilson, R.P. and Solomon, A.M., 1993, The global terrestrial carbon cycle. *Water, Air and Soil Pollution,* **70**: 19–37.

Solomon, A.M., Prentice, I.C., Leemans, R. and Cramer, W.P., 1993, The interaction of climate and land use in future terrestrial carbon storage and release. *Water, Air and Soil Pollution,* **70**: 595–614.

Solomon, A.M. and Leemans, R., 1997, Boreal forest carbon stocks and wood supply: Past, present and future responses to changing climate, agriculture and species availability. *Agricultural and Forest Meteorology*, **84**: 137–151.

Spanner, M.A., Bass, J.A. and Peterson, D.L., 1984, Feature selection and the information content of Thematic Mapper simulator data for forest structural assessment. *IEEE Transactions on Geoscience and Remote Sensing*, **22**: 482–489.

Spanner, M.A., Pierce, L.L., Peterson, D.L. and Running, S.W., 1990, Remote sensing of temperate coniferous forest leaf area index: The influence of canopy closure, understory vegetation and background reflectance. *International Journal of Remote Sensing*, **11**: 95–111.

Spanner, M.A., Johnson, L., Miller, J., McCreight, R., Freemantle, J., Runyon, J. and Gong, P., 1994, Remote sensing of seasonal leaf area index across the Oregon transect. *Ecological Applications*, **4**: 258–271.

Sprugel, D.G., Ryan, M.G., Brooks, J.R., Vogt, K.A. and Martin, T.A., 1995, *Respiration From the Organ Level to the Stand.* In Smith, W.K. and Hinckley, T.M. (eds.), Resource Physiology of Conifers, Acquisition, Allocation and Utilisation. Academic Press, San-Diego: 255–299.

Stein, A., van der Meer, F. and Gorte, B. (eds.), 1999, *Spatial Statistics for Remote Sensing.* Kluwer, Dordrecht.

Steven, M.D., 1987, Ground truth: An underview. *International Journal of Remote Sensing*, **8**: 1033–1038.

Stewart, J.B., Engman, E.T., Feddes, R.A. and Kerr, Y. (eds.), 1996, *Scaling up in Hydrology Using Remote Sensing.* Wiley, Chichester.

Stewart, J.B., El Abidine, A.Z. and Bernier, P.Y., 1995, Stomatal and mesophyll limitations of photosynthesis in black spruce seedlings during multiple cycles of drought. *Tree Physiology*, **15**: 57–64.

Steyaert, L.T., Hall, F.G. and Loveland, T.R., 1997, Land cover mapping, fire regeneration and scaling studies in the Canadian boreal forest with 1 km AVHRR and Landsat TM data. *Journal of Geophysical Research*, **102**: 29581–29598.

Strahler, A.H., Woodcock, C.E. and Smith, J.A., 1986, On the nature of models in remote sensing. *Remote Sensing of Environment*, **20**:121–139.

Street, H.E. and Öpik, H., 1970, *The Physiology of Flowering Plants: Their Growth and Development.* Arnold, London.

Stoddart, D.R., 1986, *On Geography.* Blackwell, Oxford.

Sulzman, E.W., Poiani, K.A. and Kittel, T.G.F., 1995, Modelling human-induced climatic change: A summary for environmental managers. *Environmental Management*, **19**: 197–224.

Sundquist, E.T., 1993, The global carbon dioxide budget. *Science*, **259**: 934–941.

Tans, P.P., Fung, I.Y. and Takahshi, T., 1990, Observational constraints on the global atmospheric CO_2 budget. *Science*, **247**: 1431–1438.

Tedrow, J.C.F., 1977, *Soils of the Polar Landscapes.* Rutgers University Press, New Jersey.

Teillet, P.M. and Holben, B.J., 1994, Towards operational radiometric calibration of NOAA AVHRR imagery in the visible and near-infrared channels. *Canadian Journal of Remote Sensing*, **20**: 1–10.

Teillet, P.M. Staenz, K. and Williams, D.J., 1997, Effects of spectral, spatial and radiometric characteristics on remote sensing vegetation indices of forested regions. *Remote Sensing of Environment*, **61**: 139–149.

Tett, S.F.B., Johns, T.C. and Mitchell, J.F.B., 1997. Global and regional variability in a coupled AOGCM. *Climate Dynamics*, **31**: 303–324.

Thomas, J.R. and Gausmann, H.W., 1977, Leaf reflectance versus leaf chlorophyll and carotenoid concentration for eight crops. *Agronomics Journal*, **69**: 799–802.

Thornley, J.H.M. and Johnson, I.R., 1990, *Plant and Crop Modelling.* Oxford University Press, Oxford.

Thornton, P.E., Running, S.W. and White, M.A., 1997, Generating surfaces of daily meteorological variables over large regions of complex terrain. *Journal of Hydrology*, **190**: 214–251.

Townshend, J.R.G., 1981, The spatial resolving power of Earth resources satellites. *Progress in Physical Geography*, **5**: 32–55.

Townshend, J.R.G., 1992, Land cover. *International Journal of Remote Sensing*, **13**: 1319–1328.

Townshend, J.R.G. and Justice, C.O., 1988, Selecting the spatial resolution of satellite sensors required for global monitoring of land transformations. *International Journal of Remote Sensing*, **9**: 187–236.

Trenberth, K.E. (ed.), 1992, *Climate System Modelling*. Cambridge University Press, Cambridge.

Trenberth, K.E., Houghton, J.T. and Filho, L.G., 1996, The climate system: An overview. In Houghton, J.T., Filho, L.G., Callender, N., Kattenberg, A. and Maskell, K. (eds.), *Climate Change 1995*. Cambridge University Press, Cambridge: 1–59.

Tripathy, G.K., Ghosh, T.K. and Shah, S.D., 1996, Monitoring of desertification process in Karnataka state of India using multi-temporal remote sensing and ancillary information using GIS. *International Journal of Remote Sensing*, **17**: 2243–2257.

Tucker, C.J., 1977a, Asymptotic nature of grass canopy spectral reflectance. *Applied Optics*, **16**: 1151–1156.

Tucker, C.J., 1977b, *Use of Near Infrared / Red Radiance Ratios for Estimating Vegetation Biomass and Physiological Status*. NASA/GSFC Report X-923-77-183.

Tucker, C.J., 1996, History of the use of AVHRR data for land applications. In D'Souza, G., Belward, A.S. and Malingreau, J.P. (eds.), *Advances in the Use of NOAA AVHRR Data for Land Applications*. Kluwer, Dordrecht: 1–19.

Tucker, C.J. and Garrett, M.W., 1977, Leaf optical system modelled as a stochastic process. *Applied Optics*, **16**: 635–642.

Tucker, C.J., Fung, I.Y., Keeling, C.D. and Gammon, R.H., 1986, Relationship between atmospheric CO_2 variations and a satellite-derived vegetation index. *Nature*, **319**: 195–199.

Turner, D.P., Winjun, J.K., Kolchugina, T.P. and Cairns, M.A., 1997, Accounting for biological and anthropogenic factors in national land-base carbon budgets. *Ambio*, **26**: 220–226.

Turner, D.P., Cohen, W.B., Kennedy, R.E., Fassnacht, K.S. and Briggs, J.M., 1999, Relationships between leaf area index and Landsat TM spectral vegetation indices across three temperate zone sites. *Remote Sensing of Environment*, **70**: 52–68.

Turner, M.D. and Congalton, R.G., 1998, Classification of multi-temporal SPOT-XS satellite data for mapping rice fields on a West African floodplain. *International Journal of Remote Sensing*, **19**: 21–41.

Tyrrell, J.B., 1897, Report on the Doobaunt, Kazan and Ferguson rivers and the north-west coast of Hudson bay to Lake Winnipeg. *Geological Survey of Canada Annual Report*, **9F**: 5–218.

Unwin, D., 1998, Computers, geoscience and geocomputation. *Computers and Geosciences*, **24**: 297–298.

Urban, D.L., Bonan, G.B., Smith, T.M., and Shugart, H.H., 1991, Spatial applications of gap models. *Forest Ecology and Management,* **42**: 95–110.

USACECERL , 1993, *GRASS 4.1 User's Reference Manual.* US Army Corps of Engineers Construction Engineering Research Laboratories, Champaign, Illinois.

van Beurden, A.U. and Douven, W.J., 1999, Aggregation issues of spatial information in environmental research. *International Journal of Geographical Information Science*, **13**: 513–527.

van Gardingen, Foody, G.M. and Curran, P.J. (eds.), 1997, *Scaling-up: From Cell to Landscape.* Cambridge University Press, Cambridge.

van Rompaey, A.J., Govers, G. and Baudet, M., 1999, A strategy for controlling error of distributed environmental models by aggregation. *International Journal of Geographical Information Science*, **13**: 577 – 590.

Vanclay, J.K. and Preston, R.A., 1990, Utility of Landsat TM data for mapping site productivity in tropical moist forests. *Photogrammetric Engineering and Remote Sensing*, **56**: 1383–1388.

VEMAP (Vegetation/Ecosystem Modelling and Analysis Project), 2000, *A User's Guide to the VEMAP Phase 1 Database.* (URL http://www.cgd.ucar.edu:80/vemap/users-guide.html).

Verstraete, M.M. and Pinty, B., 1992, Extracting surface properties from satellite data in visible and NIR wavelengths. In Mather, P.M. (ed.), *TERRA-1: Understanding the Terrestrial Environment.* Taylor and Francis, London: 203–209.

Verstraete, M.M. and Pinty, B., 1996, Designing optimal spectral vegetation indices for remote sensing applications. *IEEE Transactions on Geoscience and Remote Sensing*, **34**: 1254–1265.

Verstraete, M.M. and Pinty, B., 1999, MERIS potential for land applications. *International Journal of Remote Sensing*, **20**: 1747–1756.

Viner, D. and Hulme, M., 1997, *The Climate Impacts LINK Project: Applying Results from the Hadley Centre's Climate Change Experiments for Climate Change Impact Assessments.* Climatic Research Unit, Norwich.

Vloedbeld, M. and Leemans, R., 1993, Quantifying feedback processes in the response of the terrestrial carbon cycle to global change: The modelling approach of Image-2. *Water, Air and Soil Pollution,* **70**: 615–628.

Vogt, K.A. and Persson, H., 1991, Measuring growth and development of roots. In Lassoie, J.P. and Hinckley, T.M. (eds.), *Techniques and Approaches in Forest Tree Ecophysiology.* CRC Press, Boca Raton.

Vose, J.M., Dougherty, P.M., Long, J.N., Smith, F.W., Gholz, H.L. and Curran, P.J., 1994, Factors influencing the amount and distribution of leaf area in pine stands. *Ecological Bulletins*, **43**: 102–114.

Waddington, J.M. and Roulet, N.T., 2000, Carbon balance of a boreal patterned peatland. *Global Change Biology*, **6**: 87–97.

Walsh, S.J., 1987, Variability of Landsat MSS spectral responses of forests in relation to stand and site characteristics. *International Journal of Remote Sensing*, **8**: 1289–1299.

Walter-Shea, E.A., 1987, *Laboratory and Field Measurements of Leaf Spectral Properties and Canopy Architecture and their Affects on Canopy Reflectance.* Unpublished Ph.D. Thesis. University of Nebraska, Lincoln.

Waring, R.H. and Franklin, J.F., 1979, The evergreen coniferous forests of the Pacific Northwest. *Science*, **204**: 1380–1386.

Waring, R.H. and Schlesinger, W.H., 1985, *Forest Ecosystems Concepts and Management.* Academic Press, San Diego.

Waring, R.H. and Running S.W., 1998, *Forest Ecosystems: Analysis at Multiple Scales* (second edition). Academic Press, San Diego.

Warnant, P., Francois, L., Strivay, D. and Gérard, J-C., 1994, CARAIB: A global model of terrestrial biological productivity. *Global Biogeochemical Cycles*, **8**: 255–270.

Watson, R.T., Zinyowera, M.C., Moss, R.H. and Dokken, D.J., 1996, *Climate Change 1995: Impacts, Adaptations and Mitigation of Climatic Change: Scientific-Technical Analyses.* IPCC, Cambridge University Press, Cambridge.

Webster, R., 1989, Is regression what you really want? *Soil Use and Management*, **5**: 47–53.

Webster, R. and Burgess, T., 1984, Sampling and bulking strategies for estimating soil properties in small regions. *Journal of Soil Science*, **35**: 127–140.

Webster, R. and Oliver, M.A., 1990, *Statistical Methods in Soil and Land Resource Survey.* Oxford University Press, New York.

Weinreb, M.P., Hamilton, G., Brown, S. and Koczor, R.J., 1990, Non-linearity corrections in calibration of Advanced Very High Resolution Radiometer infrared channels. *Journal of Geophysical Research*, **95**: 7381–7388.

Welch, R., 1982, Spatial resolution requirements for urban studies. *International Journal of Remote Sensing*, **3**: 139–146.

Wellens, J., 1997, Rangeland vegetation dynamics and moisture availability in Tunisia: an investigation using satellite and meteorological data. *Journal of Biogeography*, **24**: 845–855.

Welles, J.M., 1990, Some indirect methods of estimating canopy structure. *Remote Sensing Reviews*, **5**: 31–43.

Welles, J.M. and Norman J.M., 1991, Instrument for indirect measurement of canopy architecture. *Agronomy Journal,* **83**: 818–825.

Welles, J.M. and Cohen, S., 1996, Canopy structure measurement by gap fraction analysis using commercial instrumentation. *Journal of Experimental Botany*, **302**: 1335–1342.

Wessman, C.A., 1992, Imaging spectrometry for remote sensing of ecosystem processes. *Advanced Space Research,* **12**: 361–368.

Wessman, C.A., 1994, Remote sensing and the estimation of ecosystem parameters and functions. In Hill, J. (ed.), Imaging Spectrometry as a Tool for Environmental Observations. Kluwer, Dordrecht: 39–56.

Wessman, C.A., Curtiss, B. and Ustin, S.L., 1990, Large scale ecosystem modelling using parameters derived from imaging spectrometer data. *SPIE, Imaging Spectroscopy of the Terrestrial Environment,* **1298**: 164–171.

Wessman, C.A., Ustin, S.L., Curtiss, B. and Gao, B.C., 1991, A conceptual framework for ecosystem modelling using remotely sensed inputs. *Proceedings of the 5th International Colloquium - Physical Measurements and Signatures in Remote Sensing*. ESA, Noordwijk, SP-319: 777–782.

White, A., Cannell, M.G.R. and Friend, A.D., 1999, Climate change impacts on ecosystems and the terrestrial carbon sink: A new assessment. *Global Environmental Change*, **9** (Supplementary Issue): 21–30.

White, J.D., Running, S.W., Nemani, R. Keane, R.E. and Ryan, K.C., 1997, Measurement and remote sensing of LAI in Rocky Mountain montane ecosystems. *Canadian Journal of Forest Research*, **27**: 1714–1727.

Wickland, D.E., 1989, Future directions for remote sensing in terrestrial ecological research. In Asrar, G. (ed.), *Theory and Applications of Optical Remote Sensing*. Wiley, New York: 691–724.

Wickland, D.E., 1991, Global ecology: The role of remote sensing. In Esser, G. and Overdieck, D. (eds.), *Modern Ecology: Basic and Applied Aspects*. Elsevier, Amsterdam: 725–750.

Wicks, T.E. and Curran, P.J., 1998, Towards the regional estimation of NPP. *Proceedings, 27th International Symposium on Remote Sensing of Environment*. Balkema, Rotterdam: 698–700.

Wicks, T.E. and Curran, P.J., 2000, Flipping forests: Implications of future climate change on boreal forest carbon sequestration. *Nature* (in preparation).

Wiegend, C.L., Richardson, A.J., and Kanemasu, E.T., 1979, Leaf area index estimates for wheat from Landsat and their implications for evapotranspiration and crop modelling. *Agronomics Journal*, **71**: 336–342.

Wigley, T.M.L., 1993, Balancing the carbon budget: Implications for projections of future carbon dioxide concentration changes. *Tellus*, **45B**: 409–425.

Wigmosta, M.S., Vail, L.W. and Lettenmaier, D.P., 1994, A distributed hydrology-vegetation model for complex terrain. *Water Resources Research*, **30**: 1665–1679.

Wilkinson, G.G., 1996, A review of current issues in the integration of GIS and remote sensing data. *International Journal of Remote Sensing*, **10**: 85–101.

Wilson, M.F., Henderson-Sellers, A., Dickenson, R.E. and Kennedy, P.J., 1987, Sensitivity of the Biosphere-Atmosphere Transfer Scheme (BATS) to the inclusion of variable soil characteristics. *Journal of Climatology and Applied Meteorology,* **26**: 341–362.

Wisniewski, J. and Sampson, R.N. (eds.), 1993, *Terrestrial Biospheric Carbon Fluxes: Quantification of Sinks and Sources of CO_2*. Kluwer, Dordrecht.

Wood, R.A., Keen, A.B., Mitchell, J.F.B. and Gregory, J.M., 1999, Changing spatial structure of the thermohaline circulation in response to atmospheric CO_2 forcing in a climate model. *Nature*, **399**: 572–575.

Woodcock, C.E. and Strahler, A.H., 1985, relating ground scenes to spatial variation in images. *Proceedings of the 3rd NASA Conference on Mathematical Pattern Recognition and Image Analysis*. NASA Goddard Space Flight Center, Greenbelt, MD: 1755–1767.

Woodcock, C.E., Strahler, A.H. and Jupp, D.L.B., 1988, The use of variograms in remote sensing. I. Scene models and simulated images. *Remote Sensing of Environment*, **25**: 323–348.

Woodcock, C.E. and Strahler, A.H., 1987, The factor of scale in remote sensing. *Remote Sensing of Environment*, **21**: 311–332.

Woodward, F.I., Smith, T.M. and Emanuel, W.R., 1995, A global land primary productivity and phyto-geography model. *Global Biogeochemical Cycles*, **9**: 471–490.

Wooster, M.J., Richards, T.S. and Kidwell, K., 1995, NOAA-11 AVHRR/2 thermal channel calibration update. *International Journal of Remote Sensing*, **16**: 359–363.

Wülder, M.A., 1998a, Optical remote sensing techniques for the assessment of forest inventory and biophysical parameters. *Progress in Physical Geography*, **22**: 449–476.

Wülder, M.A., 1998b, The prediction of leaf area index from forest polygons decomposed through the integration of remote sensing, GIS, UNIX and C. *Computers and Geoscience*, **24**: 151–157.

Wülder, M.A., Franklin, S.E. and Lavigne, M.B., 1996, Statistical texture properties of forest structure for improved LAI estimates from CASI. *Proceedings of the 18th Canadian Symposium on Remote Sensing: Vancouver*. Canadian Aeronautics and Space Institute, Ottawa: 161–164.

Xu, J. and Lathrop, R.G., 1995, Improving simulation accuracy of spread phenomena in a raster-based GIS. *International Journal of Geographical Information Systems*, **9**: 153–168.

Yoder, B., 1992, *Photosynthesis of Conifers: Influential Factors and Potential for Remote Sensing*. Unpublished Ph.D. Thesis, Oregon State University, Corvallis, Oregon.

Yoder, B.J. and Waring, R.H., 1994, The normalised difference vegetation index of small Douglas-fir canopies with varying chlorophyll concentrations. *Remote Sensing of Environment*, **49**: 81–91.

Zhang, J. and Kirby, R.P., Alternative criteria for defining fuzzy boundaries based on fuzzy classification of air photos and satellite images. *Photogrammetric Engineering and Remote Sensing*, **65**: 1379–1387.

Zhang, R., Warrick, A.W. and Myers, D.E., 1990, Variance as a function of sample support size. *Mathematical Geology*, **22**: 107–122.